

Progressive keratoconus: Insights into etiopathogenesis, diagnosis, and treatment

Edited by

Cristina Nicula and Adriana Elena Bulboaca

Published in

Frontiers in Medicine



FRONTIERS EBOOK COPYRIGHT STATEMENT

The copyright in the text of individual articles in this ebook is the property of their respective authors or their respective institutions or funders. The copyright in graphics and images within each article may be subject to copyright of other parties. In both cases this is subject to a license granted to Frontiers.

The compilation of articles constituting this ebook is the property of Frontiers.

Each article within this ebook, and the ebook itself, are published under the most recent version of the Creative Commons CC-BY licence. The version current at the date of publication of this ebook is CC-BY 4.0. If the CC-BY licence is updated, the licence granted by Frontiers is automatically updated to the new version.

When exercising any right under the CC-BY licence, Frontiers must be attributed as the original publisher of the article or ebook, as applicable.

Authors have the responsibility of ensuring that any graphics or other materials which are the property of others may be included in the CC-BY licence, but this should be checked before relying on the CC-BY licence to reproduce those materials. Any copyright notices relating to those materials must be complied with.

Copyright and source acknowledgement notices may not be removed and must be displayed in any copy, derivative work or partial copy which includes the elements in question.

All copyright, and all rights therein, are protected by national and international copyright laws. The above represents a summary only. For further information please read Frontiers' Conditions for Website Use and Copyright Statement, and the applicable CC-BY licence.

ISSN 1664-8714
ISBN 978-2-8325-4020-6
DOI 10.3389/978-2-8325-4020-6

About Frontiers

Frontiers is more than just an open access publisher of scholarly articles: it is a pioneering approach to the world of academia, radically improving the way scholarly research is managed. The grand vision of Frontiers is a world where all people have an equal opportunity to seek, share and generate knowledge. Frontiers provides immediate and permanent online open access to all its publications, but this alone is not enough to realize our grand goals.

Frontiers journal series

The Frontiers journal series is a multi-tier and interdisciplinary set of open-access, online journals, promising a paradigm shift from the current review, selection and dissemination processes in academic publishing. All Frontiers journals are driven by researchers for researchers; therefore, they constitute a service to the scholarly community. At the same time, the *Frontiers journal series* operates on a revolutionary invention, the tiered publishing system, initially addressing specific communities of scholars, and gradually climbing up to broader public understanding, thus serving the interests of the lay society, too.

Dedication to quality

Each Frontiers article is a landmark of the highest quality, thanks to genuinely collaborative interactions between authors and review editors, who include some of the world's best academicians. Research must be certified by peers before entering a stream of knowledge that may eventually reach the public - and shape society; therefore, Frontiers only applies the most rigorous and unbiased reviews. Frontiers revolutionizes research publishing by freely delivering the most outstanding research, evaluated with no bias from both the academic and social point of view. By applying the most advanced information technologies, Frontiers is catapulting scholarly publishing into a new generation.

What are Frontiers Research Topics?

Frontiers Research Topics are very popular trademarks of the *Frontiers journals series*: they are collections of at least ten articles, all centered on a particular subject. With their unique mix of varied contributions from Original Research to Review Articles, Frontiers Research Topics unify the most influential researchers, the latest key findings and historical advances in a hot research area.

Find out more on how to host your own Frontiers Research Topic or contribute to one as an author by contacting the Frontiers editorial office: frontiersin.org/about/contact

Progressive keratoconus: Insights into etiopathogenesis, diagnosis, and treatment

Topic editors

Cristina Nicula — University of Medicine and Pharmacy Iuliu Hatieganu, Romania
Adriana Elena Bulboaca — University of Medicine and Pharmacy Iuliu Hatieganu, Romania

Citation

Nicula, C., Bulboaca, A. E., eds. (2023). *Progressive keratoconus: Insights into etiopathogenesis, diagnosis, and treatment*. Lausanne: Frontiers Media SA.
doi: 10.3389/978-2-8325-4020-6

Table of contents

- 04 **Editorial: Progressive keratoconus: insights into etiopathogenesis, diagnosis, and treatment**
Cristina Ariadna Nicula and Adriana Elena Bulboaca
- 06 **Delayed Re-epithelialization After Epithelium-Off Crosslinking: Predictors and Impact on Keratoconus Progression**
Chiara Bonzano, Carlo Alberto Cutolo, Donatella Musetti, Ilaria Di Mola, Chiara Pizzorno, Riccardo Scotto and Carlo Enrico Traverso
- 12 **Associations Between Keratoconus and the Level of Sex Hormones: A Cross-Sectional Study**
Xiaorui Zhao, Yifei Yuan, Tong Sun, Yu Zhang and Yueguo Chen
- 18 **Comparison of Corneal Collagen Cross-Linking and Voriconazole Treatments in Experimental Fungal Keratitis for *Aspergillus fumigatus***
Zhennan Zhao, Xueli Chen, Yi Shao and Tingting Shao
- 28 **Determining the center of a keratoconus: Comparison of different tomographic parameters and impact of disease severity**
Gernot Steinwender, Alexander Kollenc, Mehdi Shajari, Michael Sommer, Andrea Borenich, Jutta Horwath-Winter, Ewald Lindner, Nora Woltsche, Wolfgang List and Andreas Wedrich
- 35 **Tear proteome profile in eyes with keratoconus after intracorneal ring segment implantation or corneal crosslinking**
Nahia Goñi, Itziar Martínez-Soraa, Oliver Ibarrondo, Mikel Azkargorta, Felix Elortza, David J. Galarreta and Arantxa Acera
- 50 **Outcome indicators for cross linking in pediatric keratoconus**
Denise Wajnsztajn, Or Shmueli, Yehuda Tarnovsky, Joseph Frucht-Pery and Abraham Solomon
- 59 **Combination of violet light irradiation and collagenase treatments in a rabbit model of keratoconus**
Hidenaga Kobashi, Takashi Yano and Kazuo Tsubota
- 65 **Medium to long term follow up study of the efficacy of cessation of eye-rubbing to halt progression of keratoconus**
Adrien Mazharian, Roxane Flamant, Sina Elahi, Christophe Panthier, Radhika Rampat and Damien Gatinel
- 75 **Development and validation to predict visual acuity and keratometry two years after corneal crosslinking with progressive keratoconus by machine learning**
Yu Liu, Dan Shen, Hao-yu Wang, Meng-ying Qi and Qing-yan Zeng
- 85 **Progressive high-fluence epithelium-on accelerated corneal crosslinking: a novel corneal photodynamic therapy for early progressive keratoconus**
Cosimo Mazzotta, Anna Pandolfi and Marco Ferrise



OPEN ACCESS

EDITED AND REVIEWED BY
Jodhbir Mehta,
Singapore National Eye Center, Singapore

*CORRESPONDENCE
Cristina Ariadna Nicula
✉ niculacristina65@yahoo.com

RECEIVED 26 September 2023
ACCEPTED 18 October 2023
PUBLISHED 13 November 2023

CITATION
Nicula CA and Bulboacă AE (2023) Editorial:
Progressive keratoconus: insights into
etiopathogenesis, diagnosis, and treatment.
Front. Med. 10:1302625.
doi: 10.3389/fmed.2023.1302625

COPYRIGHT
© 2023 Nicula and Bulboacă. This is an
open-access article distributed under the terms
of the [Creative Commons Attribution License](#)
(CC BY). The use, distribution or reproduction
in other forums is permitted, provided the
original author(s) and the copyright owner(s)
are credited and that the original publication in
this journal is cited, in accordance with
accepted academic practice. No use,
distribution or reproduction is permitted which
does not comply with these terms.

Editorial: Progressive keratoconus: insights into etiopathogenesis, diagnosis, and treatment

Cristina Ariadna Nicula^{1*} and Adriana Elena Bulboacă²

¹Department of Maxi-lo-Facial Surgery and Radiology, Dental Implantology, "Iuliu Hatieganu" University of Medicine and Pharmacy, Cluj-Napoca, Romania, ²"Iuliu Hatieganu" University of Medicine and Pharmacy, Cluj-Napoca, Romania

KEYWORDS

keratoconus (KCN), cross-linking, KCN treatment, KCN progression, corneal tomography

Editorial on the Research Topic

[Progressive keratoconus: insights into etiopathogenesis, diagnosis, and treatment](#)

Keratoconus (KCN) is a bilateral and asymmetric corneal ectatic dystrophy with onset during the second decade of life. The development of modern topographic, tomographic, and biomechanical examinations has increased the accuracy of keratoconus diagnosis, particularly in the subclinical stages of the disease. [Steinwender et al.](#) analyzed deviations between the locations of different tomographic parameters and identified low consistency between different methods for describing the location of a keratoconus. This study suggested that elevation- or pachymetry-based measures (such as ELEB, ELEF, or Pachymin) are suitable for clinical applications requiring an accurate cone center ([Steinwender et al.](#)). Furthermore, [Mazharian et al.](#) suggested that a significant proportion of KCN patients are likely to remain stable if close monitoring and strict eye rubbing cessation are achieved, without the need for further intervention. Moreover, [Zhao X. et al.](#) analyzed the levels of sex hormones associated with KCN and revealed that testosterone levels were reduced in the plasma of both female and male KCN patients, whereas plasma estradiol levels were increased in only male KCN patients. Moreover, when analyzing tear samples from KCN patients, [Goñi et al.](#) found A-kinase anchor protein 13 among the deregulated proteins detected, deserving special attention for its involvement in corneal thinning and its strong overexpression in the tears of patients with more active KC and faster disease progression.

In recent decades, cross-linking therapy has been successfully applied to stop or arrest KCN. [Wajnsztajn et al.](#) studied the best outcome indicators for cross-linking in pediatric KCN (logMAR visual acuity, maximal corneal power, pachymetry, and refractive cylinder). They concluded that non-accelerated treatment was more effective than accelerated treatment and that corneas with advanced disease had a greater effect on CXL ([Wajnsztajn et al.](#)). Moreover, [Liu et al.](#) demonstrated the application of a machine-learning approach using the XGBoost model, which produced predicted values closest to the actual values for both the CDVA and maximal corneal power changes in the testing ($R^2 = 0.9993$ and 0.9888) and validation ($R^2 = 0.8956$ and 0.8382) sets. [Kobashi et al.](#) suggested an experimental model using collagenase treatment to induce KCN by steepening the keratometric and astigmatic values. This study identified no significant difference in the

observed elastic behaviors of normal and ectatic corneas under physiologically relevant stress levels. Moreover, ultraviolet irradiation did not cause the regression of corneal steepening in a collagenase-induced model during short-term observation (Kobashi et al.). Mazzotta et al. introduced a novel cross-linking technique, the higher-fluence pulsed light Epi-ON accelerated crosslinking nomogram (PFPL M Epi-On ACXL), for the treatment of progressive KCN. A non-randomized interventional study showed that the pachymetry-based PFPL M Epi-On ACXL nomogram stabilized ectasia progression and higher fluence Epi-On ACXL increased CXL penetration with better functional outcomes in the absence of complications. Furthermore, the coma value improved significantly by the 6 month in all groups (Mazzotta et al.). Bonzano et al. investigated the demographic and corneal factors associated with the occurrence of delayed re-epithelialization after epithelium-off CXL (epi-off CXL) and concluded that the association between delayed re-epithelialization and age may reflect an age-related decrease in the corneal healing response without changing the efficacy of cross-linking.

Zhao Z. et al. showed that voriconazole combined with cross-linking was effective in treating *Aspergillus*-infected keratitis. They concluded that combination therapy could effectively inhibit *Aspergillus*, accelerate corneal repair, and shorten the disease course (Zhao Z. et al.).

Author contributions

CN: Writing—original draft, Writing—review & editing. AB: Writing—original draft, Writing—review & editing.

Funding

The author(s) declare that no financial support was received for the research, authorship, and/or publication of this article.

Conflict of interest

The authors declare that the research was conducted in the absence of any commercial or financial relationships that could be construed as a potential conflict of interest.

Publisher's note

All claims expressed in this article are solely those of the authors and do not necessarily represent those of their affiliated organizations, or those of the publisher, the editors and the reviewers. Any product that may be evaluated in this article, or claim that may be made by its manufacturer, is not guaranteed or endorsed by the publisher.



Delayed Re-epithelialization After Epithelium-Off Crosslinking: Predictors and Impact on Keratoconus Progression

Chiara Bonzano*, Carlo Alberto Cutolo, Donatella Musetti, Ilaria Di Mola, Chiara Pizzorno, Riccardo Scotto and Carlo Enrico Traverso

Eye Clinic, DiNOGMI, University of Genoa and IRCCS San Martino Polyclinic Hospital, Genoa, Italy

OPEN ACCESS

Edited by:

Mee Kum Kim,
Seoul National University, South Korea

Reviewed by:

Betul Bayraktutar,
Tufts Medical Center, United States
Katarzyna Krysiak,
Wojewódzki Szpital Specjalistyczny nr
5 Sosnowiec, Poland

*Correspondence:

Chiara Bonzano
oculistabonzano@gmail.com

Specialty section:

This article was submitted to
Ophthalmology,
a section of the journal
Frontiers in Medicine

Received: 24 January 2021

Accepted: 16 September 2021

Published: 15 October 2021

Citation:

Bonzano C, Cutolo CA, Musetti D, Di
Mola I, Pizzorno C, Scotto R and
Traverso CE (2021) Delayed
Re-epithelialization After
Epithelium-Off Crosslinking: Predictors
and Impact on Keratoconus
Progression. *Front. Med.* 8:657993.
doi: 10.3389/fmed.2021.657993

Purpose: To investigate the demographic and corneal factors associated with the occurrence of delayed reepithelialization (DRE) after epithelium-off crosslinking (epi-off CXL).

Design: Retrospective case series.

Methods: A chart review was performed to identify patients treated with epi-off CXL. DRE was defined as a corneal epithelial defect detected by fluorescein staining that persisted for more than 10 days. Slit-lamp examination, anterior segment optical coherence tomography, corneal topography, and corneal *in vivo* confocal microscopy (IVCM) were always performed preoperatively and at each follow-up visit (1, 3, 6, 12 months). A generalized estimating equation was used to assess the baseline factors associated with DRE.

Results: Data from 153 eyes were analyzed. The mean age of patients was 24.9 ± 8.5 years, and 47 (30.7%) were women. The average reepithelialization time was 4.7 ± 1.8 days. Six eyes (3.9%) experienced DRE. In the multivariate model, both the age of the patient ($OR = 1.30$; $p = 0.02$) and the corneal steepest meridian ($OR = 0.44$, $p = 0.047$) were associated with DRE. Baseline nerve count was also associated with DRE (0.87 , $p = 0.03$). Male gender was associated with a slower early nerve regrowth (1–6 months) ($p = 0.048$), but not with the occurrence of DRE ($p = 0.27$). Preoperative central corneal thickness was not related to DRE ($p = 0.16$). DRE was not associated with keratoconus progression after epi-off CXL ($p = 0.520$).

Conclusions: The association between DRE and age may reflect the age-related decrease in the corneal healing response. Also, low baseline corneal nerve count is associated with DRE. Gender seems to affect reinnervation measured by IVCM but not the reepithelialization time. DRE does not seem to affect the efficacy of epi-off CXL.

Keywords: epithelium-off crosslinking, accelerated corneal crosslinking, keratoconus, delayed re-epithelialization, bandage contact lens

INTRODUCTION

Keratoconus (KC) is a non-inflammatory corneal disease characterized by progressive ectasia, in which stromal thinning and cornea weakening can lead to an increase of anterior and posterior corneal curvature (1). The resulting irregular astigmatism, myopia together with the progressive corneal scarring, is responsible for visual loss (2).

Corneal collagen crosslinking (CXL) is a parasurgical technique of corneal tissue strengthening. Riboflavin activated by irradiation with ultraviolet-A (UVA) light increases the intra and interfibrillar covalent bonds, thereby increasing the mechanical strength and slowing the progression of corneal ectasia (3).

The epithelium-off CXL (epi-off CXL) technique is deemed a safe procedure for the treatment of progressive KC (4–8).

To reduce discomfort and to promote fast and safe epithelial healing, patients are generally given daily topical antibiotics and corticosteroids for 1 to 2 weeks following the epi-off CXL with close follow-up. A bandage contact lens is usually placed following the procedure, night and day up to 3–5 consecutive days. Three days later, after lens removal, complete epithelial healing is observed at the biomicroscopic examination in most of the cases (9).

Delayed reepithelialization (DRE), defined as a corneal epithelial defect detected by fluorescein-staining that persisted for more than 10 days after treatment, is a possible complication of epi-off CXL.

This study aims to investigate the demographic and corneal factors associated with DRE.

PATIENTS AND METHODS

A retrospective chart review was performed to identify patients treated with epi-off CXL at ClinicaOculistica, University of Genova, Italy. All subjects provided written informed consent.

Inclusion criteria were as follows: patients affected by grade II–III KC (Amsler-Krumeich (AK) grading); clinical and instrumental progression documented by repeated corneal topography over at least 6 months intended as an increase in the steep meridian value (K_{\max}) of 1.0 diopter or more; and willingness to undergo epi-off CXL.

Diagnosis of KC was established by using the AK classification, based on spectacle refraction, central keratometry, corneal transparency, and corneal thickness.

We included eyes with early to moderate progressive KC, corneal thickness $>400\ \mu\text{m}$, and with minimum of 12 months follow-up after epi-off CXL.

Exclusion criteria were advanced KC with stromal scarring, corneal hydrops, herpetic keratitis, autoimmune and other systemic diseases, pregnancy, and breastfeeding.

Patient Assessment

Slit-lamp examination implemented with corneal epithelial fluorescein staining, anterior segment optical coherence tomography (AS-OCT) (RTVue, Optovue Inc., Fremont, CA), corneal topography measurement using TMS-4 topographer (Tomey Corporation, Tokyo, Japan) with surface regularity

index, and corneal *in vivo* confocal microscopy (IVCM) (Heidelberg Retina Tomograph II, Rostock Cornea Module) were always performed preoperatively and at each follow-up visit (1, 3, 6, and 12 months).

Surgical Technique

Epi-off CXL was always performed by the same surgeon (C.B.) using the accelerated protocol that uses equivalent total irradiance [$9\ \text{mW}/\text{cm}^2$ for 10 min, $5.4\ \text{J}/\text{cm}^2$ (A9/10-CXL)] (10).

The procedure was always performed under sterile operating conditions using topical anesthesia oxybuprocaine hydrochloride 0.4% (Alfa Intes—Ind.Ter.Splendore) anesthetic drops. Topical pilocarpine 2.0% was administered 20 min before treatment.

After the application of an eyelid speculum, epithelial removal (9-mm) was achieved using a blunt knife. Riboflavin (0.1% in 20% dextran solution; Ricrolin; Sooft, Montegiorgio, Italy) was administered topically every minute for 15 min. The administration was continued every 2 min during UVA exposure.

The UVA irradiation was performed with a CBM X-Linker Vega using a $9\ \text{mW}/\text{cm}^2$ to obtain 10 min of UVA irradiation on balance while delivering a standard energy dose of $5.4\ \text{J}/\text{cm}^2$.

The post-CXL medication consisted of antibiotic eye drops solution (Netilmicin 0.3%) (3mg/ml) (four times daily for 1 week) and dexamethasone sodium phosphate (0.1%) (1mg/ml) (four times daily for 1 week and tapered over the following 7 days). Preservative-free isotonic solution (hyaluronic acid (HA) 0.4% and taurine (TAU) 0.5%) and preservative-free B2 vitamin eye drops (Ribolisin free, SOOFT italia) were used for 4 weeks. Oral pain medications (Tramadol 50 mg, 1–2 per day; diclofenac 25 mg, 1–2 per a day) were prescribed on the treatment day and the day after. A specific bandage lens for injured tissues, with a regenerating, anti-inflammatory, and analgesic effect (Regenera Therapeutic Lens) (16,5 mm, hydrogel Filcon II 3 e 75% H_2O , Dk = 42) was placed after the procedure to reduce the discomfort and to promote the epithelial healing. It was removed after 3 days if the epithelial healing was complete.

Delayed reepithelialization was defined as a corneal epithelial defect detected by fluorescein staining at the slit lamp examination that persisted for more than 10 days after epi-off CXL.

Delayed reepithelialization was managed conservatively with topical medication and bandage contact lens that was replaced every 3 days until complete healing. In one case, debridement was performed for redundant or loose epithelial margins. Additional surgical procedures were not needed in our cohort of patients (11, 12).

Statistical Analysis

Data are reported as mean (standard deviation) for continuous parameters or as frequencies for categorical parameters.

A generalized estimating equation was used to assess the baseline factors associated with DRE and to account for the correlation between fellow eyes. DRE was considered as the dependent variable in the analysis. Then a multivariate model was built. Criteria for model selection were guided by the univariate analysis and clinical significance of the variables. Univariate linear regression was also used to assess the association between

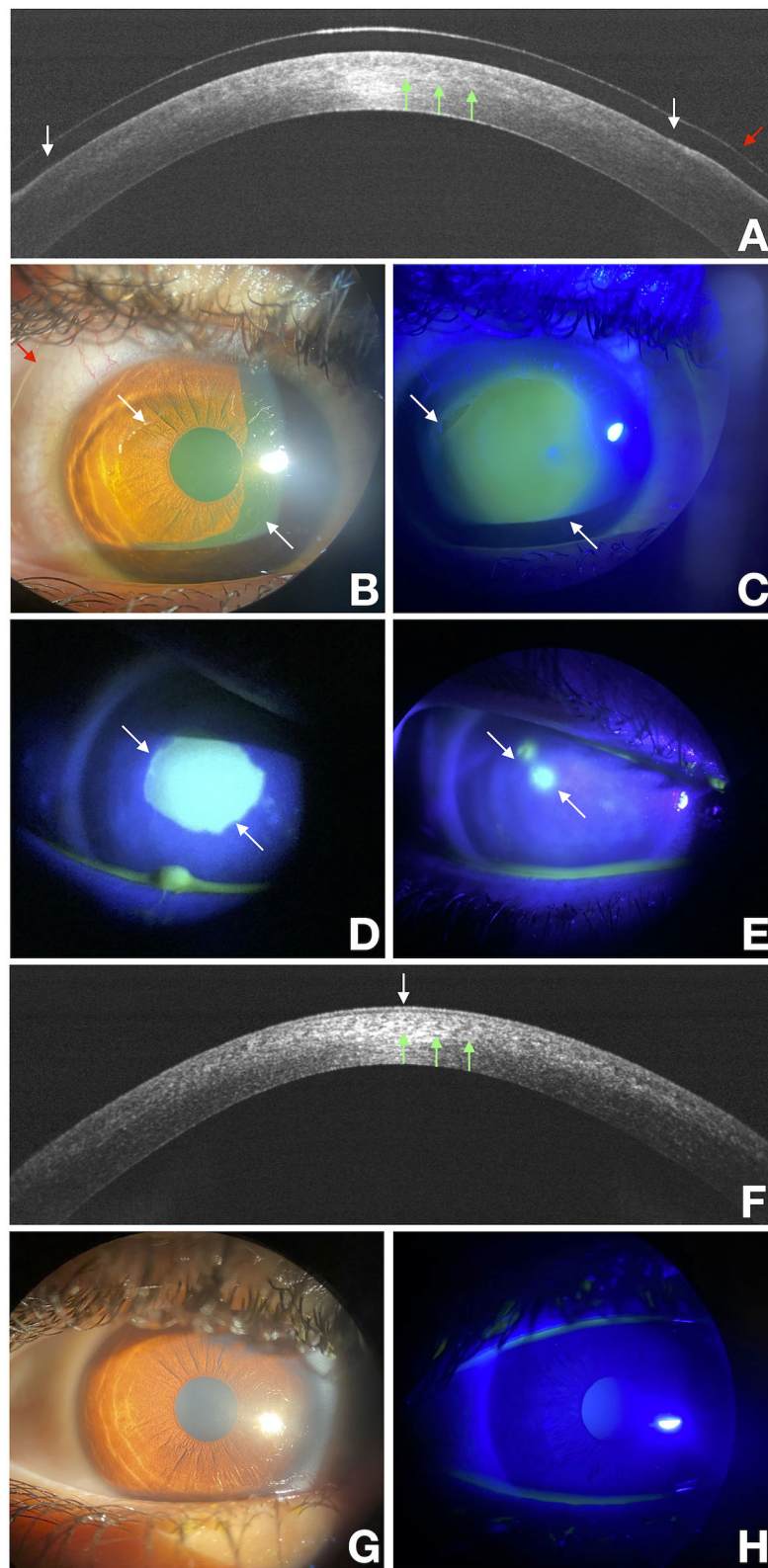


FIGURE 1 | Delayed re-epithelialization after the epithelium-off CXL (epi-off CXL) imaged with a multimodal approach. White arrows point at the edges of the epithelial fronts and green arrows points to the demarcation line, and the red arrow points to the bandage lens. OCT scan over the disepithelialized area at baseline **(A)**.

(Continued)

FIGURE 1 | Photograph obtained at baseline with diffuse white light (**B**) and with fluorescein staining (green) photograph obtained under cobalt-blue light illumination (**C**) imaged at baseline. (**D,E**) were acquired at the end of treatment at 3 and 10 days respectively. They show a residual corneal epithelial disepithelialization. OCT scan over the re-epithelialization area at day 15 (**F**). Photograph obtained at day 15 with diffuse white light (**G**) and with fluorescein staining (green) photograph obtained under cobalt-blue light illumination (**H**).

TABLE 1 | Demographic and clinical details for patients that experienced.

	No DRE (N = 147)	DRE (N = 6)	p-value
Age, (mean ± sd) years old	24.5 ± 8.3	33.6 ± 7.5	0.01
Gender, female	45 (30.6%)	2 (33%)	0.88
K2, (mean ± sd), diopters	44.2 ± 2.2	45.9 ± 3.7	0.31
CCT at thinnest point, (mean ± sd), μm	497 ± 34	479 ± 19.4	0.20
CCTmin, (mean ± sd), μm	463 ± 35	442 ± 11	0.16
GAT IOP, (mean ± sd), mmHg	13.0 ± 2.0	11.5 ± 1.7	0.14
BCVA, (mean ± sd), decimals	6.8 ± 2.5	8.3 ± 1.9	0.14
SF, (mean ± sd), diopters	−1.2 ± 2.8	−0.38 ± 1.59	0.46
CYL, (mean ± sd), diopters	5.6 ± 2.9	4.2 ± 1.3	0.30
SRI (mean ± sd)	1.02 ± 0.37	0.85 ± 0.15	0.36
Nerve, (mean ± sd), n	70.4 ± 19.8	36.5 ± 4.9	0.01
Dendritic cells, (mean ± sd), n	17.1 ± 15.6	16.0 ± 4.2	0.91

DRE, Delayed re-epithelialization; K2, steepest meridian reading; CCT, central corneal thickness; IOP, intraocular pressure measured with Goldmann tonometry; BVCA, best corrected visual acuity; SF, sphere; CYL, Cylinder; SRI, surface regularity index.

baseline characteristics and the speed of nerve regrowth between 1 and 6 months. All statistical analyses were performed with Stata version 15.1 (StataCorp LP, College Station, TX). The alpha level (type I error) was set at 0.05 for all analyses.

RESULTS

Based on inclusion and exclusion criteria, we analyzed data from 153 patients. The average reepithelialization time was 4.7 ± 1.8 days (SD). Postoperative corneal biomicroscopic examination performed on the third day after treatment showed a clear cornea, little edema, and no opacities before and immediately after therapeutic contact lens removal. Seventy-two hours after epithelium removal, almost all the patients had complete reepithelialization as shown by the fluorescein dye test instilled in the eye, only six eyes (3.9%) experienced DRE (**Figure 1**). Among these no one reported either a corneal infection or KC progression after epi-off CXL. Patient demographics and baseline ocular characteristics of the two groups are summarized in **Table 1**. The mean age of patients was 24.5 ± 8.3 in patients who did not experience DRE, and 33.6 ± 7.5 in patients with DRE ($p = 0.01$). As regard ocular characteristics, nerve count was 70.4 ± 19.8 and 36.5 ± 4.9 in the patient without and with DRE ($p = 0.01$), respectively. No significant differences were observed between the two groups regarding other demographic or ocular characteristics. As described in the methods, a model was built to better identify ocular and demographic characteristics associated with DRE (**Table 2**). The age of the patient and corneal nerve count were associated with DRE in univariate analysis with OR =

1.11 ($p = 0.02$) and OR = 0.89 ($p = 0.01$), respectively. Then, we have built two different multivariate models, not including nerve count (model 1) or age (model 2), to avoid multicollinearity. In both the multivariate models, age and nerve count remained significantly associated with DRE. Nerve count and age were also found negatively correlated ($r = -0.27$; $p = 0.028$). In model 1 the steepest meridian value was associated with DRE whereas in model 2 this variable was only marginally associated with DRE. Then, the same variables were tested for association with nerve regrowth (1–6 months), and it was found that the male gender was the only variable significantly associated with a slower early nerve regrowth ($p = 0.048$). Of note, even if gender was included in the multivariate models, it did not associate with DRE ($p = 0.27$ model 1). We also tested the hypothesis that DRE could affect the efficacy of epi-off CXL, and we found that DRE was not associated with KC progression after treatment ($p = 0.520$).

DISCUSSION

The association between DRE and age may reflect the age-related decrease in the corneal healing response. Gipson et al. (13) and some other studies reported that corneal wound healing declines with age (13–16). Major well-known changes in the cornea with age include the thickening of both the epithelial and endothelial basement membranes.

By regulating the growth factor activity, the basement membrane plays a key role in the cellular reparative process (17). Its hemidesmosome-anchoring fibrils bind the basal cells membrane to the Bowman's layer and form anchoring complexes by binding to the stromal plaques (18). The anchoring fibrils seem to become disrupted with increasing age, and the membrane thickness exceeds fibril length, and it could effectively block linkage between the anchoring fibrils and Bowman's layer (19). Furthermore, there is a well-known diminution of sex hormones that occurs with age in both sexes that affect the glandular functions and compromise the ocular surface system, and consecutively the cascade of healing mechanisms (20). Besides, the number of nerves in the corneal epithelial subbasal plexus decreases with age, leading perhaps to the loss of sensitivity observed with age involving at first the corneal periphery and successively spreading toward the central zone (16, 21). We have to keep in mind that the corneal sensation has already nearly disappeared in the early post epi-off CXL period, it improved to its baseline levels only at sixth postoperative month according to Ozgurhan et al. (22). The lower the corneal sensitivity, the lower the trend of the corneal epithelium to heal. In our analysis, we showed that baseline nerve count seems to play a role in the corneal healing process. Last but not least, an aging-related decrease in the number of conjunctival keratocytes has been reported (23). It could mean a lower level of Muc16, conjunctival

TABLE 2 | Analysis of the association between baseline demographic and anatomical parameters with DRE.

	Univariate			Multivariate (model 1)			Multivariate (model 2)		
	OR	95% CI	p	OR	95% CI	p	OR	95% CI	p
Age (years)	1.11	1.01–1.20	0.02	1.30	1.04–1.62	0.019			
Female	1.13	0.20–6.41	0.89	0.24	0.02–3.00	0.270	0.37	0.02–9.16	0.547
Steepest meridian (diopters)	0.84	0.59–1.17	0.26	0.44	0.19–0.99	0.047	0.61	0.34–1.09	0.099
Cylinder (diopters)	0.80	0.52–1.22	0.25						
CCT (μm)	0.98	0.96–1.01	0.20						
CCT at thinnest point (μm)	0.98	0.96–1.01	0.16	0.95	0.91–1.00	0.066	0.96	0.91–1.02	0.147
IOP (mmHg)	0.71	0.44–1.13	0.15						
BCVA (decimals)	1.35	0.89–2.03	0.15						
Sphere (diopter)	1.24	0.71–2.14	0.45						
SRI	0.34	0.03–3.50	0.35						
Nerve	0.89	0.81–0.97	0.01				0.87	0.76–0.98	0.026
Dendritic cells	0.99	0.90–1.10	0.92						

OR, Odds ratio; CCT, central corneal thickness; IOP, intraocular pressure measured with Goldmann tonometry; BCVA, best corrected visual acuity; SRI, surface regularity index.

mucin, which affects the behaviors of the corneal epithelium and keratocytes (24).

Gender seems to affect reinnervation measured by IVCN but not the reepithelialization time. Up to now, different studies stated that gender does not have any influence on reepithelialization as in our experience (25). Instead, no reports in literature found any impact of gender on the corneal reinnervation, unlike our observation. This study is limited by the small number of eyes who experienced complications after CXL and DRE. Even if CXL is a safe procedure, it is clinically meaningful to identify patients at risk for DRE.

The association between corneal steepest meridian readings and DRE is an interesting issue. It has been pointed out that the epithelium at the cone apex is thinner, where the stroma is steeper.

An overall thinning of the epithelium across the ectatic cornea and an apparent difference in epithelial thickness, which is lower in the central region and higher toward the inferior keratoconic cornea, is observed. Such irregularity could explain a slower reepithelialization. Vinciguerra et al. reported that the epithelium could act as a smoothing agent that reduces corneal power, astigmatism, and cornea irregularity after epi-off CXL (26). The reepithelialization and the following remodeling effect of CXL can take about 6 months to flatten and regularize the keratoconic shape of the cornea (26). This slower epithelium remodeling process when the cone is steeper could explain why topography obtained 1 month after CXL paradoxically shows an increase in the steepness of the cone.

The present study suggests that patients who experienced DRE did not derive less efficacy from epi-off CXL.

CONCLUSION

The association between DRE and age may reflect the age-related decrease in the corneal healing response.

Also, low baseline corneal nerve count is associated with DRE. Gender seems to affect reinnervation measured by IVCN, but not the reepithelialization time. DRE does not seem to affect the efficacy of epi-off CXL treatment.

DATA AVAILABILITY STATEMENT

The raw data supporting the conclusions of this article will be made available by the authors, without undue reservation.

ETHICS STATEMENT

Ethical review and approval was not required for the study on human participants in accordance with the local legislation and institutional requirements. Written informed consent to participate in this study was provided by the participants' legal guardian/next of kin.

AUTHOR CONTRIBUTIONS

CB: conceptualization, methodology, investigation, writing, and editing the final manuscript. CC: conceptualization, methodology, formal analysis, and editing the final manuscript. DM, RS, ID, and CP: resources and data curation. CT: supervision and reviewing.

ACKNOWLEDGMENTS

The content of this manuscript has been presented in part at the 2019 European Society of Ophthalmology (SOE) meeting, Nice, France.

REFERENCES

- Sharif R, Bak-Nielsen S, Hjortdal J, Karamichos D. Pathogenesis of keratoconus: the intriguing therapeutic potential of prolactin-inducible protein. *Prog Retin Eye Res.* (2018) 67:150–67. doi: 10.1016/j.preteyeres.2018.05.002
- Rabinowitz YS. Keratoconus. *Surv Ophthalmol.* (1998) 42:297–319. doi: 10.1016/S0039-6257(97)00119-7
- Wollensak G, Spoerl E, Seiler T. Riboflavin/ultraviolet-a-induced collagen crosslinking for the treatment of keratoconus. *Am J Ophthalmol.* (2003) 135:620–7. doi: 10.1016/S0002-9394(02)02220-1
- Mazzotta C, Baiocchi S, Bagaglia SA, Fruschelli M, Meduri A, Rechichi M. Accelerated 15 mW pulsed-light crosslinking to treat progressive keratoconus: two-year clinical results. *J Cataract Refract Surg.* (2017) 43:1081–8. doi: 10.1016/j.jcrs.2017.05.030
- Wittig-Silva C, Chan E, Islam FMA, Wu T, Whiting M, Snibson GR, et al. Randomized, controlled trial of corneal collagen cross-linking in progressive keratoconus. *Ophthalmology.* (2014) 121:812–21. doi: 10.1016/j.ophtha.2013.10.028
- Raiskup F, Theuring A, Pillunat LE, Spoerl E. Corneal collagen crosslinking with riboflavin and ultraviolet-A light in progressive keratoconus: ten-year results. *J Cataract Refract Surg.* (2015) 41:41–6. doi: 10.1016/j.jcrs.2014.09.033
- O'Brart DPS, Patel P, Lascaratos G, et al. Corneal cross-linking to halt the progression of keratoconus and corneal ectasia: seven-year follow-up. *Am J Ophthalmol.* (2015) 160:1154–63. doi: 10.1016/j.ajo.2015.08.023
- Raiskup-Wolf F, Hoyer A, Spoerl E, Pillunat LE. Collagen crosslinking with riboflavin and ultraviolet-A light in keratoconus: long-term results. *J Cataract Refract Surg.* (2008) 34:796–801. doi: 10.1016/j.jcrs.2007.12.039
- Soeters N, Wisse RPL, Godefrooij DA, Imhof SM, Tahzib NG. Transepithelial versus epithelium-off corneal cross-linking for the treatment of progressive keratoconus: a randomized controlled trial. *Am J Ophthalmol.* (2015) 159:821–828.e3. doi: 10.1016/j.ajo.2015.02.005
- Lang PZ, HafeziNL, Khandelwal SS, Torres-Netto EA, Hafezi F, Randleman JB. Comparative functional outcomes after corneal crosslinking using standard, accelerated, and accelerated with higher total fluence protocols. *Cornea.* (2019) 38:433–41. doi: 10.1097/ICO.0000000000001878
- Krysiak K, Dobrowolski D, Wylegała EA, Lyssek-Boroń A, Amniotic membrane as a main component in treatment supporting healing and patch grafts in corneal melting and perforations. *J Ophthalmol.* (2020) 4238919:1–7. doi: 10.1155/2020/4238919
- Leccisotti A, Mitomycin C. in photorefractive keratectomy: effect on epithelialization and predictability. *Cornea.* (2008) 27:288–91. doi: 10.1097/ICO.0b013e31815c5a51
- Gipson IK. Age-related changes and diseases of the ocular surface and cornea. *Investigat Ophthalmol Visual Sci.* (2013) 54:ORSF48. doi: 10.1167/iops.13-12840
- Faragher RG, Mulholland B, Tuft SJ, Sandeman S, Khaw PT. Aging and the cornea. *Br J Ophthalmol.* (1997) 81:814–7. doi: 10.1136/bjo.81.10.814
- Rao SN, Chuck RS, Chang AH, LaBree L, McDonnell PJ. Effect of age on the refractive outcome of myopic photorefractive keratectomy. *J Cataract Refract Surg.* (2000) 26:543–6. doi: 10.1016/S0886-3350(99)00465-4
- Niederer RL, Perumal D, Sherwin T, McGhee CNJ. Age-related differences in the normal human cornea: a laser scanning in vivo confocal microscopy study. *Br J Ophthalmol.* (2007) 91:1165–9. doi: 10.1136/bjo.2006.112656
- Torricelli AAM, Singh V, Santhiago MR, Wilson SE. The Corneal epithelial basement membrane: structure, function, and disease. *Investigat Ophthalmol Visual Sci.* (2013) 54:6390. doi: 10.1167/iops.13-12547
- Mantelli F, Mauris J, Argüeso P. The ocular surface epithelial barrier and other mechanisms of mucosal protection: from allergy to infectious diseases. *Curr Opin Allergy Clin Immunol.* (2013) 13:563–8. doi: 10.1097/ACI.0b013e3283645899
- Alvarado J, Murphy C, Juster R. Age-related changes in the basement membrane of the human corneal epithelium. *Invest Ophthalmol Vis Sci.* (1983) 24:1015–28.
- Knop E, Knop N, Millar T, Obata H, Sullivan DA. The International workshop on meibomian gland dysfunction: report of the subcommittee on anatomy, physiology, and pathophysiology of the meibomian gland. *Investigat Ophthalmol Visual Sci.* (2011) 52:1938. doi: 10.1167/iops.10-6997c
- Roszkowska AM, Colosi P, Ferreri FMB, Galasso S. Age-related modifications of corneal sensitivity. *Ophthalmologica.* (2004) 218:350–5. doi: 10.1159/000079478
- Ozgunhan EB, Celik U, Bozkurt E, Demirok A. Evaluation of subbasal nerve morphology and corneal sensation after accelerated corneal collagen cross-linking treatment on keratoconus. *Curr Eye Res.* (2015) 40:484–9. doi: 10.3109/02713683.2014.932387
- Berlau J, Becker H-H, Stave J, Oriwol C, Guthoff RF. Depth and age-dependent distribution of keratocytes in healthy human corneas: a study using scanning-slit confocal microscopy in vivo. *J Cataract Refract Surg.* (2002) 28:611–6. doi: 10.1016/S0886-3350(01)01227-5
- Shirai K, Okada Y, Cheon D-J, et al. Effects of the loss of conjunctival Muc16 on corneal epithelium and stroma in mice. *Investigat Ophthalmol Vis Sci.* (2014) 55:3626. doi: 10.1167/iops.13-12955
- Pastar I, Stojadinovic O, Yin NC, et al. Epithelialization in wound healing: a comprehensive review. *Adv Wound Care.* (2014) 3:445–64. doi: 10.1089/wound.2013.0473
- Vinciguerra P. Intraoperative and postoperative effects of corneal collagen cross-linking on progressive keratoconus. *Archiv Ophthalmol.* (2009) 127:1258. doi: 10.1001/archophthalmol.2009.205

Conflict of Interest: The authors declare that the research was conducted in the absence of any commercial or financial relationships that could be construed as a potential conflict of interest.

Publisher's Note: All claims expressed in this article are solely those of the authors and do not necessarily represent those of their affiliated organizations, or those of the publisher, the editors and the reviewers. Any product that may be evaluated in this article, or claim that may be made by its manufacturer, is not guaranteed or endorsed by the publisher.

Copyright © 2021 Bonzano, Cutolo, Musetti, Di Mola, Pizzorno, Scotto and Traverso. This is an open-access article distributed under the terms of the Creative Commons Attribution License (CC BY). The use, distribution or reproduction in other forums is permitted, provided the original author(s) and the copyright owner(s) are credited and that the original publication in this journal is cited, in accordance with accepted academic practice. No use, distribution or reproduction is permitted which does not comply with these terms.



Associations Between Keratoconus and the Level of Sex Hormones: A Cross-Sectional Study

Xiaorui Zhao^{1,2}, Yifei Yuan^{1,2}, Tong Sun^{1,2}, Yu Zhang^{1,2} and Yueguo Chen^{1,2*}

¹ Department of Ophthalmology, Peking University Third Hospital, Beijing, China, ² Beijing Key Laboratory of Restoration of Damaged Ocular Nerve, Peking University Third Hospital, Beijing, China

OPEN ACCESS

Edited by:

Eray Atalay,
Eskişehir Osmangazi University, Turkey

Reviewed by:

Ahmed Abdelkareem Elmassry,
Alexandria University, Egypt
Stefan Lang,
University Hospital Freiburg, Germany

*Correspondence:

Yueguo Chen
chenyueguo@263.net

Specialty section:

This article was submitted to
Ophthalmology,
a section of the journal
Frontiers in Medicine

Received: 03 December 2021

Accepted: 01 February 2022

Published: 24 February 2022

Citation:

Zhao X, Yuan Y, Sun T, Zhang Y and
Chen Y (2022) Associations Between
Keratoconus and the Level of Sex
Hormones: A Cross-Sectional Study.
Front. Med. 9:828233.
doi: 10.3389/fmed.2022.828233

Purpose: To analyze the level of sex hormone in relation to keratoconus (KC).

Methods: Sixty-two eyes of 62 patients (12 females, 50 males) classified as KC and 120 eyes of 120 patients (21 females, 99 males) with mild to moderate myopia and astigmatism were analyzed. Plasma samples were collected and analyzed using a chemiluminescence immunoassay to determine the concentrations of estriol (E_3), estradiol (E_2), progesterone (P), and testosterone (T). Corneal morphological parameters, such as the central corneal thickness (CCT), thinnest corneal thickness (TCT), and maximum simulated keratometry (K_{max}), were measured using Pentacam and Sirius.

Results: The mean age was 23.73 ± 5.16 years for patients with KC and 23.68 ± 6.10 years for patients treated with laser vision correction (LVC). Among the patients with KC, 12 were female (19.35%) and 50 were male (80.65%). The majority of patients with KC were between 20 and 30 years old. In female patients, the concentration of T in the KC group was significantly lower than that in the LVC group (0.86 ± 0.33 vs. 1.18 ± 0.58 nmol/L; $P = 0.044$). There were positive correlations between T, CCT ($r = 0.395$, $P = 0.023$) and TCT ($r = 0.378$, $P = 0.030$) in female patients. In male patients, E_2 was higher in the KC group than the LVC group (143.75 ± 34.82 vs. 124.80 ± 43.56 pmol/L; $P = 0.013$), while T was significantly lower (11.59 ± 2.85 vs. 13.58 ± 4.77 nmol/L; $P = 0.026$). A positive correlation was found between E_2 and K_{max} ($r = 0.222$, $P = 0.007$) in male patients.

Conclusions: Conclusively, our results showed that T level was reduced in both female and male KC plasma, while E_2 was increased in male KC plasma. Different levels of sex hormones are correlated with KC, which, may provide the basis of a new technique for screening and diagnosing KC with or without the assistance of current imaging techniques. Moreover, the correlations between sex hormone alterations and KC provide compelling insight into KC etiopathogenesis.

Keywords: keratoconus, sex hormone, etiopathogenesis, proinflammatory cytokine, matrix metalloproteinases

INTRODUCTION

Keratoconus (KC) is a bilateral progressive ectatic disease with central and/or paracentral thinning and steepening of the cornea. It was first described in 1936 by Dr. Benedict Duddell. Since then, extensive research has been conducted to understand the pathophysiology of the disease (1, 2). The incidence rate is 0.05–0.23% worldwide; and the ratio of male to female incidence is 0.9–2.5:1 (3). It appears during puberty and progresses until the third or fourth decade of life (4, 5). Males develop the disease earlier and progress more rapidly than females (5).

Patients with KC always develop irregular astigmatism and myopia, leading to mild-to-marked impairment in visual acuity and quality of vision. Central or paracentral stromal thinning, rupture in the Bowman's layer, ring-shaped ferritin deposition at the basal layer of the epithelium (Fleischer's ring), fine vertical lines in the deep stroma of Descemet's membrane (Vogt's striae), and Munson's sign are typical clinical manifestations of KC (6, 7). Numerous hypotheses have been proposed, including genes, sex, eye rubbing, contact lens use, age, sun exposure, inflammation, and even pollution (2, 8–11). Recently, scientists have found that hormones, including sex hormones, prolactin, gonadotropins, thyroid hormones, glucocorticoids, and relaxin may be involved in the development of KC (8, 12–20). However, the exact mechanisms remain unclear. Many studies have shown that sex hormones cause and promote the progression of KC by influencing corneal matrix metalloproteinases (MMP) (21–23).

The present study aimed to investigate the association between sex hormones and KC, and analyze their possible mechanisms.

MATERIALS AND METHODS

This study was conducted at the Peking University Third Hospital Eye Center, Beijing, China. This study was approved by the Medical Science Research Ethics Committee of Peking University Third Hospital, and followed the tenets of the Declaration of Helsinki. Informed written consent was obtained from all subjects.

Patient Selection

All subjects were enrolled continuously in the Peking University Third Hospital Eye Center in 2020. Patients were divided into two groups: (1) 62 eyes of 62 patients (12 females, 50 males) classified as KC and scheduled to be treated with corneal collagen cross-linking (CXL). (2) Hundred and twenty eyes of 120 patients (21 females, 99 males) with mild to moderate myopia and astigmatism were scheduled to be treated with laser vision correction (LVC). In the KC group, only the operative eye data were included. In the control group, one eye from each patient was randomly selected for comparison. All patients in the control group were examined at least twice before surgery to ensure that the patients' myopia or astigmatism was stable and conformed to the surgical indications. The diagnosis of KC was based on the presence of clinical signs (such as cornea ectasia, Fleischer's ring, Vogt's striae), central or paracentral steepening in the corneal curvature, cornea thickness, and other necessary parameters measured using topographic and tomographic maps.

All diagnoses were confirmed by an experienced specialist in CXL and LVC surgery. Patients with a trend of progression in the past 12 months and that met one of the following conditions were treated with CXL: the maximum K reading increased by >1 D, mean corneal refractive power increased by >1 D, astigmatism increased by >1 D, and the spherical equivalent of manifest refraction increased by >1 D with best spectacle-corrected distance visual acuity having lost more than one line. Exclusion criteria included hormone supplementation therapy, previous ocular surgery, trauma, and systemic diseases such as immunodeficiency and desmosis.

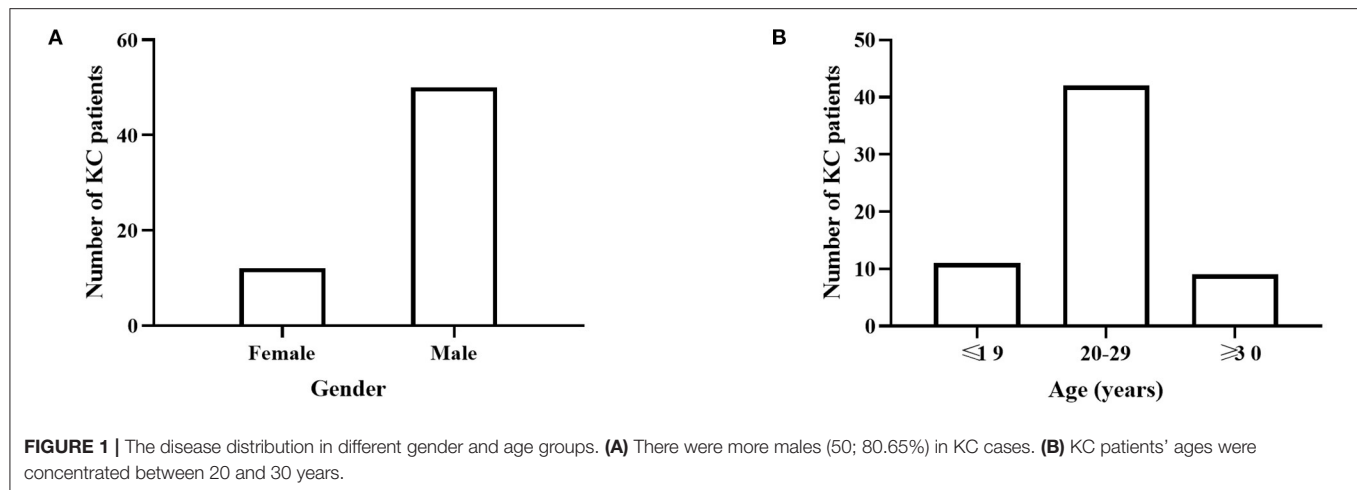
Examination Protocol

All subjects underwent a complete standard ophthalmological examination. The refraction errors were evaluated with a KR-8100 auto kerato-refractometer (Topcon, Tokyo, Japan), visual acuity was measured with the Standard Logarithmic Visual Acuity Chart. The anterior segment and fundus were examined with a slit-lamp microscope (YZ5F, Suzhou, China), intraocular pressure was measured with non-contact tonometers (Canon, Tokyo, Japan), and corneal parameters such as the central corneal thickness (CCT), thinnest corneal thickness (TCT), and maximum simulated keratometry (K_{max}) were measured using a Pentacam (Oculus, Wetzlar, Germany) and Sirius (Costruzione Strumenti Oftalmici, Florence, Italy).

Blood samples were obtained at 10:00–13:00 from all subjects. For males, 2–3 ml blood samples were collected from the outpatient venous blood collection area 3 days before surgery, and were sent to the Laboratory of Endocrinology, Reproductive Center, Peking University Third Hospital to test the levels of sex hormones, including estriol (E_3), estradiol (E_2), progesterone (P), and testosterone (T) using chemiluminescence immunoassay by Immulite 2000 (Siemens, Flanders, USA). In consideration of the effect of the menstrual cycle on female sex hormones, blood samples were collected from females during their secretory phase. Once received, the levels of the four hormones are processed within approximately 24 h. For males, normal E_2 ranges were 0.00–143.00 pmol/L and normal P ranges were 0.86–2.90 nmol/L. Male androgen had no normal ranges. For females, normal E_2 ranges were 111.00–1007.00 pmol/L, normal P ranges were 3.00–68.00 nmol/L, and normal T ranges were 0.00–2.53 nmol/L.

Data Analysis

Statistical analyses were performed using SPSS version 26 (SPSS, Inc., Chicago, IL, USA). The normality distribution was checked for all parameters using the Kolmogorov-Smirnov test. Age, sex hormone levels, and corneal parameters were analyzed descriptively, and the results were expressed as the mean and standard deviation for the two study groups. Because of the known sex bias for hormones, we thought analysis by sex was essential. The Mann-Whitney U test was used to evaluate differences in parameters between female and male patients. Spearman correlation analysis was used to correlate sex hormone levels, CCT, TCT, K_{max} , and age. Statistical significance was set at $P < 0.05$.

**TABLE 1 |** Clinical and laboratory parameters.

		KC	LVC	P value
All	Gender (female/male)	62 (12/50)	120 (21/99)	0.740
	Age (years)	23.73 ± 5.16	23.68 ± 6.10	0.350
Female	Patients (N)	12	21	
	Age (years)	24.08 ± 4.42	25.05 ± 6.12	0.548
	E ₃ (nmol/L)	0.24 ± 0.00	0.25 ± 0.04	0.450
	E ₂ (pmol/L)	528.00 ± 372.86	400.27 ± 340.71	0.178
	T (nmol/L)	0.86 ± 0.33	1.18 ± 0.58	0.044
	P (nmol/L)	9.16 ± 10.13	10.92 ± 12.37	0.567
	CCT (μm)	472.67 ± 33.25	553.19 ± 39.31	<0.001
	TCT (μm)	455.17 ± 33.03	547.62 ± 39.24	<0.001
	K _{max} (D)	49.25 ± 3.23	44.46 ± 1.93	<0.001
Male	Patients (N)	50	99	
	Age (years)	23.64 ± 5.36	23.38 ± 6.09	0.274
	E ₃ (nmol/L)	0.24 ± 0.00	0.25 ± 0.02	0.186
	E ₂ (pmol/L)	143.75 ± 34.82	124.80 ± 43.56	0.013
	T (nmol/L)	11.59 ± 2.85	13.58 ± 4.77	0.026
	P (nmol/L)	1.44 ± 0.46	1.50 ± 0.44	0.445
	CCT (μm)	470.82 ± 35.82	553.13 ± 30.68	<0.001
	TCT (μm)	445.14 ± 39.52	548.85 ± 30.68	<0.001
	K _{max} (D)	61.89 ± 10.06	44.13 ± 1.62	<0.001

LVC, laser vision correction; KC, keratoconus; E₃, estriol; E₂, estradiol; P, progesterone; T, testosterone; CCT, central corneal thickness; TCT, thinnest corneal thickness; K_{max}, maximum simulated keratometry. All data are expressed as mean ± SD.

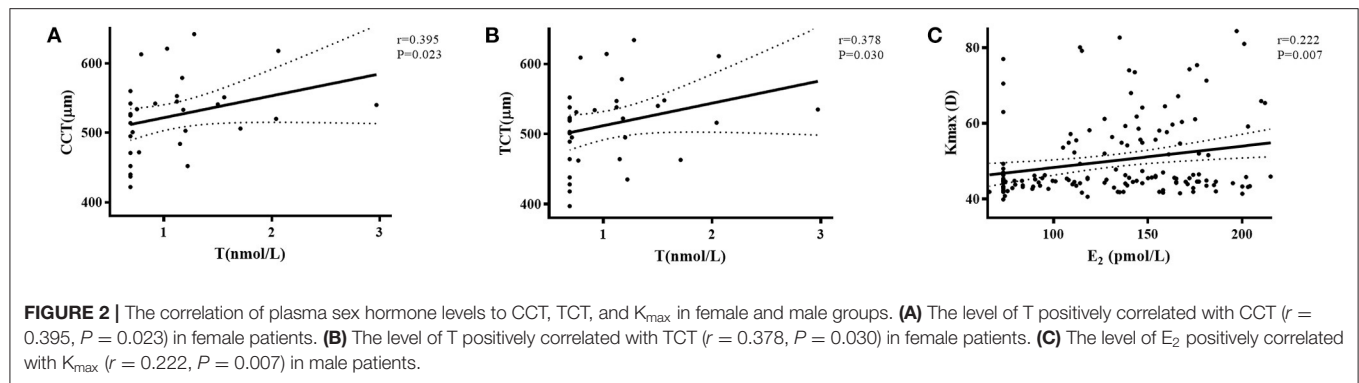
RESULTS

Sixty-two patients with KC (12 females, 50 males) and 120 LVC patients (21 females, 99 males) were included in this study. The mean age was 23.73 ± 5.16 years for KC patients and 23.68 ± 6.10 years for LVC patients, with no significant difference between groups. Among the KC cases, there were more males (50; 80.65%), and the KC patients' ages were concentrated between 20 and 30 years (**Figure 1; Table 1**).

Table 1 shows the demographic, morphological, and laboratory parameters of the female KC and LVC groups. From the data above, we could find that the concentration of T in

the KC group was significantly lower than the LVC group (0.86 ± 0.33 vs. 1.18 ± 0.58 nmol/L; $P = 0.044$). We performed Pentacam and Sirius examinations, and CCT, TCT, and K_{max} were recorded for each patient. The mean CCT, TCT, and K_{max} values differed significantly between the groups ($P < 0.001$). In the male KC group, E₂ was higher than in the LVC group (143.75 ± 34.82 vs. 124.80 ± 43.56 pmol/L; $P = 0.013$), while T was significantly lower (11.59 ± 2.85 vs. 13.58 ± 4.77 nmol/L; $P = 0.026$). However, there was no difference between the KC and LVC groups in terms of E₃ and P ($P = 0.186$, $P = 0.445$).

Figure 2 shows that the level of T positively correlated with CCT ($r = 0.395$, $P = 0.023$) and TCT ($r = 0.378$, $P = 0.030$) in



female patients. A positive correlation was found between E_2 and K_{\max} ($r = 0.222$, $P = 0.007$) in male patients. E_3 and P were not correlated with any of the KC parameters.

DISCUSSION

With the progression of science and technology, the early diagnosis and treatment of KC are more and increasingly accurate and cutting-edge, but the etiopathogenesis of this important kind of corneal ectasia disease has not been completely investigated. Exploring the etiopathogenesis of KCs is difficult, but essential. Hypotheses have proposed that genetic, immunological, metabolic, and endocrinological factors may be involved in the progression of KC. Furthermore, many reports have shown a significant relationship between sex hormones and KC. Some case reports have shown increased tendency for corneal ectasia in pregnancy and hormone replacement therapies and reveal corneal graft rejection in pregnancy. Yuksel et al. found that females treated with *in-vitro* fertilization always have progression in KC (24). In Emilio's report, a 49-year-old woman with previously stable KC had got late-onset KC progression when starting treatment for endometriosis using an estrogenic activity regulator with tibolone (12). Spoerl et al. exposed porcine corneas to 10 $\mu\text{mol/L}$ of β -estradiol for 7 days, and found that the corneal thickness increased, but the biomechanics decreased (25). Indeed, studies have reported that sex hormones and the expression of matrix metalloproteinase-9 (MMP-9) and MMP-2 in the corneal epithelium, stroma, and tear fluid of patients with KC may be associated with the severity of KC. Taken together, the fluctuating levels of MMP-2, MMP-9 in corneas with KC and tear fluid may be regulated by sex hormones, and may additively contribute to the progression of corneal ectasia.

Plasma concentration screening, clinical observations, and clinical examinations were used to determine the correlation between KC and sex hormones. It was thought that increased levels of sex hormones may be associated with the etiopathogenesis and progression of KC due to some mechanism of action. First, c-fos, an estrogen-target gene, is involved in cell proliferation, differentiation, apoptosis, oncogenesis, and invasion. Pan found that both c-fos and MMP-9 protein levels were higher in females with endometriosis than in those without

endometriosis. A positive correlation between c-fos and MMP-9 protein levels was found, which suggests that c-fos may be regulated by sex hormones and promote the gene expression of MMP-9 in the development of endometriosis (26). Therefore, estrogen may induce the expression of MMP-9 with KC in a similar way. Second, inflammatory cytokines have been reported as key factors in the pathogenesis of KC, which are stimulated by sex hormone receptors and then stimulate MMP genes in the human cornea (27). Sex hormone receptor mRNA exists in various ocular tissues, including the cornea. Ayan et al. found that the expression of progesterone and androgen receptors in the corneal epithelium was higher in patients with KC by using quantitative polymerase chain reaction (qPCR) (28). Suzuki et al. studied the expression of proinflammatory cytokines, estrogen, and MMP genes in the human cornea, and found that 17 β -estradiol could stimulate the expression of various proinflammatory cytokines, such as IL-6, IL-1 β , IL-8, and GM-CSF, and stimulate MMP genes in immortalized human corneal epithelial cells (29, 30). T level regulates some systemic factors, such as IL-16 and stem cell factors which may affect the corneal microenvironment (31). There is a direct link between enhanced proinflammatory cytokines and thinner corneas in patients with KC, and the phenomenon of increased curvature and enhanced inflammatory factors shows that inflammatory factors may contribute to disease severity. Activated MMP-9 and -2 can degrade the basement membrane, lead to cytokine release, and regulate proinflammatory cytokines.

Although the plasma levels of sex hormones were approximately in the normal range in patients with KC and LVC, the plasma levels of E_2 and T showed a statistically difference, suggesting that even in the normal range, the sex hormone might have certain influences on the cornea.

This study has several limitations. The present study had a cross-sectional design, and the findings must be confirmed via longitudinal studies that require larger patient populations. Sex hormones were not measured in the tear fluid. In addition, there are changes in many other hormones, such as growth hormone, around the age of 25. Thus, further research is required that examines their role in KC.

In conclusion, although the specific mechanism between sex hormones and KC appears not to have been investigated, it is proposed that sex hormones may play an essential role in the

development of KC. The results of our study might be helpful as a basis for further studies to elucidate the etiopathogenesis of KC and explore the role of sex hormones in the treatment of KC in the future.

DATA AVAILABILITY STATEMENT

The raw data supporting the conclusions of this article will be made available by the authors, without undue reservation.

ETHICS STATEMENT

The studies involving human participants were reviewed and approved by The Medical Science Research Ethics Committee of Peking University Third Hospital. Written informed consent to participate in this study was provided by the participants or their legal guardian/next of kin.

REFERENCES

- Grzybowski A, McGhee CN. The early history of keratoconus prior to Nottingham's landmark 1854 treatise on conical cornea: a review. *Clin Exp Optom.* (2013) 96:140–5. doi: 10.1111/cxo.12035
- Ferrari G, Rama P. The keratoconus enigma: a review with emphasis on pathogenesis. *Ocul Surf.* (2020) 18:363–73. doi: 10.1016/j.jtos.2020.03.006
- Imbornoni LM, McGhee CNJ, Belin MW. Evolution of keratoconus: from diagnosis to therapeutics. *Klin Monbl Augenheilkd.* (2018) 235:680–8. doi: 10.1055/s-0044-100617
- Godefrooij DA, de Wit GA, Uiterwaal CS, Imhof SM, Wisse RP. Age-specific incidence and prevalence of keratoconus: a nationwide registration study. *Am J Ophthalmol.* (2017) 175:169–72. doi: 10.1016/j.ajo.2016.12.015
- Ferdi AC, Nguyen V, Gore DM, Allan BD, Rozema JJ, Watson SL. Keratoconus natural progression: a systematic review and meta-analysis of 11 529 eyes. *Ophthalmology.* (2019) 126:935–45. doi: 10.1016/j.ophtha.2019.02.029
- Loukovitis E, Kozeis N, Gatzoufas Z, Kozei A, Tsotridou E, Stoila M, et al. The proteins of keratoconus: a literature review exploring their contribution to the pathophysiology of the disease. *Adv Ther.* (2019) 36:2205–22. doi: 10.1007/s12325-019-01026-0
- Romero-Jiménez M, Santodomingo-Rubido J, Wolffsohn JS. Keratoconus: a review. *Contact Lens Anter Eye.* (2010) 33:157–66. doi: 10.1016/j.clae.2010.04.006
- Appelbaum A. KERATOCONUS. *Arch Ophthalmol.* (1936) 15:900–21. doi: 10.1001/archoph.1936.00840170112011
- Lim L, Lim EWL. Current perspectives in the management of keratoconus with contact lenses. *Eye (Lond).* (2020) 34:2175–96. doi: 10.1038/s41433-020-1065-z
- Valgaeren H, Koppen C, Van Camp G. A new perspective on the genetics of keratoconus: why have we not been more successful? *Ophthalmic Genet.* (2018) 39:158–74. doi: 10.1080/13816810.2017.1393831
- Crawford AZ, Zhang J, Gokul A, McGhee CNJ, Ormonde SE. The enigma of environmental factors in keratoconus. *Asia Pac J Ophthalmol (Phila).* (2020) 9:549–56. doi: 10.1097/APO.0000000000000334
- Torres-Netto EA, Randleman JB, Hafezi NL, Hafezi F. Late-onset progression of keratoconus after therapy with selective tissue estrogenic activity regulator. *J Cataract Refract Surg.* (2019) 45:101–4. doi: 10.1016/j.jcrs.2018.08.036
- Coco G, Kheirikhah A, Foulsham W, Dana R, Ciolino JB. Keratoconus progression associated with hormone replacement therapy. *Am J Ophthalmol Case Rep.* (2019) 15:100519. doi: 10.1016/j.ajoc.2019.100519
- Bilgihan K, Hondur A, Sul S, Ozturk S. Pregnancy-induced progression of keratoconus. *Cornea.* (2011) 30:991–4. doi: 10.1097/ICO.0b013e3182068adc

AUTHOR CONTRIBUTIONS

XZ, YY, and TS were responsible for the initial plan, study design, data collection, data extraction, data interpretation, manuscript drafting, statistical analysis, and conducting the study. YZ and YC were responsible for data collection, extraction, and critical revisions of the manuscript. YC was the guarantor for this article and has full responsibility for this study. All authors contributed to the article and approved the submitted version.

FUNDING

This study was supported by grant of Key Clinical Innovation Program of Peking University Third Hospital, Category A, No. Y65495–05.

ACKNOWLEDGMENTS

We thank all participants of the study at our team.

- Karamichos D, Barrientes B, Nicholas S, Ma S, Van L, Bak-Nielsen S, et al. Gonadotropins in keratoconus: the unexpected suspects. *Cells.* (2019) 8:1494–507. doi: 10.3390/cells8121494
- Anders P, Song X, Gyorgy B, Szentmary N, Seitz B, Gatzoufas Z. Effect of prolactin on normal and keratoconus human corneal stromal fibroblasts *in vitro*. *PLoS ONE.* (2021) 16:e0249344. doi: 10.1371/journal.pone.0249344
- Karamichos D, Escandon P, Vasini B, Nicholas SE, Van L, Dang DH, et al. Anterior pituitary, sex hormones, and keratoconus: beyond traditional targets. *Prog Retin Eye Res.* (2021) 2021:101016. doi: 10.1016/j.preteyeres.2021.101016
- Natarajan R, Ravindran R. Progression of keratoconus resulting from hormone replacement therapy. *J Cataract Refract Surg.* (2019) 45:1055. doi: 10.1016/j.jcrs.2019.04.038
- Sharif R, Bak-Nielsen S, Hjortdal J, Karamichos D. Pathogenesis of keratoconus: the intriguing therapeutic potential of prolactin-inducible protein. *Prog Retin Eye Res.* (2018) 67:150–16. doi: 10.1016/j.preteyeres.2018.05.002
- Lenk J, Spoerl E, Stalder T, Schmiedgen S, Herber R, Pillunat Lutz E, et al. Increased hair cortisol concentrations in patients with progressive keratoconus. *J Refract Surg.* (2017) 33:383–8. doi: 10.3928/1081597X-20170413-01
- Martino Ed, Ali M, Inglehearn CF. Matrix metalloproteinases in keratoconus – too much of a good thing? *Exp Eye Res.* (2019) 182:137–43. doi: 10.1016/j.exer.2019.03.016
- Du G, Liu C, Li X, Chen W, He R, Wang X, et al. Induction of matrix metalloproteinase-1 by tumor necrosis factor- α is mediated by interleukin-6 in cultured fibroblasts of keratoconus. *Exp Biol Med (Maywood).* (2016) 241:2033–41. doi: 10.1177/1535370216650940
- Chen S, Mienaltowski MJ, Birk DE. Regulation of corneal stroma extracellular matrix assembly. *Exp Eye Res.* (2015) 133:69–80. doi: 10.1016/j.exer.2014.08.001
- Yüksel E, Yalinbas D, Aydin B, Bilgihan K. Keratoconus progression induced by *in vitro* fertilization treatment. *J Refract Surg.* (2016) 32:60–3. doi: 10.3928/1081597X-20151207-10
- Kilavuzoglu AEB, Cosar CB, Bildirici I, Cetin O, Ozbasli E. Estrogen- and progesterone-induced variation in corneal parameters according to hormonal status. *Eye Contact Lens.* (2018) 44:S179–S84. doi: 10.1097/ICL.0000000000000376
- Pan H, Sheng JZ, Tang L, Zhu R, Zhou TH, Huang HF. Increased expression of c-fos protein associated with increased matrix metalloproteinase-9 protein expression in the endometrium of endometriotic patients. *Fertil Steril.* (2008) 90:1000–7. doi: 10.1016/j.fertnstert.2007.07.1386

27. Ionescu C, Corbu CG, Tanase C, Jonescu-Cuypers C, Nicula C, Dascalescu D, et al. Inflammatory biomarkers profile as microenvironmental expression in keratoconus. *Dis Markers*. (2016) 2016:1243819. doi: 10.1155/2016/1243819
28. Ayan B, Yuksel N, Carhan A, Gumuskaya Ocal B, Akcay E, Cagil N, et al. Evaluation estrogen, progesterone and androgen receptor expressions in corneal epithelium in keratoconus. *Cont Lens Anter Eye*. (2019) 42:492–6. doi: 10.1016/j.clae.2018.11.015
29. Suzuki T, Sullivan DA. Estrogen stimulation of proinflammatory cytokine and matrix metalloproteinase gene expression in human corneal epithelial cells. *Cornea*. (2005) 24:1004–9. doi: 10.1097 / 01.ico.0000160973.04072.a5
30. Glicéria J, Valbon BF, Santos RT, Ambrósio RA Jr. Pregnancy-induced progression of keratoconus in a 37-year-old patient. *Int J Kerat Ectat Corn Dis*. (2013) 2:84–8. doi: 10.5005/jp-journals-10025-1057
31. McKay TB, Hjortdal J, Sejersen H, Asara JM, Wu J, Karamichos D. Endocrine and metabolic pathways linked to keratoconus: implications for the role of hormones in the stromal microenvironment. *Sci Rep*. (2016) 6:25534. doi: 10.1038/srep25534

Conflict of Interest: The authors declare that the research was conducted in the absence of any commercial or financial relationships that could be construed as a potential conflict of interest.

Publisher's Note: All claims expressed in this article are solely those of the authors and do not necessarily represent those of their affiliated organizations, or those of the publisher, the editors and the reviewers. Any product that may be evaluated in this article, or claim that may be made by its manufacturer, is not guaranteed or endorsed by the publisher.

Copyright © 2022 Zhao, Yuan, Sun, Zhang and Chen. This is an open-access article distributed under the terms of the Creative Commons Attribution License (CC BY). The use, distribution or reproduction in other forums is permitted, provided the original author(s) and the copyright owner(s) are credited and that the original publication in this journal is cited, in accordance with accepted academic practice. No use, distribution or reproduction is permitted which does not comply with these terms.



Comparison of Corneal Collagen Cross-Linking and Voriconazole Treatments in Experimental Fungal Keratitis for *Aspergillus fumigatus*

OPEN ACCESS

Edited by:

Cristina Nicula,
Iuliu Hațieganu University of Medicine
and Pharmacy, Romania

Reviewed by:

Cosimo Mazzotta,
University of Sassari, Italy
Yingxue Zhang,
Wayne State University, United States

*Correspondence:

Tingting Shao
shaotingting@fudan.edu.cn
Yi Shao
freebee99@163.com

[†]These authors have contributed
equally to this work and share first
authorship

[‡]These authors have contributed
equally to this work and share last
authorship

Specialty section:

This article was submitted to
Ophthalmology,
a section of the journal
Frontiers in Medicine

Received: 04 February 2022

Accepted: 07 June 2022

Published: 28 June 2022

Citation:

Zhao Z, Chen X, Shao Y and Shao T
(2022) Comparison of Corneal
Collagen Cross-Linking and
Voriconazole Treatments in
Experimental Fungal Keratitis for
Aspergillus fumigatus.
Front. Med. 9:869429.
doi: 10.3389/fmed.2022.869429

Zhennan Zhao^{1,2,3†}, Xueli Chen^{1,2,3†}, Yi Shao^{4*‡} and Tingting Shao^{1,2,3*‡}

¹ Eye Institute and Department of Ophthalmology, Eye Ear Nose and Throat Hospital of Fudan University, Shanghai, China,

² NHC Key Laboratory of Myopia Fudan University, Laboratory of Myopia, Chinese Academy of Medical Sciences, Shanghai, China, ³ Key Laboratory of Visual Impairment and Restoration of Shanghai, Shanghai, China, ⁴ Department of Ophthalmology, The First Affiliated Hospital of Nanchang University, Nanchang, China

Aims: To compare the antifungal efficacy of corneal cross-linking (CXL) and voriconazole in experimental *Aspergillus* keratitis models.

Methods: Thirty-nine New Zealand rabbits were divided into three groups: a control group, a voriconazole group (M group), and a voriconazole combined with CXL group (CXL-M group). The ulcer area was measured via slit lamp imaging, the corneal and corneal epithelial thickness, and ulcer depth was measured via anterior segment optical coherence tomography (AS-OCT). The existence time of the hyphae was observed via *in vivo* confocal microscopy (IVCM), and the cornea was taken for pathological examination after modeling and at the end of the study to determine the hyphae and corneal repair. The observation times were as follows: at successful modeling and at 1, 4, 7, 14, 21, and 28 days after intervention.

Results: In the CXL-M group, ulcer area and depth decreased continuously from Day 4 to Day 28 after CXL (all $P < 0.05$). In the CXL-M group, ulcer area and depth were smaller than those in the other two groups from Day 4 to Day 21 after CXL (all $P < 0.05$, except ulcer area in the CXL-M vs. M group on Day 21). The duration of hyphae in the CXL-M group was significantly shorter than in the other two groups ($P = 0.025$). On Day 28, in CXL-M group, corneal thickness was thicker than baseline ($P < 0.05$). Meanwhile, in CXL-M group, corneal and corneal epithelial thickness were significantly thinner than in the other two groups ($P < 0.001$). The CXL-M group had no complications, such as corneal perforation, at the end of the study.

Conclusions: Voriconazole combined with CXL is effective in treating *Aspergillus*-infected keratitis. Combined therapy could effectively inhibit *Aspergillus*, accelerate corneal repair, and shorten the course of the disease.

Keywords: corneal cross-linking (CXL), fungal keratitis, *Aspergillus fumigatus*, rabbit, voriconazole

INTRODUCTION

Fungal keratitis is a serious blinding corneal disease that accounts for about 50% of all infectious keratitis and is the leading cause of infectious keratitis in the world (1–3). In addition, the current clinical lack of specific antifungal therapy makes treatment difficult (4, 5), especially in developing countries (6, 7). Corneal collagen cross-linking therapy (CXL) is a photochemotherapy that enhances corneal strength (8, 9). In recent years, researchers have applied it to the treatment of infectious corneal ulcers and achieved promising results (10–15). Marstin et al. found that ultraviolet radiation plus riboflavin can inhibit *Streptococcus pneumoniae*, *Staphylococcus aureus*, *Pseudomonas aeruginosa*, methicillin-resistant *Staphylococcus epistaxis*, and other bacteria *in vitro* (16). Bilgihan et al. had further confirmed that corneal cross-linking has inhibitory effects on common fungi *in vitro*, such as *Fusarium*, *Candida* and *Aspergillus* (17). Our previous results show that CXL combined with voriconazole and natamycin has a better effect on fungal corneal ulcers than drugs alone in patients (18). However, similar to the results of other clinical observation studies (11–13, 19, 20), the therapeutic effect of CXL on a single fungus has not been evaluated.

The common infections of fungal keratitis are *Candida*, *Fusarium*, and *Aspergillus* (21, 22), with the latter two being more common in developing countries (23). Preliminary studies have focused on the effects of CXL on *Fusarium* and *Candida* (10–16), while studies on *Aspergillus*, which has the same high incidence rate (23, 24), are rare.

Therefore, this study constructed an animal model of *Aspergillus* infection to demonstrate whether CXL combined with voriconazole is better than voriconazole alone in the treatment of fungal keratitis caused by *Aspergillus* infection based on ulcer area, ulcer depth, hyphae number change, and pathological results.

MATERIALS AND METHODS

Aspergillus fumigatus

Aspergillus fumigatus was provided by the Department of Infectious Diseases, Huashan Hospital, Affiliated with Fudan University; transplanted on Potato dextrose agar (PDA) medium; and incubated in a fungal incubator at 25°C for 5 days. After amplification, it was diluted with a small amount of saline to prepare a suspension, adjusting the concentration to that required (10^6 CFU/mL) with a turbidimetric meter.

Laboratory Animal

Thirty-nine male New Zealand white rabbits weighing 2.5–3.0 Kg that were healthy and SPF (Special pathogen free, SPF) were selected. These rabbits were provided by the Department of Animal Medicine, School of Medicine, Fudan University (Shanghai, China). All experimental methods involved in this research follow the Declaration of Helsinki, and the animal experiments were in accordance with the Association of Vision and Ophthalmology (ARVO) regulations on the use of experimental animals in ophthalmic research and approved

by the Animal Ethics Committee of Fudan University School of Medicine (Shanghai, China).

Rabbit Corneal *Aspergillus fumigatus* Infection Model

All rabbits were given an intramuscular injection of 35 mg/kg of intramuscular ketamine hydrochloride and 5 mg/kg of xylazine for general anesthesia, and oxybucaine hydrochloride eye drops were used for local anesthesia (Santen Pharmaceutical Co., Ltd.). Then, 50 μ L of 10^6 CFU/mL *Aspergillus fumigatus* suspension were drawn with a microsyringe to inject 1/3–2/3 of the full corneal thickness of the corneal stroma. Seventy-two hours after injection, typical ulcer formation and *in vivo* confocal microscopy (IVCM; HRT3-RCM, Heidelberg Engineering, GmbH, Heidelberg, Germany) showed hyphae to be determined as *Aspergillus fumigatus* infection. This was recorded as Day 0, and experimental observations began.

Grouping and Follow-Up

The rabbits were randomly divided into three groups: a control group (C; no antifungal treatment), a medication group (M; 1% voriconazole (Vfend IV, Pfizer Pharmaceuticals, New York, USA), 3 h/time, 4 times/day), and a medication combined with cross-linking group (CXL-M; cross-linking, followed by 1% voriconazole, 3 h/time, 4 times/day). During the study, data were collected on Days 0, 1, 4, 7, 14, 21, and 28; in addition, before modeling, all rabbits underwent anterior segment optical coherence tomography (AS-OCT; RTVue Version 6.9 Optovue Inc., Fremont, CA, USA) scans to record the corneal and corneal epithelial thickness. After successful modeling, one rabbit was executed in each group, and the remainder of the rabbits in each group were executed at the end of the study. The corneal tissue of the eye was taken for pathological analysis.

Corneal CXL Procedure

In the CXL group, on Day 0, the corneal epithelium and necrotic tissue in the central area (diameter 9 mm, including the ulcer area) were removed with a round blunt scalpel, and 0.1% riboflavin drops (Medio-Cross riboflavin/dextran solution) were applied to the eyes for 3 min/time for 30 min. Phoenix UV-A system (Peschke Meditrade GmbH, Huenenberg, Switzerland) was applied to CXL. The ultraviolet light irradiation parameters were set to 3 mW/cm², and the cross-linking time was 30 min (total UVA energy 5.4 J/cm²). The positioning cross was irradiated in the center of the ulcer, the diameter of the spot was adjusted to 11 mm, and 0.1% Riboflavin was added every 5 min. After the cross-linking, clindamycin was used to prevent bacterial infections.

Ophthalmologic Examinations

A uniform magnification and scale plate was applied for slit lamp imaging, and ImageJ software was used to analyze the corneal ulcer area. The corneal cross-section images were obtained by AS-OCT. Cross-sectional images of the cornea at six angles, 0–180°, 30–210°, 60–240°, 90–270°, 120–300°, and 150–330°, were captured for each eye. The acquired data were processed by AS-OCT software to measure the following parameters:

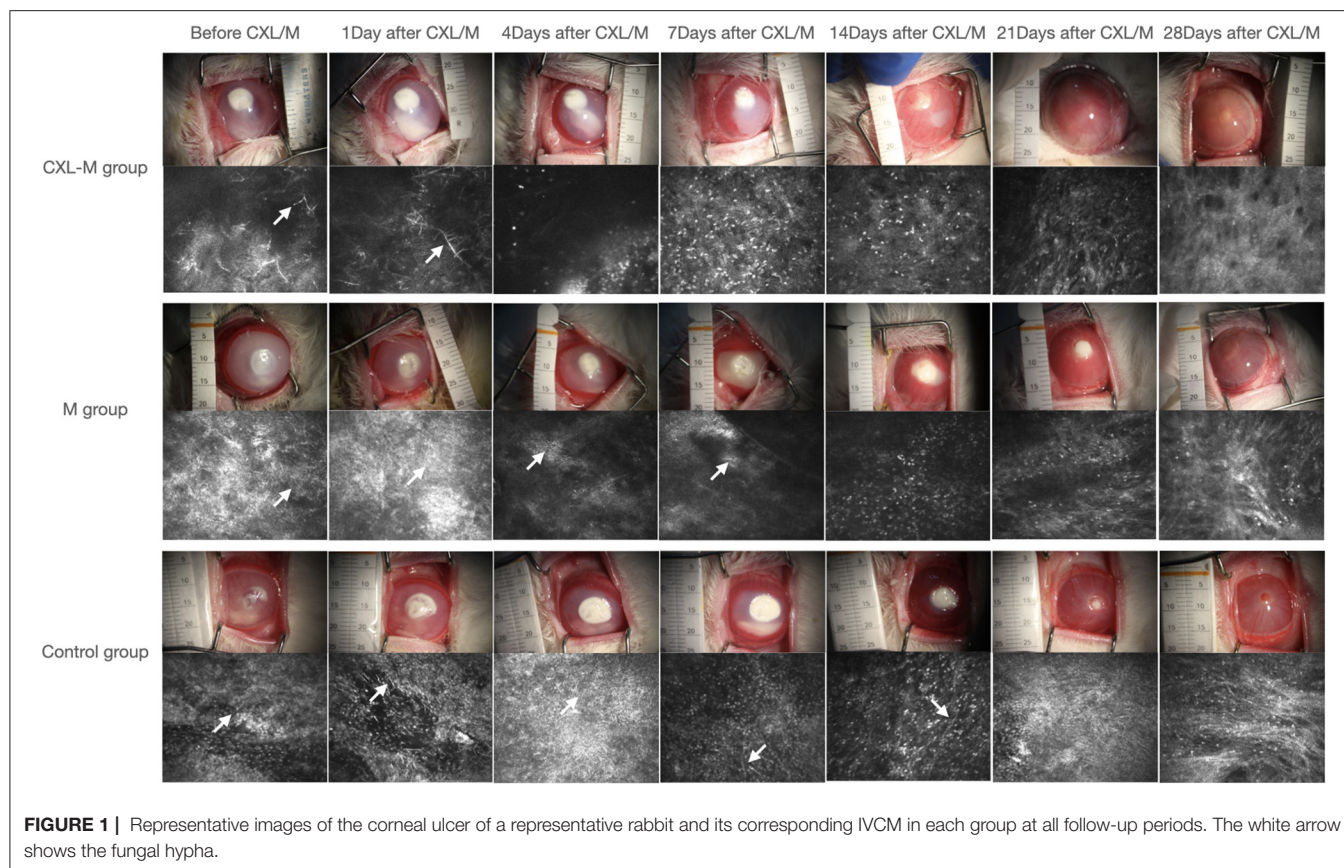


FIGURE 1 | Representative images of the corneal ulcer of a representative rabbit and its corresponding IVCM in each group at all follow-up periods. The white arrow shows the fungal hyphae.

maximum ulcer depth and corneal and epithelial thickness after ulcer healing. *In vivo* confocal microscopy was used to observe the hyphae and spores of *Aspergillus fumigatus* and ulcer development in each group of corneal ulcer areas and their surroundings.

Hematoxylin-Eosin (HE) Staining

After successful modeling and at the end of the study, corneal materials were taken, and the corneal tissue was fixed with 4% neutral formaldehyde solution, dehydrated, paraffin-embedded, and continuously sliced. The slice thickness was 3 to 4 μm . Bake slices at 60°C for 1 h, HE staining, xylene transparent, neutral gum sealing. The imageJ software was used to analyze the inflammatory cell density.

Statistical Analysis

The Statistical Package for the Social Sciences Version 23.0 was used to analyze the data. The comparison of ulcer area and depth, corneal and corneal epithelium thickness, and inflammatory cell density between groups was performed using a multivariate analysis of a one-way analysis of variance (ANOVA), which was tested for least significant difference (LSD) if the variance was homogeneous, and Dunnett's T3 test if the variance was uneven. The area and depth of the ulcers in the groups were compared using a repeated measures ANOVA, followed by Bonferroni analysis. The comparison of corneal and corneal epithelium thickness at baseline and after 28 days of treatment in each group

was performed using *t*-test. Descriptive statistical values are expressed as means \pm standard deviations ($\pm\text{SD}$), with $p < 0.05$ representing a significant difference.

RESULTS

Seventy-two hours after corneal stroma injection, corneal epithelium defects and typical ulcer formation were seen in all three groups (Figure 1), and hyphae were seen upon IVCM (Figure 1). One corneal section was taken from each group for HE staining. Obvious hyphae can be seen (Figure 2), and was determined that the modeling of rabbit *Aspergillus fumigatus* keratitis was successful. Ultimately, twelve rabbits (twelve eyes) in each group were enrolled in the analysis. Corneal ulcer-representative images observed via slit-lamp in each group are shown in Figure 1.

Figure 3 shows that the ulcer area in the control group was larger than that before intervention on Days 1–14 (all $p < 0.05$), and the ulcer area reached its peak on the seventh day after intervention ($73.20 \pm 8.21 \text{ mm}^2$). Twenty-one days after the intervention, the ulcer area was smaller than that before intervention, but this difference was not statistically significant ($P = 0.5671$). At the end of the study, the ulcer area was $10.20 \pm 3.41 \text{ mm}^2$, which was significantly reduced as compared with that before the intervention ($P = 0.0005$). In the M group, the ulcer area was larger than that before the medication on the

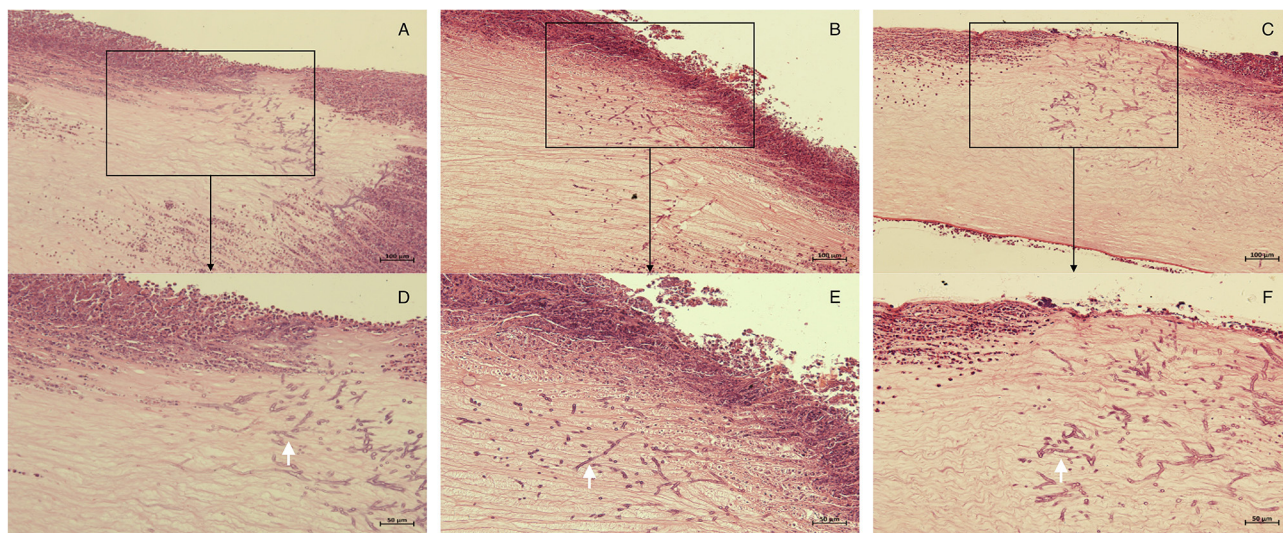


FIGURE 2 | Histopathology of corneas in each group 72 h after corneal stroma injection. The corneal tissue of rabbit in each group was subject to HE staining. (A,D), control group; (B,E), M group; (C,F), CXL-M group. (D–F) (X40) are the magnification of the content of the boxes in (A–C) (X20), respectively; and the white arrow refers to the fungal hyphae.

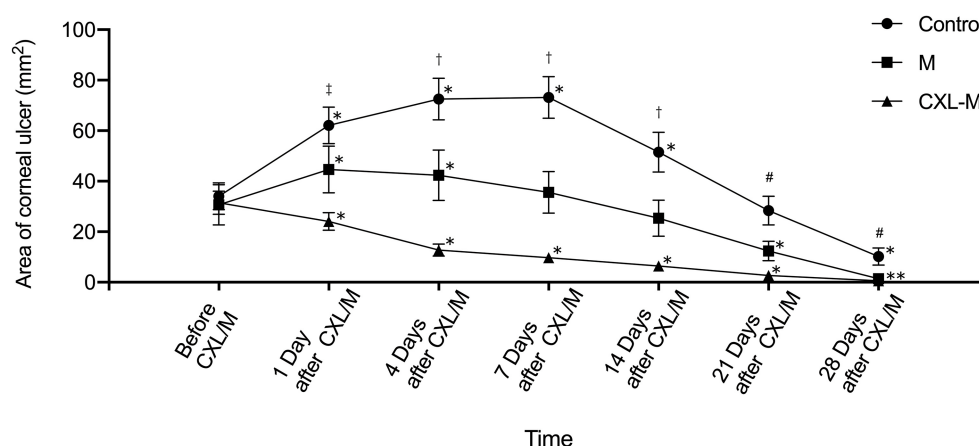


FIGURE 3 | The area of corneal ulcer in three groups. *The corneal ulcer area was significantly different at different follow-up time point in each group compared with that before treatment ($P < 0.05$ for all). †There were significant differences in the areas of corneal ulcer between each group at one follow-up time point ($P < 0.05$ for all). #There were significant differences in the areas of corneal ulcer between control group and other two groups ($P < 0.05$). ‡There was significant difference in the area of corneal ulcer between control group and CXL-M group ($P < 0.05$).

first and fourth days after the medication was applied, and the difference was statistically significant ($P = 0.0146$, $P = 0.0378$). On the 7th day after the medication was provided, the ulcer area was still larger than that before the medication, but the difference was not statistically significant ($P = 0.2311$). On the 14th day after the medication was provided, the ulcer area was smaller than that before the medication was given, but the difference was not statistically significant ($P = 0.3152$); on the 21st and 28th days after the medication provided, the ulcer area was significantly smaller than before the medication ($P = 0.0334$, $P = 0.0182$). In the CXL-M group, ulcer area decreased on Day 1 after CXL, but the difference was not statistically significant (P -value). From postoperative Day 4 to Day 28,

ulcer area was significantly smaller than that before CXL (all $P < 0.05$).

The comparison between the three groups at the same time point is shown in **Figure 3**. Before the intervention (including CXL and medication), the corneal ulcer area between the three groups was not statistically significant ($P = 0.9176$). On the first day after the intervention, the ulcer area in the control group ($62.08 \pm 7.22 \text{ mm}^2$) was significantly larger than that in the CXL-M group ($24.09 \pm 3.52 \text{ mm}^2$) ($P = 0.0026$). Additionally, in terms of ulcer area, the control group > M group and M group > CXL group, but the differences were not statistically significant ($P = 0.2102$, $P = 0.1338$, respectively). On the 4, 7, and 14th days after the intervention, the control group > M group

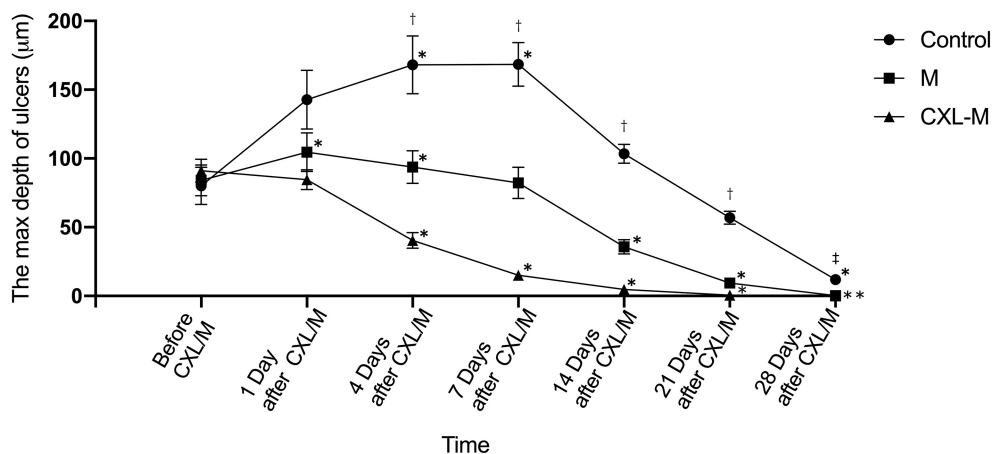


FIGURE 4 | The depth of corneal ulcer in three groups. *The corneal ulcer depth was significantly different at different follow-up time point in each group compared with that before treatment ($P < 0.05$ for all). †There were significant differences in the depth of corneal ulcer between each group at one follow-up time point ($P < 0.05$ for all). ‡There were significant differences in the depth of corneal ulcer between control group and other two groups ($P < 0.05$).

> CXL group (all $P < 0.05$). On the 21st day after intervention, the ulcer area of control group was larger than that of M group ($P = 0.0336$) and CXL-M group ($P = 0.0007$), while the ulcer area of the M group was larger than that of the CXL group, but the difference was not statistically significant ($P = 0.271$). On the 28th day after the intervention, the difference among the three groups was the same as that on the 21st day.

Changes in the depth of the corneal ulcer are shown in **Figure 4**. In the control group, although the ulcer depth deepened significantly on the first day after the intervention, the difference was not statistically significant ($P = 0.1208$). On the 7th day after the intervention, the ulcer depth reached the peak at $168.40 \pm 47.48 \mu\text{m}$ ($P = 0.0147$). On the 14th day after the intervention, the ulcer depth was deeper than that before the intervention, while on the 21st day, the ulcer depth was shallower than that before the intervention, but these differences were not statistically significant ($P = 0.339$, $P = 0.3949$, respectively). Some ulcers remained unhealed 28 days after the intervention ($n = 2$) in the control group. In the M group, the ulcers deepened on the 1st and 4th days after medication ($P = 0.047$, $P = 0.0346$); On the 7th day after medication, the ulcer depth was shallower than before medication, but this difference was not statistically significant ($P = 0.9962$). From the 14th day to the 21st day after the medication was provided, the ulcer was obviously shallower than before medication ($P = 0.0095$, $P < 0.0001$, respectively). On the 28th day, most ulcer depths were 0 ($n = 10$). In the CXL-M group, on the first day after CXL, ulcer depth was slightly shallower than before CXL, but this difference was not statistically significant ($P = 0.719$). From Day 4 to Day 28 after CXL, ulcer depth was significantly shallower than that before CXL (all $P < 0.05$). On the 21st day after CXL, only two eyes still had mild ulcers, and at the end of the study, all the ulcers had healed.

There was no significant difference in ulcer depth between the three groups before and on the first day after the intervention ($P = 0.8184$, $P = 0.0604$, respectively). From 4 to 21 days

after the intervention, there was a difference in ulcer depth between the three groups: CXL group < M group < control group (All $P < 0.05$), and this difference peaked on Day 7 (CXL group vs. M group, $T = 67.33 \mu\text{m}$, $P = 0.0014$; M group vs. control group, $T = 86.11 \mu\text{m}$, $P < 0.0001$). On the 28th day after intervention, control group > M group/CXL-M group ($P = 0.0007$, $P < 0.0001$).

Two rabbits in the control group experienced corneal perforation on the 7th and 14th days, respectively. Corneal perforation occurred in one rabbit in the M group on Day 7. No corneal perforation was observed in CXL-M group.

Representative ulcers observed via IVCN in each group are shown in **Figure 1**, and the average number of days of hyphae duration among the three groups was different: control group (15.75 ± 4.95 days) > M group (10.50 ± 3.742 days) > CXL group (5.125 ± 1.553 days) ($P = 0.025$).

Corneal and corneal epithelium thickness were measured via AS-OCT (**Table 1**). Before modeling (baseline level), there were no significant differences in corneal and corneal epithelial thickness between the three groups ($P = 0.9586$, $P = 0.9886$, respectively). On the 28th day after modeling and intervention, the corneal thickness in the three groups was significantly thicker than baseline (all $P < 0.05$). The thickness differences between the three groups were as follows: M group > control group > CXL group ($P < 0.0001$). Meanwhile, the corneal epithelium in the CXL-M group was slightly thicker than baseline, but this difference was not statistically significant ($P = 0.0958$), and corneal epithelium thicknesses in the control group and M group were significantly thicker than baseline (all $P < 0.001$). There were also differences in corneal epithelial thickness between the three groups, with the CXL-M group having thinner values than the other two groups ($P < 0.0001$).

The HE-stained sections of each group at 28 days after the intervention are shown in **Figure 5**. In the control group, there was more than 12 corneal structural damage, scar repair, diffuse

TABLE 1 | Corneal and corneal epithelium thickness in three groups.

		Base line	28 days after M/CXL	P
Corneal epithelium thickness (μm)	Control (n/n' = 12/8)	45.56 \pm 2.186	74.89 \pm 5.905	<0.0001
	M (n/n' = 12/10)	45.42 \pm 2.234	79.42 \pm 7.229	<0.0001
	CXL-M (n/n' = 12/12)	45.25 \pm 2.121	47.89 \pm 3.940	0.0958
	P	0.9596	<0.0001	
Corneal thickness (μm)	Control (n/n' = 12/8)	381.25 \pm 24.42	608.80 \pm 34.62	<0.0001
	M (n/n' = 12/10)	380.80 \pm 21.68	736.60 \pm 36.34	<0.0001
	CXL-M (n/n' = 12/12)	382.10 \pm 17.54	517.40 \pm 29.25	<0.0001
	P	0.9886	<0.0001	

M, voriconazole only; CXL-M, cross-link combined with voriconazole; The test used for statistical analysis among groups was t-test and between groups was one-way ANOVA. n/n', number of rabbits at base line/ number of rabbits with perforation and non-healing excluded at 28 days after treatment.

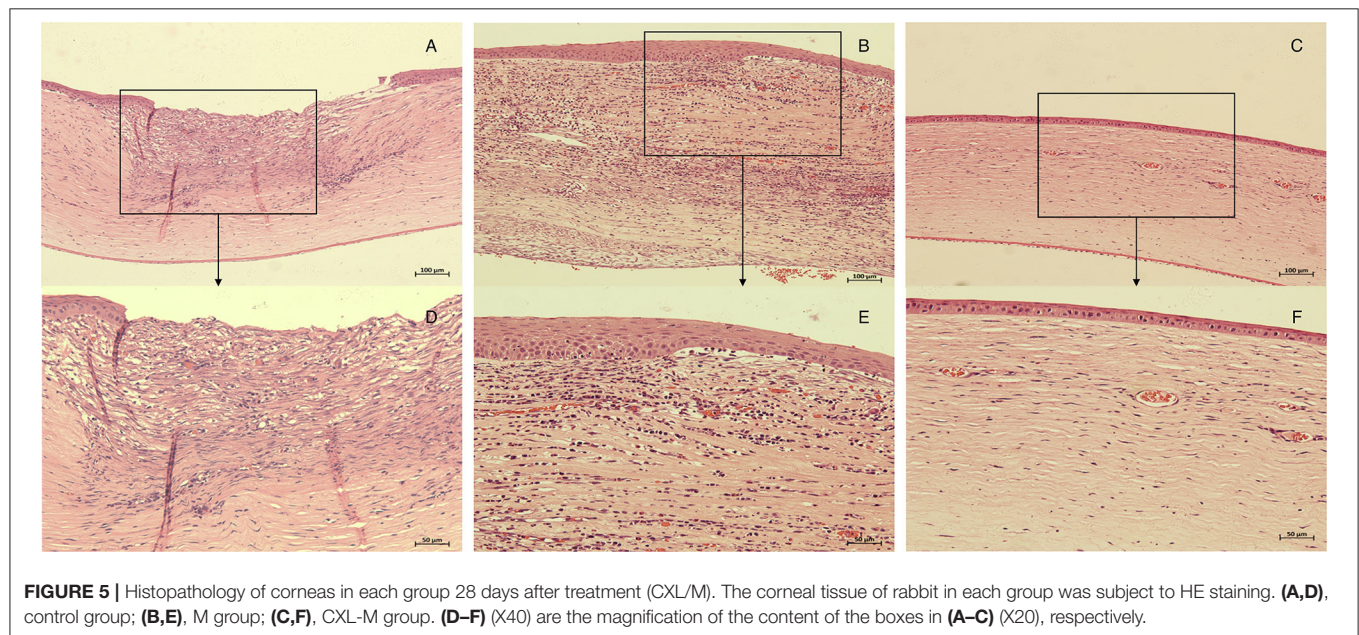


FIGURE 5 | Histopathology of corneas in each group 28 days after treatment (CXL/M). The corneal tissue of rabbit in each group was subject to HE staining. (A,D), control group; (B,E), M group; (C,F), CXL-M group. (D–F) (X40) are the magnification of the content of the boxes in (A–C) (X20), respectively.

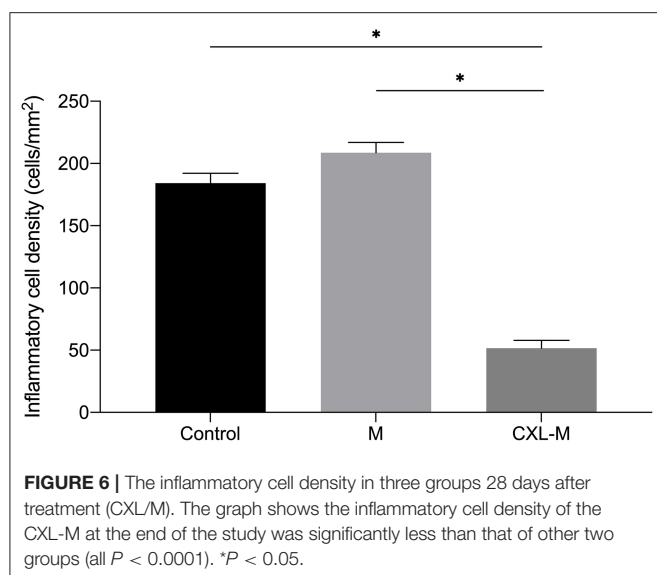
thickening of cornea, abundant proliferation of corneal stromal fibroblasts, fibrosis and extremely chaotic fiber arrangement, massive inflammatory cells and neovascularization, a thickened epithelial layer with a multi-layered cell arrangement, and local epithelial defect. In the M group, there was diffuse thickening of the entire cornea, with a large amount of inflammatory cell infiltration and neovascularization; a large number of fibroblasts in the stromal layer with chaotic fiber arrangement; and obvious thickening of the corneal epithelium with multilayer cells. In the CXL group, the proliferation of fibrous tissue in the stroma was regular, some neovascularization could be seen locally, and the corneal epithelium was flat and arranged in a single layer. The inflammatory cell density of CXL-M group was significantly lower than that of the other two groups ($P < 0.001$, **Figure 6**).

DISCUSSION

This study used conventional voriconazole combined with CXL in treating rabbit fungal keratitis infected by *Aspergillus*, which is the first drug-combined-with-CXL study for an animal model

of *Aspergillus* infection. We found that voriconazole combined with CXL can significantly curb the development of corneal ulcers caused by *Aspergillus* infection, accelerate healing, and reduce complications.

In this study, the average hypha duration for the CXL-M group was significantly shorter than that of the other two groups. Bilgihan et al. and Sun et al. demonstrated that CXL has inhibitory effects on *Aspergillus*, *Fusarium*, and *Candida in vitro* (17, 25). During the crosslinking process, oxygen radicals produced by the photooxidation of riboflavin via ultraviolet radiation can damage the genetic material of the fungus, destroy the DNA of the pathogen, and kill the pathogen (26, 27); at the same time, the reaction process consumes oxygen, creating an oxygen-deficient environment, affecting the replication and growth of the fungus (27, 28). Interestingly, Sauer et al. found that CXL had no antifungal effect on *Candida*, *Fusarium*, and *Aspergillus in vitro*, while after pretreatment with amphotericin B, CXL had a significant antifungal effect (29). The author believes that cross-linking promotes the distribution of amphotericin B, which helps anti-fungi (29). However, the manner of adding



riboflavin in their study may have led to the result that CXL alone had no antifungal activity *in vitro* (25). It is also believed that the results obtained via *in vitro* studies cannot effectively reflect effectiveness *in vivo* (29). Therefore, tissue culture or animal studies may better detect the effectiveness of cross-linking on infectious keratitis. In this animal study, our results show that the combination of voriconazole and CXL had excellent anti-*Aspergillus* effects, controlling the infection earlier and more effectively compared to voriconazole treatment alone.

The ulcer area in the control group and M group both increased from the first day after the intervention and continued to increase for 14 and 7 days respectively. By the end of the study, some rabbits still had incomplete ulcer healing in both groups. However, the area of ulcers in the CXL-M group began to shrink from the first day of the intervention, and all the rabbits had ulcer healed at the end of the experiment. Further analysis of the ulcer area between the three groups at the same time point showed that the ulcer area of the CXL-M group was significantly smaller than that of the other two groups during the entire study after the intervention (except for the 1st and 28th days of M group). The changes in the depth of ulcers within and between the three groups showed a trend similar to that of the area of corneal ulcers. It is suggested that voriconazole combined with CXL is significantly better than voriconazole treatment alone in terms of onset time and ulcer healing (ulcer area and depth).

There are few randomized controlled studies on CXL in the treatment of fungal corneal ulcers, and the previous results are also conflicting. Ozdemir et al. and Galperin et al. report the effectiveness of cross-linking against *Fusarium* and *Candida* infectious keratitis in rabbits (14, 30). Similarly, cross-linking was also beneficial in treating *Fusarium* infectious keratitis in mice (31). Although our previous clinical study and Jeyalatha Mani et al. both reported that CXL had a significant adjuvant effect of CXL in treating fungal keratitis compared to standalone antifungal treatment (18, 32), further analysis of various fungal

species has not been conducted. Uddaraju et al. and Price et al. found that CXL has a poor response to the healing of fungal corneal ulcers (20, 33). These researchers believe that the deeper and larger ulcers before the intervention are responsible for the poor response. Vajpayee et al. observed the healing time of fungal corneal ulcers after CXL and found no difference between CXL and medication alone (34). However, in comparing the healing time of aspergillus-infected corneal ulcer in their study, the CXL group was superior to the medication group. Thus far, there has been no animal study or clinical observation report on the effects of CXL on *Aspergillus* infection alone. This study is the first drug combination cross-linking study for *Aspergillus* infectious corneal ulcers in rabbit; the results showed that the healing of ulcers in the CXL-M group was significantly better than that in the M group and the control group.

Aspergillus can produce proteases, such as metalloproteinase and serine proteinase, which can degrade collagen (35). However, the large amount of singlet oxygen produced during CXL may damage the protease and protect the corneal stroma (36). Corneal collagen cross-linking can also change the tertiary structure between collagen fibers, thereby preventing protease from acting on its specific enzymatic site (37). On the other hand, corneal collagen crosslinking can improve the mechanical strength and stability of the cornea and enhance its tolerance of enzyme digestion (36, 38). After CXL, the cornea hardens, and its permeability will decrease, which prevent the invasion of fungi into the deep cornea (17, 38, 39).

Corneal perforation was observed in both the control group and the M group during follow-up, while no corneal perforation was observed in the CXL-M group in this study. Said et al. report the effectiveness of CXL in severe infectious keratitis with kerolysis (38). In their study, no corneal perforation occurred in the cross-linking group, and about 40% of cases were aspergillus infections. In addition, both Z. Li et al. and Galperin et al. reported that CXL was effective in treating fungal keratitis without complications (13, 30). However, it was also found that the perforation rate of patients with deep stromal fungal keratitis after CXL was higher than that in the control group (33). These researchers suggested that CXL responds poorly to deeper ulcers and may even increase the risk of perforation for deeper corneal ulcers (12, 20, 33). The differences in the reported results may be caused by the various fungal species and their abilities to invade the corneal stroma. In addition, in animal studies, the initial depth of corneal ulcer may also be different after modeling, and most of the previous studies did not measure ulcer depth. The use of different cross-linking schemes may also have contributed to this difference. In addition, Uddaraju et al. believe that CXL may have specific effects on certain fungi (33).

In this study, the ulcer depth was quantitatively measured by AS-OCT, and it was found that the average ulcer depth in the CXL-M group was 91 μm before intervention, while no abnormality of the corneal endothelium was found in pathological sections of the CXL-M group. Shetty et al. suggest that the superficial corneal stroma infiltration of the anterior one-third depth responds better to CXL (12). Therefore, we speculated that voriconazole combined with CXL can safely and effectively control *aspergillus*-infected corneal ulcers at an ulcer

depth of at least 90 μm in rabbit. Further studies are needed to confirm whether use for ulcers beyond this depth is still effective and safe.

On the 28th day after the intervention, although the corneal thickness of all three groups were thicker than the baseline before modeling, the CX-M group was significantly thinner than that of the other two groups. The corneal epithelial thickness of the CXL-M group was also thinner than that of the other two groups, but there was no significant difference between the CXL-M group and baseline level, while the other two groups were thicker than the baseline level. This result is similar to the results of our previous clinical observation research (18). We speculated that the corneal inflammation in the CXL-M group was milder at this time and that the corneal shape was closer to the normal. Pathological sections also confirmed that the corneal epithelium of the cross-linking group was monolayer; stromal fiber was regular; and inflammatory cells, neovascularization, and fibroblasts were significantly less than in the other two groups at this time.

The corneal epithelial cells recognize fungi through pattern recognition receptors (40), such as Toll-like receptors (TLR) and C-type Lectin receptors (CLR). *Aspergillus fumigatus* encounter during fungal keratitis have been reported to be sensed by TLR (41), which can induce production of chemokines and recruit neutrophils (are more than 90% of the infiltrating cells) (40). Jeyalatha Mani et al. found that the expression of pro-inflammatory factors (IL-1 β , IL-8, and IFN- γ) and TLRs (TLR-3/4/6) were significantly downregulated after CXL treatment in patients with fungal keratitis (32), suggesting that CXL may exerts an anti-inflammatory effect via TLRs pathway. In addition, photooxidation during CXL can inactivate leukocytes and reduce and regulate inflammatory response (42), which may also participate in the effect observed. Wollensak et al. found that cross-linking can significantly reduce the edema coefficient in the cross-linking area (43), and Holopainen et al. found that the corneal thickness decreased by an average of $19 \pm 7\%$ after crosslinking (44), suggesting that the anti-edema effect of cross-linking may also be one of the reasons for thinner corneal thickness in the CXL-M group as compared with the other two groups.

The sample size of this study is small, and the follow-up time is short. The results must be further verified in subsequent large-sample and long-term studies. Currently, no

report has recommended CXL as a standalone first-line therapy, so this study did not include CXL treatment alone group, and relevant studies will be carried out in the future. To date, there is an absolute empiric use and no protocol consensus and agreement or fungal-agent-specific CXL or customized CXL nomogram. This experimental setting finally studied an organism-specific response to clarify that the adjuvant effect of CXL may be dependent on the specific fungal organism. In addition, only traditional CXL (3 mW/cm², total UVA energy 5.4 J/cm²) combined with voriconazole and voriconazole alone were compared in this study. The question of whether there are differences between different CXL protocols (such as 9 mW, 18 mW, and 30 mW CXL, etc.) and different antifungal agents (such as natamycin, amphotericin, etc.) could not be answered in this study, but subsequent studies should investigate this matter further.

This study found that voriconazole combined with corneal collagen crosslinking can significantly inhibit fungal keratitis caused by *aspergillus* infection and accelerate ulcer healing. It can be used as an adjunctive treatment for fungal keratitis of *aspergillus* infection, especially for early and superficial corneal ulcers.

DATA AVAILABILITY STATEMENT

The original contributions presented in the study are included in the article/supplementary material, further inquiries can be directed to the corresponding authors.

ETHICS STATEMENT

The animal study was reviewed and approved by Animal Ethics Committee of Fudan University School of Medicine (Shanghai, China).

AUTHOR CONTRIBUTIONS

TS and YS contributed to conception and design of the study. ZZ and XC collected and measured the data. ZZ performed the statistical analysis and wrote the first draft of the manuscript. XC wrote sections of the manuscript. TS revised the manuscript. All authors contributed to manuscript revision, read, and approved the submitted version.

REFERENCES

- Manikandan P, Abdel-Hadi A, Randhir Babu Singh Y, Revathi R, Anita R, Banawas S, et al. Fungal keratitis: epidemiology, rapid detection, and antifungal susceptibilities of fusarium and aspergillus isolates from corneal scrapings. *Biomed Res Int.* (2019) 2019:6395840. doi: 10.1155/2019/6395840
- Ghosh AK, Gupta A, Rudramurthy SM, Paul S, Hallur VK, Chakrabarti A. Fungal keratitis in North India: spectrum of agents, risk factors and treatment. *Mycopathologia.* (2016) 181:843–50. doi: 10.1007/s11046-016-0042-3
- Ng JK, Fraunfelder FW, Winthrop KL. Review and update on the epidemiology, clinical presentation, diagnosis, and treatment of fungal keratitis. *Curr Fungal Infect Rep.* (2013) 7:293–300. doi: 10.1007/s12281-013-0163-9
- Mahmoudi S, Masoomi A, Ahmadikia K, Tabatabaei SA, Soleimani M, Rezaei S, et al. Fungal Keratitis: An overview of clinical and laboratory aspects. *Mycoses.* (2018) 61:916–30. doi: 10.1111/myc.12822
- Kalkanci A, Yesilirmak N, Ozdemir HB, Unal EA, Erdogan M, Seker T, et al. Impact of iontophoresis and Pack-Cxl corneal concentrations of antifungals in an *in vivo* model. *Cornea.* (2018) 37:1463–7. doi: 10.1097/ICO.0000000000001696

6. Ansari Z, Miller D, Galor A. Current thoughts in fungal keratitis: diagnosis and treatment. *Curr Fungal Infect Rep.* (2013) 7:209–18. doi: 10.1007/s12281-013-0150-1
7. Wu J, Zhang WS, Zhao J, Zhou HY. Review of clinical and basic approaches of fungal keratitis. *Int J Ophthalmol.* (2016) 9:1676–83. doi: 10.18240/ijo.2016.11.23
8. Wollensak G, Spoerl E, Seiler T. Riboflavin/Ultraviolet-a-induced collagen crosslinking for the treatment of keratoconus. *Am J Ophthalmol.* (2003) 135:620–7. doi: 10.1016/S0002-9394(02)02220-1
9. Wollensak G. Crosslinking treatment of progressive keratoconus: new hope. *Curr Opin Ophthalmol.* (2006) 17:356–60. doi: 10.1097/01.icu.0000233954.86723.25
10. Iseli HP, Thiel MA, Hafezi F, Kampmeier J, Seiler T. Ultraviolet a/Riboflavin corneal cross-linking for infectious keratitis associated with corneal melts. *Cornea.* (2008) 27:590–4. doi: 10.1097/ICO.0b013e318169d698
11. Igal V, Pikkell Igal YS, Pikkell YY. Corneal cross-linking as a treatment for fungal keratitis associated with corneal melting. *Case Rep Ophthalmol.* (2017) 8:148–51. doi: 10.1159/000456537
12. Shetty R, Nagaraja H, Jayadev C, Shivanna Y, Kugar T. Collagen crosslinking in the management of advanced non-resolving microbial keratitis. *Br J Ophthalmol.* (2014) 98:1033–5. doi: 10.1136/bjophthalmol-2014-304944
13. Li Z, Jhanji V, Tao X, Yu H, Chen W, Mu G. Riboflavin/ultraviolet light-mediated crosslinking for fungal keratitis. *Br J Ophthalmol.* (2013) 97:669–71. doi: 10.1136/bjophthalmol-2012-302518
14. Ozdemir HB, Kalkanci A, Bilgihan K, Gocun PU, Ogut B, Karakurt F, et al. Comparison of corneal collagen cross-linking (Pack-Cxl) and voriconazole treatments in experimental fungal keratitis. *Acta Ophthalmol.* (2019) 97:e91–e6. doi: 10.1111/aos.13829
15. Papaioannou L, Miligkos M, Papanthassiou M. Corneal Collagen cross-linking for infectious keratitis: a systematic review and meta-analysis. *Cornea.* (2016) 35:62–71. doi: 10.1097/ICO.0000000000000644
16. Martins SA, Combs JC, Noguera G, Camacho W, Wittmann P, Walther R, et al. Antimicrobial Efficacy of Riboflavin/Uva Combination (365 Nm) *in vitro* for bacterial and fungal isolates: a potential new treatment for infectious keratitis. *Invest Ophthalmol Vis Sci.* (2008) 49:3402–8. doi: 10.1167/iovs.07-1592
17. Bilgihan K, Kalkanci A, Ozdemir HB, Yazar R, Karakurt F, Yuksel E, et al. Evaluation of antifungal efficacy of 01% and 025% Riboflavin with Uva: a Comparative *in vitro* study. *Curr Eye Res.* (2016) 41:1050–6. doi: 10.3109/02713683.2015.1088956
18. Wei A, Wang K, Wang Y, Gong L, Xu J, Shao T. Evaluation of corneal cross-linking as adjuvant therapy for the management of fungal keratitis. *Graefes Arch Clin Exp Ophthalmol.* (2019) 257:1443–52. doi: 10.1007/s00417-019-04314-1
19. Tabibian D, Richoz O, Riat A, Schrenzel J, Hafezi F. Accelerated photoactivated chromophore for keratitis-corneal collagen cross-linking as a first-line and sole treatment in early fungal keratitis. *J Refract Surg.* (2014) 30:855–7. doi: 10.3928/1081597X-20141113-06
20. Price MO, Tenkman LR, Schrier A, Fairchild KM, Trokel SL, Price FW Jr. Photoactivated riboflavin treatment of infectious keratitis using collagen cross-linking technology. *J Refract Surg.* (2012) 28:706–13. doi: 10.3928/1081597X-20120921-06
21. Kalkanci A, Ozdek S. Ocular fungal infections. *Curr Eye Res.* (2011) 36:179–89. doi: 10.3109/02713683.2010.533810
22. Lakhundi S, Siddiqui R, Khan NA. Pathogenesis of microbial keratitis. *Microb Pathog.* (2017) 104:97–109. doi: 10.1016/j.micpath.2016.12.013
23. Sharma S, Kunimoto DY, Gopinathan U, Athmanathan S, Garg P, Rao GN. Evaluation of corneal scraping smear examination methods in the diagnosis of bacterial and fungal keratitis: a survey of eight years of laboratory experience. *Cornea.* (2002) 21:643–7. doi: 10.1097/00003226-200210000-00002
24. Leck AK, Thomas PA, Hagan M, Kalamurthy J, Ackuaku E, John M, et al. Aetiology of suppurative corneal ulcers in Ghana and South India, and epidemiology of fungal keratitis. *Br J Ophthalmol.* (2002) 86:1211–5. doi: 10.1136/bjo.86.11.1211
25. Sun B, Li ZW, Yu HQ, Tao XC, Zhang Y, Mu GY. Evaluation of the *in vitro* antimicrobial properties of ultraviolet a/riboflavin mediated crosslinking on *Candida Albicans* and *fusarium solani*. *Int J Ophthalmol.* (2014) 7: 205–10.
26. Pouget JP, Douki T, Richard MJ, Cadet J, DNA. Damage induced in cells by *F* and Uva radiation as measured by Hplc/Gc– Ms and Hplc– Ec and comet assay. *Chem Res Toxicol.* (2000) 13:541–9. doi: 10.1021/tx000020e
27. Hiraku Y, Ito K, Hirakawa K, Kawanishi S. Photosensitized DNA damage and its protection *via* a novel mechanism. *Photochem Photobiol.* (2007) 83:205–12. doi: 10.1562/2006-03-09-IR-840
28. Baier J, Maisch T, Maier M, Engel E, Landthaler M, Bäumler W. Singlet oxygen generation by Uva light exposure of endogenous photosensitizers. *Biophys J.* (2006) 91:1452–9. doi: 10.1529/biophysj.106.082388
29. Sauer A, Letscher-Bru V, Speeg-Schatz C, Touboul D, Colin J, Candolfi E, et al. *In vitro* efficacy of antifungal treatment using Riboflavin/Uv-a (365 Nm) combination and Amphotericin B. *Invest Ophthalmol Vis Sci.* (2010) 51:3950–3. doi: 10.1167/iovs.09-4013
30. Galperin G, Berra M, Tau J, Boscaro G, Zarate J, Berra A. Treatment of fungal keratitis from *fusarium* infection by corneal cross-linking. *Cornea.* (2012) 31:176–80. doi: 10.1097/ICO.0b013e318221cec7
31. Zhu Z, Zhang H, Yue J, Liu S, Li Z, Wang L. Antimicrobial efficacy of corneal cross-linking *in vitro* and *in vivo* for *fusarium solani*: a potential new treatment for fungal keratitis. *BMC Ophthalmol.* (2018) 18:65. doi: 10.1186/s12886-018-0727-0
32. Jeyalatha Mani V, Parthasarathy D, Padmanabhan P, Narayanan N, Lakshmiopathy M, Pachayappan SK, et al. Therapeutic effect of corneal crosslinking on fungal keratitis: efficacy of corneal collagen crosslinking as an adjuvant therapy for fungal keratitis in a tertiary eye hospital in South India. *Ocul Immunol Inflamm.* (2021) 29:1648–55. doi: 10.1080/09273948.2020.1770296
33. Uddaraju M, Mascarenhas J, Das MR, Radhakrishnan N, Keenan JD, Prajna L, et al. Corneal cross-linking as an adjuvant therapy in the management of recalcitrant deep stromal fungal keratitis: a randomized trial. *Am J Ophthalmol.* (2015) 160:131–4 e5. doi: 10.1016/j.ajo.2015.03.024
34. Vajpayee RB, Shafi SN, Maharana PK, Sharma N, Jhanji V. Evaluation of corneal collagen cross-linking as an additional therapy in mycotic keratitis. *Clin Exp Ophthalmol.* (2015) 43:103–7. doi: 10.1111/ceo.12399
35. Gopinathan U, Ramakrishna T, Willcox M, Rao CM, Balasubramanian D, Kulkarni A, et al. Enzymatic, clinical and histologic evaluation of corneal tissues in experimental fungal keratitis in rabbits. *Exp Eye Res.* (2001) 72:433–42. doi: 10.1006/exer.2000.0971
36. Spoerl E, Wollensak G, Seiler T. Increased resistance of crosslinked cornea against enzymatic digestion. *Curr Eye Res.* (2004) 29:35–40. doi: 10.1080/02713680490513182
37. Hovakimyan M, Guthoff RF, Stachs O. Collagen cross-linking: current status and future directions. *J. Ophthalmol.* (2012) 2012:406850. doi: 10.1155/2012/406850
38. Said DG, Elalfy MS, Gatziofias Z, El-Zakouk ES, Hassan MA, Saif MY, et al. Collagen cross-linking with photoactivated riboflavin (Pack-Cxl) for the treatment of advanced infectious keratitis with corneal melting. *Ophthalmology.* (2014) 121:1377–82. doi: 10.1016/j.ophtha.2014.01.011
39. Stewart JM, Lee OT, Wong FF, Schultz DS, Lamy R. Cross-linking with ultraviolet-a and riboflavin reduces corneal permeability. *Invest Ophthalmol Vis Sci.* (2011) 52:9275–8. doi: 10.1167/iovs.11-8155
40. Suman S, Kumar A, Saxena I, Kumar M. *Fungal keratitis: recent advances in diagnosis and treatment.* *Infect Eye Dis Recent Adv Diagn Treat.* (2021):55. doi: 10.5772/intechopen.98411
41. Wu J, Zhang Y, Xin Z, Wu X. The crosstalk between Tlr2 and Nod2 in *aspergillus fumigatus* keratitis. *Mol Immunol.* (2015) 64:235–43. doi: 10.1016/j.molimm.2014.11.021

42. Wollensak G, Spoerl E, Wilsch M, Seiler T. Keratocyte apoptosis after corneal collagen cross-linking using Riboflavin/Uva treatment. *Cornea*. (2004) 23:43–9. doi: 10.1097/00003226-200401000-00008
43. Wollensak G, Aurich H, Pham DT, Wirbelauer C. Hydration behavior of porcine cornea crosslinked with riboflavin and ultraviolet A. *J Cataract Refract Surg*. (2007) 33:516–21. doi: 10.1016/j.jcrs.2006.11.015
44. Holopainen JM, Krotila K. Transient corneal thinning in eyes undergoing corneal cross-linking. *Am J Ophthalmol*. (2011) 152:533–6. doi: 10.1016/j.ajo.2011.03.023

Conflict of Interest: The authors declare that the research was conducted in the absence of any commercial or financial relationships that could be construed as a potential conflict of interest.

Publisher's Note: All claims expressed in this article are solely those of the authors and do not necessarily represent those of their affiliated organizations, or those of the publisher, the editors and the reviewers. Any product that may be evaluated in this article, or claim that may be made by its manufacturer, is not guaranteed or endorsed by the publisher.

Copyright © 2022 Zhao, Chen, Shao and Shao. This is an open-access article distributed under the terms of the Creative Commons Attribution License (CC BY). The use, distribution or reproduction in other forums is permitted, provided the original author(s) and the copyright owner(s) are credited and that the original publication in this journal is cited, in accordance with accepted academic practice. No use, distribution or reproduction is permitted which does not comply with these terms.



OPEN ACCESS

EDITED BY

Yan Li,
Oregon Health and Science University,
United States

REVIEWED BY

Robert Herber,
University Hospital Carl Gustav
Carus, Germany
FangJun Bao,
Affiliated Eye Hospital of Wenzhou
Medical College, China

*CORRESPONDENCE

Gernot Steinwender
steinwender.gernot@gmail.com

SPECIALTY SECTION

This article was submitted to
Ophthalmology,
a section of the journal
Frontiers in Medicine

RECEIVED 13 June 2022

ACCEPTED 30 August 2022

PUBLISHED 20 September 2022

CITATION

Steinwender G, Kollenc A, Shajari M,
Sommer M, Borenich A,
Horwath-Winter J, Lindner E,
Woltsche N, List W and Wedrich A
(2022) Determining the center of a
keratoconus: Comparison of different
tomographic parameters and impact
of disease severity.
Front. Med. 9:968318.
doi: 10.3389/fmed.2022.968318

COPYRIGHT

© 2022 Steinwender, Kollenc, Shajari,
Sommer, Borenich, Horwath-Winter,
Lindner, Woltsche, List and Wedrich.
This is an open-access article
distributed under the terms of the
[Creative Commons Attribution License](#)
(CC BY). The use, distribution or
reproduction in other forums is
permitted, provided the original
author(s) and the copyright owner(s)
are credited and that the original
publication in this journal is cited, in
accordance with accepted academic
practice. No use, distribution or
reproduction is permitted which does
not comply with these terms.

Determining the center of a keratoconus: Comparison of different tomographic parameters and impact of disease severity

Gernot Steinwender^{1*}, Alexander Kollenc¹, Mehdi Shajari²,
Michael Sommer¹, Andrea Borenich³, Jutta Horwath-Winter¹,
Ewald Lindner¹, Nora Woltsche¹, Wolfgang List¹ and
Andreas Wedrich¹

¹Department of Ophthalmology, Medical University Graz, Graz, Austria, ²Department of Ophthalmology, Medical University Frankfurt, Frankfurt, Germany, ³Institute for Medical Informatics, Statistics and Documentation, Medical University Graz, Graz, Austria

Purpose: There exists remarkable variation in definitions for the location of the center of a keratoconus. The objective of this study was to analyze deviations between locations obtained by different tomographic maps for that purpose. Furthermore, it was investigated whether these deviations are influenced by disease severity.

Methods: In 162 eyes with keratoconus, corneal tomographic maps derived by Scheimpflug technology were retrospectively analyzed to determine the cone location with 5 different methods: maximum axial curvature of the front surface (Kmax), maximum tangential curvature of the front surface (tKmax), minimum pachymetry (Pachymin), maximum elevation of the front surface (ELEF), and maximum elevation of the back surface (ELEB). Distances between the locations were calculated and tested for a correlation with keratoconus severity and distance between cone and corneal vertex.

Results: Cone locations derived from the curvature maps (Kmax, tKmax) showed the lowest agreement with the locations determined by pachymetry or elevation maps. The largest distances were found between Kmax and Pachymin [Median and Interquartile range: 1.19 mm (0.87, 1.60)], Kmax and ELEB [1.12 mm (0.79, 1.41)], and Kmax and ELEF [0.97 mm (0.64, 1.27)]. Low distances (<0.5 mm) were calculated between ELEB and ELEF, and ELEB and Pachymin. All of the calculated distances between the locations showed a significant negative correlation with keratoconus severity and most of them increased significantly with a more peripheral position of the cone ($p < 0.05$).

Conclusions: There was low consistency between different methods for describing the location of a keratoconus. Curvature-based determinations of the cone center (Kmax, tKmax) showed the highest deviations and should not be used for that purpose. However, the discrepancies between different cone location methods diminished with increasing disease severity and more central position of the cone.

KEYWORDS

keratoconus, corneal tomography, cornea, customized cross-linking, ectasia

Introduction

Keratoconus is a localized biomechanical disorder of the cornea that changes the natural shape of the cornea into a more cone-like shape (1). Refractive consequences of ectatic protrusion and thinning of the cornea in keratoconic eyes are irregular astigmatism and myopia, reducing patients quality of life (2, 3).

There is currently no cure for the disease, although patients can be helped to compensate visual impairment with spectacles or hard contact lenses. In progressive cases of ectasia the condition can be halted with interventions such as corneal cross-linking (CXL), which increases the biomechanical strength of the cornea (4).

In the standard CXL protocol first described by Wollensak et al., the cornea is soaked with riboflavin solution before exposure to a uniform beam of ultraviolet (UV) radiation (5). In a newer approach, only the affected part of the ectatic cornea instead of the entire cornea is addressed by UV energy due to a defined intensity beam profile. Thus, such customized CXL can reduce the size of the exposed cornea and could provide the same or even better therapeutic efficacy than the standard protocol with less UV energy (6–8).

An important issue in customized CXL is to identify the location of the weakest area of the cornea (6, 9, 10). As no objective clinical quantification of the biomechanically affected area is currently available, recently published studies relied on geometrical measurements of the cornea. Some investigators located the center of the UV beam at the point of maximum elevation of the posterior corneal surface (6, 8), while others decided to center the treatment at the points of axial or tangential steepest curvature of the anterior corneal surface (10).

Beside those new therapeutic approaches also a widely used diagnostic method for describing and staging keratoconus based on Scheimpflug-derived tomographic data is based on a certain definition of the center of a keratoconic cornea. With the aim of enhancing early ectatic changes in the elevation map, Belin and Duncan determined the thinnest point as the center of the disordered corneal region and eliminated a small diameter optical zone centered around that point from the standard best-fit-sphere computation (11).

Apparently, there exists remarkable variation in definitions of the center of a keratoconus and thus, the objective of this study was to analyze deviations between locations of different tomographic parameters proposed for that purpose. Furthermore, we wanted to investigate whether these deviations are influenced by disease severity.

Methods

In this retrospective study, corneal tomography maps of 162 right and left eyes of 92 clinically diagnosed keratoconus patients

TABLE 1 Patient characteristics.

Parameter	Mean \pm SD
Patients (<i>n</i> = 92)	
Age (years)	27.7 \pm 7.8
Eyes (<i>n</i> = 162)	
Right eyes	81 (49.7%)
D-value	7.8 \pm 3.7
Kmax (D)	54.4 \pm 6.1
Pachymin (μ m)	471 \pm 37

enrolled in the Department of Ophthalmology of the Medical University of Graz (Graz, Austria) between 2008 and 2018 were reviewed. Approval of the institutional ethics committee was obtained and the study was conducted in accordance with the tenets of the Declaration of Helsinki.

Inclusion criteria were the diagnosis of manifest or subclinical keratoconus made by an experienced cornea specialist (G.S.) based on typical tomographic patterns. Exclusion criteria included corneal diseases other than keratoconus, extensive corneal scarring, corneal edema, and a history of ocular surgery such as corneal cross-linking, implantation of intracorneal rings or corneal refractive surgery.

For each patient, a Scheimpflug (Pentacam, Software version 6.09r40, Oculus Optikgeräte GmbH, Wetzlar, Germany) measurement was performed. Only images with a quality check status of “ok” were included. Analyzed locations to potentially describe the center of the keratoconus included: point of maximum axial curvature of the front surface (Kmax), point of maximum tangential curvature of the front surface (tKmax), point of minimum pachymetry (Pachymin), point of maximum elevation of the front surface (ELEF), and point of maximum elevation of the back surface (ELEB).

To calculate the distances between the described locations, cartesian coordinate system provided by the Pentacam System was used. The origin point of the coordinate system is the corneal vertex, the corneal intersect with the patients line of sight (12). While the coordinates of Kmax and Pachymin are automatically displayed by the Pentacam Software, the coordinates of tKmax, ELEF, and ELEB had to be determined manually by moving the computer mouse cursor to the desired position of the curvature or elevation map followed by extracting the displayed coordinates into a separate data file. After collecting coordinates of all locations, distances between points were calculated using the Pythagorean Theorem.

As a measure for keratoconus severity we used the D-value, a multimetric combination index composed of keratometric, pachymetric, pachymetric progression and elevation parameters which is provided by the Belin/Ambrosio Enhanced Ectasia Software of the Pentacam System.

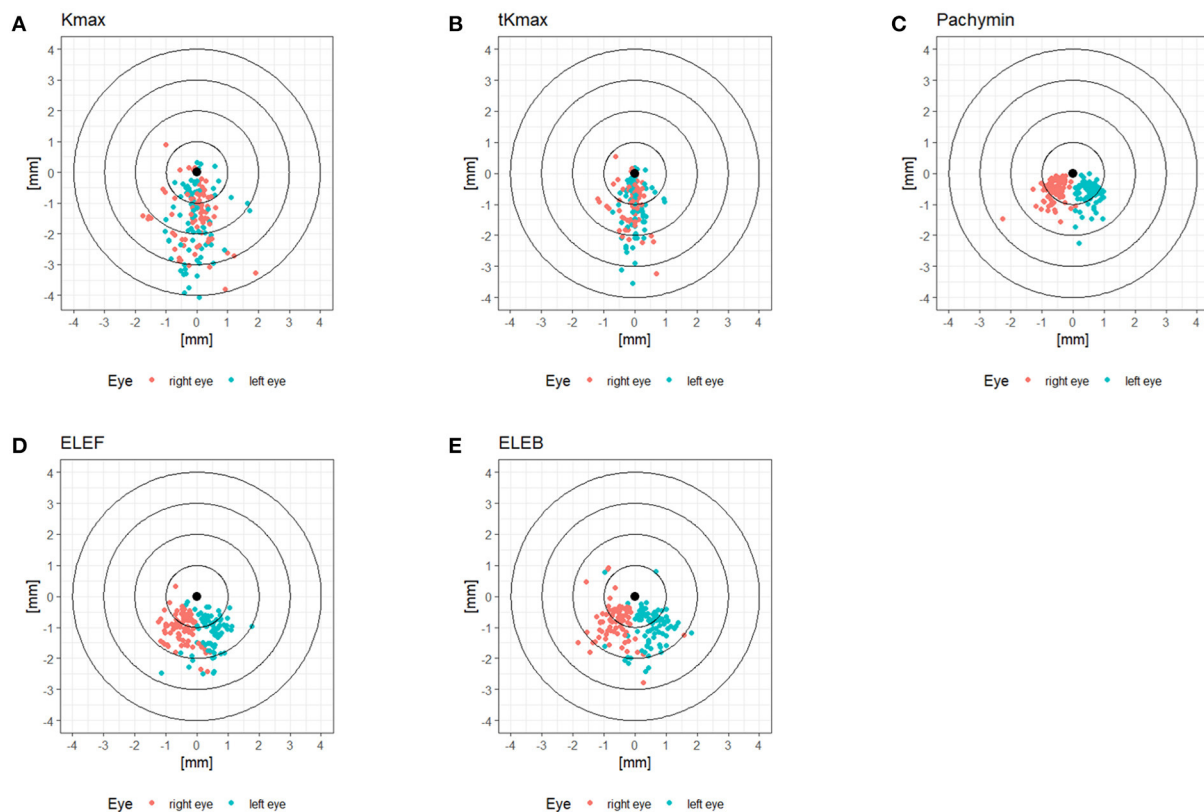


FIGURE 1
(A–E) Locations of tomographic parameters relative to the corneal vertex.

Patient characteristics were reported as absolute and relative frequencies for categorical data and numerical data as mean and standard deviation. Correlations were determined using Spearman's correlation coefficient. For calculating correlations, only 1 randomized eye per patient was included. All statistical analyses were conducted using R version 4.1.2 (<https://www.r-project.org>).

Results

The patient characteristics are displayed in Table 1. The cohort comprised keratoconic eyes from subclinical to advanced stages, represented by a range of *D*-value from 1.0 to 20.5. The locations of Kmax, tKmax, Pachymin, ELEF, and ELEB relative to the corneal vertex are shown in Figure 1. While Pachymin, ELEF and ELEB were predominantly located in the inferior-nasal quadrant, the positions of Kmax and tKmax showed inferior clusters with a less pronounced lateral shifting.

Distances between the different points are shown in Table 2. The largest distances between locations were found between Kmax and Pachymin, Kmax and ELEB, and Kmax and ELEF (Figure 2). Thus, cone locations derived from the axial curvature

map (Kmax) showed the lowest agreement with the locations determined by pachymetry or elevation maps. Low distances (<0.5 mm) were calculated between ELEB and ELEF, and ELEB and Pachymin.

Significant correlations ($p < 0.05$) were found between keratoconus severity and all of the calculated distances between the locations (Figure 3). Higher *D*-values and thus more advanced keratoconus showed a moderate correlation to smaller distances between ELEB and Kmax, ELEB and Pachymin, Kmax and Pachymin, and Kmax and tKmax. The majority of the distances between locations were positively correlated with the distance of those locations from the corneal vertex, meaning that more peripheral cones showed higher deviations between the locations. This observation was most pronounced for the distance between Kmax and Pachymin.

Discussion

In our study, we analyzed deviations between different parameters which could be used to determine the center of a keratoconus and how they are impacted by disease severity. We revealed clinically significant inconsistencies of the location of

TABLE 2 Distances between locations of different tomographic parameters.

Characteristic	Overall, N = 162 ^a	Right eye, N = 81 ^a	Left eye, N = 81 ^a
Distance Pachymin-ELEB	0.37 (0.24, 0.58)	0.35 (0.25, 0.56)	0.38 (0.24, 0.59)
Distance Pachymin-ELEF	0.58 (0.40, 0.72)	0.58 (0.42, 0.65)	0.54 (0.34, 0.76)
Distance Pachymin-Kmax	1.19 (0.87, 1.60)	1.20 (0.88, 1.54)	1.17 (0.84, 1.73)
Distance Pachymin-tKmax	0.77 (0.55, 1.01)	0.78 (0.56, 0.97)	0.77 (0.53, 1.02)
Distance ELEB-ELEF	0.27 (0.17, 0.38)	0.29 (0.20, 0.41)	0.23 (0.16, 0.37)
Distance ELEB-Kmax	1.12 (0.79, 1.41)	1.07 (0.79, 1.32)	1.13 (0.77, 1.43)
Distance ELEB-tKmax	0.70 (0.41, 0.98)	0.67 (0.38, 0.95)	0.73 (0.45, 0.98)
Distance ELEF-Kmax	0.97 (0.64, 1.27)	0.89 (0.61, 1.26)	1.05 (0.69, 1.27)
Distance ELEF-tKmax	0.57 (0.36, 0.81)	0.49 (0.35, 0.78)	0.64 (0.39, 0.87)
Distance Kmax-tKmax	0.54 (0.35, 0.78)	0.54 (0.38, 0.77)	0.55 (0.32, 0.81)

^aMedian (IQR).

the cone center when determined by different morphological maps, including axial or tangential curvature, pachymetry, or elevation maps.

The distribution patterns of the cone center relative to the corneal vertex differed between locations derived from axial or tangential curvature maps of the front surface (Kmax, tKmax) and locations based on pachymetry (Pachymin) or elevation data (ELEF, ELEB). While pachymetry and elevation data resulted in quite regular clusters in the inferior-nasal quadrant, the distribution of the curvature data showed more variability with less lateral shifting and only a moderate inferior predominance (Figure 1). These differences could be attributed to the masking effect of the corneal epithelium. Front stromal surface cones may be fully or partially masked by epithelial remodeling characterized by compensatory thinning over the stromal cone with a surrounding annulus of thicker epithelium (13). In early stages of keratoconus these effects may be great enough to mask stromal irregularities from curvature maps of the front surface, and in more advanced disease stages at least the location of the cone center could be obscured.

To quantify the discrepancies between locations of the cone center, we calculated the distances between locations for a pairwise comparison. The highest deviations were found between curvature-based locations (Kmax, tKmax) and pachymetry- or elevation-based locations (Pachymin, ELEF, ELEB). One reason for Kmax being the least consistent location may be that axial maps assume center points of surface curvature to be always located on the central reference axis hence reducing the sensitivity in identifying surface irregularities (14). Tangential curvature maps typically are more sensitive for describing focal corneal irregularities although they therefore also have higher noise-to-signal ratios. Hence, tKmax showed intermediate deviations in our cohort, better than Kmax, but less consistent than pachymetric- or elevation-based location data. The shortest distance and thus the highest consistency occurred between the elevation (ELEF, ELEB) and

the pachymetry maps (Pachymin). As locations derived from the posterior corneal surface are less influenced by epithelial masking, we assume ELEB is the most accurate location for describing the center of a keratoconus. Showing only small deviations from ELEB, ELEF and Pachymin may be good alternatives for that purpose. Kmax and tKmax seem to be the least suitable options for clinical applications requiring the accurate center of the cone, as they had the least consistency with ELEB.

Our findings are in accordance with Sedaghat et al., who analyzed 90 keratoconic eyes and observed no considerable agreement between the elevation and axial curvature map in locating the center of the cone. Furthermore, similar to our study, the cone was found in the inferotemporal quadrant in the majority of cases (~95%) on the elevation map, while this quadrant contained only 18% of the cone center on the axial curvature map (15).

On the basis from the data of our study, we suggest that using axial or tangential curvature maps (Kmax and tKmax) is not a suitable option for locating a keratoconus. Clinical applications requiring the accurate center of the cone can be more efficient with elevation or pachymetry maps.

The pachymetry map is used for the Belin/Ambrosio enhanced best-fit sphere method, a popular method for the detection of early or subclinical keratoconus as well as for evaluating disease progression (16–18). With this method, the height of the cone is obtained by the difference in elevation between the best-fit sphere of the whole cornea and the best-fit sphere after excluding a fixed area around the thinnest point. Our study provides support for the reasonability to use pachymetry data for determining the cone location, as Pachymin showed only minor deviations from elevation-derived cone locations. Cunha et al. had a different view and decided to use Kmax for defining the keratoconus center in their recent study analyzing keratoconus enlargement as a predictor of keratoconus progression (19).

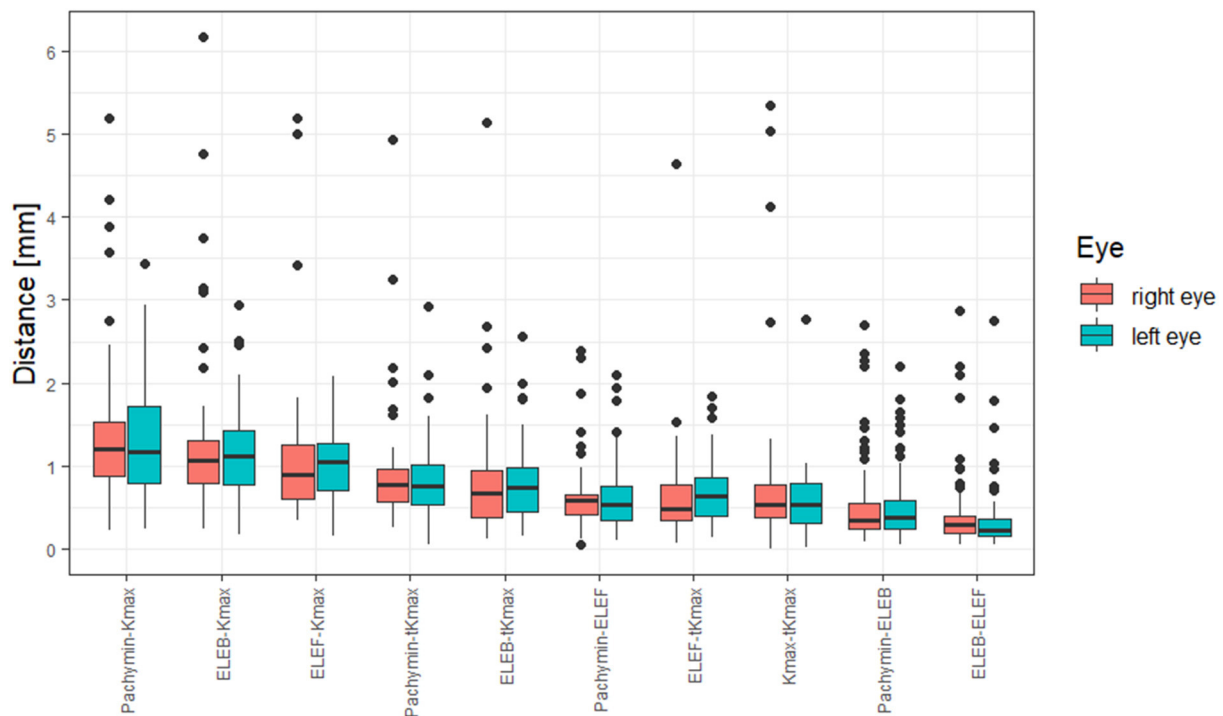


FIGURE 2
Box and whisker plot of distances between locations of different tomographic parameters.

Another important application requiring a precise definition of the cone center is customized cross-linking, which is associated with more corneal flattening and a better visual outcome compared to conventional cross-linking. Seiler et al. (6) and Cassagne et al. (8) defined the keratoconus center based on the posterior elevation map, while Shetty et al. (10) decided to use axial and tangential curvature maps. A recent study from Lopes et al. confirmed remarkable variations in finding the center of a keratoconus with low agreement even in corneal specialists (20).

Our results showed evidence that with increased disease severity, the distances between the cone locations reduced. We suggest that with more pronounced ectatic alterations of the cornea the obscuring effects including epithelial masking and mathematical assumptions for curvature calculation diminish. On the other hand, special consideration should be given in defining the cone location during early stages of the disease, since larger differences between the locations can be expected. In contrast to our findings, Sedaghat et al. reported no considerable change of their results after re-analysis of data in different stages of keratoconus (15). Interestingly, in their investigation of 309 keratoconic patients Eliasy et al. demonstrated a reduction of the distance from the cone center to the corneal vertex

with increased keratoconus severity. However, they did not analyze differences between cone locations obtained by different morphological maps (21).

When testing correlations, we detected a significant increase of deviations between the different locations with increasing distance from the corneal vertex. Thus, more peripheral cones showed higher discrepancies than more central cones. This observation was most pronounced for the distance between Kmax and Pachymin, which may be attributed to a relative central shift of the thinnest point of an ectatic cornea (Pachymin) due to the normal thickness profile of a human cornea, being thinnest centrally.

In conclusion, we found low consistency between different methods for describing the location of a keratoconus. As curvature-based determinations (like Kmax or tKmax) of the cone center showed the highest deviations, they should not be used for that purpose. Elevation- or pachymetry-based measures (like ELEB, ELEF, or Pachymin) are more suitable options for clinical applications requiring the accurate center of the cone. However, the discrepancies between the different cone location methods diminished with increasing disease severity and more central position of the cone.

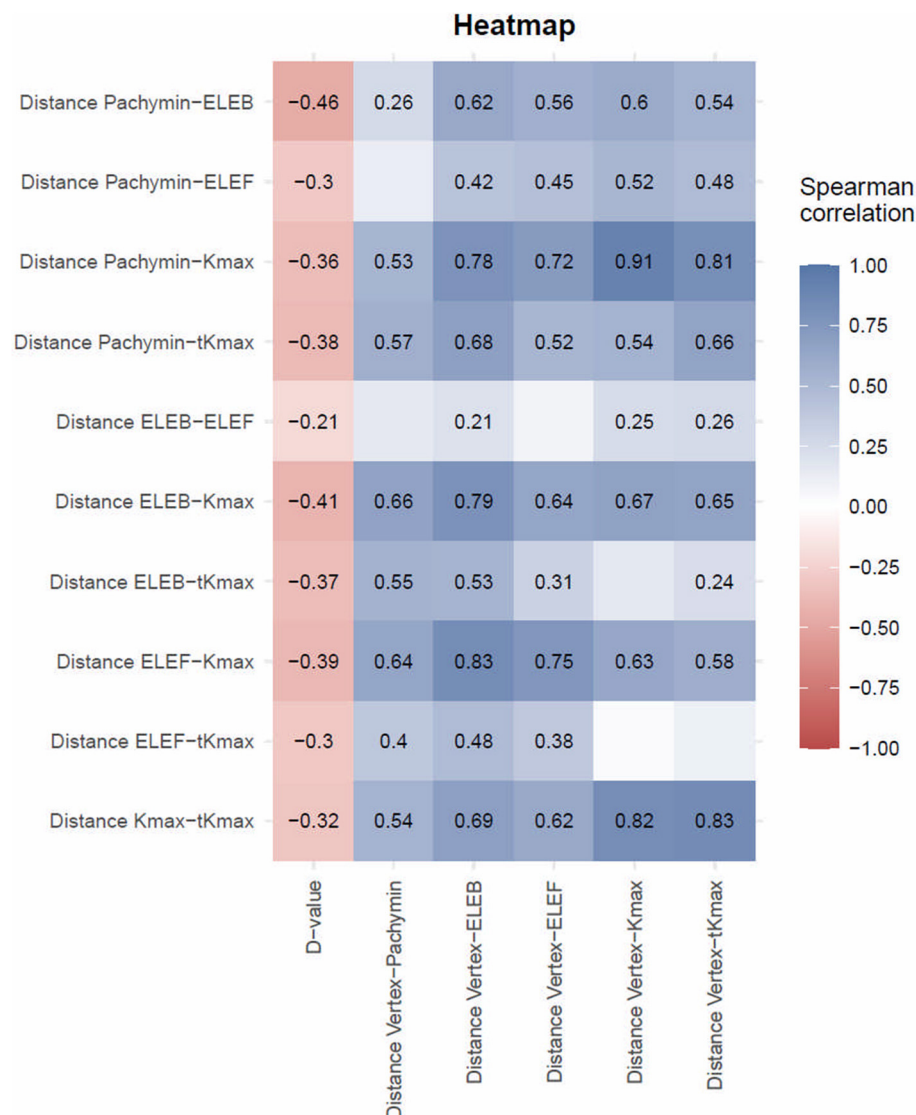


FIGURE 3

Spearman Correlation between distances between locations of different tomographic parameters and D-values or distances between locations and corneal vertex. The Spearman correlation coefficient is only presented in fields reaching statistical significance ($p < 0.05$). Discrepancy between different measures decreased with disease severity and increased with increasing distance from the corneal vertex.

Data availability statement

The raw data supporting the conclusions of this article will be made available by the authors, without undue reservation.

Ethics statement

The studies involving human participants were reviewed and approved by Ethics Committee of the Medical University of Graz. Written informed consent from the participants' legal guardian/next of kin was not required to participate in this study in accordance with

the national legislation and the institutional requirements. Written informed consent was not obtained from the minor(s)' legal guardian/next of kin for the publication of any potentially identifiable images or data included in this article.

Author contributions

GS, AK, and MSh contributed to conception and design of the study. AK and MSo organized the database. AB performed the statistical analysis and wrote sections of the manuscript. GS wrote the first draft of the manuscript with

constructive inputs of JH-W, EL, NW, WL, and AW. All authors contributed to manuscript revision, read, and approved the submitted version.

Conflict of interest

The authors declare that the research was conducted in the absence of any commercial or financial relationships that could be construed as a potential conflict of interest.

References

- Scarcelli G, Besner S, Pineda R, Kalout P, Yun SH. *In vivo* biomechanical mapping of normal and keratoconus corneas. *JAMA Ophthalmol.* (2015) 133:480. doi: 10.1001/jamaophthalmol.2014.5641
- Krachmer JH, Feder RS, Belin MW. Keratoconus and related noninflammatory corneal thinning disorders. *Surv Ophthalmol.* (1984) 28:293–322. doi: 10.1016/0039-6257(84)90094-8
- Jones-Jordan LA, Walline JJ, Sinnott LT, Kymes SM, Zadnik K. Asymmetry in keratoconus and vision-related quality of life. *Cornea.* (2013) 32:267–72. doi: 10.1097/ICO.0b013e31825697c4
- Spoerl E, Huhle M, Seiler T. Induction of cross-links in corneal tissue. *Exp Eye Res.* (1998) 66:97–103. doi: 10.1006/exer.1997.0410
- Wollensak G, Spoerl E, Seiler T. Riboflavin/ultraviolet-a-induced collagen crosslinking for the treatment of keratoconus. *Am J Ophthalmol.* (2003) 135:620–7. doi: 10.1016/S0002-9394(02)02220-1
- Seiler TG, Fischinger I, Koller T, Zapp D, Frueh BE, Seiler T. Customized corneal cross-linking: one-year results. *Am J Ophthalmol.* (2016) 166:14–21. doi: 10.1016/j.ajo.2016.02.029
- Nordström M, Schiller M, Fredriksson A, Behndig A. Refractive improvements and safety with topography-guided corneal crosslinking for keratoconus: 1-year results. *Br J Ophthalmol.* (2017) 101:920–5. doi: 10.1136/bjophthalmol-2016-309210
- Cassagne M, Pierné K, Galiacy SD, Asfaux-Marfaing M-P, Fournié P, Malecaze F. Customized topography-guided corneal collagen cross-linking for keratoconus. *J Refract Surg Thorofare NJ* 1995. (2017) 33:290–7. doi: 10.3928/1081597X-20170201-02
- Sinha Roy A, Dupps WJ. Patient-specific computational modeling of keratoconus progression and differential responses to collagen cross-linking. *Investig Ophthalmology Vis Sci.* (2011) 52:9174. doi: 10.1167/iops.11-7395
- Shetty R, Pahuja N, Roshan T, Deshmukh R, Francis M, Ghosh A, et al. Customized corneal cross-linking using different UVA beam profiles. *J Refract Surg.* (2017) 33:676–82. doi: 10.3928/1081597X-20170621-07
- Belin M, Duncan J. Keratoconus: the ABCD grading system. *Klin Monatsblstter Fon Augenheilkd.* (2016) 233:701–7. doi: 10.1055/s-0042-100626
- Mandell RB, Chiang CS, Klein SA. Location of the major corneal reference points. *Optom Vis Sci Off Publ Am Acad Optom.* (1995) 72:776–84. doi: 10.1097/00006324-199511000-00002
- Silverman RH, Urs R, RoyChoudhury A, Archer TJ, Gobbe M, Reinstein DZ. Epithelial remodeling as basis for machine-based identification of keratoconus. *Investig Ophthalmology Vis Sci.* (2014) 55:1580. doi: 10.1167/iops.13-12578
- Lopes BT, Ramos IC, Dawson DG, Belin MW, Ambrósio R. Detection of ectatic corneal diseases based on pentacam. *Z Fen Med Phys.* (2016) 26:136–42. doi: 10.1016/j.zemedi.2015.11.001
- Sedaghat M-R, Momeni-Moghaddam H, Azimi Khorasani A, Belin MW, Monfared N, Wolffsohn JS, et al. Comparison of keratoconus cone location of different topo/tomographical parameters. *Curr Eye Res.* (2021) 46:1666–72. doi: 10.1080/02713683.2021.1931343
- Luz A, Lopes B, Hallahan KM, Valbon B, Ramos I, Faria-Correia F, et al. Enhanced combined tomography and biomechanics data for distinguishing forme fruste keratoconus. *J Refract Surg.* (2016) 32:479–94. doi: 10.3928/1081597X-20160502-02
- Belin MW, Meyer JJ, Duncan JK, Gelman R, Borgstrom M. Assessing progression of keratoconus and cross-linking efficacy: the Belin ABCD progression display. *Int J Keratoconus Ectatic Corneal Dis.* (2017) 6:1–10. doi: 10.5005/jp-journals-10025-1135
- Shajari M, Steinwender G, Herrmann K, Kubiak KB, Pavlovic I, Plawetzki E, et al. Evaluation of keratoconus progression. *Br J Ophthalmol.* (2019) 103:551–7. doi: 10.1136/bjophthalmol-2017-311651
- Cunha AM, Correia PJ, Alves H, Torráo L, Moreira R, Falcão-Reis F, et al. Keratoconus enlargement as a predictor of keratoconus progression. *Sci Rep.* (2021) 11:21079. doi: 10.1038/s41598-021-00649-0
- Lopes B, Padmanabhan P, Zhang H, Abass A, Eliasy A, Bandeira F, et al. Clinical validation of the automated characterization of cone size and center in keratoconic corneas. *J Refract Surg.* (2021) 37:414–21. doi: 10.3928/1081597X-20210315-03
- Eliasy A, Abass A, Lopes BT, Vinciguerra R, Zhang H, Vinciguerra P, et al. Characterization of cone size and centre in keratoconic corneas. *J R Soc Interface.* (2020) 17:20200271. doi: 10.1098/rsif.2020.0271

Publisher's note

All claims expressed in this article are solely those of the authors and do not necessarily represent those of their affiliated organizations, or those of the publisher, the editors and the reviewers. Any product that may be evaluated in this article, or claim that may be made by its manufacturer, is not guaranteed or endorsed by the publisher.



OPEN ACCESS

EDITED BY

Cristina Nicula,
Iuliu Hațieganu University of Medicine
and Pharmacy, Romania

REVIEWED BY

Reta Birhanu Kitata,
Pacific Northwest National Laboratory
(DOE), United States
Shi Song Rong,
Massachusetts Eye and Ear Infirmary
and Harvard Medical School,
United States

*CORRESPONDENCE

Arantxa Acera
aacara71@gmail.com

SPECIALTY SECTION

This article was submitted to
Ophthalmology,
a section of the journal
Frontiers in Medicine

RECEIVED 15 May 2022

ACCEPTED 23 August 2022

PUBLISHED 20 September 2022

CITATION

Goñi N, Martínez-Soraa I, Ibarrondo O,
Azkargorta M, Elortza F, Galarreta DJ
and Acera A (2022) Tear proteome
profile in eyes with keratoconus after
intracorneal ring segment implantation
or corneal crosslinking.
Front. Med. 9:944504.
doi: 10.3389/fmed.2022.944504

COPYRIGHT

© 2022 Goñi, Martínez-Soraa,
Ibarrondo, Azkargorta, Elortza,
Galarreta and Acera. This is an
open-access article distributed under
the terms of the [Creative Commons
Attribution License \(CC BY\)](https://creativecommons.org/licenses/by/4.0/). The use,
distribution or reproduction in other
forums is permitted, provided the
original author(s) and the copyright
owner(s) are credited and that the
original publication in this journal is
cited, in accordance with accepted
academic practice. No use, distribution
or reproduction is permitted which
does not comply with these terms.

Tear proteome profile in eyes with keratoconus after intracorneal ring segment implantation or corneal crosslinking

Nahia Goñi^{1,2}, Itziar Martínez-Soraa^{1,2}, Oliver Ibarrondo³,
Mikel Azkargorta⁴, Felix Elortza⁴, David J. Galarreta⁵ and
Arantxa Acera^{6,7*}

¹Department of Ophthalmology, Hospital Universitario Donostia, San Sebastian, Spain, ²Department of Ophthalmology, University of the Basque Country UPV/EHU, Leioa, Spain, ³RS-Statistics, Arrasate-Mondragón, Spain, ⁴Proteomics Platform, CIC bioGUNE, Basque Research and Technology Alliance (BRTA), CIBERehd, Derio, Spain, ⁵Department of Ophthalmology, Hospital Clínico Universitario de Valladolid, Valladolid, Spain, ⁶Department of Cell Biology and Histology, Experimental Ophthalmology-Biology Group (GOBE: www.ehu.eus/gobe), University of the Basque Country UPV/EHU, Leioa, Spain, ⁷IKERBASQUE, Basque Foundation for Science, Bilbao, Spain

Purpose: Keratoconus (KC) is a corneal ectasia characterized by structural changes, resulting in progressive thinning and biomechanical weakening that can lead to worsening visual acuity due to irregular astigmatism. Corneal collagen Crosslinking (CXL) and Intracorneal Ring Segment (ICRS) are widely used treatments in KC disease, but the alterations they cause in biomechanical mediators are still poorly understood. The aim of this study was to analyze the tear proteome profile before and after treatments to identify biomarkers altered by surgery.

Materials and methods: An observational, prospective, case-control pilot study was conducted, analyzing tear samples from KC patients by nano-liquid chromatography-mass spectrometry (nLC-MS/MS). Data are available via ProteomeXchange with identifier PXD035655. Patients with KC who underwent ICRS surgery ($n = 4$), CXL ($n = 4$), and healthy subjects (Ctrl, $n = 4$) were included in this study. Clinical parameters were measured and tear samples were collected before and 18 months after surgery. Proteins with ≥ 2 expression change and p -value < 0.05 between groups and times were selected to study their role in post-operative corneal changes.

Results: These analyses led to the identification of 447 tear proteins, some of which were dysregulated in KC patients. In comparisons between the two surgical groups and Ctrl, the biological processes that were altered in KC patients at baseline were those that were dysregulated as a consequence of the disease and not of the surgical intervention. Among the biological processes seen to be altered were: immune responses, cytoskeleton components, protein synthesis and metabolic reactions. When comparing the two treatment groups (ICRS and CXL), the process related to cytoskeleton components was the most altered, probably due to corneal thinning which was more pronounced in patients undergoing CXL.

Conclusion: The changes observed in tears after 18 months post-operatively could be due to the treatments performed and the pathology. Among the deregulated proteins detected, A-kinase anchor protein 13 (AKAP-13) deserves special attention for its involvement in corneal thinning, and for its strong overexpression in the tears of patients with more active KC and faster disease progression. However, it should be kept in mind that this is a pilot study conducted in a small number of patients.

KEYWORDS

keratoconus, tear film, intracorneal ring segment, crosslinking, biomarker

Introduction

Keratoconus (KC) is the most common primary corneal ectasia with an estimated incidence of 1 in 2,000 among the general population (1). It is a bilateral and asymmetric pathology that is characterized by a progressive thinning and protrusion of the cornea, predominantly in its inferotemporal or central region. It usually commences at puberty and progresses until the third or fourth decade of life, at which point it does not progress further (2). Less frequently it may initiate earlier in life, following a more aggressive and rapid progression (2–4). There is some variability in the presentation and evolution of this condition, although changes in ocular refraction provoked by the development of irregular astigmatism and the consequent loss of visual acuity (VA) are characteristic features of KC (5–7). The macroscopic and microscopic alterations that can be observed depend on the stage of KC and they include central or paracentral stromal thinning, the protrusion of the cornea as a cone, Fleischer rings, Vogt's striae, prominent corneal nerves, Munson's and Rizzuti's signs, sub-epithelial opacity, and stromal scarring (1).

Despite the studies carried out to date the precise details of the physiopathology of KC remain unknown. It appears to be of multifactorial origin, combining genetic and environmental factors (8–13). Among the factors identified are atopy, chronic eye rubbing or exposure to ultraviolet (UV) light, although there is no clear consensus as to the overall importance of each of these in the physiopathology of the disease (12). Over and above the risk factors that favor the development of this disease are the internal events that give rise to the structural changes associated with this pathology. Proteomics studies of the distinct corneal layers, the tear film and the aqueous humor have provided fundamental information in order to understand the processes that take place during the development of KC (14). Accordingly, inflammation, oxidative stress, enzyme deregulation and cellular hypersensitivity are the pathophysiological events most often described (14–20). Over the years, several studies have been conducted to characterize the human tear proteome using

different proteomic approaches. Based on the most recent literature, the tear proteome is estimated to be around 1500 proteins (21) of which 10% are extracellular. However, although the number of extracellular proteins is not so high, it is instead in terms of their relative concentration and this is due not only to the contribution of the lacrimal gland, but also to the contribution of both corneal and conjunctival epithelial cells. Studies of the tear proteome have identified different patterns of proteins associated with specific pathologic conditions (22, 23). These studies illustrated the usefulness and importance of tear component analysis as a source of insight into the pathologic mechanisms involved in ocular surface disorders. Studies on KC have demonstrated the presence of alterations in the corneal epithelium (24) and stroma (25), but complementary and useful information can also be obtained by biochemical analysis of tears, which are relatively easy to obtain. Tear film stability is a prerequisite for proper optical and metabolic functioning of the eye. It is important to know and understand the terms related to tear stability, the phenomena involved in the different theories proposed, and the techniques to evaluate it in order to make a more accurate diagnosis, leading to effective treatments.

The optimal treatment of KC includes personalized approaches that take into account an evaluation of the patient's visual demands, the degree of KC, its progression or stability, age, and tolerance to visual correction with glasses or contact lenses. Conservative treatment with glasses or contact lenses is reserved for those patients with stable KC or after a surgical procedure, such as cross-linking (CXL), intracorneal ring segment (ICRS) implantation or keratoplasty. The therapeutic approach in young patients with progressive KC has been modified by the introduction of CXL, a surgical procedure that halts its progression. This is a procedure particularly recommended for young patients (especially under 25 years of age) with progressive KC, pachymetry above 400 microns, a clear cornea and keratometry values below 60 diopters (D). By contrast, in patients with stable KC, visual affectation and poor adaptation to optical correction, a minimal pachymetry of 400 microns, a clear central cornea and keratometry values

below 60D the recommended procedure is ICRS. Deep Anterior Lamellar Keratoplasty (DALK) and Penetrating Keratoplasty (PK) are only considered in cases that do not meet these indications (26–28).

Crosslinking is a chemical reaction that involves the covalent binding of two or more molecules, changing their physicochemical properties. This is achieved by stimulating crosslinking molecules with physical agents (UV light, heat, pressure), chemical catalysis, or a combination of both (29). The efficacy of CXL with UVA radiation and riboflavin was described in patients with KC, producing a 328.9% increase in the rigidity of the cornea that would explain the positive benefits of CXL in stabilizing KC (30). This efficacy of this approach was later confirmed in clinical studies (31–35). Subsequently, the conventional Dresden protocol was proposed that involved the desepithelialization of the cornea by applying a riboflavin solution (0.1%) for 30 min, followed by irradiation at a wavelength of 370 nm and with a potency of 3 mW/cm² (36). Subsequently, distinct variations of this technique were published using the same surgical technique to limit the adverse effects of conventional CXL. Accelerated CXL, for example, reduces surgical time by applying a higher irradiation dose for a shorter period of time (37).

The implantation of ICRS (33), circular segments of poly(methyl methacrylate) flattens the cornea and recovers its curvature, reducing any astigmatism and representing an alternative to improve the patients vision when astigmatism is strong and/or they tolerate contact lenses poorly (38, 39). These implants act as passive spacers and when placed on the cornea, they provoke the local separation of the corneal layers, which results in a shortening of the anterior corneal curvature and a flattening of the central cornea (29). When only one segment is used, flattening only occurs in that region and there is an increase in curvature in the opposite direction of the ring. Moreover, the thicker the segment, the greater the flattening produced (40). The ICRS can be implanted manually or using a femtosecond laser. Both these procedures have similar clinical results but the use of femtosecond laser is associated with fewer intraoperative complications, and greater precision and predictability (41–43). The distribution of the stress on shortening the layers and changing the shape of the cornea will alter the cycle and the pattern of progressive decompensation, permitting the cornea to adopt a more regular shape over time. Likewise, the natural evolution of the disease toward a stable state could be a determinant in the post-operative progression. However, at present it is unclear what the impact of this treatment might be on the underlying processes (44). The tear is a complex biological fluid that contains mucin, proteins/peptides, electrolytes, lipids, and metabolites.

Despite its relatively small volumes, the tear composition reflects the physiological status of the eye and its underlying systems, and it can provide information regarding ophthalmological and systemic pathologies (21). In fact,

studying the variations in the composition of the tear is a good approach to discover biomarkers. As such, proteomic studies of the tear could explain the changes that occur in the cornea and at the eye surface after CXL and ICRS implantation. The objective of this study was to describe the proteomic changes induced in the tear of patients with KC after performing these two surgical procedures.

Materials and methods

Study cohort

An observational, prospective, interventional case-control pilot study was designed, in which 8 patients with KC and 4 healthy subjects (Ctrl) were included. Patients with KC underwent 2 types of surgery and as such, they were divided into two groups. Group 1 underwent Ferrara ICRS implantation surgery and group 2 underwent corneal accelerated CXL. Group 3 consisted of the 4 Ctrl. This research was carried out by qualified medical personnel after receiving approval from the Ethics Committee at the Hospital Universitario Donostia (Code 2015120). The study was carried out in strict accordance with the principles of the Helsinki Declaration on Biomedical Research Involving Human Subjects. Prior to sample collection, signed informed consent was obtained from all subjects or their legal representatives (in the case of patients under 18 years of age) after the nature and possible consequences of the study were explained.

Patients were recruited consecutively at the Ophthalmology Service of the Hospital Universitario Donostia (San Sebastian, Gipuzkoa, Spain) during outpatient consultations, between January 2018 and February 2019. The follow-up of the patients continued until February 2020. The inclusion criteria applied to the group of patients was the prior diagnosis of KC [mild, moderate or severe (6)], age between 14 and 45 years, and the need to perform a surgical procedure to treat their KC (27). The diagnostic criteria used to confirm KC were based on the topographic criteria of Rabinowitz (1) and the Belin-Ambrosi o algorithm incorporated into the Pentacam® Software (Pentacam HR; Oculus Optikgeräte GmbH, Wetzlar, Germany) regarding corneal thickness (Belin/Ambrosio Enhanced Ectasia Display). The exclusion criteria included any eye surgery carried out prior to recruitment, systemic corticoid or anti-depressive medication, chronic eye medication except for artificial tears or topical anti-histamines, a mean keratometry above 60D or pachymetry below 400 microns. Contact lens wearers were asked to desist from wearing contact lenses for 15 days prior to any testing to avoid any possible interference in the interpretation of results and all patients were asked to avoid scratching their eyes prior to surgeries. Preliminary eye tests and sample collection was performed on the same day. Two visits were

performed, a pre-surgical baseline visit and a post-surgical visit 18 months later.

The patients that displayed a reduction in at least 1 line of vision, an increase of one diopter (D) in the K maximum (Kmax), or a decrease in corneal thickness at its thinnest point of 2% in a period of 6 months or that were at risk of progression [under 16-years-old with central cone defects and decrease in the corrected VA (4)] were included in the CXL group. The patients that did not tolerate contact lenses or that suffered difficulties in adapting to them, or those with greater visual demands than those obtained by optical correction were included in the ICRS implantation group. The demographic and clinical data collected included gender, age, patient's ocular history, medical history (allergy and eye rubbing), and topical and systemic treatments.

Ophthalmological examination

The basal pre-operative and post-operative exploration at 18 months included the uncorrected distance visual acuity (UDVA) and the corrected distance visual acuity (CDVA) as the logarithm of the minimum angle of resolution, the determination of the spherical equivalent (SE) with an autorefractometer and the exploration of the anterior segment by slit lamp biomicroscopy. A Pentacam® (Pentacam HR; Oculus Optikgeräte GmbH, Wetzlar, Germany) apparatus was used for the tomography study of the cornea, through which the following study variables were registered: flat keratometry (K1), steep keratometry (K2), K max, mean keratometry (Mean-K), and the minimal corneal thickness (MCT).

To assess the ocular surface variables and tear function, complementary tests were performed such as the measurement of tear osmolarity (OSM) (TearLab Osmolarity System: Reader, TearLab Co., San Diego, CA, United States), the Ocular Surface Disease Index (OSDI) questionnaire, tear break up time (TBUT), and the Schirmer test (SCH) with anesthesia. These tests were always carried out in the same order at the consultations.

Intracorneal ring segment surgery

All the surgical procedures were carried out as outpatient treatments under topical anesthesia (double Colircusi anesthesia: a collyrium containing 1 mg/ml of tetracaine hydrochloride and 4 mg/ml oxibuprocaine hydrochloride), and strict aseptic conditions of the eye (5% iodinated povidone) and periocular area (10% iodinated povidone). For ICRS implantation, the surgical plan envisaged the number of rings to be implanted, the position of the incisions, the thickness, and the arc of the ring and the diameter of the optic zone in each case. During the intervention, the central point of the cornea

was first marked and the eyeball was fixed through a vacuum system, to which the laser interface was coupled. The corneal tunnel is configured previously to work at a depth of 70–80% of the thinnest point in the rings' trajectory. After making an opening with the femtosecond laser (Technolas, Bausch and Lomb (B&L), Munich, Germany), the rings were introduced with the aid of a Ferrara spatula at the predetermined position. After surgery, post-operative treatment with Tobradex eye drops® (1 mg/ml Dexamethasone and 3 mg/ml Tobramycin) was recommended with a schedule diminishing over 1 month.

Crosslinking

For the CXL procedure, corneal desepithelialization was performed at 9 mm from the central diameter with 20% alcohol and riboflavin (0.1%: VibeX Rapid™, Avedro; Waltham, MA, United States) was applied every 2 min over 10 min. Subsequently, the LED lamp (Avedro® KXL; Waltham, MA, United States) was put in place to apply the UVA radiation with on/off pulses over 8 min, administering a total irradiation of 7.2 J/cm². Finally, the eye was cleaned with abundant physiological serum and a drop Tobradex® was applied, thereafter placing a therapeutic contact lens until re-epithelialization was completed. These patients were recommended to follow the same post-operative treatment as the patients subjected to ICRS.

Tear sample collection

All the tear samples were collected using calibrated 10 µl glass microcapillary tubes (BLAUBRAND intraMark, Wertheim, Germany). Tear samples were obtained from the inferior temporal tear meniscus, minimizing any irritation of the ocular surface or lid margin, and without the installation of anesthesia. The tear samples were collected from both eyes of each participant and immediately placed in precooled Eppendorf tubes. After tear collection, the samples were stored at −80°C in the Basque Biobank¹ following standard operation procedures with appropriate approval of the Ethical and Scientific Committees until their analyses.

Proteomics analyses

The proteomics analyses were carried out at the CIC bioGUNE Proteomics Platform (Derio, Bizkaia, Spain), using the Filter Aided Sample Preparation (FASP) protocol for sample processing and digestion with minor variations (45). Briefly, samples were solubilized in a buffer containing 7M Urea 2M

¹ www.biobancovasco.org

Thiourea and 4% CHAPS and submitted to buffer exchange steps using 30 kDa cutoff AMICON filters, as described in the protocol described by Wiśniewski et al. (45). Trypsin was added at a trypsin:protein ratio of 1:50, and the mixture was incubated overnight at 37°C, dried in a RVC2 25 Speedvac concentrator (Christ) and resuspended in 0.1% Formic Acid (FA). The peptides obtained were desalted and resuspended in 0.1% FA using C18 stage tips (Millipore, St. Louis, MO, United States).

Samples (4 biological replicates except for the control condition, where 5 replicates were used) were analyzed in a novel hybrid trapped ion mobility quadrupole time of flight mass spectrometer (timsTOF Pro with PASEF: Bruker Daltonics, Bremen, Germany), coupled online to a nanoElute liquid chromatograph (Bruker, Coventry, United Kingdom). This mass spectrometer takes advantage of a novel scan mode, termed parallel accumulation serial fragmentation (PASEF), which multiplies the sequencing speed without any loss of sensitivity, and it has been proven to provide outstanding analytical speed and sensitivity for proteomics analyses. Samples (200 ng) were loaded directly onto a 15 cm Bruker nanoelute FIFTEEN C18 analytical column (Bruker) and resolved at 400 nl/min. Mass spectrometer was operated in DDA PASEF mode using the standard method provided by the manufacturer. A 30 min linear gradient (3–40% acetonitrile) was used to resolve and analyze the samples. The column was heated to 50°C in an oven.

Protein identification and quantification was carried out using the PEAKS software (Bioinformatics Solutions, Waterloo, ON, Canada). Searches against a database of canonical human Uniprot/Swissprot entries (2020_03 release, 20368 entries, no isoforms considered), with precursor and fragment tolerances of 20 ppm and 0.05 Da. Area-based label-free protein quantification was performed using the PEAKS Q module available in the PEAKS software. Only proteins identified with at least two peptides at a False Discovery Rate (FDR) < 1% at peptide level and present in at least 70% of the samples from one of the experimental groups analyzed were considered for further analysis. The data was loaded onto the Perseus platform and further processed (log2 transformation, imputation) before the application of a Student's *t*-test for differential protein expression analysis.

The mass spectrometry proteomics data have been deposited to the ProteomeXchange Consortium via the PRIDE (46) partner repository with the dataset identifier PXD035655 and 10.6019/PXD035655.

Statistical analyses

A descriptive analysis of the variables by different groups was performed using absolute and relative frequencies in the case of categorical variables, and the median and interquartile

range (IQR) in the case of continuous variables. The non-parametric Mann–Whitney test was used to compare the medians of the groups.

The intensity of the spectrometry signals was transformed to the binary logarithm to reduce the effect of the variability in the results and the subsequent normalization is achieved by iterative rank-order normalization (IRON). The data obtained by mass spectrometry was compared to the human protein database (Homo sapiens database) for identification. The normal distribution of the resulting samples was assessed through a Shapiro–Wilk test and the statistical significance of the mean differences was measured using a Student *t*-test. The pooled comparison of the three groups were established by ANOVA analysis. The *p*-values calculated determine the probability that the association between the proteins in the dataset and a given canonical pathway, functional network or upstream regulator is explained by chance alone, based on a Fisher's exact test with a *p*-value < 0.05 considered to be significant. We also produced volcano plots to identify the differences between the groups in terms of their protein composition, with a 2-fold change and $\alpha = 0.05$ obtained in the test *t*-Student using a Benjamini-Hochberg FDR of 5% as the correction for the multiple tests. The differences in protein expression in each group were determined by calculating the ratios of protein expression per group. Levels of expression between 0.5 and 2-fold were considered similar. The identification of the proteins with the greatest differences between the groups (the most strongly over- or under-expressed) were established by calculating the Euclidean distance. All the data was analyzed using the R-Statistics programming software.

Results

Patients and clinical parameters

Control group

The clinical study of the Ctrl group was performed at only one-time point. This group consisted of four patients with a median age of 33 years (IQR 13.25), with no known ophthalmological or systemic pathologies of interest, nor were they receiving any topical or systemic treatments. Their visual function, refractive and topographic values, and those in reference to the eye surface and tear function were recorded (see Table 1).

The intracorneal ring segment group

The median of age of this group was of 37.5 years and 75% of these patients suffered from allergic disease such as atopic dermatitis, asthma, or allergic conjunctivitis, but unlike the CXL group only 25% of the patients indicated having or having had a habit of rubbing their eyes. Moreover, 25% of them used contact lenses. In the pre-surgical baseline condition, 50% of the eyes

TABLE 1 Comparison of results after treatment with baseline values.

Variable	Ctrl	ICRS			CXL		
	Baseline	Baseline	18 month	P-value	Baseline	18 month	P-value
UDVA (logMAR)	−0.04 (IRQ: 0.29)	0.73 (IQR: 0.30)	0.60 (IQR: 0.36)	0.486	0.55 (IQR: 0.27)	0.61 (IQR: 0.16)	1.000
CDVA (logMAR)	−0.13 (IRQ: 0.10)	0.22 (IQR: 0.21)	0.10 (IQR: 0.07)	0.234	0.28 (IQR: 0.17)	0.12 (IQR: 0.07)	0.309
SE (D)	0.32 (IRQ: 0.65)	−4.31 (IQR: 2.32)	−3.25 (IQR: 2.75)	0.800	−7.75 (IQR: 4.00)	−6.77 (IQR: 3.60)	0.800
K1 (D)	42.35 (IRQ: 0.93)	47.55 (IQR: 3.25)	45.95 (IQR: 2.47)	0.486	46.80 (IQR: 1.85)	46.75 (IQR: 2.60)	0.686
K2 (D)	43.25 (IRQ: 0.88)	54.50 (IQR: 7.10)	49.85 (IQR: 6.92)	0.343	51.50 (IQR: 1.90)	50.85 (IQR: 1.25)	0.886
Kmax (D)	43.60 (IRQ: 0.95)	62.00 (IQR: 6.55)	58.00 (IQR: 2.27)	0.200	61.40 (IQR: 6.20)	62.05 (IQR: 9.05)	1.000
Mean-K (D)	42.80 (IRQ: 0.83)	53.45 (IQR: 3.25)	47.65 (IQR: 4.93)	0.110	48.35 (IQR: 1.20)	48.50 (IQR: 1.30)	0.657
MCT (μ)	558.00 (IRQ: 58.25)	429.50 (IQR: 6.00)	435.50 (IQR: 6.25)	0.486	451.00 (IQR: 24.00)	436.00 (IQR: 40.00)	0.886
OSM (mOsm/L)	275.50 (IRQ: 3.50)	304.00 (IQR: 0.00)	290.50 (IQR: 9.25)	0.100	304.50 (IQR: 9.75)	313.50 (IQR: 8.50)	0.057
OSDI	2.00 (IRQ: 1.00)	6.50 (IQR: 10.0)	1.00 (IQR: 3.25)	0.301	18.00 (IQR: 12.50)	16.50 (IQR: 13.75)	0.772
TBUT (sec)	11.50 (IRQ: 3.75)	13.50 (IQR: 5.50)	16.00 (IQR: 2.50)	0.306	10.00 (IQR: 2.50)	13.50 (IQR: 7.50)	0.661
SCH (mm)	13.50 (IRQ: 4.00)	14.50 (IQR: 2.75)	10.50 (IQR: 8.25)	0.561	12.00 (IQR: 16.00)	10.50 (IQR: 15.25)	0.663

Values are expressed as median and interquartile range (IQR).

UDVA, uncorrected distance visual acuity (logMAR); CDVA, corrected distance visual acuity (logMAR); SE, spherical equivalent (diopters); K1, flat keratometry (diopters); K2, steep keratometry (diopters); Kmax, maximum keratometry (diopters); Mean-K, mean keratometry (diopters); MCT, minimal corneal thickness (μ); OSM, tear osmolarity (mOsm/L); OSDI, ocular surface disease index; TBUT, tear break up time (seconds); SCH, Schirmer's test (mm). $P < 0.05$ show statistically significant differences.

had moderate KC (K2 45–52D) and the rest had severe KC (K2 > 52D). Only 25% of the patients had chronic treatment with oral iron. The rest had no oral or topical prescription. In the post-operative study of these patients, a functional and refractive improvement from 0.73 to 0.60 for logMAR UCVA and from 0.22 to 0.10 for logMAR BCVA was detected. Moreover, the SE fell by 1,06D. After 18 months, the topographic values indicated a medium flattening of the cornea by 1.6D in K1, 4.65D in K2, 4D in Kmax, and 5.8D in Kmean. The increase in corneal thickness at its thinnest point was 6 microns post-operatively. The complementary ocular surface evaluation tests, OSM, TBUT, SCH, and OSDI questionnaire remained stable over time and with normal values. The differences detected were not statistically significant (Table 1).

Crosslinking group

The group of patients subjected to CXL had a median of age of 17.5 years and all these patients had allergic condition. Although all these patients reported chronic eye rubbing only 50% of them used topical anti-histamines. In addition, 50% of the patient were being treated with topical (inhaled) extraocular corticosteroids and 25% with systemic leukotrien receptor antagonist. Also, half of these patients were occasional users of contact lenses. In the pre-surgical baseline condition, 75% of the eyes showed moderate KC (K2 45–52D) and the rest severe KC (K2 > 52D).

After 18 months, functional and refractive outcomes demonstrated non-significant changes; worsening from 0.55 to 0.61 in UDVA logMAR, improvement from 0.28 to 0.12 in CDVA logMAR, and a reduction of 1D SE (from −7.75 to −6.77). As for the topographic values analyzed (K1, K2, Kmax,

K-mean), there was less than 0.75D variability in each of these parameters and the median of MCT decreased by 15 microns after surgery. As for the complementary tests used to assess changes in ocular surface and tear function, there were no significant changes for either of these variables. However, there was a change in OSM which increased to pathological values (to mild dry eye). None of the changes recorded in the post-operative studies of this group of patients were statistically significant (Table 1).

The nano-liquid chromatography-mass spectrometry data

A total of 447 tear proteins were identified in the samples analyzed here, in agreement with previous tear proteomic studies (21, 23). Several group-specific alterations of the tear proteome were evident in KC patients relative to the controls and proteins with different abundances were detected in all the groups studied. Comparative analyses were performed between the basal state of the three groups, Ctrl versus ICRS, Ctrl versus CXL, and ICRS versus CXL. Moreover, each group was analyzed separately at baseline and 18 months after treatment.

Volcano maps of gene expression were obtained to compare the three groups of patients (ICRS vs. Ctrl, CXL vs. Ctrl, and CXL vs. ICRS), distinguishing between the two time periods considered (baseline and 18 months after the intervention, Figure 1). When the two surgical techniques were compared (CXL vs. ICRS, Figure 1C), differences in protein expression between these techniques were represented at each of the two

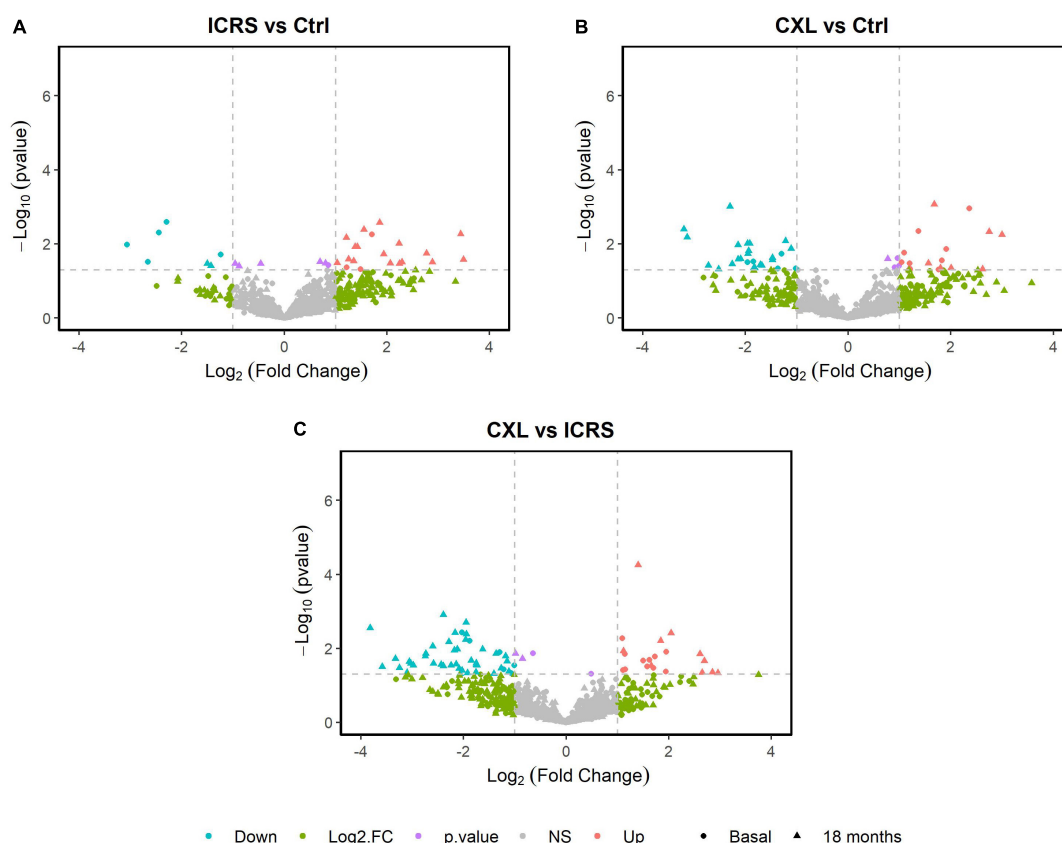


FIGURE 1

Volcano map of protein expression was performed for the pairwise comparison of the three groups; ICRS vs. Ctrl (A), CXL vs. Ctrl (B), and CXL vs. ICRS (C), differentiating between the two time periods considered (Baseline and 18 months).

time points but not a comparison for the two time points for each group (CXL and ICRS). The proteins that displayed the greatest differences in expression (4-fold overexpression and 4-fold under-expression) when comparing the two surgical techniques (ICRS vs. Ctrl, CXL vs. Ctrl, and CXL vs. ICRS) at the baseline and after 18 months are reflected in [Table 2](#). The most relevant selection of the proteins was established through their position in the volcano plots, ordering them according to the differences in the Euclidean distance calculated between their origin and the distance represented by the Fold change [\log_2 (Fold)] and the p -value [$-\log_{10}$ (p -value)]. The proteins with the largest distances represented those with the strongest changes in expression between the groups compared.

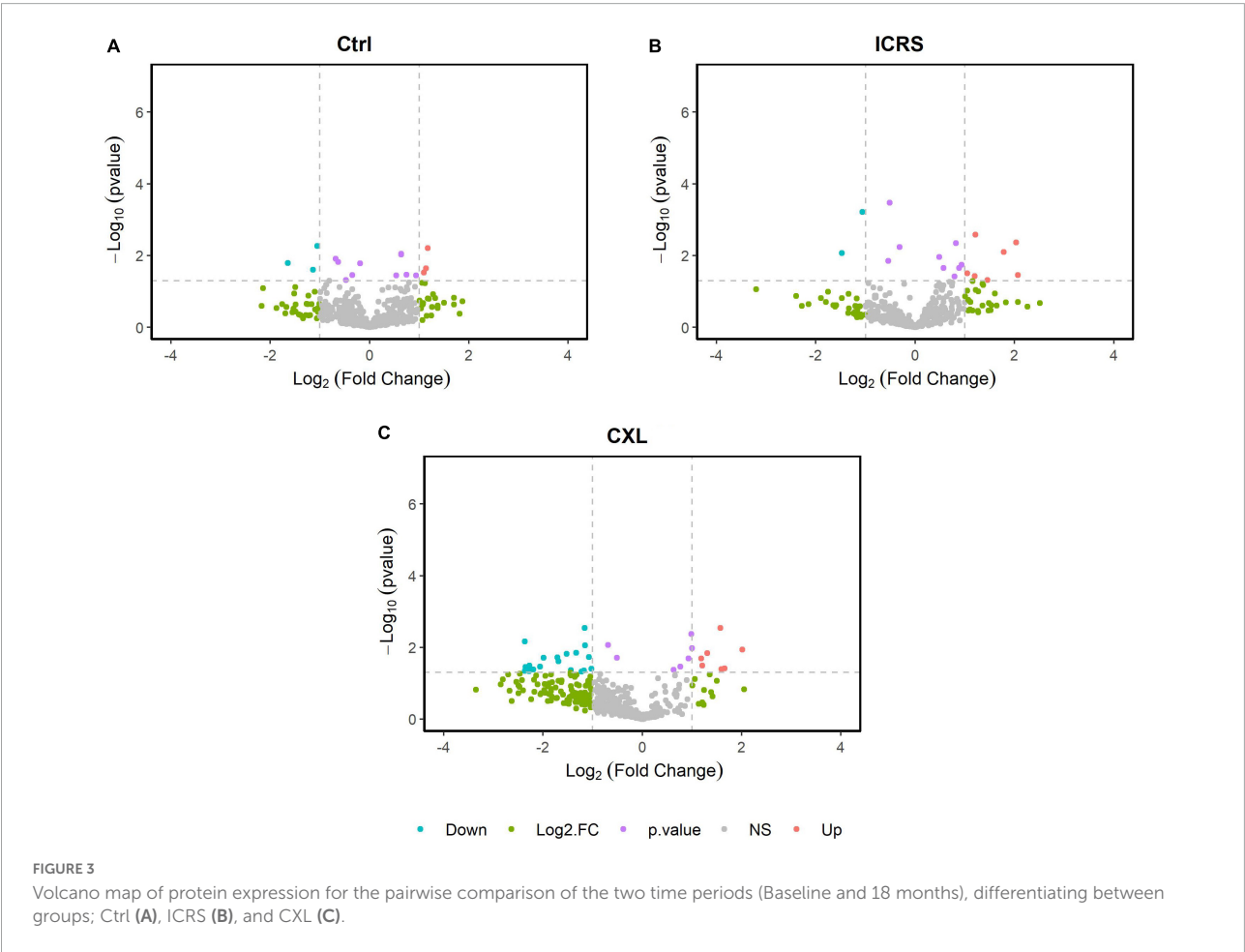
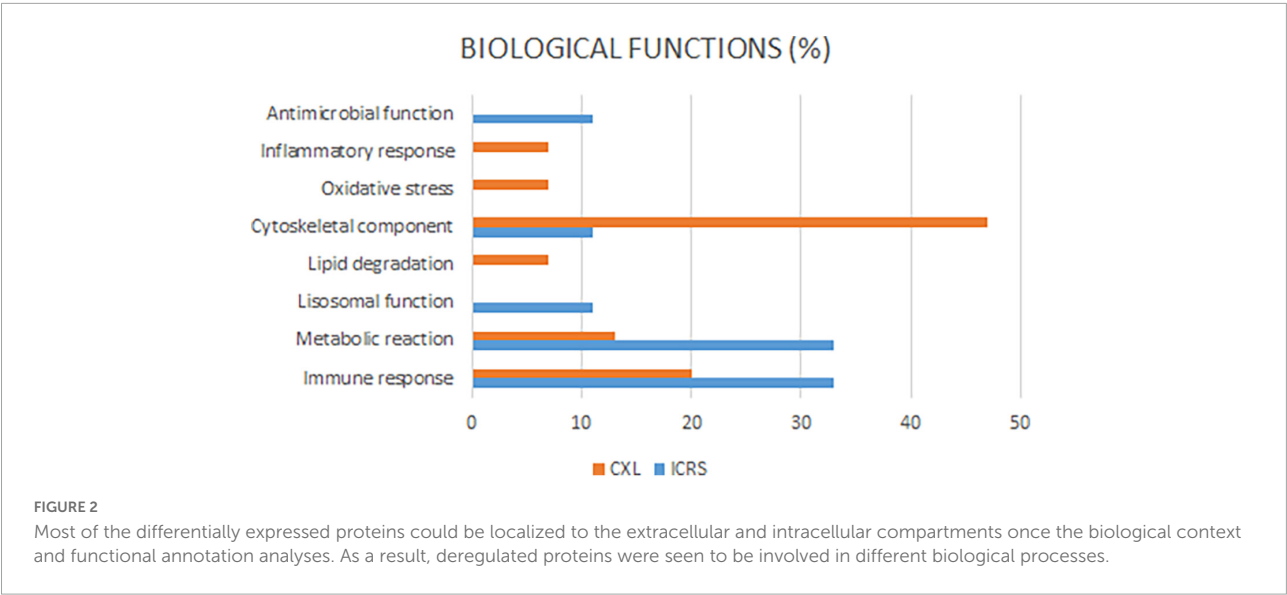
Most of the differentially expressed proteins could be localized to the extracellular and intracellular compartments once the biological context and functional annotation analyses were performed using the different gene ontology (GO) terms. As a result, deregulated proteins were seen to be involved in different biological processes. In the comparisons between the two surgical groups and the Ctrl, the biological processes that were altered in the KC patients (ICRS + CXL) at baseline were those that were deregulated as a consequence of the disease and

not of the surgical intervention. Among the biological processes seen to be altered were: Immune responses (Ig kappa chain V-I region WEA), cytoskeletal components (Desmoplakin), protein synthesis (Proline-rich protein 4), metabolic reactions (Sodium/potassium-transporting ATPase subunit alpha-4, DNA dC → dU-editing enzyme) ([Figure 2](#)). On comparing the two treatment groups (ICRS and CXL), of all the processes altered the most significant was that related to collagen degradation, which was probably provoking the corneal thinning that was most pronounced in the patients subjected to CXL. This was reflected in the 26.98-fold overexpression of the protein A-kinase anchor protein 13 in the tears of the patients in the CXL group relative to that in the tear of patients subjected to ICRS. There was weaker expression of this protein after both of the surgical procedures, although it continues to be more strongly overexpressed in the CXL group than in the ICRS group 18 months after surgery (13.4-fold). The pachymetry was thinner after surgery in the CXL group than in the ICRS group. This is consistent with the corneal collagen fibers remodeling and compaction after CXL, with a difference in corneal pachymetry between the measurement at baseline and after 18 months of -15 and $+6$ microns, respectively. The

TABLE 2 Changes between surgical techniques and control group by time period and expression type.

Period	Group	Entry name	Description	Fold	P-value	
Basal	ICRS/Ctrl	ASC-1	Activating signal cointegrator 1 complex subunit 3	3.26	0.006	
		KV118	Ig kappa chain V-I region WEA	2.81	0.048	
		DSP	Desmoplakin	2.32	0.043	
		CALR	Calreticulin	0.20	0.003	
		AT1A4	Sodium/potassium-transporting ATPase subunit alpha-4	0.18	0.005	
		PROL-4	Proline-rich protein 4	0.16	0.030	
		APOBEC-3A	DNA dC → dU-editing enzyme APOBEC 3A	0.12	0.011	
		CXL/Ctrl	DSP	Desmoplakin	5.13	0.001
			PRG2	Bone marrow proteoglycan	3.77	0.014
			ALS	Insulin-like growth factor-binding protein complex acid	3.55	0.028
	ABCA1		ATP-binding cassette sub-family A member 1	2.58	0.005	
	AMY1		Alpha-amylase 1	0.41	0.019	
	PROM1		Prominin-1	0.39	0.047	
	GLU2B		Glucosidase 2 subunit beta	0.28	0.030	
	MUC5B		Mucin-5B	0.26	0.031	
	CXL/ICRS		AKP13	A-kinase anchor protein 13	26.98	0.019
			ALS	Insulin-like growth factor-binding protein complex acid	3.87	0.012
		CATD	Cathepsin D	3.31	0.017	
		PEDF	Pigment epithelium-derived factor	2.13	0.005	
	18 months	ICRS/Ctrl	ASCC3	Activating signal cointegrator 1 complex subunit 3	0.43	0.037
			CALU	Calumenin	0.41	0.013
			OLFM4	Olfactomedin-4	0.27	0.006
			GLU2B	Glucosidase 2 subunit beta	0.25	0.004
			CO7	Complement component C7	11.23	0.027
MDHM			Malate dehydrogenase mitochondrial	10.83	0.005	
ASAH1			Acid ceramidase	7.38	0.031	
ELNE			Neutrophil elastase	6.83	0.018	
MUC5B			Mucin-5B	0.37	0.039	
PEDF			Pigment epithelium-derived factor	0.35	0.034	
CXL/Ctrl		CO7	Complement component C7	7.97	0.006	
		HPTR	Haptoglobin-related protein	6.70	0.005	
		TFF1	Trefoil factor 1	6.14	0.047	
		ZA2G	Zinc-alpha-2-glycoprotein	3.19	0.001	
		CAP1	Adenylyl cyclase-associated protein 1	0.20	0.001	
		LV211	Ig lambda chain V-II region NIG-84	0.15	0.038	
		IGHG2	Ig gamma-2 chain C region	0.11	0.007	
		MUC5B	Mucin-5B	0.11	0.004	
		CXL/ICRS	AKP13	A-kinase anchor protein 13	13.40	0.05
			APOE	Apolipoprotein E	7.76	0.046
K1C16			Keratin type I cytoskeletal 16	6.09	0.014	
HPTR			Haptoglobin-related protein	4.12	0.004	
ZA2G			Zinc-alpha-2-glycoprotein	2.64	0.000	
CO1			Complement factor I	0.19	0.001	
MMP9	Matrix metalloproteinase-9		0.10	0.019		
ELNE	Neutrophil elastase		0.08	0.031		
CAP1	Adenylyl cyclase-associated protein 1	0.07	0.003			

$P < 0.05$ show statistically significant differences.



changes produced between the two time points (basal and 18 months' post-surgery) were also analyzed for each of the two surgical approaches (Figure 3). At 18 months' post-surgery, up- and downregulated proteins were detected in the two patient groups (Table 3). The changes were established separately for each of the surgical groups, allowing us to see which proteins

TABLE 3 Proteins with the most relevant expression changes before and after the intervention by surgery type.

Group	Entry name	Description	Fold	P-value
ICRS	LV001	Ig lambda chain V region 4A	4.19	0.035
	HS90B	Heat shock protein HSP 90-beta	4.09	0.004
	GYLG	Glycogenin-1	3.44	0.008
	KV113	Ig kappa chain V-I region Lay	2.74	0.048
	LV301	Ig lambda chain V-III region SH	2.32	0.003
	CATD	Cathepsin D	2.30	0.038
	DESP	Desmoplakin	2.07	0.031
	LC1L1	Putative lipocalin 1-like protein 1	0.48	0.001
	AK1A1	Alcohol dehydrogenase [NADP(+)]	0.36	0.009
	AL1A1	Alcohol dehydrogenase [NADP(+)]	0.36	0.009
CXL	K1C9	Keratin type I cytoskeletal 9	4.03	0.012
	TPM2	Tropomyosin beta chain	3.15	0.039
	C1R	Complement C1r subcomponent	3.02	0.040
	ZA2G	Zinc-alpha-2-glycoprotein	2.98	0.003
	SLPI	Antileukoprotease	2.47	0.014
	K1C10	Keratin type I cytoskeletal 10	2.30	0.032
	CY24B	Cytochrome b-245 heavy chain	2.27	0.020
	AHNK	Neuroblast differentiation-associated protein	0.45	0.003
	ML12A	Myosin regulatory light chain 12A	0.25	0.020
	F11	Protein F11	0.22	0.042
	MYH14	Myosin-14	0.21	0.033
	KV206	Ig kappa chain V-II region RPMI 6410	0.21	0.046
	SSPO	SCO-spondin	0.20	0.035
	PROF1	Profilin-1	0.19	0.045
	PGAM1	Phosphoglycerate mutase 1	0.19	0.007

P < 0.05 show statistically significant differences.

were affected in each group of patients as a consequence of surgery. The **Table 3** shows the proteins with the greatest changes in expression after each of the procedures performed.

After ICRS (18 months) the deregulated proteins were mainly implicated in: immune responses (Ig lambda chain V region 4 A, Ig kappa chain V-I region Lay, Ig lambda chain V-III region SH), metabolic reactions (Heat shock protein HSP 90-beta, Glycogenin-1, Alcohol dehydrogenase [NADP (+)]), antimicrobial activity (Putative lipocalin 1-like protein 1), and the cytoskeleton (Cathepsin D, Desmoplakin). By contrast, after

CXL the proteins deregulated were implicated in inflammatory responses (Antileukoprotease), oxidative stress (Cytochrome B-245 heavy chain), metabolic reactions (Phosphoglycerate mutase 1, Zinc-alpha-2-glycoprotein) and immune responses (Complement C1r sub-component, Ig kappa chain V-II region RPMI 6410), and above all they included cytoskeletal components (Keratin type I cytoskeletal 9, Tropomyosin beta chain, Keratin type I cytoskeletal 10, Neuroblast differentiation-associated protein, Myosin regulatory light chain 12A, Myosin-14, Profilin-1: **Table 3**).

Discussion

The pathology of KC was classically not considered an inflammatory disease since it did not possess the typical pattern of cellular infiltrate and vascularization. However, studies in this past decade indicate that an inflammatory cascade may occur at the ocular surface of KC patients due to the presence of enzymes related to collagen degradation and corneal thinning, or through the release of pro-inflammatory cytokines or certain genetic mutations (15, 47). Elsewhere, evidence of oxidative stress was obtained through alterations to antioxidant enzymes, and the accumulation of lipid peroxidation products, elements in the nitric oxide pathways and impaired mitochondrial membrane potentials (48–51).

Here tear samples were analyzed from Ctrl subjects and KC patients subjected to two treatments, CXL or ICRS, obtained at baseline and 18 months after the intervention. From a clinical point of view, the presurgical features of these patients differ. The CXL patients are generally younger and with a greater risk of disease progression, while the ICRS patients are older and with KC that has evolved over a longer period, and that is more stable and severe (e.g., median K2 51.50D CXL, 54.40D ICRS). In addition, the need for treatment for allergic disease is higher in CXL group than in ICRS group, probably because of being a younger group, as part of asthmatic and atopic dermatitis patients show improvement of symptoms in early adulthood (52, 53). Despite these differences, the characteristics of each group did not change throughout the study period, which leads us to believe that the changes observed in patients tear proteomics may be secondary to the procedures performed in each group.

The study of the clinical parameters did not show statistically significant differences between the two study moments. The main explanation for this lack of significance could be the sample size we have ($n = 4$ in each group), the major limitation of the study. Variables related to ocular surface status did not change significantly at the 18-month post-operative period. Therefore, it seems that the changes observed in the tear proteome correspond to the effects of the surgery itself on the cornea and not to changes induced by the procedures on the ocular surface.

Intracorneal ring segment is an effective technique to regulate the cornea that can be explained by the Barraquer thickness law, whereby removing tissue from the center of the cornea or adding tissue to the periphery flattens the curvature of the cornea. This effect is directly proportional to the thickness and inversely proportional to the ring diameter (54). Ferrara rings are made of biocompatible and inert poly (methyl methacrylate). Prior to their implantation in humans their biocompatibility was demonstrated in rabbit corneas, with good medium term tolerance and maintaining the transparency of the central cornea (55). However, the corneal response to this biomaterial is still under study and as yet, aspects such as the importance of the changes in protein expression in the cornea following ICRS and how this may affect the stability of the refractive and visual consequences, as well as in any post-operative complications remains unclear.

For introduction of the Ferrara rings, it is necessary to make of intrastromal tunnel manually or using a femtosecond laser. This laser employs thousands of very short pulses of light close to the infrared spectrum (1053 nm) to create microcavities that separate the corneal tissue (56). As such, both the creation of the intrastromal tunnels with the femtosecond laser as well as the implantation of the rings could induce structural and biomechanical changes, on top of the biological changes in the cornea, which could be reflected in the alterations to the tear proteome of these patients. To better understand the biological processes initiated by this surgery and that develop as a consequence of these procedures, the basal proteome of the tear was compared with that at 18 months' post-surgery of patients subjected to ICRS.

At baseline, proteomic differences were evident in these patients relative to the Ctrl, with the overexpression of some proteins and the downregulation of others. At 18 months' post-surgery, significant differences relative to the baseline were seen for 9 proteins, 7 of which were overexpressed, and 2 downregulated. Among the overexpressed proteins were desmoplakin and cathepsin D, both of which are related to desmosomes. These cell structures are fundamental for intercellular adhesion and the adhesion between cells and the cytoskeleton, as well as in the resistance of the epithelium to mechanical stress (57). However, these proteins have opposing roles, whereby desmoplakin is a desmosome protein that couples intermediate filaments (IFs) to the desmosome plaque (58), while cathepsin D is a protease that acts on fibronectin and laminin in the extracellular matrix (ECM), the expression of which in the desmosomes potentially producing cell shedding (59).

The overexpression of both these proteins could be explained by the findings *in vivo* and *ex vivo* from corneas subjected to ICRS. Confocal microscopy identified large hyperreflective nuclei in the transition from the basal epithelial layers to the intermediate layers in the region covering the rings of some such corneas, as well as signs of an increase in epithelial

mitosis (60). The increase in desmoplakin expression could correspond to the stimulation of epithelial mitosis. Moreover, epithelial hypoplasia in the epithelium covering the rings has been observed, whilst the central epithelium retains a normal structure (61, 62). The epithelium between these two zones is hypertrophic (62), which is related to the biological stress produced by the implant (60). In fact, on removing the rings a recovery of the epithelium is observed (61). The increased cathepsin D expression could be related to this hypoplasia, given that it favors cell shedding.

In addition to epithelial changes, an increase in cell density has been described in the stroma adjacent to the rings (52, 55). However, a reduction in CD34⁺ cells has also been observed in the stroma immediately above and below the rings, which might be related to a reduction in the number of keratocytes, as well as to the changes produced in their phenotype, probably toward phenotypes generating collagen (61). Likewise, anomalous ECM components have been detected around the intrastromal rings that are not evident in the healthy cornea but that appear during repair processes. These components include tenascin-C, fibrillin-1, and proteinases specific to collagen type III, IV (α1/α2), and XIV. In particular stromelysins and some cathepsin F and H have been detected (63). It has been proposed that this overexpression may be due to the participation of keratocytes in stromal remodeling and in degrading the excess fibrosis in the ECM that surrounds the rings as part of the reparative events observed after ring implantation (63). The over expression of cathepsin D in our patients could also form part of this remodeling process. Other members of the cathepsin family have been seen to be elevated in the tear and cornea of patients with KC, like cathepsin S (CATS), relating the amounts in the tear to the increase in corneal curvature (64). Cathepsin B, G and F are also related to secondary fibrosis in ruptures of the Bowman membrane (64), although these other cathepsins were not seen to be overexpressed in our patients.

Both in the pre-operative and post-operative analysis, overexpression of some Immunoglobulin (Ig) chains was seen in the ICRS patients. In the post-operative period, there was a significant increase in the basal expression of Ig chains lambda V region 4A, Ig kappa V-I region Lay, and Ig lambda chain V-III region SH. These chains constitute the light chains of the IgG, IgA, IgM, IgD, and IgE isotypes (65). IgA is the principal Ig in the tear and it has been seen to be downregulated in patients with KC, reinforcing the inflammatory and immunological aspects of the pathology (66). In terms of the light and heavy Ig chains, some differences in their expression have been reported in patients with KC (65, 67), although the significance of this deregulation is unclear. The atopic condition of these patients must be borne in mind given the distinct immunological profile of these patients relative to the control subjects.

The other treatment used, CXL prevents KC by increasing the covalent bonding between the collagen fibers of the corneal stroma, thereby improving the mechanical resistance of the

cornea to deformation (68). Several studies have shown that corneal collagen CXL can delay or prevent the progression of KC, and prevent post-operative corneal dilation (69, 70). After CXL, the diameter of the collagen fibers in the anterior matrix of the cornea increases and there is a loss of keratocytes in the treated area. It might be speculated that the change in corneal hardness after CXL could be due to the differential expression of proteins present in the cornea.

To understand the biological changes in the cornea during corneal remodeling after CXL, we studied the changes in protein expression in the tear of patients before and 18 months after surgery, identifying significant differences in the expression of certain proteins. We focused on proteins that exhibited a tendency to change their expression over time. As indicated previously (67), there were more deregulated proteins at baseline relative to the Ctrl, probably due to an increase in the proteases present in KC and a decrease in keratocyte secretion. However, 18 months after CXL more overexpressed proteins appeared than at baseline, probably due to the changes that occur as a result of the treatment.

Many of the proteins that appear to be overexpressed at 18 months after CXL surgery were components of the cytoskeleton, with Keratin type I cytoskeletal 9 (4.03-fold) and Tropomyosin beta chain (3.15-fold) those most strongly expressed. Keratins are proteins that form the cytoskeleton of epithelial cells, and changes in keratin expression have contributed to the evolutionary adaptation of epithelia to different environments (71). The keratins present in the corneal epithelium and other proteins related to the cytoskeleton could be altered by the effect of UV light on the riboflavin used in the surgical procedure. A significant decrease in collagen types I, III, V, and XII, as well as in the lumican proteins has been proposed in keratoconic corneas (72), as has a reduction in the interfibrillar distance of collagen lamellae and an increase in proteoglycans with abnormalities in their configuration as the disease progresses (73). However, the increase in collagen-related proteins and cytoskeleton components after CXL reflects an active process affecting collagen fibers, strengthening these even though corneal thinning was not stabilized as it is in the ICRS patients. In the patients with more active and aggressive KC who were to undergo CXL, Insulin-like growth factor (IGF) was overexpressed at baseline in the tear. As reported previously when the *ex vivo* modulation of the healing process was studied in keratoconic corneas, more fibroblast growth factor 2 (FGF-2), platelet-derived growth factor (PDGF) and epidermal growth factor (EGF) was found in keratoconic corneas than in the controls, although secondary injury *ex vivo* reduced the EGF, FGF-2, and PDGF concentrations to undetectable levels (74, 75). Accordingly, it was proposed that dysregulation of repair pathways in KC causes the cornea to appear in a state of perpetual injury, even though some repair responses to secondary injuries such as rubbing or contact lens wear are shown.

Here, IGF does not appear in the tears of patients with KC at 18 months in either the CXL or ICRS groups, concluding that the treatments provoked an aggression that caused a decrease in its initial concentration. In addition, proteins related to inflammation were overexpressed, like the antileukoproteinase inhibitor (SLPI, 2.47-fold), and Cytochrome b-245 heavy chain (CY24B, 2.27-fold) related to oxidative stress, indicating that 18 months after treatment, active processes may persist in the corneal microenvironment. The inflammatory process has already been reported and either corneal rubbing of the eyelid, the use of contact lenses or other secondary reactions occurring in the cornea produce markers of inflammation to appear in the tear of patients with KC (47, 64, 76–78). Here, the SLPI protein was seen to be overexpressed, probably due to the intracellular activity caused by treatment. By contrast, the metalloproteinase 9 (MMP-9) that has been widely reported in KC is significantly downregulated (0.10-fold) 18 months after CXL. The decrease in MMP-9 expression at 18 months was greater in CXL patients than in ICRS patients, which may be due to the effect of covalent bonding between collagen fibers that strengthens their resistance and prevents the action of metalloproteases that degrade collagen.

Cells respond to environmental signals by mobilizing signal transduction cascades involving protein kinases and phosphatases. The correct organization of these enzymes in space and time drives the efficient and precise transmission of chemical signals. Cyclic AMP-dependent protein kinase A is compartmentalized through its association with the AKAPs, a family of scaffolds that constrain signaling enzymes to drive essential physiological events. Recently, it was recognized that defective signaling in certain endocrine disorders and cancers proceeds through pathological AKAP complexes (79). Among these proteins, AKAP4 and AKAP9 have been extensively studied as cancer-promoting factors, whereas AKAP12 and recently AKAP13 have been shown to play the opposite role, although their mechanism of action has not been studied in depth. After 18 months of CXL treatment patients still had a corneal thinning of 15 microns compared to the baseline. This may be explained by the strong tear overexpression of the protein A-kinase anchor protein 13 (AKAP13) at baseline and post-surgery, up to 26- and 13-fold, respectively, and it was more strongly expressed in CXL patients whose thinning is more active than in patients with a more stable KC that underwent ICRS.

The cornea is a collagen-rich tissue whose thickness is closely related to normal vision. In a metanalysis on corneal thinning 16 new loci were identified in more than 20,000 European and Asian individuals, some of which conferred a relatively high risk for KC, highlighting the possible involvement of genes associated with the pathogenesis of this disease (80). Functional annotations prioritized eight genes harboring SNPs with strong evidence of regulatory potential (ADAMTS6,

ARID5B, FOXO1, AKAP13, COL4A3, COL8A2, TBL1XR1, and KCMB2). The genes associated with corneal thinning were also shown to be implicated in pathways related to collagen physiology and the KC phenotype, and some of them were implicated in an interaction network involving both (80). Further studies on AKAP13 in KC patients are needed, as its strong overexpression even after treatment (13-fold) makes us suspect that it could be a good tear biomarker for KC patients with strong collagen degradation and corneal thinning.

In conclusion, the study performed here demonstrates the changes in the tear protein profile of KC patients 18 months after two surgical treatments, ICRS and CXL. The changes observed are probably due to the treatments performed and to the pathology, and not so much to the changes produced by the treatments on the ocular surface. Indeed, at 18 months after surgery there were no alterations to the variables used to assess the eye surface. Among the deregulated proteins detected, AKAP-13 deserves special attention because of its involvement in corneal thinning, and due to its strong overexpression in the tears of patients with more active KC and with a more rapid disease progression. However, it should be noted that the results obtained here cannot be directly extrapolated as this was a pilot study performed on a small number of patients, although they should serve as the basis for future studies on larger populations to see if these results are reproducible.

Data availability statement

The mass spectrometry proteomics data have been deposited to the ProteomeXchange Consortium *via* the PRIDE (46) partner repository with the dataset identifier: [10.6019/PXD035655](https://doi.org/10.6019/PXD035655).

Ethics statement

The studies involving human participants were reviewed and approved by Ethics Committee at the Hospital Universitario Donostia (Code: 2015120). Written informed consent to

participate in this study was provided by the participants' legal guardian/next of kin.

Author contributions

AA contributed to conception and design of the study, contributed to analysis and interpretation of the data, and drafted the manuscript. All authors contributed to acquisition of data, revised the manuscript critically for important intellectual content, read and approved the final version of this manuscript, and agreed to be accountable for all aspects of the work in terms of the accuracy or integrity of any part of the work.

Funding

The authors wish to acknowledge the financial support received to carry out this work from: MINECO-Retos Fondos Fender (RTC-2016-48231), ELKARTEK (KK-2019/00086), MINECO-Retos (PID2019-111139RB-I00), ELKARTEK (KK-2021-00023), Proyecto de Investigación y Desarrollo en Salud (GV-2021333047), and FISS-21-RD21/0002/0041.

Conflict of interest

The authors declare that the research was conducted in the absence of any commercial or financial relationships that could be construed as a potential conflict of interest.

Publisher's note

All claims expressed in this article are solely those of the authors and do not necessarily represent those of their affiliated organizations, or those of the publisher, the editors and the reviewers. Any product that may be evaluated in this article, or claim that may be made by its manufacturer, is not guaranteed or endorsed by the publisher.

References

1. Rabinowitz YS. Keratoconus. *Surv Ophthalmol.* (1998) 42:297–319.
2. Mukhtar S, Ambati BK. Pediatric keratoconus: a review of the literature. *Int Ophthalmol.* (2018) 38:2257–66.
3. Olivo-Payne A, Abdala-Figuerola A, Hernandez-Bogantes E, Pedro-Aguilar L, Chan E, Godefrooij D. Optimal management of pediatric keratoconus: challenges and solutions. *Clin Ophthalmol.* (2019) 13:1183–91. doi: 10.2147/OPTH.S183347
4. Soeters N, Van Der Valk R, Tahzib NG. Corneal cross-linking for treatment of progressive keratoconus in various age groups. *J Refract Surg.* (2014) 30:454–60.
5. Wagner H, Barr JT, Zadnik K. Collaborative longitudinal evaluation of keratoconus (CLEK) study: methods and findings to date. *Contact Lens Anterior Eye.* (2007) 30:223–32.
6. Zadnik K, Barr JT, Edrington TB, Everett DE, Jameson M, McMahon TT, et al. Baseline findings in the collaborative longitudinal evaluation of keratoconus (CLEK) study. *Investig Ophthalmol Vis Sci.* (1998) 39:2537–46.
7. Krachmer JH, Feder RS, Belin MW. Keratoconus and related noninflammatory corneal thinning disorders. *Surv Ophthalmol.* (1984) 28:293–322.

8. Mas Tur V, MacGregor C, Jayaswal R, O'Brart D, Maycock N. A review of keratoconus: diagnosis, pathophysiology, and genetics. *Surv Ophthalmol.* (2017) 62:770–83. doi: 10.1016/j.survophthal.2017.06.009
9. Omer K. Epidemiology of Keratoconus worldwide. *Open Ophthalmol J.* (2018) 12:289–99.
10. Millodot M, Shneur E, Albou S, Atlani E, Gordon-Shaag A. Prevalence and associated factors of Keratoconus in Jerusalem: a cross-sectional study. *Ophthalmic Epidemiol.* (2011) 18:91–7. doi: 10.3109/09286586.2011.560747
11. Gordon-Shaag A, Millodot M, Shneur E, Liu Y. The genetic and environmental factors for keratoconus. *Biomed Res Int.* (2015) 2015:24–32.
12. Hashemi H, Heydarian S, Hooshmand E, Saatchi M, Yekta A, Aghamirsalam M, et al. The prevalence and risk factors for Keratoconus: a systematic review and meta-analysis. *Cornea.* (2020) 39:263–70.
13. Woodward MA, Blachley TS, Stein JD. The association between sociodemographic factors, common systemic diseases, and Keratoconus. *Ophthalmology.* (2016) 123:457–65.e2.
14. Soiberman U, Foster J, Jun A, Chakravarti S. Pathophysiology of keratoconus: what do we know today. *Open Ophthalmol J.* (2017) 11:252–61. doi: 10.2174/1874364101711010252
15. Galvis V, Sherwin T, Tello A, Merayo J, Barrera R, Acera A. Keratoconus: an inflammatory disorder? *Eye.* (2015) 29:843–59.
16. Volatier TLA, Figueiredo FC, Connon CHEJ. Keratoconus at a molecular level: a review. *Anat Rec.* (2019) 303:1–9. doi: 10.1002/ar.24090
17. Wisse RPL, Kuiper JJW, Gans R, Imhof S, Radstake TRDJ, Van Der Lelij A. Cytokine expression in keratoconus and its corneal microenvironment: a systematic review. *Ocul Surf.* (2015) 13:272–83. doi: 10.1016/j.jtos.2015.04.006
18. Loukovitis E, Katsanos A, Kozei A, Anogeianakis G, Sfakianakis K, Tsotridou E, et al. The proteins of Keratoconus: a literature review exploring their contribution to the pathophysiology of the disease. *Adv Ther.* (2019) 36:2205–22. doi: 10.1007/s12325-019-01026-0
19. McMonnies CW. Inflammation and keratoconus. *Optom Vis Sci.* (2015) 92:e35–41.
20. Khaled ML, Helwa I, Drewry M, Seremwe M, Estes A, Liu Y. Molecular and histopathological changes associated with keratoconus. *Biomed Res Int.* (2017) 2017:7803029. doi: 10.1155/2017/7803029
21. Zhou L, Beuerman RW. Tear analysis in ocular surface diseases. *Prog Retin Eye Res.* (2012) 31:527–50. doi: 10.1016/j.preteyeres.2012.06.002
22. Tomosugi N, Kitagawa K, Takahashi N, Sugai S, Ishikawa I. Diagnostic potential of tear proteomic patterns in Sjögren's syndrome. *J Proteome Res.* (2005) 4:820–5. doi: 10.1021/pr0497576
23. de Souza GA, Godoy LMF, Mann M. Identification of 491 proteins in the tear fluid proteome reveals a large number of proteases and protease inhibitors. *Genome Biol.* (2006) 7:1–11. doi: 10.1186/gb-2006-7-8-R72
24. Nielsen K, Vorum H, Fagerholm P, Birkenkamp-Demtröder K, Honoré B, Ehlers N, et al. Proteome profiling of corneal epithelium and identification of marker proteins for keratoconus, a pilot study. *Exp Eye Res.* (2006) 82:201–9. doi: 10.1016/j.exer.2005.06.009
25. Wilson SE, Liu JJ, Mohan RR. Stromal-epithelial interactions in the cornea. *Prog Retin Eye Res.* (1999) 18:293–309.
26. Andreanos K, Petrelli M, Droutsas K, Georgalas I, Kymionis G, Hashemi K. Keratoconus treatment algorithm. *Ophthalmol Ther.* (2017) 6:245–62.
27. Mohammadpour M, Heidari Z, Hashemi H. Updates on managements for Keratoconus. *J Curr Ophthalmol.* (2018) 30:110–24. doi: 10.1016/j.joco.2017.11.002
28. Mandathara PS, Stapleton FJ, Willcox MDP. Outcome of keratoconus management: review of the Past 20 Years' contemporary treatment modalities. *Eye Contact Lens.* (2017) 43:141–54. doi: 10.1097/ICL.0000000000000270
29. Adamiak K, Sionkowska A. Current methods of collagen cross-linking: review. *Int J Biol Macromol.* (2020) 161:550–60. doi: 10.1016/j.ijbiomac.2020.06.075
30. Wollensak G, Spoerl E, Seiler T. Stress-strain measurements of human and porcine corneas after riboflavin-ultraviolet-A-induced cross-linking. *J Cataract Refract Surg.* (2003) 29:1780–5. doi: 10.1016/s0886-3350(03)00407-3
31. Poli M, Cornut PL, Balmitgere T, Aptel F, Janin H, Burillon C. Prospective study of corneal collagen cross-linking efficacy and tolerance in the treatment of keratoconus and corneal ectasia: 3-year results. *Cornea.* (2013) 32:583–90. doi: 10.1097/ICO.0b013e31825e8414
32. Chunyu T, Xiujun P, Zhengjun F, Xia Z, Feihu Z. Corneal collagen cross-linking in keratoconus: a systematic review and meta-analysis. *Sci Rep.* (2014) 4:25–31.
33. Goldich Y, Barkana Y, Lior OW, Marcovich AL, Hirsh A, Avni I, et al. Corneal collagen cross-linking for the treatment of progressive keratoconus: 3-year prospective outcome. *Can J Ophthalmol.* (2014) 49:54–9. doi: 10.1016/j.cjco.2013.09.002
34. Kobashi H, Rong SS. Corneal collagen cross-linking for Keratoconus: systematic review. *Biomed Res Int.* (2017) 2017:8145651.
35. Zotov VV, Pashtaev NP, Pozdeeva NA. Corneal collagen cross-linking for keratoconus. *Vestn Oftalmol.* (2015) 131:88–93.
36. Wollensak G, Spoerl E, Seiler T. Riboflavin/ultraviolet-A-induced collagen crosslinking for the treatment of keratoconus. *Am J Ophthalmol.* (2003) 135:620–7.
37. Sorkin N, Varssano D. Corneal collagen crosslinking: a systematic review. *Ophthalmologica.* (2014) 232:10–27.
38. Vega-Estrada A, Alio JL, Brenner LF, Javaloy J, Plaza Puche AB, Barraquer RI, et al. Outcome analysis of intracorneal ring segments for the treatment of keratoconus based on visual, refractive, and aberrometric impairment. *Am J Ophthalmol.* (2013) 155:575–84.e1. doi: 10.1016/j.ajo.2012.08.020
39. Torquetti L, Ferrara G, Almeida F, Cunha L, Araujo LPN, Machado AP, et al. Intrastromal corneal ring segments implantation in patients with keratoconus: 10-year follow-up. *J Refract Surg.* (2014) 30:22–6. doi: 10.3928/1081597X-20131217-02
40. Burris TE, Baker PC, Ayer CT, Loomas BE, Mathis ML, Silvestrini TA. Flattening of central corneal curvature with intrastromal corneal rings of increasing thickness: an eye-bank eye study. *J Cataract Refract Surg.* (1993) 19:182–7. doi: 10.1016/S0886-3350(13)80404-X
41. Shabayek MH, Alió JL. Intrastromal corneal ring segment implantation by femtosecond laser for Keratoconus correction. *Ophthalmology.* (2007) 114:1643–52.
42. Ertan A, Kamburoğlu G, Bahadır M. Intacs insertion with the femtosecond laser for the management of keratoconus. one-year results. *J Cataract Refract Surg.* (2006) 32:2039–42. doi: 10.1016/j.jcrs.2006.08.032
43. Kubaloglu A, Sari ES, Cinar Y, Cingu K, Koçtak A, Coşkun E, et al. Comparison of mechanical and femtosecond laser tunnel creation for intrastromal corneal ring segment implantation in keratoconus: prospective randomized clinical trial. *J Cataract Refract Surg.* (2010) 36:1556–61. doi: 10.1016/j.jcrs.2010.04.028
44. Ertan A, Kamburoğlu G. Intacs implantation using a femtosecond laser for management of keratoconus: comparison of 306 cases in different stages. *J Cataract Refract Surg.* (2008) 34:1521–6. doi: 10.1016/j.jcrs.2008.05.028
45. Wiśniewski JR, Zougman A, Nagaraj N, Mann M. Universal sample preparation method for proteome analysis. *Nat Methods.* (2009) 6:359–62.
46. Perez-Riverol Y, Bai J, Bandla C, Garcia-Seisdedos D, Hewapathirana S, Kamathinathan S, et al. The PRIDE database resources in 2022: a hub for mass spectrometry-based proteomics evidences. *Nucleic Acids Res.* (2022) 50:D543–52. doi: 10.1093/nar/gkab1038
47. Lema I, Sobrino T, Durán JA, Brea D, Díez-Feijoo E. Subclinical keratoconus and inflammatory molecules from tears. *Br J Ophthalmol.* (2009) 93:820–4. doi: 10.1136/bjo.2008.144253
48. Buddi R, Lin B, Atilano SR, Zorapapel NC, Kenney MC, Brown DJ. Evidence of oxidative stress in human corneal diseases. *J Histochem Cytochem.* (2002) 50:341–51.
49. Udar N, Atilano SR, Small K, Nesburn AB, Kenney MC. SOD1 haplotypes in familial keratoconus. *Cornea.* (2009) 28:902–7.
50. Atilano SR, Coskun P, Chwa M, Jordan N, Reddy V, Le K, et al. Accumulation of mitochondrial DNA damage in keratoconus corneas. *Investig Ophthalmol Vis Sci.* (2005) 46:1256–63.
51. Kenney MC, Brown DJ, Rajeev B. Everett Kinsey lecture. The elusive causes of keratoconus: a working hypothesis. *CLAO J.* (2000) 26:10–3.
52. Margolis JS, Abuabara K, Bilker W, Hoffstad O, Margolis DJ. Persistence of mild to moderate atopic dermatitis. *JAMA Dermatol.* (2014) 150:593–600.
53. Holgate ST, Wenzel S, Postma DS, Weiss ST, Renz H, Sly PD. Asthma. *Nat Rev Dis Prim.* (2015) 1:1–22.
54. Zare MA, Hashemi H, Salari MR. Intracorneal ring segment implantation for the management of keratoconus: safety and efficacy. *J Cataract Refract Surg.* (2007) 33:1886–91.

55. D'Hermies F, Hartmann C, von Ey F, Holzkämper C, Renard G, Pouliquen Y. Biocompatibility of a refractive intracorneal PMMA ring. *Fortschr Ophthalmol Zeitschrift Dtsch Ophthalmol Gesellschaft*. (1991) 88:790–3.
56. Donate D, Albert O, Colliac JP, Tubelis P, Sabatier P, Mourou G, et al. Laser femtoseconde: système de micro-usinage pour chirurgie de la cornée. *J Fr Ophthalmol*. (2004) 27:783–9.
57. Kowalczyk AP, Green KJ. Structure, function, and regulation of desmosomes. *Prog Mol Biol Transl Sci*. (2013) 116:95–118.
58. Bornslaeger EA, Corcoran CM, Stappenbeck TS, Green KJ. Breaking the connection: displacement of the desmosomal plaque protein desmoplakin from cell-cell interfaces disrupts anchorage of intermediate filament bundles and alters intercellular junction assembly. *J Cell Biol*. (1996) 134:985–1001. doi: 10.1083/jcb.134.4.985
59. Patel S, Homaei A, El-Seedi HR, Akhtar N. Cathepsins: proteases that are vital for survival but can also be fatal. *Biomed Pharmacother*. (2018) 105:526–32.
60. Ruckhofer J, Böhnke M, Alzner E, Grabner G. Confocal microscopy after implantation of intrastromal corneal ring segments. *Ophthalmology*. (2000) 107:2144–51.
61. Samimi S, Leger F, Touboul D, Colin J. Histopathological findings after intracorneal ring segment implantation in keratoconic human corneas. *J Cataract Refract Surg*. (2007) 33:247–53. doi: 10.1016/j.jcrs.2006.08.059
62. Andregretti E, Hashimoto M, Domingues MAC, Antunes VAC, Segundo Pde S, Silva MR. Biocompatibility of Ferrara intracorneal ring segment with and without chondroitin sulfate coating: clinical and histopathological evaluation in rabbits. *Acta Cir Bras*. (2013) 28:632–40. doi: 10.1590/s0102-86502013000900002
63. Maguen E, Rabinowitz YS, Regev L, Saghizadeh M, Sasaki T, Ljubimov AV. Alterations of extracellular matrix components and proteinases in human corneal buttons with INTACS for post-laser in situ keratomileusis keratectasia and keratoconus. *Cornea*. (2008) 27:565–73. doi: 10.1097/ICO.0b013e318165b1cd
64. Balasubramanian SA, Mohan S, Pye DC, Willcox MDP. Proteases, proteolysis and inflammatory molecules in the tears of people with keratoconus. *Acta Ophthalmol*. (2012) 90:303–9. doi: 10.1111/j.1755-3768.2011.02369.x
65. McKay TB, Serjersen H, Hjortdal J, Zieske JD, Karamichos D. Characterization of tear immunoglobulins in a small-cohort of keratoconus patients. *Sci Rep*. (2020) 10:1–8. doi: 10.1038/s41598-020-66442-7
66. Balasubramanian SA, Pye DC, Willcox MDP. Levels of lactoferrin, secretory IgA and serum albumin in the tear film of people with keratoconus. *Exp Eye Res*. (2012) 96:132–7. doi: 10.1016/j.exer.2011.12.010
67. Acera A, Vecino E, Rodríguez-Agüirretxe I, Aloria K, Arizmendi JM, Morales C, et al. Changes in tear protein profile in keratoconus disease. *Eye*. (2011) 25:1225–33.
68. Spoerl E, Huhle M, Seiler T. Induction of cross-links in corneal tissue. *Exp Eye Res*. (1998) 66:97–103.
69. Wollensak G. Corneal collagen crosslinking: new horizons. *Expert Rev Ophthalmol*. (2010) 5:201–15.
70. Gomes JAP, Tan D, Rapuano CJ, Belin MW, Ambrósio R, Guell JL, et al. Global consensus on keratoconus and ectatic diseases. *Cornea*. (2015) 34:359–69.
71. Osborn M, Weber K. Tumor diagnosis by intermediate filament typing: a novel tool for surgical pathology. *Lab Invest*. (1983) 48:372–94.
72. Chaerkady R, Shao H, Scott SG, Pandey A, Jun AS, Chakravarti S. The keratoconus corneal proteome: loss of epithelial integrity and stromal degeneration. *J Proteomics*. (2013) 87:122–31. doi: 10.1016/j.jpro.2013.05.023
73. Takahashi A, Nakayasu K, Okisaka S, Kanai A. [Quantitative analysis of collagen fiber in keratoconus]. *Nihon Ganka Gakkai Zasshi*. (1990) 94:1068–73.
74. Cheung IMY, Mcghee CNJ, Sherwin T. A new perspective on the pathobiology of keratoconus: interplay of stromal wound healing and reactive species-associated processes. *Clin Exp Optom*. (2013) 96:188–96. doi: 10.1111/cxo.12025
75. Cheung IM, Mcghee CN, Sherwin T. Deficient repair regulatory response to injury in keratoconic stromal cells. *Clin Exp Optom*. (2014) 97:234–9. doi: 10.1111/cxo.12118
76. Lema I, Durán JA, Ruiz C, Díez-Feijoo E, Acera A, Merayo J. Inflammatory response to contact lenses in patients with keratoconus compared with myopic subjects. *Cornea*. (2008) 27:758–63. doi: 10.1097/ICO.0b013e31816a3591
77. Lema I, Durán JA. Inflammatory molecules in the tears of patients with keratoconus. *Ophthalmology*. (2005) 112:654–9.
78. Recalde JJ, Durán JA, Rodríguez-Agüirretxe I, Soria J, Sánchez-Tena MA, Pereiro X, et al. Changes in tear biomarker levels in keratoconus after corneal collagen crosslinking. *Mol Vis*. (2019) 25:12–21.
79. Bucko PJ, Scott JD. Drugs that regulate local cell signaling: AKAP targeting as a therapeutic option. *Annu Rev Pharmacol Toxicol*. (2021) 61:361–79. doi: 10.1146/annurev-pharmtox-022420-112134
80. Mirshahi A, Hewitt AW, Koehn D, Hysi PG, Ramdas WD, Zeller T, et al. Lu 2013 – genome-wide association analyses identify multiple loci associated. *Nat Genet*. (2014) 45:155–63.



OPEN ACCESS

EDITED BY

Cristina Nicula,
University of Medicine and Pharmacy Iuliu
Hatieganu, Romania

REVIEWED BY

Mehmet Cem Sabaner,
Kutahya Evliya Celebi Training and Research
Hospital, Türkiye
Qingyan Zeng,
Aier Eye Hospital of Wuhan University, China

*CORRESPONDENCE

Abraham Solomon
✉ dr.avi.solomon@gmail.com

†These authors have contributed equally to this work and share first authorship

RECEIVED 22 January 2023

ACCEPTED 24 April 2023

PUBLISHED 12 May 2023

CITATION

Wajnsztajn D, Shmueli O, Tarnovsky Y,
Frucht-Pery J and Solomon A (2023) Outcome
indicators for cross linking in pediatric
keratoconus.

Front. Med. 10:1149641.

doi: 10.3389/fmed.2023.1149641

COPYRIGHT

© 2023 Wajnsztajn, Shmueli, Tarnovsky,
Frucht-Pery and Solomon. This is an open-
access article distributed under the terms of
the [Creative Commons Attribution License
\(CC BY\)](https://creativecommons.org/licenses/by/4.0/). The use, distribution or reproduction
in other forums is permitted, provided the
original author(s) and the copyright owner(s)
are credited and that the original publication in
this journal is cited, in accordance with
accepted academic practice. No use,
distribution or reproduction is permitted which
does not comply with these terms.

Outcome indicators for cross linking in pediatric keratoconus

Denise Wajnsztajn[†], Or Shmueli[†], Yehuda Tarnovsky,
Joseph Frucht-Pery and Abraham Solomon*

Department of Ophthalmology, Hadassah-Hebrew University Medical Center, Jerusalem, Israel

Purpose: To evaluate the predictive factors for successful corneal collagen cross-linking (CXL) in pediatric patients with Keratoconus (KC).

Methods: This retrospective study was conducted using a prospectively built database. Patients (18 years old or younger) underwent CXL for KC between 2007 and 2017, with a 1-year follow-up period or longer. The outcomes included changes in Kmax (delta $[\Delta]$ $K_{max} = K_{max_{last}} - K_{max_{pre}}$) and LogMAR visual acuity ($\Delta LogMAR = LogMAR_{last} - LogMAR_{pre}$).

The effects of CXL type (accelerated or non-accelerated), demographics (age, sex, background of ocular allergy, ethnicity), preoperative LogMAR visual acuity, maximal corneal power (Kmax), pachymetry (CCT_{pre}), refractive cylinder, and follow-up (FU) time on the outcomes were analyzed.

Results: One hundred thirty-one eyes of 110 children were included (mean age, 16 ± 2 years; range, 10–18 years). Kmax and LogMAR improved from baseline to last visit: from $53.81 D \pm 6.39 D$ to $52.31 D \pm 6.06 D$ ($p < 0.001$) and from 0.27 ± 0.23 LogMAR units to 0.23 ± 0.19 LogMAR units ($p = 0.005$), respectively. A negative ΔK_{max} (meaning corneal flattening) was associated with a long FU, low CCT_{pre} , high $K_{max_{pre}}$, high $LogMAR_{pre}$, and non-accelerated CXL on univariate analysis. High $K_{max_{pre}}$ and non-accelerated CXL were associated with negative ΔK_{max} in the multivariate analysis.

A negative $\Delta LogMAR$ (meaning vision improvement) was associated with a high $LogMAR_{pre}$ in univariate analysis.

Conclusion: CXL is an effective treatment option in pediatric patients with KC. Our results showed that the non-accelerated treatment was more effective than the accelerated treatment. Corneas with advanced disease had a greater effect on CXL.

KEYWORDS

keratoconus, cross-linking, outcome indicators, predictive factors, efficacy, pediatric

Introduction

Keratoconus (KC) is a progressive corneal ectasia characterized by progressive central or paracentral thinning, protrusion, and irregular astigmatism, with the potential for severe visual loss. KC onset occurs between the first decade of life and puberty. Younger patients, especially young males (1), often present with more advanced and severe disease, a rapidly progressive course, and significant asymmetry (2–4). Advanced KC causes significant visual impairment and is of particular concern to this population because it may critically impact young patients' social, educational, and professional development.

Corneal collagen cross-linking (CXL) is used to strengthen the cornea by photochemically creating new covalent bonds within and between amino acid residues in the collagen fibers of the cornea through a combination of vitamin B₂ (riboflavin) and longer-wavelength ultraviolet A radiation (370 nm). This increases the biomechanical strength of the keratoconic cornea and halts ectasia progression of ectasia (5).

To date, the maximum corneal power (K_{\max}) and visual acuity (measured as the minimum angle of resolution [logMAR]) are acceptable parameters for evaluating CXL efficacy and safety, respectively (6). The success of CXL in pediatric patients is conflicting. While some studies agree that CXL in this population can stop KC progression (7–13), others claim that this treatment is insufficient or only partially effective, showing disease progression in up to 55% of treated eyes (14–19).

The main shortcomings of the current literature on pediatric CXL are the small number of studies with more than 100 eyes and short follow-up times, with only one randomized controlled study to date (20). Moreover, most studies compared final outcomes to baseline preoperative measures, and there is a lack of studies that systematically evaluated the factors predicting CXL success using a multivariate analysis approach (21).

Our study used multivariate analysis to evaluate long-term outcomes and preoperative predictors of successful CXL treating KC in children.

Materials and methods

Study design and patient selection

This was a retrospective cohort study. We collected data from patients with KC treated with CXL between 2007 and 2017 at the Department of Ophthalmology Cornea Service of Hadassah-Hebrew University Medical Center (Jerusalem, Israel).

This study adhered to the principles of the Declaration of Helsinki. Approval was obtained from the Institutional Review (IRB) Board/Ethics Committee (approval number 18-0221).

The included patients were aged 18 years or younger at the time of treatment and underwent CXL for progressive KC. Informed consent was obtained from the legal guardian (aged <18 years), allowing for treatment. The IRB waived the requirement for informed consent for participation in this study owing to the retrospective and anonymous nature of data analysis.

KC was diagnosed based on topographic features (EyeSys 2000; EyeSys Vision Inc., Houston, Texas, USA) (22).

Progression of KC was defined as an increase of at least 1.00 D in K_{\max} or in the refractive cylinder within 1 year or a patient's report of deteriorating visual acuity without any other underlying cause in cases where previous refraction or topographic assessment was not possible.

Before CXL, we performed a complete eye examination with anterior segment evaluation, intraocular pressure measurement, Schirmer test, and central corneal thickness measurement [CCT (Corneo-Gage Plus™, Sonogage, Cleveland, OH, USA)]. Any abnormalities were managed before CXL was performed.

Follow-up lasted for at least 1 year after CXL treatment.

Exclusion criteria included insufficient follow-up time (less than 1 year after CXL) and insufficient critical data for calculating primary outcomes (e.g., lack of $K_{\max_{\text{pre}}}$ measurement).

CXL was not performed in patients with active ocular surface disease, a history of herpes, stable KC, or pregnant women.

Corneal cross-linking procedure

All CXL procedures involve epithelium-off (epi-off). After the application of topical anesthetics, a slit lamp-assisted corneal abrasion of 8 mm diameter was made using a blunt spatula, and isotonic [0.1% riboflavin, 20% dextran (MedioCROSS D, Avedro)] or hypotonic (0.1% riboflavin (MedioCROSS H, Avedro) in corneas <400 μm) riboflavin was applied every 3 min for 30 min. Pachymetry was performed to ensure CCT >400 μm before UVA exposure. None of the patients in our study required general anesthesia.

The cornea was subsequently exposed to a 3-mW/cm² 365-nm UV light source for 30 min in the non-accelerated (Dresden) protocol, or to a 9-mW/cm² 365-nm UV light source for 10 min in the accelerated protocol (UV-X™ Specifications, IROC, Zurich, Switzerland). In both protocols, a total of 5.4 J/cm² energy was delivered.

Subsequently, a 17 mm soft bandage contact lens (BCL; Sophlex, Israel) was placed on the cornea for at least 7 days or until complete re-epithelialization was evident. The patients received topical 0.1% dexamethasone and 0.3% gentamycin three and four times a day, respectively, for a week. After 7 days or when complete epithelialization was evident, BCL was removed, and topical fluorometholone 0.1% was applied three times a day for an additional 3 months.

Follow-up examinations were performed at 1, 3, 6, and 12 months of the first year and then yearly, including topography, uncorrected and corrected distance visual acuity (CDVA), and manifest refraction.

Data collection

We retrospectively recorded data from a prospectively built database of patients who underwent CXL for KC at the Cornea Service of The Ophthalmology Department of Hadassah Medical Center. The predictive factors documented included age at treatment, gender, a background of ocular allergy (diagnosis of allergic keratoconjunctivitis, vernal keratoconjunctivitis (VKC), undefined ocular allergy, or significant papillary reaction), ethnicity (Arabic or Jewish origin), follow-up period (in months), CCT at treatment (CCT_{pre} in microns), accelerated or non-accelerated (Dresden) protocol, K_{\max} before

Abbreviations: CDVA, Corrected distance visual acuity; K_{\max} , Maximal corneal curvature; $K_{\max_{\text{pre}}}$, Maximal corneal curvature before cross-linking; $K_{\max_{\text{last}}}$, Maximal corneal curvature after cross-linking at last follow up; $\log MAR_{\text{pre}}$, Logarithm of minimal angle of resolution; $\log MAR_{\text{pre}}$, Logarithm of minimal angle of resolution before cross-linking; $\log MAR_{\text{last}}$, Logarithm of minimal angle of resolution after cross-linking at last follow up; Cyl_{pre} , Refractive cylinder before cross-linking; CCT_{pre} , Central corneal thickness before cross linking; SE_{pre} , Spherical equivalent before cross-linking; CXL, Cross-linking; KC, Keratoconus; SD, Standard deviation.

treatment ($K_{\max_{\text{pre}}}$, in diopters), CDVA in LogMAR before treatment ($\text{LogMAR}_{\text{pre}}$), and refractive cylinder before treatment (Cyl_{pre} , in diopters).

Data were collected between 2007 and 2017. Visual acuity was tested using a Snellen chart and was converted to a logMAR visual acuity score. Cyl was extracted from manifest refraction, and CCT was obtained using the Corneo-Gage Plus™. The maximal corneal power (K_{\max}) was obtained using EyeSys through an axial numeric map provided by the topographer. The highest values were recorded and used for comparison (23).

Data analysis

The two study outcome measures were changes in K_{\max} (Delta K_{\max}) and visual acuity (Delta LogMAR) after CXL.

Delta K_{\max} was defined as the difference between the maximal corneal power (in diopters) at the last follow-up ($K_{\max_{\text{last}}}$) and the maximal corneal power before CXL ($K_{\max_{\text{pre}}}$): $\Delta K_{\max} = K_{\max_{\text{last}}} - K_{\max_{\text{pre}}}$.

Delta logMAR was defined as the difference in logMAR CDVA between the last follow-up ($\text{LogMAR}_{\text{last}}$) and logMAR before treatment ($\text{LogMAR}_{\text{pre}}$): $\Delta \text{LogMAR} = \text{LogMAR}_{\text{last}} - \text{LogMAR}_{\text{pre}}$.

A value of 0 or negative values in Delta K_{\max} or Delta LogMAR indicated no decrease (stabilization) or improvement in K_{\max} or CDVA, respectively, demonstrating a favorable effect of CXL.

Delta K_{\max} and Delta LogMAR were analyzed using paired Student's *t*-tests to evaluate the significance of the changes.

We first tested the effects of the independent variables on the outcome measures (Delta K_{\max} and Delta LogMAR) using a univariate analysis. We used the paired *t*-test, Mann–Whitney test and Pearson's correlation (with *r* coefficient) for continuous variables, including age, $\text{LogMAR}_{\text{pre}}$, $K_{\max_{\text{pre}}}$, CCT_{pre} , Cyl_{pre} , and follow-up time. We used the chi-squared test for categorical variables, including accelerated or non-accelerated CXL, sex, ocular allergic background, and ethnicity.

Subsequently, variables that demonstrated a significant effect on either outcome measure in the univariate analysis were included in the multivariate analysis using stepwise linear regression.

p values < 0.05 were considered statistically significant.

Data were analyzed using SPSS version 24.0 (IBM).

Results

We included 131 eyes of 110 patients. The mean follow-up was 32.76 ± 21.03 months (range: 12–104.47 months). The baseline patient characteristics are presented in Table 1. Hypotonic riboflavin was applied before CXL in 10 eyes with $\text{CCT} < 400 \mu\text{m}$. All these eyes except for two achieved a minimal CCT of $400 \mu\text{m}$ after the instillation of hypotonic riboflavin before UVA treatment. These two eyes had CCT of 380 and $397 \mu\text{m}$, respectively. Treatment was performed because of the potentially high risk of vision loss due to advanced KC. There were no complications in these eyes, including corneal edema or scarring.

Annual post-CXL data were unavailable for all patients throughout follow-up; the number of patients and eyes for which data were available for analysis are indicated in the tables and figures below.

TABLE 1 Baseline patient's characteristics.

Baseline continuous variables			
Variables	¹ N	Median	Mean± ² SD (Min–Max)
Age (years)	131	16.00	15.71 ± 2.07 (10; 18)
Follow up (months)	131	24.97	32.76 ± 21.03 (12.0; 104.47)
³ Pachymetry (microns)	128	470.00	464.78 ± 44.71 (328– 575)
⁴ Kmax _{pre} (D)	131	52.40	53.81 ± 6.39 (42.70– 70.10)
⁵ LogMAR _{pre}	129	0.22	0.27 ± 0.23 (0–1.96)
⁶ Cyl _{pre} (D)	120	–3.25	–4.11 ± 3.00 (–12.50; 0)
Baseline categorical variables			
Accelerated/ non-accelerated	N = 131	Non-accelerated	41 eyes
		Accelerated	90 eyes
Gender	N = 131	Male	102 eyes
		Female	29 eyes
Ethnicity	N = 128	Jewish	101 eyes
		Arabic	27 eyes
Allergy	N = 131	Allergy	35 eyes
		No allergy	96 eyes
Baseline characteristics of accelerated\ non-accelerated treatment groups			
Variable	Non- accelerated	Accelerated	p-value
Age (years)	16.22	15.48	0.057
Follow up (months)	55.23	23.02	<0.001**
Pachymetry (microns)	453.90	469.55	0.068
Kmax _{pre}	56.4810	52.5900	0.001
LogMAR _{pre}	0.3387	0.2359	0.018
Cyl _{pre} (D)	–4.016	–4.145	0.810
Sex (male)	80.5%	76.7%	0.625
Allergy	14.6%	32.2%	0.035
Ethnicity (Jewish)	71.1%	82.2%	0.157

Continuous variables are presented by Mean, median, standard deviation and minimum/maximum values. Comparison of baseline characteristics of accelerated/non-accelerated treatment groups was analyzed with *t*-test and χ^2 test, respectively. Bold values are for *p*-values of significance.

¹N = number of eyes with available data.

²SD = standard deviation.

³Pachymetry was measured before corneal epithelial removal.

⁴ $K_{\max_{\text{pre}}}$ = maximal corneal power before cross-linking.

⁵ $\text{LogMAR}_{\text{pre}}$ = Logarithm of minimal angle of resolution before cross-linking.

⁶ Cyl_{pre} = refractive cylinder before cross-linking.

**p* < 0.05.

***p* < 0.01.

K_{\max} and Delta K_{\max} outcome

A total of 131 eyes of 110 children had available K_{\max} results for a minimum of 1 year and were included in this analysis. Mean K_{\max}

decreased from $53.81 \text{ D} \pm 6.39 \text{ D}$ to $52.31 \text{ D} \pm 6.06 \text{ D}$ ($p < 0.001$) at the last follow-up.

The mean Delta Kmax was $-1.495 \pm 2.946 \text{ D}$ (median -1.200).

Among the eyes, 52.6% had Delta Kmax $\leq -1\text{D}$ (improvement following treatment), 31.6% had Delta Kmax between -1D and $+1\text{D}$ (stable), and 15.8% had Delta Kmax $\geq +1\text{D}$ (post-treatment progression).

Mean Delta Kmax values did not differ significantly between hypotonic (10 eyes; Mean Delta Kmax $= -3.9$) and isotonic (121 eyes; Mean Delta Kmax $= -1.3$) riboflavin pre-CXL instillation ($p = 0.33$; Mann-Whitney test).

Delta Kmax: univariate analysis

Correlation analysis demonstrated a significant correlation between a longer follow-up time ($r = -0.435$; $p < 0.001$) and negative Delta Kmax values, indicating that the treatment effect was greater the further it was measured from the time of treatment (Figure 1).

A significant correlation was also found between a more negative Delta Kmax and thinner corneas ($r = 0.222$; $p = 0.012$; Figure 2), higher Kmax_{pre} ($r = -0.341$; $p < 0.001$; Figure 3), and higher LogMAR_{pre} values ($r = -0.221$; $p = 0.012$; the results of the correlation analysis are presented in Table 2).

More negative Delta Kmax values were observed with the non-accelerated CXL protocol ($p < 0.001$) than with the accelerated CXL protocol (Figure 4).

Other variables had no significant effect on Delta Kmax (Table 2), including age ($p = 0.842$), sex ($p = 0.824$), ethnicity (Jewish or Arabic; $p = 0.177$), Cyl_{pre} ($p = 0.065$), and the presence of ocular allergy ($p = 0.824$).

The percentage of eyes with Delta Kmax ≤ -1 was 82.9% in the non-accelerated protocol group and 38.9% in the accelerated protocol group ($p < 0.001$; Table 3).

Delta Kmax: a multivariate analysis

Only two variables remained significant in the multivariate analysis ($R^2 = 23.2\%$; Table 2). In order of significance, these were accelerated/non-accelerated CXL protocols ($\beta = -2.453$; $p < 0.001$) and Kmax_{pre} ($\beta = -0.096$; $p < 0.001$). Together, these results indicate that the non-accelerated CXL protocol and a higher Kmax pre-CXL positively influenced corneal flattening following CXL treatment in pediatric patients with KC.

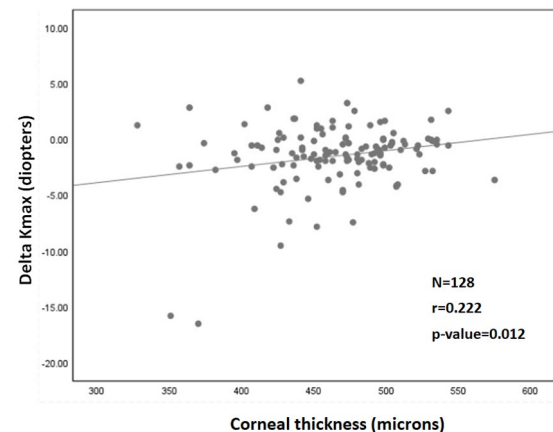


FIGURE 2

Correlation between corneal thickness (pachymetry) and ¹Delta Kmax. More negative Delta Kmax values significantly correlated with thinner corneas, indicating that a thinner cornea can predict a better treatment outcome. However, the correlation coefficient is low, with $r^2 = 0.05$. Thus, although the correlation is significant, it is relatively weak. ¹Delta Kmax = (maximal corneal power after cross-linking) – (maximal corneal power before cross-linking), measured in diopters. ²r = Pearson correlation coefficient.

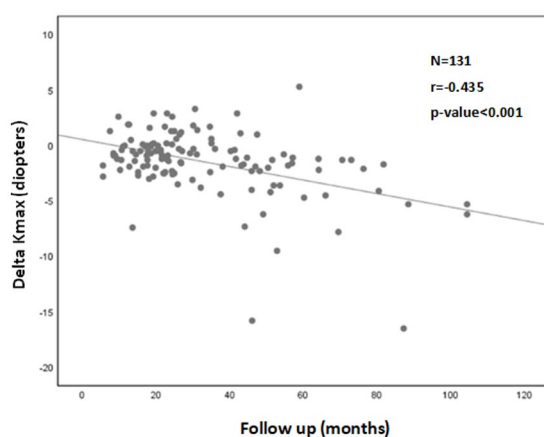


FIGURE 1

Correlation between follow-up time and ¹Delta Kmax. More negative Delta Kmax values were correlated with longer follow-up times, indicating the treatment effect was greater with longer follow-up times. However, the correlation coefficient is low, with $r^2 = 0.19$. Thus, although the correlation is significant, it is relatively weak.

¹Delta Kmax = (maximal corneal power after cross-linking) – (maximal corneal power before cross-linking), measured in diopters.

²r = Pearson correlation coefficient.

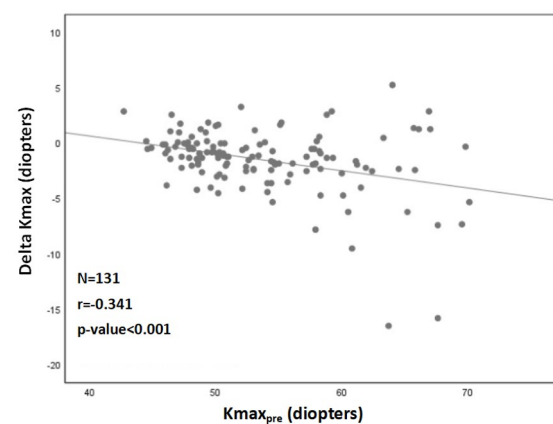


FIGURE 3

Correlation between ¹Kmax_{pre} and ²Delta Kmax. More negative Delta Kmax values significantly correlated with higher Kmax_{pre} values (more severe baseline keratoconus). However, the correlation coefficient is low, with $r^2 = 0.13$. Thus, although the correlation is significant, it is relatively weak. ¹Kmax_{pre} = maximal corneal power before cross-linking. ²Delta Kmax = (maximal corneal power after cross-linking) – (maximal corneal power before cross-linking), measured in diopters. ³r = Pearson correlation coefficient.

TABLE 2 Analysis of variables affecting ¹Delta Kmax.

Univariate analysis of continuous variables				
Variables	² N	Pearson Correlation (³ r)		p-value
Age	131	−0.018		0.842
Pachymetry	128	0.222		0.012*
⁴ LogMAR _{pre}	129	−0.221		0.012*
Follow-up time	131	−0.435		<0.001**
⁵ Kmax _{pre}	131	−0.341		<0.001**
⁶ Cyl _{pre} (D)	120	0.170		0.065
Univariate analysis of categorical variables				
Variables	N	Mean	Median	p-value
Accelerated	90	−0.56	−0.60	<0.001**
Non-Accelerated	41	−3.55	−2.40	
Male	102	−1.46	−1.20	0.824
Female	29	−1.60	−0.90	
Jewish	101	−1.28	−1.10	0.177
Arab	27	−2.14	−1.30	
Allergy	35	−1.40	−0.50	0.824
No allergy	96	−1.53	−1.25	
Multivariate stepwise regression analysis				
Variables	N	β		p-value
Accelerated\	90	−2.453		<0.001**
Non-accelerated	41			
Kmax _{pre}	131	−0.096		0.013
LogMAR _{pre}	129	−0.15		0.875
Follow-up time	131	−0.179		0.122
Pachymetry	128	−0.60		0.557
Model's R ²	23.2%			

Univariate analysis was done with correlation analysis for continuous variables and Chi-square test for categorical variables. Variables that were significant in the univariate analysis were included in multivariate analysis using stepwise approach linear regression.

¹Delta Kmax = (maximal corneal power after cross-linking) − (maximal corneal power before cross-linking).

²N = number of patients.

³r = Pearson correlation coefficient.

⁴LogMAR_{pre} = Logarithm of minimal angle of resolution before cross-linking.

⁵Kmax_{pre} = maximal corneal power before cross-linking.

⁶Cyl_{pre} = refractive cylinder before cross-linking.

* $p < 0.05$.

** $p < 0.01$.

Bold values are for p -values of significance.

LogMAR and Delta LogMAR outcome

A total of 123 eyes of 108 children had available LogMAR results for a minimum of 1 year and were included in this analysis. Mean LogMAR decreased from 0.27 ± 0.23 to 0.22 ± 0.19 ($p = 0.005$) at the last follow up. Mean Delta LogMAR was -0.05 ± 0.18 (median -0.05).

12.8% of patients had Delta LogMAR ≤ -0.2 (improvement), 80% of patients had Delta LogMAR between -0.2 and $+0.2$ (stable), 7.2% of patients had Delta LogMAR $\geq +0.2$ (worsen). Figure 5 shows the distribution of delta logMAR following CXL.

Mean Delta LogMAR values did not differ significantly between hypotonic (10 eyes; Mean Delta LogMAR = -0.13) and isotonic (113

eyes; Mean Delta Kmax = -0.04) riboflavin pre-CXL instillation ($p = 0.77$; Mann–Whitney test).

Delta LogMAR: univariate analysis

The only variable found to be significantly correlated with a more negative Delta LogMAR (Table 4) was LogMAR_{pre} ($r = -0.596$; $p < 0.001$). Other variables were not significantly correlated with Delta LogMAR (Table 4), including age ($p = 0.527$), pachymetry ($p = 0.853$), follow-up time ($p = 0.164$), Kmax_{pre} ($p = 0.712$), Cyl_{pre} ($p = 0.701$), CXL protocol type (accelerated or non-accelerated; $p = 0.350$), sex ($p = 0.663$), ethnicity ($p = 0.571$), or ocular allergy ($p = 0.502$).

As only one variable was associated with a significant change in Delta LogMAR, the multivariate analysis was not relevant. These results demonstrate that lower preoperative visual acuity only influences the improvement of visual function following CXL in pediatric patients with KC.

The percentage of patients with Delta LogMAR ≤ -0.2 (gain of two or more Snellen lines) was 24.4% in the non-accelerated protocol group and 7.1% in the accelerated protocol group ($p = 0.006$; Table 3). However, the accelerated group had a larger proportion of stable eyes with Delta LogMAR between -0.2 and $+0.2$ (86.9% vs. 60.1% in the non-accelerated group; $p = 0.008$) and a non-significant trend towards a smaller proportion of eyes with Delta LogMAR $\geq +0.2$ (6% vs. 14.6% in the non-accelerated group; $p = 0.17$).

Discussion

We analyzed the effects of preoperative predictors of successful CXL in pediatric patients with progressive KC by using an extensive database of patients with a long-term follow-up period. We used two primary outcome measures: changes in Kmax and visual acuity, over the follow-up period. Our study showed that CXL in this group not only successfully stabilized KC progression over time, but the mean negative Delta Kmax and Delta LogMAR results also indicated improvement of corneal shape and visual function, respectively. In addition, to the best of our knowledge, our study is the first to demonstrate that, in a multivariate analysis, non-accelerated CXL and higher Kmax pre-CXL positively influenced corneal flattening, whereas lower preoperative visual acuity only influenced the improvement of visual function. These results suggest that CXL may have a more potent effect in children with advanced KC.

In the adult population, there is robust evidence of CXL success and long-lasting effects in long-term follow-up (24, 25). The results in the pediatric keratoconus patients are still controversial. Overall, epithelium-off studies show stability or flattening of the cornea while maintaining or improving the CDVA (7–11). However, some authors report significant KC progression post-CXL, with increasing rates over time (14–18). Kodavoor (18) reported Kmax worsening in 8.6% of treated eyes at one-year post-CXL. Godefrooij (17) reported Kmax progression of up to 7.2D in 22% of treated eyes in the last follow-up, with no significant changes in visual acuity. Padmanabhan (15) showed an increase of more than 1D in Kmax in 15% of treated eyes at 2 years, 21% at 4 years, and 24% beyond that period, with a decrease in visual acuity of 30.9% after 4 years. A similar CXL regression effect was noted by Mazzota (16), with a 24% progression rate over a 10-year

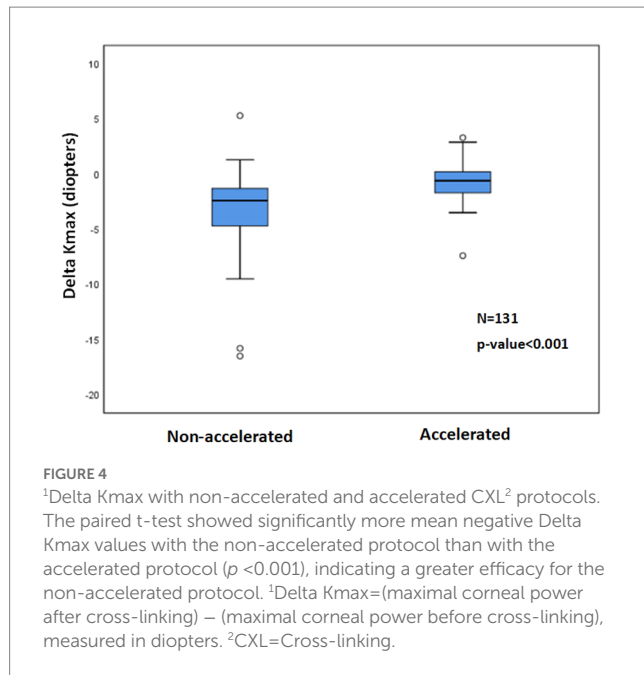


TABLE 3 Success rates of non-accelerated vs. accelerated cross-linking.

Variables	Non-accelerated	Accelerated	<i>p</i> -value
¹Delta Kmax			
Delta Kmax ≤ −1	82.9%	38.9%	< 0.001**
+1 > Delta Kmax > −1	12.2%	40%	0.003**
Delta Kmax ≥ +1	4.9%	21.1%	0.019*
²Delta LogMAR			
Delta LogMAR ≤ −0.2	24.4%	7.1%	0.01*
+0.2 > Delta LogMAR > −0.2	60.1%	86.9%	0.008**
Delta LogMAR ≥ +0.2	14.6%	6%	0.17

Analysis was done with and Chi-square test.

¹Delta Kmax = (maximal corneal power after cross-linking) – (maximal corneal power before cross-linking).

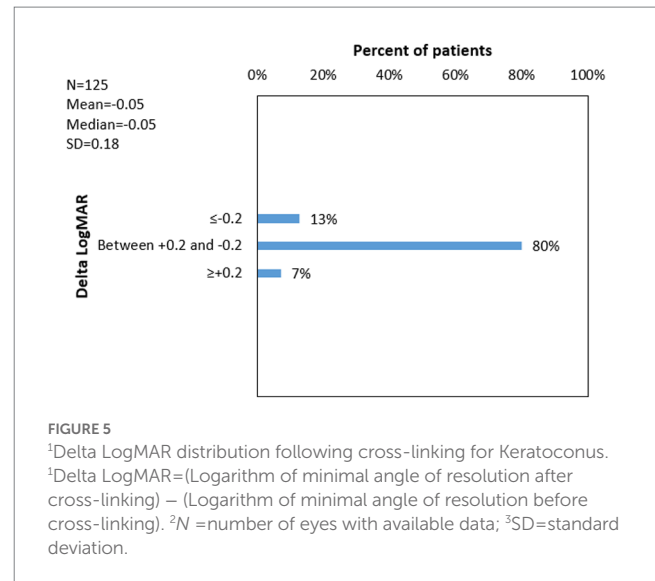
²Delta LogMAR = (LogMAR after cross-linking) – (LogMAR before cross-linking).

* $p < 0.05$.

** $p < 0.01$.

Bold values are for *p*-values of significance.

follow-up period. Chatzis and Hafezi (14) reported the highest rate of progression, with 55% of treated eyes showing an increase of 1D or more after 3 years. In addition, the only randomized controlled trial (20) on this population showed KC progression in 7% of the treated eyes after 18 months. In general, the loss of CXL effect is poorly understood. While some authors may attribute this finding to eye rubbing secondary to chronic ocular allergic disease (14, 16, 18), it could be secondary to the more aggressive course of KC in this population (2, 26), the lack of natural cross-links in pediatric young corneas, and the corneal collagen turnover (16). Our results showed an increase of ≥ 1.0 D in Kmax in 15.8% of the eyes with a loss of ≥ 2

TABLE 4 Analysis of variables affecting ¹Delta LogMAR.

Univariate analysis of continuous variables				
Variables	² <i>N</i>	Pearson Correlation (³ <i>r</i>)		<i>p</i> -value
Age	123	0.058		0.527
Follow-up	123	−0.127		0.164
Pachymetry	120	0.017		0.853
⁴ LogMAR _{pre}	123	−0.596		<0.001**
⁵ Kmax _{pre}	123	−0.034		0.712
⁶ Cyl _{pre}	114	−0.036		0.701
Univariate analysis of categorical variables				
Variables	<i>N</i>	Mean	Median	<i>p</i> -value
Accelerated	83	−0.04	0	0.350
Non-Accelerated	40	−0.07	−0.07	
Male	97	−0.04	−0.05	0.663
Female	26	−0.06	−0.05	
Jewish	95	−0.05	−0.05	0.571
Arab	26	−0.03	−0.04	
Allergy	35	−0.03	0	0.502
No allergy	88	−0.05	−0.05	

Univariate analysis was done with correlation analysis for continuous variables and Chi-square test for categorical variables.

¹Delta LogMAR = (LogMAR after cross-linking) – (LogMAR before cross-linking).

²*N* = number of patients.

³*r* = Pearson correlation coefficient.

⁴LogMAR_{pre} = Logarithm of minimal angle of resolution before cross-linking.

⁵Kmax_{pre} = maximal corneal power before cross-linking.

⁶Cyl_{pre} = refractive cylinder before cross-linking.

* $p < 0.05$.

** $p < 0.01$.

Bold values are for *p*-values of significance.

Snellen lines in 7.2%. Interestingly, in the univariate analysis, a longer follow-up period was correlated with a more negative Delta Kmax, indicating that the CXL effect was maintained or increased over time. However, no significant differences were found in multivariate analysis.

A higher K_{max_pre} correlated with a significantly more negative delta K_{max} . Although studies performed in the adult population support our findings (27, 28), reports on the pediatric population failed to establish a correlation between K_{max_pre} and Delta K_{max} (11, 17, 21). Interestingly, Padmanabhan (15) showed that the decrease in K_{max} post-CXL was maximal in eyes with a moderate grade of disease than in the severe and mild groups.

The explanation for greater CXL flattening effect seen with higher K_{max_pre} is still not clear. As far as we are concerned, the existing literature in adults, with similar findings as ours, fails to establish a clear cause for this effect. Sloot et al. (28) speculate that there “might be a difference in the corneal stroma in mild to moderate cases versus advanced cases of KC.” In addition, the authors believe that “treatment might be more deeply located in the stroma in advanced cases because these have thinner corneas.” (28) Our work shows that indeed in univariate analysis, pre-operatively thinner corneas were also correlated with a more negative K_{max} . Although this was not the case in the multivariate analysis, as we explained in the manuscript, stepwise linear regression grades variables according to the strength of their correlation with the outcome. It might be the case that K_{max_pre} correlated better with delta k_{max} and since steeper corneas usually are thinner, the pre-operative thickness was excluded from the multivariate analysis.

Like Uçakhan (11), we did not find an association between K_{max_pre} and Delta LogMAR.

In univariate analysis, thinner corneas were correlated with a more negative Delta K_{max} . This finding is in contrast with those of other published reports. Sarac (21) found that eyes with corneas thinner than 450 μm had an OR of 4.54 to progress after CXL. The authors believe that, in this group, the driving factors for KC progression are especially stronger in the more advanced (thinner) diseased corneas, and the use of hypotonic riboflavin during treatment in these eyes provided a weaker CXL effect. Kodavoor (18) showed that 1-year post-CXL, patients with a thinner cornea (between 350 and 400 μm) had a mean K_{max} of 3 D more than those with thicker corneas ($>400 \mu m$). In contrast, while searching for predictors of KC progression post-CXL, Godefrooij (17) did not find a correlation between pachymetry and outcomes. The Siena CXL Pediatrics study (8) found that both groups of eyes with corneas $>$ or $<450 \mu m$ had statistically significant flattening of K_{max} during all follow-up periods, with a similar mean decrease in K_{max} . Similarly, with an accelerated protocol, Ulusoy (12) showed that keratometry and CDVA improved from baseline after 1 year in eyes with corneas $<$ and $\geq 450 \mu m$. We believe that our results better reflect clinical CXL effects because we analyzed corneal thickness in a large cohort as a continuous variable rather than using a categorical variable approach. Moreover, corneal thickness was correlated with KC severity. Thus, eyes with thinner corneas had more severe topographic characteristics (such as K_{max_pre}) at baseline. Stepwise linear regression grade variables according to the strength of their correlation with the outcome. Other parameters (K_{max_pre}) probably correlated better with the outcome; hence, pachymetry was found to be nonsignificant in the multivariate analysis. Pachymetry was not associated with logMAR changes, similar to the findings of other studies (16, 18).

Worse baseline visual acuity (higher LogMAR_{pre}) was significantly correlated with corneal flattening and better visual acuity post-CXL

in univariate analysis. Although studies on the adult population support our findings (29–31) data on pediatric patients contradict our results. Uçakhan (11) did not find an association between preoperative vision and improvement in uncorrected or corrected distance visual acuity in 40 eyes during 48 months of follow-up. While evaluating predictive factors for the progression of KC post-CXL, Sarac (21) and Godefrooij (17) did not find a significant effect of CDVA on an increase in $K_{max} \geq 1$ D. Interestingly, despite the usual vision worsening with KC progression, some studies have reported no vision change with an increase in K_{max} post-CXL (14, 17). In a previous work by Wisse et al. (31), worse baseline visual acuity correlated with more central cones, which demonstrated greater CXL effect, presumably due to a more perpendicular incident angle of UVA rays, as compared with more peripheral cones. However, we did not evaluate cone eccentricity in our study. It seems that further studies are needed to elucidate the mechanism explaining the observation of greater visual improvement with worse baseline visual acuity.

Non-accelerated CXL correlated with significant K_{max} flattening compared with accelerated CXL. Amer (32) found that the CDVA and K_{max} improved more in the non-accelerated group. Turhan (33) found a significant decrease in K_{max} in both accelerated and non-accelerated groups. However, after 2 years, CDVA only improved from baseline in the non-accelerated group. Sarac (34) found no difference in the outcomes between the non-accelerated and accelerated groups. However, the post-CXL progression rates in the non-accelerated and accelerated CXL groups were 13.1 and 16.3%, respectively ($p=0.754$).

Although the exact mechanism explaining superior efficacy of the non-accelerated protocol is not clear to us, a previous study on porcine corneas found non-accelerated CXL to produce greater anterior stromal stiffening, as compared to the accelerated protocol (35).

In contrast, a prospective randomized contralateral eye study (36) showed better improvement in vision and K_{max} with the accelerated protocol after 3 years. The authors stated that conventional and accelerated CXL are effective options for managing KC in children. Accelerated CXL is more appealing to both doctors and patients because of its shorter duration and, therefore, better patient comfort and compliance during local anesthesia. However, we believe that the benefits of non-accelerated treatment outweigh its disadvantages, with a significantly more potent effect characterized by 95 vs. 79% stabilization or flattening of K_{max} in children.

Age did not affect any of the outcome measures in this study. Other studies (11, 17, 21) also failed to demonstrate a correlation with age. However, Mazzotta (16) observed that a treatment regression rate of 24% over 10 years could be considered for patients aged 15 years at the time of treatment. When evaluating the accelerated CXL protocol, Ozer (19) found keratometric progression in 35% of patients aged ≤ 14 years and 4% of patients aged 15–18 years ($p=0.014$). Although some may argue that younger patients have more severe allergic eye diseases and are less compliant with ceasing eye rubbing (19), in addition to having more aggressive KC (2–4), we believe that our results are consistent because age was analyzed as a continuous variable (and not dichotomously, as in those studies).

Our previous work evaluated success predictors of CXL in adult KC in 517 eyes, with a mean followed for 2.3 years (37). The ethnic populations were similar to the present study in children. In

resemblance with the present study, Delta Kmax was influenced negatively by a longer follow-up, thinner corneas, non-accelerated protocol, higher Kmaxpre and higher LogMARpre in univariate analysis and non-accelerated protocol and higher Kmax in multivariate analysis. Similarly, the only significant feature when analyzing the Delta LogMAR was a higher LogMARpre. The results of both studies corroborate the idea that CXL effect is higher in more advanced diseases regardless of age and that the non-accelerated protocol is more effective than the accelerated CXL. In addition, although pediatric corneas have fewer natural cross-links and are subjected to more aggressive disease, CXL treatment behaves alike.

Allergy was not associated with changes in the CDVA and Kmax. Previous studies have linked allergy and eye rubbing to CXL failure or regression (14, 18). KC is more severe and progresses faster in patients with VKC and ocular allergies than in those without VKC (38). Nonetheless, in a study comparing CXL in pediatric patients with KC with and without VKC, there were no differences in outcome, complications, or KC progression between the groups (39).

Middle Eastern populations are known to have a greater incidence and severity of KC (3). Nevertheless, our study did not find a correlation between Jewish or Arabic origin and CXL success in Israel. However, the pathogenesis of KC is not yet completely understood. Some KC features suggest a strong genetic component (40). Our study population comprised both the Jewish and Arabic populations of Jerusalem and its surroundings. High rates of consanguineous marriages characterize these two subsets of the local population; therefore, genetic diseases are relatively more common. We believe that similar marital habits might explain the similarities in the outcomes between the two groups.

Our study has significant advantages over the existing literature. First, the sample size was significantly larger than those reported in previous studies. Second, we followed the patients for an extended period of up to 8 years. Third, many variables in this study were analyzed as continuous (Kmax, LogMAR, age, CCT, and follow-up) and not categorically as in previous studies. Fourth, we included the effects of allergic eye disease and ethnicity on the CXL outcomes. Finally, this is one of the few studies to present a systematic analysis of multiple predictors of CXL success using univariate and multivariate statistical tools.

Our study has some limitations. This was a retrospective analysis; therefore, some data were missing from a small proportion of the cohort. Second, the study cohort lacked control eyes that had not been treated with CXL. However, as the efficacy of CXL has been demonstrated in many previous studies, it is unethical to not perform this procedure in patients with progressive KC. In addition, our analysis included cases from 2007, when CXL was less popular and well known and was not yet introduced to the Israeli National Health basket until 2014. This means that cases performed in the early years might have had a more advanced KC, whereas those performed in the later years might have had a more moderate KC. As the procedure gained acceptance and popularity, and with the growing awareness of its efficacy, more community ophthalmologists and optometrists referred more patients with KC at earlier stages. Lastly, it mainly comprises Middle Eastern patients, who are known to have a more aggressive progression of KC than other populations (3).

In conclusion, our results show that CXL is an effective treatment for decrease in Kmax and to improve vision in pediatric patients with

KC. Patients with an advanced KC may benefit more from the late effects of CXL, with a decrease in Kmax, than patients with early KC do. However, early detection and treatment are critical for patient benefit, and treatment should not be delayed to achieve maximum effects. Finally, we demonstrated that the non-accelerated protocol had a greater impact on corneal flattening than the accelerated protocol did.

Data availability statement

The raw data supporting the conclusions of this article will be made available by the authors, without undue reservation.

Ethics statement

The studies involving human participants were reviewed and approved by this study adhered to the principles of the Declaration of Helsinki. Approval was obtained from the Institutional Review (IRB) Board/Ethics Committee of Hadassah medical center, Jerusalem, Israel (approval number 18-0221). Written informed consent from the participants' legal guardian/next of kin was not required to participate in this study in accordance with the national legislation and the institutional requirements.

Author contributions

DW, JF-P, and AS: conceptualization. DW, OS, YT, JF-P, and AS: data curation and formal analysis. DW, OS, JF-P, and AS: methodology. AS: project administration, resources, and supervision. YT and AS: validation. DW, OS, YT, and AS: writing—original draft. DW, OS, and AS: writing—review and editing. All authors contributed to the article and approved the submitted version.

Acknowledgments

We sincerely thank the author Tali Bdolach (statistics expert).

Conflict of interest

The authors declare that the research was conducted in the absence of any commercial or financial relationships that could be construed as a potential conflict of interest.

Publisher's note

All claims expressed in this article are solely those of the authors and do not necessarily represent those of their affiliated organizations, or those of the publisher, the editors and the reviewers. Any product that may be evaluated in this article, or claim that may be made by its manufacturer, is not guaranteed or endorsed by the publisher.

References

- Yang K, Gu Y, Xu L, Fan Q, Zhu M, Wang Q, et al. Distribution of pediatric keratoconus by different age and gender groups. *Front Pediatr.* (2022) 10:937246. doi: 10.3389/fped.2022.937246
- Léoni-Mesplé S, Mortemousque B, Touboul D, Malet F, Praud D, Mesplé N, et al. Scalability and severity of keratoconus in children. *Am J Ophthalmol.* (2012) 154:56–62.e1. doi: 10.1016/j.ajo.2012.01.025
- Ferdi AC, Nguyen V, Gore DM, Allan BD, Rozema JJ, Watson SL. Keratoconus natural progression: a systematic review and meta-analysis of 11 529 eyes. *Ophthalmology.* (2019) 126:935–45. doi: 10.1016/j.ophtha.2019.02.029
- Olivo-Payne A, Abdala-Figuerola A, Hernandez-Bogantes E, Pedro-Aguilar L, Chan E, Godefrooij D. Optimal management of pediatric keratoconus: challenges and solutions. *Clin Ophthalmol.* (2019) 13:1183–91. doi: 10.2147/OPTH.S183347
- Wollensak G, Spoerl E, Seiler T. Riboflavin/ultraviolet-A-induced collagen crosslinking for the treatment of keratoconus. *Am J Ophthalmol.* (2003) 135:620–7. doi: 10.1016/S0002-9394(02)02220-1
- Koller T, Mrochen M, Seiler T. Complication and failure rates after corneal crosslinking. *J Cataract Refract Surg.* (2009) 35:1358–62. doi: 10.1016/j.jcrs.2009.03.035
- Vinciguerra P, Albé E, Frueh BE, Trazza S, Epstein D. Two-year corneal cross-linking results in patients younger than 18 years with documented progressive keratoconus. *Am J Ophthalmol.* (2012) 154:520–6. doi: 10.1016/j.ajo.2012.03.020
- Caporossi A, Mazzotta C, Baiocchi S, Caporossi T, Denaro R, Balestrazzi A. Riboflavin-UVA-induced corneal collagen cross-linking in pediatric patients. *Cornea.* (2012) 31:227–31. doi: 10.1097/ICO.0b013e31822159f6
- Zotta PG, Diakonis VF, Kymionis GD, Grentzelos M, Moschou KA. Long-term outcomes of corneal cross-linking for keratoconus in pediatric patients. *J AAPOS.* (2017) 21:397–401. doi: 10.1016/j.jaapos.2017.07.205
- Wise S, Diaz C, Termote K, Dubord PJ, McCarthy M, Yeung SN. Corneal cross-linking in pediatric patients with progressive Keratoconus. *Cornea.* (2016) 35:1441–3. doi: 10.1097/ICO.0000000000000923
- Uçakhan ÖO, Bayraktutar BN, Sağlik A. Pediatric corneal collagen cross-linking: long-term follow-up of visual, refractive, and topographic outcomes. *Cornea.* (2016) 35:162–8. doi: 10.1097/ICO.0000000000000702
- Ulusoy DM, Göktaş E, Duru N, Özköse A, Atas M, Yuvacı İ, et al. Accelerated corneal crosslinking for treatment of progressive keratoconus in pediatric patients. *Eur J Ophthalmol.* (2017) 27:319–25. doi: 10.5301/eye.5000848
- Ozgurhan EB, Kara N, Cankaya KI, Kurt T, Demirok A. Accelerated corneal cross-linking in pediatric patients with keratoconus: 24-month outcomes. *J Refract Surg.* (2014) 30:843–9. doi: 10.3928/1081597X-20141120-01
- Chatzis N, Hafezi F. Progression of keratoconus and efficacy of corneal collagen cross-linking in children and adolescents. *J Refract Surg.* (2012) 28:753–8. doi: 10.3928/1081597X-20121011-01
- Padmanabhan P, Rachapalle Reddi S, Rajagopal R, Natarajan R, Iyer G, Srinivasan B, et al. Corneal collagen cross-linking for Keratoconus in pediatric patients - long-term results. *Cornea.* (2017) 36:138–43. doi: 10.1097/ICO.0000000000001102
- Mazzotta C, Traversi C, Baiocchi S, Bagaglia S, Caporossi O, Villano A, et al. Corneal collagen cross-linking with riboflavin and ultraviolet A light for pediatric Keratoconus: ten-year results. *Cornea.* (2018) 37:560–6. doi: 10.1097/ICO.0000000000001505
- Godefrooij DA, Soeters N, Imhof SM, Wisse RPL. Corneal cross-linking for pediatric Keratoconus: long-term results. *Cornea.* (2016) 35:954–8. doi: 10.1097/ICO.0000000000000819
- Kodavoor SK, Arsiwala AZ, Ramamurthy D. One-year clinical study on efficacy of corneal cross-linking in Indian children with progressive keratoconus. *Cornea.* (2014) 33:919–22. doi: 10.1097/ICO.0000000000000197
- Ozer MD, Batur M, Mesen S, Tekin S, Seven E, Yasar T. Comparison of the efficacy of accelerated corneal cross-linking therapy in different pediatric age groups having progressive keratoconus. *Int Ophthalmol.* (2020) 40:2651–8. doi: 10.1007/s10792-020-01446-w
- Larkin DFP, Chowdhury K, Burr JM, Raynor M, Edwards M, Tuft SJ, et al. Effect of corneal cross-linking versus standard care on Keratoconus progression in young patients: the KERALINK randomized controlled trial. *Ophthalmology.* (2021) 128:1516–26. doi: 10.1016/j.ophtha.2021.04.019
- Sarac O, Caglayan M, Cakmak HB, Cagil N. Factors influencing progression of keratoconus 2 years after corneal collagen cross-linking in pediatric patients. *Cornea.* (2016) 35:1503–7. doi: 10.1097/ICO.0000000000001051
- Maeda N, Klyce SD, Smolek MK. Comparison of methods for detecting Keratoconus using Videokeratography. *Arch Ophthalmol.* (1995) 113:870. doi: 10.1001/archophth.1995.01100070044023
- Koppen C, Gobin L, Mathysen D, Wouters K, Tassinon MJ. Influence of contact lens wear on the results of ultraviolet A/riboflavin cross-linking for progressive keratoconus. *Br J Ophthalmol.* (2011) 95:1402–5. doi: 10.1136/bjophthalmol-2011-300329
- O'Brart DPS, Patel P, Lascaratos G, Wagh VK, Tam C, Lee J, et al. Corneal cross-linking to halt the progression of Keratoconus and corneal ectasia: seven-year follow-up. *Am J Ophthalmol.* (2015) 160:1154–63. doi: 10.1016/j.ajo.2015.08.023
- Raiskup F, Theuring A, Pillunat LE, Spoerl E. Corneal collagen crosslinking with riboflavin and ultraviolet-a light in progressive keratoconus: ten-year results. *J Cataract Refract Surg.* (2015) 41:41–6. doi: 10.1016/j.jcrs.2014.09.033
- McMahon TT, Edrington TB, Szczotka-Flynn L, Olafsson HE, Davis LJ, Schechtman KB, et al. Longitudinal changes in corneal curvature in keratoconus. *Cornea.* (2006) 25:296–305. doi: 10.1097/01.icc.0000178728.57435.df
- Koller T, Pajic B, Vinciguerra P, Seiler T. Flattening of the cornea after collagen crosslinking for keratoconus. *J Cataract Refract Surg.* (2011) 37:1488–92. doi: 10.1016/j.jcrs.2011.03.041
- Sloot F, Soeters N, Van Der Valk R, Tahzib NG. Effective corneal collagen crosslinking in advanced cases of progressive keratoconus. *J Cataract Refract Surg.* (2013) 39:1141–5. doi: 10.1016/j.jcrs.2013.01.045
- Toprak I, Yaylali V, Yildirim C. Factors affecting outcomes of corneal collagen crosslinking treatment. *Eye.* (2014) 28:41–6. doi: 10.1038/eye.2013.224
- Godefrooij DA, Boom K, Soeters N, Imhof SM, Wisse RPL. Predictors for treatment outcomes after corneal crosslinking for keratoconus: a validation study. *Int Ophthalmol.* (2017) 37:341–8. doi: 10.1007/s10792-016-0262-z
- Wisse RPL, Godefrooij DA, Soeters N, Imhof SM, Van Der Lelij A. A multivariate analysis and statistical model for predicting visual acuity and keratometry one year after cross-linking for keratoconus. *Am J Ophthalmol.* (2014) 157:519–525.e2. doi: 10.1016/j.ajo.2013.11.001
- Amer I, Elaskary A, Mostafa A, Hazem HA, Omar A, Abdou A. Long-term visual, refractive and topographic outcomes of “epi-off” corneal collagen cross-linking in pediatric keratoconus: standard versus accelerated protocol. *Clin Ophthalmol.* (2020) 14:3747–54. doi: 10.2147/OPTH.S275797
- Turhan SA, Yargi B, Tokar E. Efficacy of conventional versus accelerated corneal cross-linking in pediatric keratoconus: two-year outcomes. *J Refract Surg.* (2020) 36:265–9. doi: 10.3928/1081597X-20200302-01
- Sarac O, Caglayan M, Uysal BS, Uzel AGT, Tanriverdi B, Cagil N. Accelerated versus standard corneal collagen cross-linking in pediatric keratoconus patients: 24 months follow-up results. *Contact Lens Anterior Eye.* (2018) 41:442–7. doi: 10.1016/j.clae.2018.06.001
- Dias J, Diakonis VF, Lorenzo M, Gonzalez F, Porras K, Douglas S, et al. Corneal stromal elasticity and viscoelasticity assessed by atomic force microscopy after different cross linking protocols. *Exp Eye Res.* (2015) 138:1–5. doi: 10.1016/j.exer.2015.06.015
- Eissa SA, Yassin A. Prospective, randomized contralateral eye study of accelerated and conventional corneal cross-linking in pediatric keratoconus. *Int Ophthalmol.* (2019) 39:971–9. doi: 10.1007/s10792-018-0898-y
- Wajnsztajn D, Shmueli O, Zur K, Frucht-Pery J, Solomon A. Predicting factors for the efficacy of crosslinking for keratoconus. *PLoS One.* (2022) 17:e0263528. doi: 10.1371/journal.pone.0263528
- Wajnsztajn DSA. Vernal keratoconjunctivitis and keratoconus. *Curr Opin Allergy Clin Immunol.* (2021) 21:507–14. doi: 10.1097/ACI.0000000000000765
- Alrobaian M, Elsayed M, Alotaibi A, Alharbi M, May W, Stone D. Safety and efficacy of corneal cross-linking in pediatric patients with keratoconus and vernal keratoconjunctivitis. *Middle East Afr J Ophthalmol.* (2019) 26:95–100. doi: 10.4103/meajo.MEJO_240_18
- Tuft SJ, Hassan H, George S, Frazer DG, Willoughby CE, Liskova P. Keratoconus in 18 pairs of twins. *Acta Ophthalmol.* (2012) 90:e482–6. doi: 10.1111/j.1755-3768.2012.02448.x



OPEN ACCESS

EDITED BY

Cristina Nicula,
University of Medicine and Pharmacy Iuliu
Hatieganu, Romania

REVIEWED BY

Yueguo Chen,
Peking University Third Hospital, China
Mehmet Serhat Mangan,
Haydarpasa Numune Training and Research
Hospital, Türkiye

*CORRESPONDENCE

Hiddenaga Kobashi
✉ hiddenaga_kobashi@keio.jp

RECEIVED 28 November 2022

ACCEPTED 28 April 2023

PUBLISHED 24 May 2023

CITATION

Kobashi H, Yano T and Tsubota K (2023)
Combination of violet light irradiation and
collagenase treatments in a rabbit model of
keratoconus. *Front. Med.* 10:1109689.
doi: 10.3389/fmed.2023.1109689

COPYRIGHT

© 2023 Kobashi, Yano and Tsubota. This is an
open-access article distributed under the terms
of the [Creative Commons Attribution License](https://creativecommons.org/licenses/by/4.0/)
(CC BY). The use, distribution or reproduction
in other forums is permitted, provided the
original author(s) and the copyright owner(s)
are credited and that the original publication in
this journal is cited, in accordance with
accepted academic practice. No use,
distribution or reproduction is permitted which
does not comply with these terms.

Combination of violet light irradiation and collagenase treatments in a rabbit model of keratoconus

Hiddenaga Kobashi^{1,2*}, Takashi Yano³ and Kazuo Tsubota^{1,2}

¹Department of Ophthalmology, School of Medicine, Keio University, Tokyo, Japan, ²Tsubota Laboratory Inc., Tokyo, Japan, ³Life Science Laboratories, Ltd., Osaka, Japan

Purpose: We evaluated the use of collagenase treatment to generate a rabbit model of keratoconus and the impact of violet light (VL) irradiation on the disease model in six Japanese White rabbits.

Methods: After epithelial debridement, the collagenase group was treated with a collagenase type II solution for 30 min; the control group was treated with a solution without collagenase. Three rabbits also underwent VL irradiation (375 nm, irradiance 310 $\mu\text{W}/\text{cm}^2$) for 3 h daily for 7 days after topical collagenase application. Slit-lamp microscopy results, steep keratometry (Ks), corneal astigmatism, central corneal thickness, and axial length were examined before and after the procedure. The corneas were obtained on day 7 for biomechanical evaluation.

Results: A significant increase in Ks and corneal astigmatism was observed in the collagenase and VL irradiation groups compared with the control group on day 7. No significant difference was found in the change in corneal thickness between the groups. The elastic modulus at 3, 5, and 10% strain was significantly lower in the collagenase group than in the control group. There was no significant difference in the elastic modulus at any level of strain between the collagenase and VL irradiation groups. The average axial length at day 7 was significantly longer in the collagenase and VL irradiation groups than in the control group. Collagenase treatment induced a model of keratoconus by steepening the keratometric and astigmatic values. There was no significant difference in the observed elastic behavior of normal and ectatic corneas under physiologically relevant stress levels.

Conclusion: VL irradiation did not cause regression of corneal steepening in a collagenase-induced model during short-term observation.

KEYWORDS

keratoconus, animal model, collagenase, violet light, corneal cross-linking

Introduction

Keratoconus (KC) is a progressive, frequently asymmetric, and corneal thinning disorder characterized by changes in the structure and organization of corneal collagen (1, 2). It results in corneal thinning and protrusion, progressive myopia, and irregular astigmatism. It is difficult to establish an *ex vivo* and *in vivo* corneal ectatic model of KC. Previous studies have examined the treatment of corneal ectasia using excimer lasers, but the corneal shape did not result in a KC model (3, 4). Hong et al. (5) reported a significant increase in corneal curvature in human donor corneas after topical collagenase application. Qiao et al. (6) mimicked KC with increased corneal keratometric parameters, corneal thinning, and a lower elastic modulus

using rabbits. Wang et al. (7) developed an *ex vivo* corneal ectatic model that mimics KC by applying collagenase and chondroitinase enzymes to rabbit corneas. However, other parameters, such as corneal astigmatism and axial length, have not been investigated. Ihalainen et al. (8) reported increased collagenase and gelatinase activities in the medium of human KC corneal cultures. The lack of preclinical animal models of KC has been an obstacle for evaluating potential new therapies. Because abnormal collagenase activity and decreased total collagen levels are present in KC, exposure of collagenous enzymes to normal tissue may simulate some aspects of acute KC disease.

Recently, we reported a novel technology, KeraVio, consisting of violet light (VL) irradiation and riboflavin treatment, in rabbit and human corneas (9). KeraVio halted disease progression in eyes with corneal ectasia, similar to corneal cross-linking (CXL). KeraVio treatment uses an eyeglass with a 375-nm-wavelength VL source applied to the cornea, and the patients wear the eyeglass daily without limitations. Corneal epithelial peeling in CXL not only induces ocular pain after surgery but also carries a potential risk of corneal infection. Some modified CXL-associated accelerated and/or transepithelial techniques have recently become popular in the treatment of KC (10, 11). KeraVio treatment avoids these complications of CXL surgery and may become another option for KC treatment, but its efficacy has not been compared with that of CXL. To simplify the treatment procedure, we preliminarily identified originally endogenous riboflavin in the human cornea without adding riboflavin drops, and a relatively low intensity of VL irradiation itself strengthened the corneal stiffness in porcine corneas (12). In a normal eye, VL is absorbed by the cornea, which contains physiological riboflavin and other photosensitizers, leading to CXL in the cornea. If physiological riboflavin originally exists in the human cornea, VL irradiation may strengthen the corneal stiffness without adding riboflavin drops in the KeraVio technique. Subsequently, a clinical trial of KeraVio without riboflavin drops was launched (jRCTs032190267). To optimize the KeraVio treatment protocols based on the dose of riboflavin and VL irradiation, we need to develop an experimental model of KC. In this study, KeraVio was defined as a treatment using VL to stop the progression of KC, regardless of riboflavin treatment. We evaluated the impact of topical collagenase on eyes treated with KeraVio without riboflavin drops, but the corneal biometry needs to be clarified.

This study aimed to evaluate corneal biometry after treatment with both collagenase and VL irradiation in rabbit eyes.

Methods

Nine female Japanese White rabbits weighing 1.5–2.0 kg were used in the study. All animals were healthy and free of ocular disease. In six rabbits, the right eyes were treated with collagenase type II, and the left eyes were treated as the control group ($n = 6$ in each group). In the other three rabbits, KeraVio treatment was applied to both eyes after topical collagenase application ($n = 6$). All animals were treated according to the Association for Research in Vision and Ophthalmology Statement for the Use of Animals in Ophthalmic and Vision Research. This study was approved by the Review Board at Life Science Laboratories, Ltd: #18-20.

A topical anesthetic consisting of 0.4% oxybuprocaine hydrochloride was applied to the eyes. After epithelial debridement, corneal trephines were placed on the corneas. In the collagenase group, a 10 mg/ml collagenase type II solution (Worthington, Lakewood, NJ) in balanced salt solution and 15% dextran was applied to the surface of the corneas for 30 min with corneal trephines, as reported by Hong et al. (5). We chose the epithelium removal technique to encourage collagenase to penetrate corneal stroma, in terms of drug delivery. The solution was then removed with cotton swabs, and the corneas were rinsed with 0.9% sodium chloride solution. The control eyes were subjected to the same protocol but without collagenase type II in the applied solution. The KeraVio process began with the application of collagenase in the same manner as in the collagenase group. VL irradiation (375 nm) was applied using a single VL diode (Nitride Semiconductors Co., Ltd., Tokushima, Japan), with an irradiance of 0.31 mW/cm² for 180 min at a distance of 60 cm from the cornea (total energy dose, 3.3 J/cm²). KeraVio treatment using only VL irradiation was continued for 7 days (total energy dose, 23.4 J/cm²) (9). The experiments were carried out at room temperature ($20 \pm 1^\circ\text{C}$).

Before surgery, the rabbit eyes were subjected to slit-lamp examinations to identify the evidence of conjunctival injection, corneal infiltration, and corneal stromal inflammation. These examinations were repeated every day during the 7-day study to assess ocular safety; an examination was carried out before the collagenase treatment and repeated every day during the 7-day study. From day 1 to day 6, measurements of corneal parameters were not performed, but slit-lamp examinations were carried out daily. Corneal keratometry and the central corneal thickness (CCT) were recorded at the baseline (the day before treatment) and 7 days after treatment using a handheld keratometer (Retinomax 3; Righton, Tokyo, Japan) and an ultrasound pachymeter (SP-100; Tomey, Nagoya, Japan), respectively, under topical anesthesia. Although the maximum measurable refractive astigmatism of the Retinomax 3 was up to 12 dioptres (D), we modified its limit and reset the maximum value up to 30 D. Regarding the axis orientation of corneal astigmatism, no data were provided because of unreliable alignment using a handheld keratometer. Three measurements were taken at each time point, and the mean value of each parameter was recorded along with the change in its value. The mean steep keratometry (Ks), corneal astigmatism, CCT, and changes in each parameter were evaluated. The axial length was also recorded at day 7 after treatment using a digital caliper. In this study, the axial length was defined as the distance from the corneal apex to the scleral apex near the optic nerve.

The rabbits were euthanized with an intravenous overdose of sodium pentobarbital on day 7. The corneas were harvested en bloc along the sclera. A 2–3 mm scleral rim was preserved, and the cornea was attached along a custom-made scale. Then, a 5-mm-wide corneal strip was resected vertically along the cornea. The corneal strips were clamped vertically at a distance of 5 mm between the jaws. The CCT at day 7 in each cornea was used to calculate the cross-sectional area of the corneal strip. After the prepared corneal strip was placed on a computer-controlled electronic universal testing machine (TA, XTplusC Texture AnalyserTM, Stable Micro Systems, Ltd., London, UK) on day 8, a fixture was applied to hold the corneoscleral limbus of the corneal strip during a uniaxial tensile test. For the actual

TABLE 1 Changes in steep keratometry over time.

	Baseline dioptres (D)	1 week (D)	Change from baseline to 1 week (D)	* <i>P</i> -value	† <i>P</i> -value
Collagenase	54.73 ± 0.74	61.81 ± 5.51	7.08 ± 5.58	0.002	n/a
KeraVio with collagenase	56.49 ± 3.77	62.59 ± 6.29	6.10 ± 5.83	0.002	0.699
Control	57.62 ± 2.01	53.06 ± 1.21	−4.56 ± 2.14	n/a	n/a

*Compared with the control group.

†Comparison between collagenase with and without KeraVio.

D, diopters; n/a, not applicable.

TABLE 2 Changes in corneal astigmatism over time.

	Baseline (D)	1 week (D)	Change from baseline to 1 week (D)	* <i>P</i> -value	† <i>P</i> -value
Collagenase	1.74 ± 0.43	20.13 ± 7.37	18.39 ± 7.51	0.002	n/a
KeraVio with collagenase	5.63 ± 1.55	20.50 ± 5.73	14.87 ± 5.19	0.002	0.240
Control	4.04 ± 1.82	2.94 ± 0.82	−1.11 ± 2.50	n/a	n/a

*Compared with the control group.

†Comparison between collagenase with and without KeraVio.

D, diopters; n/a, not applicable.

measurement, the sample was stretched at a velocity of 1.8 mm/min up to a maximum force of 5 N. The elastic modulus was defined as the ratio of tensile stress (amount of force causing deformation per unit trans-sectional area of the corneal strip) to tensile strain (percentage change in the length caused by the stress). For the subsequent statistical analysis, the elastic modulus was consistently evaluated at 3, 5, and 10% strain.

Analyses were performed with Statistical Analysis Software (version 9.4; SAS Institute, Cary, NC). The outcome measures were reported as the mean ± standard deviation. The normality of all data samples was first checked by the Kolmogorov–Smirnov test. The Mann–Whitney U-test was used to compare the data between the two groups. A *P*-value of < 0.05 was considered statistically significant. The sample size ($n = 6$ in each group) in this study offered 88% statistical power at the 5% level to detect a 12-D difference in corneal astigmatism between the two groups when the standard deviation of the mean difference was 6 D. To determine the repeatability of Ks and astigmatism, intraclass correlation coefficients (ICCs) were calculated for the three repeated measurements at the baseline point in each eye. The ICC was determined based on the analysis of variance for mixed models for each situation, as proposed by Bartko and Carpenter (13). The ICC ranges from 0 to 1 and is commonly classified as follows: an ICC < 0.75 indicates poor repeatability; an ICC of 0.75 to < 0.90 indicates moderate repeatability; and an ICC > 0.90 indicates high repeatability.

Results

After collagenase treatment, daily slit-lamp examinations showed no conjunctival infection, corneal infiltration, or corneal stromal inflammation throughout the follow-up period. Fluorescein staining examinations showed complete corneal epithelial healing at ~7 days after the surgery.

TABLE 3 Repeatability of three measurements at the baseline by the ICC.

	ICC (95% CI)
Steep keratometry	0.908 (0.872–0.937)
Corneal astigmatism	0.904 (0.883–0.929)

ICC, intraclass correlation coefficient; CI, confidence interval.

At the baseline, the Ks values in the collagenase and KeraVio with collagenase groups did not differ from that in the control group ($P = 0.058$ and $P = 0.180$, respectively). Table 1 shows the Ks values from the baseline throughout the 1-week observation period. The change in Ks in the collagenase and KeraVio with collagenase groups was significant on day 7 compared with that in the control group (each $P = 0.002$).

At the baseline, corneal astigmatism in the collagenase and KeraVio with collagenase groups did not differ from that in the control group ($P = 0.065$ and $P = 0.197$, respectively). No significant difference was found in baseline corneal astigmatism between the KeraVio and collagenase groups ($p = 0.055$). Table 2 demonstrates the corneal astigmatism values from the baseline throughout the 1-week observation period. The changes in corneal astigmatism in the collagenase and KeraVio with collagenase groups were significant on day 7 compared with that in the control group (each $P = 0.002$).

Table 3 shows the repeatability of Ks and corneal astigmatism with the handheld keratometer. The repeatability of these parameters was excellent, with an ICC higher than 0.900.

At the baseline, the CCT in the collagenase and KeraVio with collagenase groups did not differ from that in the control group ($P = 0.150$ and $P = 0.355$, respectively). Table 4 presents the CCT values from the baseline throughout the 1-week observation period. The change in the CCT in the collagenase group was significantly different on day 7 compared with that in the control group ($P = 0.002$) but not the KeraVio with the collagenase group ($P = 0.132$).

TABLE 4 Changes in central corneal thickness over time.

	Baseline (μm)	1 week (μm)	Change from baseline to 1 week (μm)	* <i>P</i> -value	† <i>P</i> -value
Collagenase	380.33 \pm 31.13	289.67 \pm 46.99	−90.67 \pm 57.11	0.002	n/a
KeraVio with collagenase	377.00 \pm 27.88	290.00 \pm 81.69	−87.00 \pm 101.48	0.132	0.818
Control	341.67 \pm 20.43	341.00 \pm 14.76	−0.67 \pm 17.10	n/a	n/a

*Compared with the control group.

†Comparison between collagenase with and without KeraVio.

n/a, not applicable.

TABLE 5 Comparison of the elastic modulus in each group.

	3% (kPa)	* <i>P</i> -value	† <i>P</i> -value	5% (kPa)	* <i>P</i> -value	† <i>P</i> -value	10% (kPa)	* <i>P</i> -value	† <i>P</i> -value
Collagenase	96.60 \pm 51.87	0.004	n/a	104.01 \pm 58.28	0.004	n/a	121.48 \pm 81.08	0.002	n/a
KeraVio with collagenase	262.84 \pm 170.17	0.394	0.065	289.69 \pm 213.20	0.310	0.132	466.35 \pm 384.02	0.310	0.132
Control	354.40 \pm 190.22	n/a	n/a	407.89 \pm 220.83	n/a	n/a	604.48 \pm 280.05	n/a	n/a

*Compared with the control group.

†Comparison between collagenase with and without KeraVio.

n/a, not applicable.

Table 5 shows the elastic modulus of the treated corneas at 3, 5, and 10% strain. We found significant differences in stress values between the collagenase and control groups at 3, 5, and 10% strain ($P = 0.004$, 0.004 , and 0.002 , respectively).

Table 6 presents the average axial length at day 7. The axial length in the collagenase and KeraVio with the collagenase groups was significantly longer than that in the control group ($P = 0.004$ and 0.009 , respectively). Figure 1 shows a representative whole collagenase-treated eye, KeraVio–collagenase-treated eye, and control eye after euthanasia.

When we compared each parameter between the collagenase and KeraVio with collagenase groups, there was no significant difference in the change in Ks, corneal astigmatism, CCT, and corneal stiffness at 3, 5, or 10% strain, or axial length.

Discussion

In the present study, collagenase treatment induced a significant increase in Ks (7.08 D) at day 7, which is consistent with the clinical characteristics of irregular corneal topography. Hong CW et al. (5) reported that collagenase treatment resulted in a significant increase in corneal curvature in human corneas by 6.6 ± 1.1 D. Wang X et al. (7) demonstrated that rabbit corneas exposed to collagenase *ex vivo* showed a significant decrease in CCT. Regarding corneal thickness during accelerated CXL in clinical KC, Ocak et al. (10) found a significant decrease at the end of ultraviolet-A irradiation. They also reported a significant decrease in endothelial cell density postoperatively (11). However, we have no data on corneal thickness and endothelial cell density before and after CXL treatments. Some studies have also focused on the relationship between corneal keratometry and time (5, 6). Our study also revealed a similar decrease in Ks in the control group. Although previous studies evaluated keratometry and corneal thickness after collagenase treatments, corneal astigmatism was not clarified (5, 6). To imitate KC, we measured corneal astigmatism

TABLE 6 Average axial length at day 7 in each group.

	Axial length at day 7 (mm)	* <i>P</i> -value	† <i>P</i> -value
Collagenase	20.28 \pm 1.63	0.004	n/a
KeraVio with collagenase	19.05 \pm 1.51	0.009	0.251
Control	16.45 \pm 1.37	n/a	n/a

*Compared with the control group.

†Comparison between collagenase with and without KeraVio.

n/a, not applicable.

as a lower-order aberration. Higher-order aberrations were not evaluated in this study because corneal topography was not available. Compared to the control group, the collagenase group exhibited a significant increase in corneal astigmatism (18.39 D) at day 7.

Regarding axial length, we previously reported that VL irradiation may have the potential to retard myopia progression (14). We assessed the impact of VL irradiation on the change in axial length in eyes treated with collagenase. However, there was no significant difference in the axial length at day 7 between eyes treated with collagenase with and without KeraVio. Although we should have assessed various collagenase concentrations and exposure times in this study, we used the same methods as those of previous investigations (5, 6). The change in the axial length was a secondary outcome after collagenase administration. Unfortunately, we did not use the ultrasound method to measure the axial length in this study. Instead, we are conducting a subsequent investigation to evaluate scleral and corneal morphological changes after collagenase treatment using ultrasound.

We found significant differences in the elastic modulus between the collagenase and control groups at 3, 5, and 10% strain. Generally, when the elastic modulus of corneal strips is compared,

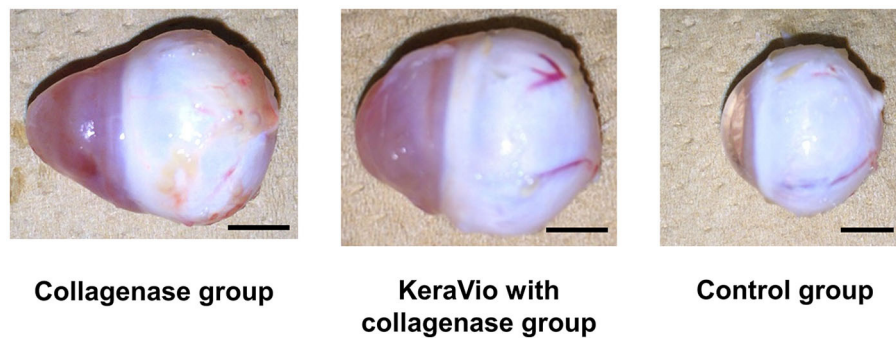


FIGURE 1

Whole eyes demonstrating the axial length in the collagenase, KeraVio with collagenase, and control groups. The scale bar represents 5 mm.

the value at 10% strain is useful and is commonly recorded (15, 16). In our study, the stress–strain curves showed an exponential increase, as in the previous investigation by Wollensak et al. (15). Compared to the results in a relevant report by Qiao et al. (6), the elastic modulus in our study demonstrated high standard deviations in each group. The discrepancy might be attributable to differences in the measurement conditions of the stress–strain test. Our higher standard deviations might be related to a day of delay in the measurement schedule due to logistics. Corneal epithelial removal induced discomfort, such as ocular pain in the rabbits, but these effects were controlled using oxybuprocaine drops.

Regarding the impact of KeraVio with collagenase on the cornea, no significant difference was found in any parameter between the collagenase and KeraVio with collagenase groups. However, the KeraVio with the collagenase group showed a slightly higher elastic modulus at 10% strain than the collagenase group. We suggest that this effect may have been due to the higher concentration of collagenase, a short-term follow-up, and an absence of riboflavin drops in the KeraVio with the collagenase group. The short-term follow-up of 7 days might be a limitation of this study because remodeling in the cornea is unstable. However, the KeraVio treatment provided sufficient VL irradiation for 7 days to produce a total energy dose that was 4.3-fold higher than the dose delivered by the standard Dresden protocol for CXL (23.4 J/cm² vs. 5.4 J/cm²). Because the current study did not include corneal changes after the CXL technique, it was difficult to determine whether KeraVio outperformed CXL in terms of preventing corneal changes. We previously compared the elastic modulus after KeraVio and standard CXL treatments without collagenase application using porcine corneas (12). The model of the previous *ex vivo* study (12) differed in terms of species from the rabbit model in this study. Further research is needed to measure the concentration of riboflavin in rabbit corneas *in vivo*. In our previous study without collagenase treatment, the KeraVio without riboflavin (VL irradiation only) and standard CXL groups showed a significantly higher elastic modulus than the control group consisting of normal eyes, whereas no significant difference between the KeraVio and CXL groups was found (12). The preliminary data indicated similar outcomes between the two treatment groups (12). To the best of our knowledge, this is the

first study to investigate corneal biometry and biomechanics after treatment with collagenase and with and without KeraVio. We are optimizing the dose of VL irradiation in preclinical investigations to move to clinical studies of KeraVio, which is similar to but distinct from CXL. To evaluate the preliminary efficacy of KeraVio using only VL irradiation without riboflavin drops, we established a collagenase animal model in the rabbit cornea.

The main limitation of the current study is that it did not assess the long-term impact of this novel corneal ectasia treatment. We avoided ethical issues regarding rabbit discomfort. No corneal complications or adverse events were observed during the 7-day follow-up period. This 1-week observation period may be too short to obtain a comprehensive understanding of this enzymatic degradation model, although, in the present study, a significant increase in Ks and a significant decrease in the elastic modulus were observed in 1 week. In addition, long-term observation is necessary for further identification of changes in Ks, corneal astigmatism, and tensile strength, which could confirm the sustainability of this novel model. Additional studies with long-term follow-up periods are warranted to better investigate the reliability and efficacy of this *in vivo* animal model of corneal ectasia. Another minor limitation is that we have no data on histopathological findings in this study. However, previous research demonstrated histopathological findings of loosely arranged collagen fibers and interlamellar clefts after collagenase treatment (6). In this study, we focused on the impact of VL irradiation under collagenase treatment. Further studies should include comprehensive assessments of histopathological images, corneal strips, and results of computer-controlled electronic universal testing machine trials. Another limitation is that in the collagenase treatment-only group, the right eye was treated while the other eye was used as a control, but in the KeraVio group, both eyes were treated when there should have been a similar monocular control.

In conclusion, a method for generating keratometric features of KC was demonstrated in rabbit eyes treated with collagenase. There was no significant difference in the observed elastic behavior of normal and ectatic corneas under physiologically relevant stress levels. KeraVio, including VL irradiation, did not cause regression of corneal steepening in this model. Further study is required to evaluate the efficacy of novel treatments for this disorder.

Data availability statement

The raw data supporting the conclusions of this article will be made available by the authors, without undue reservation.

Ethics statement

All animals were treated according to the Association for Research in Vision and Ophthalmology Statement for the Use of Animals in Ophthalmic and Vision Research. This study was approved by the Review Board at Life Science Laboratories, Ltd: #18-20.

Author contributions

HK, TY, and KT were involved in the design and conducted the study, collection, management, analysis, interpretation of data, preparation, review, and final approval of the manuscript. All authors contributed to the article and approved the submitted version.

References

- Rabinowitz YS. Keratoconus. *Surv Ophthalmol.* (1998) 42:297–319. doi: 10.1016/S0039-6257(97)00119-7
- Krachmer JH, Feder RS, Belin MW. Keratoconus and related noninflammatory corneal thinning disorders. *Surv Ophthalmol.* (1984) 28:293–322. doi: 10.1016/0039-6257(84)90094-8
- Liu YC, Konstantopoulos A, Riau AK, Bhayani R, Lwin NC, Teo EP, et al. Repeatability and reproducibility of corneal biometric measurements using the Visante Omni and a rabbit experimental model of post-surgical corneal Ectasia. *Trans Vis Sci Technol.* (2015) 4:16. doi: 10.1167/tvst.4.2.16
- Dawson DG, Grossniklaus HE, McCarey BE, Edelhauser HF. Biomechanical and wound healing characteristics of corneas after excimer laser keratorefractive surgery: is there a difference between advanced surface ablation and sub-Bowman's keratomileusis? *J Refract Surg.* (2008) 24:S90–6. doi: 10.3928/1081597X-20080101-16
- Hong CW, Sinha-Roy A, Schoenfield L, McMahon JT, Dupps WJ Jr. Collagenase-mediated tissue modeling of corneal ectasia and collagen cross-linking treatments. *Invest Ophthalmol Vis Sci.* (2012) 53:2321–7. doi: 10.1167/iovs.11-9327
- Qiao J, Li H, Tang Y, et al. A rabbit model of corneal Ectasia generated by treatment with collagenase type II. *BMC Ophthalmol.* (2018) 18:94. doi: 10.1186/s12886-018-0760-z
- Wang X, Huang Y, Jastaneiah S, Majumdar S, Kang JU, Yiu SC, et al. Protective effects of soluble collagen during ultraviolet-a crosslinking on enzyme-mediated corneal Ectatic models. *PLoS ONE.* (2015) 10:e0136999. doi: 10.1371/journal.pone.0136999
- Ihalainen A, Salo T, Forsius H, Peltonen L. Increase in type I and type IV collagenolytic activity in primary cultures of keratoconus cornea. *Eur J Clin Invest.* (1986) 16:78–84. doi: 10.1111/j.1365-2362.1986.tb01311.x
- Kobashi H, Torii H, Toda I, Kondo S, Itoi M, Tsubota K. Clinical outcomes of KeraVio using violet light: emitting glasses and riboflavin drops for corneal ectasia: a pilot study. *Br J Ophthalmol.* (2021) 105:1376–82. doi: 10.1136/bjophthalmol-2020-316974
- Ocak SY, Mangan MS, Elçioglu MN. The intraoperative corneal pachymetry changes during accelerated corneal cross-linking in progressive keratoconus patients with thin corneas. *Korean J Ophthalmol.* (2021) 35:438–42. doi: 10.3341/kjo.2021.0111
- Yurttaser Ocak S, Mangan MS. Endothelial cell loss after accelerated corneal crosslinking using pachymetry-guided hypo-osmolar riboflavin dosing in thin keratoconic corneas. *J Cataract Refract Surg.* (2021) 47:1530–4. doi: 10.1097/j.jcrs.0000000000000686
- Kobashi H, Yunoki S, Kato N, Shimazaki J, Ide T, Tsubota K. Evaluation of the physiological corneal intrastromal riboflavin concentration and the corneal elastic modulus after violet light irradiation. *Transl Vis Sci Technol.* (2021) 10:12. doi: 10.1167/tvst.10.5.12
- Bartko JJ, Carpenter WT Jr. On the methods and theory of reliability. *J Nerv Ment Dis.* (1976) 163:307–17. doi: 10.1097/00005053-197611000-00003
- Torii H, Ohnuma K, Kurihara T, Tsubota K, Negishi K. Violet light transmission is related to myopia progression in adult high myopia. *Sci Rep.* (2017) 7:14523. doi: 10.1038/s41598-017-09388-7
- Wollensak G, Spoerl E, Seiler T. Stress-strain measurements of human and porcine corneas after riboflavin-ultraviolet-A-induced cross-linking. *J Cataract Refract Surg.* (2003) 29:1780–5. doi: 10.1016/S0886-3350(03)00407-3
- Hammer A, Richoz O, Arba Mosquera S, Tabibian D, Hoogewoud F, Hafezi F. Corneal biomechanical properties at different corneal cross-linking (CXL) irradiances. *Invest Ophthalmol Vis Sci.* (2014) 55:2881–4. doi: 10.1167/iovs.13-13748

Conflict of interest

HK and KT are employed by Tsubota Laboratory Inc. TY is employed by Life Science Laboratories, Ltd.

Publisher's note

All claims expressed in this article are solely those of the authors and do not necessarily represent those of their affiliated organizations, or those of the publisher, the editors and the reviewers. Any product that may be evaluated in this article, or claim that may be made by its manufacturer, is not guaranteed or endorsed by the publisher.

Supplementary material

The Supplementary Material for this article can be found online at: <https://www.frontiersin.org/articles/10.3389/fmed.2023.1109689/full#supplementary-material>



OPEN ACCESS

EDITED BY

Cristina Nicula,
University of Medicine and Pharmacy Iuliu
Hatieganu, Romania

REVIEWED BY

Mehran Zarei-Ghanavati,
Tehran University of Medical Sciences, Iran
Swaminathan Sethu,
Narayana Nethralaya Foundation, India

*CORRESPONDENCE

Damien Gatinel
✉ gatinel@gmail.com

RECEIVED 27 January 2023

ACCEPTED 28 April 2023

PUBLISHED 24 May 2023

CITATION

Mazharian A, Flamant R, Elahi S, Panthier C,
Rampat R and Gatinel D (2023) Medium to long
term follow up study of the efficacy of
cessation of eye-rubbing to halt progression of
keratoconus.

Front. Med. 10:1152266.

doi: 10.3389/fmed.2023.1152266

COPYRIGHT

© 2023 Mazharian, Flamant, Elahi, Panthier,
Rampat and Gatinel. This is an open-access
article distributed under the terms of the
[Creative Commons Attribution License \(CC BY\)](https://creativecommons.org/licenses/by/4.0/).
The use, distribution or reproduction in other
forums is permitted, provided the original
author(s) and the copyright owner(s) are
credited and that the original publication in this
journal is cited, in accordance with accepted
academic practice. No use, distribution or
reproduction is permitted which does not
comply with these terms.

Medium to long term follow up study of the efficacy of cessation of eye-rubbing to halt progression of keratoconus

Adrien Mazharian, Roxane Flamant, Sina Elahi,
Christophe Panthier, Radhika Rampat and Damien Gatinel*

Centre d'Explorations et de Recherche en Optique Visuelle (CEROV), Hôpital Fondation Rothschild,
Paris, France

Purpose: To study the progression of keratoconus after cessation of eye rubbing with a minimum follow up of three-years.

Design: Retrospective, monocentric, longitudinal cohort study of keratoconus patients with a minimum of 3 years follow-up.

Participants: One hundred fifty three eyes of seventy-seven consecutive patients with keratoconus were included.

Methods: Initial examination consisted of anterior and posterior segment evaluation using slit-lamp biomicroscopy. At the initial visit, patients were thoroughly informed of their pathology and instructed to stop rubbing their eyes. Eye rubbing cessation was assessed at all the follow-up visits at 6 months, 1 year, 2 years, 3 years, and yearly afterward. Corneal topography using the Pentacam® (Oculus®, Wetzlar, Germany) was used to obtain maximum and average anterior keratometry readings (Kmax and Kmean), as well as thinnest pachymetry (Pachymin, μm) in both eyes.

Main outcome measures: The main outcomes measured were maximum keratometry (Kmax), mean keratometry (Kmean), and thinnest pachymetry (Pachymin) values at various time points to assess for keratoconus progression. Keratoconus progression was defined as a significant augmentation of Kmax ($>1\text{D}$), Kmean ($>1\text{D}$), or significant diminution of Pachymin ($>5\%$) throughout the total follow-up duration.

Results: One hundred fifty three eyes of seventy-seven patients (75.3% males) aged 26.4 years old, were followed for an average of 53 months. Over the course of the follow-up, there was no statistically significant variation of ΔKmax ($+0.04 \pm 0.87$; $p=0.34$), ΔKmean ($+0.30 \pm 0.67$; $p=0.27$) nor $\Delta\text{Pachymin}$ (-4.36 ± 11.88 ; $p=0.64$). Among the 26 of the 153 eyes which had at least one criterion of KC progression, 25 admitted continuing eye rubbing, or other at-risk behaviors.

Conclusion: This study suggests that a significant proportion of keratoconus patients are likely to remain stable if close monitoring and strict ARB cessation are achieved, without the need for further intervention.

KEYWORDS

eye-rubbing, keratoconus, cornea, ectasia, corneal topography, progression

1. Introduction

Keratoconus (KC) is characterized by a progressive, asymmetric deformation of the cornea associated with central or paracentral corneal thinning, usually first diagnosed in adolescents or young adults. The condition results in ectasia, which can lead to significant visual impairment, sometimes severe enough to require corneal graft surgery (1).

The reported prevalence of eye-rubbing in KC patients is between 66% et 73% (2, 3). Although many different pathways such as biochemical, genetic, environmental, mechanical or multi-factorial origin have been investigated, the specific underlying cause of this condition is not fully understood (4).

Some hypothesized that repetitive, external, biomechanical stress can induce weakening and deformation of the cornea (5–7). Gatinel put forth the conjecture that KC is not a dystrophy of unknown genetics and biomolecular substratum, but rather a syndrome caused by eye rubbing, resulting in the progressive deformation and thinning of the corneal wall, the hallmarks of the disease (8, 9). If eye rubbing is an indispensable circumstance, then removing this mechanical stress could lead to stabilization of the induced corneal deformation (10, 11). This mechanical stress is often in the form of repetitive eye rubbing. Other at-risk behaviors (ARB) such as incorrect sleeping position (12–15) and applying overnight pressure on the cornea, may also play a role to some extent. While eye rubbing and allergy have recognized associations (16) with keratoconus, their precise causative relationship and contribution to disease progression is still debated. This study aimed to determine if eye rubbing, and other ARB cessation alone, may be effective in stabilizing keratoconus.

2. Materials and methods

2.1. Study design

This was a single-center retrospective cohort study of naïve keratoconus patients with a minimum of 3 years follow-up at the Rothschild Foundation, Paris, France.

The initial examination consisted of anterior and posterior slit lamp examination, corneal topography, maximum and mean keratometry (Kmax and Kmean, respectively), as well as thinnest pachymetry (Pachymin) (Pentacam®, Oculus®, Wetzlar, Germany). Objective refractive measures (Sphere and cylinder) recorded at initial visits were not included in the follow-up visits due to poor repeatability demonstrated in keratoconus patients (17). The study was conducted in accordance with the tenets of the 1964 Declaration of Helsinki. Informed consent was obtained from all the study subjects when anonymization was impossible.

2.2. Inclusion/exclusion criteria

Patients with keratoconus aged between 12 and 40 years old at the first visit were included based on the « Global consensus on keratoconus and corneal ectasia 2015 » criteria, defined as abnormal posterior ectasia, clinical non-inflammatory corneal thinning and abnormal corneal thickness distribution (18). Examinations were performed 3 days after soft contact lens and 2 weeks after rigid/scleral

contact lens removal. Patients with consultations preceding their referrals often had missing or inconsistent data, clinical information, or underwent investigations using other imaging methods with poor comparability; the reference point (baseline) was defined as the first visit to our center. Patients with prior cross-linking, or surgical intervention were excluded as well as patients with factors leading to compulsive eye-rubbing (19) or poor compliance such as autism, Tourette's syndrome, and Down Syndrome, a history of infectious corneal pathology, or presence of any inflammatory corneal condition, except for ocular allergies.

2.3. Outcome measures

The primary outcome measured was the absence of keratoconus progression, based on Wittig-Silva et al.'s criteria (20) of a significant increase in Kmax or Kmean ($> 1.0D$) or decrease in Pachymin ($> 5\%$) over the course of the follow-up (defined as ΔK_{max} , ΔK_{mean} , and $\Delta PachyMin$). The standard criteria are variations over a one-year duration, but we restricted our study to the same criteria over the course of the entire follow-up duration to ensure that slowly-progressing eyes (i.e., $< 1D$ progression per year) do not falsely meet the absence of progression criteria.

2.4. Follow-up

Patients were examined and underwent topographic measurements at 6 months, 1 year, 2 years, 3 years, and yearly afterwards.

Most patients had multimodal imaging using several topographers, but the Pentacam® was chosen for this study because of its repeatability and reproducibility, as described in the literature (17, 21, 22). A subgroup of 100 anonymized patients consented to make their medical records, with clinical photographs and investigation reports available on the website: <https://defeatkeratoconus.com> (23).

2.5. Evaluation of at-risk behaviors

To evaluate the presence and extent of ARB, a detailed history was taken to establish the presence, frequency, and specific manner (frequency, intensity, dominant hand, time of day) of eye rubbing and other ARB, often aided by interrogation of family members and close relatives in patients suspected of anosognosia. This was repeated at each visit, and the importance of ARB cessation was reinforced. Patients describing ocular itch or discomfort were prescribed topical antihistamines and/or ocular lubricants. Patients with potentially damaging sleeping positions (prone or side-sleeping position with ocular compression) were systematically offered a rigid eye shields as nighttime protection and encouraged to modify their sleeping position (12–15).

Only repeated and daily eye-rubbing with the testimony of relatives was considered pathological. We have collected all of these testimonials, including making case reports with photos by putting them on the following site: <https://defeatkeratoconus.com/> (23).

We have yet to find another way to characterize this behavior, which remains mainly based on the patient's declaration.

Sleeping with either eyes dug in the pillow or nocturnal eye-rubbing was considered pathological. Sleeping on the back or the opposite side was not counted as an ARB. Therefore, a patient reporting a predominant right-sided sleeping position had only the right eye included in the ARB group.

2.6. Statistical analysis

Results were reported as mean \pm standard deviation (SD). ΔK_{\max} , ΔK_{mean} , $\Delta \text{Pachymin}$ were defined as the difference between the values at the latest visit and the baseline.

A statistically significant difference between means and between timepoints was determined using paired or unpaired Student *t*-test, as well as a categorical pairwise comparison using Tukey's method. value of $p < 0.05$ were considered statistically significant. All statistical analyses were performed using Stata software (v14.0 StataCorp, TX, United States).

3. Results

3.1. Baseline patient characteristics

Out of 396 patients diagnosed with keratoconus during the studied period, 176 met the inclusion criteria, and 77 completed the 3-year follow-up. The study included 153 eyes (77 patients, 75.3% males) with keratoconus over a follow-up of 53 ± 20.8 months. The average age was 26.4 years (range 12–40 years). Table 1 displays demographic and baseline characteristics. Figure 1 shows the distribution of dominant hand in the studied population. Table 2 displays demographic and baseline characteristics in each studied sub-group: absence of At-Risk Behavior (ARB) or Recurrent Eye-Rubbing (RER), presence of ARB only, presence of RER only and presence of both ARB and RER.

3.2. Keratometry measures (K_{\max} and K_{mean})

The variation in keratometry at various time points is presented in Tables 3, 4. There is no statistically significant difference between

ΔK_{\max} means at all time points, as displayed on Table 3. Similar results were observed for ΔK_{mean} with almost no significant difference at all time points except between year 2 and year 3 (0.09 ± 0.86 vs. 0.56 ± 1.97 , $p = 0.03$) (Table 4). The variation in keratometry at various time point has also been analyzed in 4 sub-groups: absence of At-Risk Behavior (ARB) or Recurrent Eye-Rubbing (RER), presence of ARB only, presence of RER only and presence of both ARB and RER. They are summarized in Tables 5, 6. There is a statistically significant difference of K_{\max} variation in the “RER only” sub-group from month from year 2 until end of follow-up for K_{\max} ($+1.48$, $p = 0.04$, $+2.32$, $p < 0.01$, $+4.01$, $p < 0.01$ and $+1.60$, $p < 0.01$) (Table 5) and year 3 until end of follow-up for K_{mean} ($+1.14$, $p < 0.01$, $+3.58$, $p < 0.01$ and $+1.17$, $p < 0.01$) (Table 6). Other sub-groups show no significant variation in both K_{\max} and K_{mean} during follow-up, except for “ARB and RER” sub-group regarding K_{mean} criteria at more than 48 months follow-up ($+0.60$, $p = 0.02$) (Tables 5, 6).

3.3. Minimal pachymetry

Variations in Pachymin are reported throughout Table 7 and show a statistically significant difference between $\Delta \text{Pachymin}$ at year 2 and year 3 (-0.24 ± 10.26 vs. -4.38 ± 14.18 , $p = 0.02$). The variation in Pachymin at various time point has also been analyzed in 4 sub-groups: no At-Risk Behavior (ARB) nor Recurrent Eye-Rubbing (RER), ARB only, RER only and both ARB and RER. They are summarized in Table 8. “Only RER” sub-group shows statistically significant difference in Pachymin variation from year 2 to year 4 (-7.33 , $p = 0.01$, -15.34 , $p = 0.03$ and -22.46 , $p < 0.01$). “ARB and RER” sub-group presents significant Pachymin variation at year 2 and 4 ($+5.38$, $p = 0.01$ and $+6.20$, $p < 0.01$). As this variation is positive, it cannot be associated with keratoconus progression. Other sub-groups display no statistically significant difference in Pachymin (Table 8).

3.4. Progression analysis

3.4.1. Primary outcome: $K_{\max} \geq 1D$

Out of the 153 studied eyes, 21 (13.73%) showed progression according to the ΔK_{\max} criteria, 20 of which (95.23%) admitted that they could not stop their ARB.

Figures 2A,B compare ΔK_{\max} at the end of the follow-up between patients who have kept both ARB and RER, one of each and patients who have managed to stop.

3.4.2. Secondary outcome: K_{mean}

Out of the 153 eyes, 16 (10.46%) showed progression according to the ΔK_{mean} secondary criteria, all of which (100%) failed to stop ARB over the course of the follow-up.

Figures 3A,B compare ΔK_{mean} at the end of the follow-up between patients who have kept both ARB and RER, one of each and patients who have managed to stop.

3.4.3. Secondary outcome: PachyMin

Out of the 153 eyes, 7 (4.58%) showed progression according to the $\Delta \text{PachyMin}$ secondary criteria, all of which (100%) failed to stop ARB during the follow-up.

TABLE 1 Baseline characteristics of patients.

	Value	SD or %
Total of patients	77	0
Number of KC eyes	153	0
Age (years)	26.4	± 7.3
Male, <i>n</i> (patients)	58/77	75.32%
Follow-up (months)	53.0	± 20.8
K_{\max}	51.6	± 6.1
K_{mean}	45.5	± 3.2
Pachymin (μm)	479.3	± 41.9

KC, Keratoconus; K_{\max} , Maximal keratometry reading; K_{mean} , Mean keratometry reading; PachyMin, Minimal corneal thickness measurement; SD, Standard Deviation.

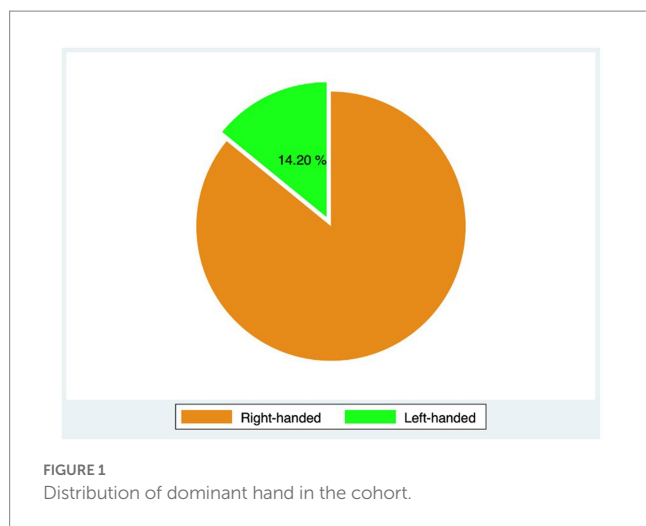


TABLE 2 Baseline characteristics of patients in each sub-group.

	No ARB/RER	RER only	ARB only	ARB & RER	p-value
Total of patients	44	15	18	10	
Number of KC eyes	80	28	28	17	
Age (years)	26.5	26.7	27.4	30.1	0.7
Follow-up (months)	46.6	41.0	53.0*	55.1*	<0.01
Kmax	52.2	50.3	51.0	50.5	0.44
Kmean	46.1	45.2	44.9	44.1	0.06
Pachymin (μm)	475.7	475.0	496.9	484.5	0.20

ARB, At-Risk Behavior; RER, Recurrent Eye-Rubbing; KC, Keratoconus; Kmax, Maximal keratometry reading, Kmean, Mean keratometry reading; PachyMin, Minimal corneal thickness measurement, *Indicates statistical significance in this sub-group ($p < 0.05$).

Figures 4A,B compare Δ Pachymin at the end of the follow-up between patients who have kept both ARB and RER, one of each and patients who have managed to stop.

Out of 153 eyes, 26 had at least one progression criterion, and among these, 23 continued ARB.

3/26 patients had disease progression despite positively denying any form of ARB. When comparing progressive and non-progressive populations, there was no statistically significant difference in terms of baseline age, Kmax, Kmean or pachymin as shown in Table 9. Table 10 details the percentage of progression for each positive criteria, in all pre-cited sub-groups. The “RER only” sub-group shows the highest progression rate for each criteria (35.71 and 21.43% for Kmean and Pachymin respectively), except for Kmax>1D: “RER and ARB” sub-group ranks first in this category (41.18% vs. 39.29% for “RER only”) as displayed in Table 10.

4. Discussion

This retrospective study describes the relationship between ARB (especially eye rubbing) and KC progression, and the possibility that

TABLE 3 Maximal Keratometry¹ variations at different timepoints.

	Mean	SD	N	p [†]
Baseline	0	0	153	
Δ M6	0.01	1.01	78	0.91
Δ M12	-0.16	0.72	107	0.23
Δ M24	-0.05	1.81	90	0.56
Δ M36	0.57	2.76	116	0.07
Δ M48	0.46	3.18	72	0.83
$\Delta > M48$	0.04	0.87	51	0.34

M, Months; SD, Standard Deviation. [†]Unpaired Student's *t*-test comparing the statistically significant difference from the previous timepoint. *Indicates statistical significance ($p < 0.05$). ¹Stand for Kmax.

TABLE 4 Mean Keratometry² variations at different timepoints.

	Mean	SD	N	p value [†]
Baseline	0	0	153	
Δ M6	0.04	0.76	86	0.52
Δ M12	-0.04	0.48	110	0.39
Δ M24	0.09	0.82	90	0.18
Δ M36	0.56	1.97	120	0.03*
Δ M48	0.66	2.48	84	0.75
$\Delta > M48$	0.30	0.67	61	0.27

M, Months; SD, Standard Deviation. [†]Unpaired Student's *t*-test comparing the statistically significant difference from the previous timepoint. *Indicates statistical significance ($p < 0.05$). ²Stand for Kmean.

solely preventing the corneas to suffer repetitive mechanical stress, may be sufficient for long-term disease stabilization (or delay in progression), thereby avoiding the risks of potentially unrequired treatments. Multiple studies have reported a higher prevalence of eye-rubbing in keratoconus patients compared to the normal population (2, 4, 6, 24–29), and the implication of eye-rubbing in development and progression of keratoconus is well-described in the literature (30–33). Eye-rubbing has been shown to be the most significant cause of keratoconus in multivariate analysis (34). However, whether eye-rubbing is merely a risk-factor, or rather a sine-qua-non condition for the disease to appear and progress, is a question that remains yet debated (8, 9, 35).

The results of this study show disease progression (according to any of the three defined criteria) in 16.9% (26/153) of the eyes. Almost all were explained by the self-admitted persistence of ARB. Only 1 of these (0.65%) showed progression in the absence of ARB. Careful and thorough evaluation of the files and clinical data did not permit to identify ARBs or risk factors explaining the progression. Due to the nature of the ARBs, which are most often subconscious and can even occur overnight while unconscious, we believe that there is a probability of anosognosia. Objective confirmation of this hypothesis is unlikely to be proven until technology makes objective continuous monitoring of ARB possible.

Ferdi et al. systematic review and meta-analysis (11,529 eyes) (36) studying keratoconus' natural progression found a significant Kmax progression of 0.7D at 12 months follow-up with significant variation depending on age and ethnicity. A significant Kmean progression was measured at 0.4D during the same period. Their

TABLE 5 Maximal Keratometry¹ variations at different timepoints for each sub-group: no ARB nor RER, ARB only, RER only and both ARB and RER.

Δ KMAX	No ARB/RER	RER only	ARB only	ARB & RER	N	p value [‡]
Baseline	0	0	0	0		
Δ M6	-0.17	0.26	-0.18	-0.89	78	0.07
Δ M12	-0.23	-0.34	0.01	-0.20	107	0.68
Δ M24	-0.53	1.48*	-0.26	0.04	90	0.04
Δ M36	0.07	2.32*	0.38	-0.06	115	<0.01
Δ M48	-0.18	4.01*	-0.03	-0.54	72	<0.01
$\Delta > M48$	-0.31	1.6*	-0.02	1.22	52	<0.01

ARB, At-Risk Behavior, RER, Recurrent Eye-Rubbing, M, Months, [‡]Unpaired Student's *t*-test comparing the statistically significant difference from the previous timepoint, *Indicates statistical significance in this sub-group ($p < 0.05$). ¹Stand for Kmax.

TABLE 6 Mean Keratometry² variations at different timepoints for each sub-group: no ARB nor RER, ARB only, RER only and both ARB and RER.

Δ KM	No ARB/RER	RER only	ARB only	ARB & RER	N	p value [‡]
Baseline	0	0	0	0		
Δ M6	-0.07	-0.10	0.08	-0.10	86	0.39
Δ M12	-0.04	-0.01	-0.10	0.00	110	0.96
Δ M24	-0.12	0.76	0.23	0.17	90	0.07
Δ M36	0.34	1.14*	0.39	0.16	119	<0.01
Δ M48	0.66	3.58*	0.31	-0.13	84	<0.01
$\Delta > M48$	0.05	1.17*	0.07	0.60*	62	0.02

ARB, At-Risk Behavior, RER, Recurrent Eye-Rubbing, M, Months, [‡]Unpaired Student's *t*-test comparing the statistically significant difference from the previous timepoint, *Indicates statistical significance in this sub-group ($p < 0.05$). ²Stand for Kmean.

meta-analysis model predicted a gradual reduction in the progression of Kmax and Kmean over the years. When comparing a control-group with a cross-linking group, Wittig-Silva et al. (20) reported a mean Kmax variation of 1.20 vs. -0.72D at 12 months and 1.75D vs. -1.03D at 36 months, respectively. Minimal pachymetry reduction at 36 months was 17.01 vs. 19.52 μ m in the control and cross-linking groups, respectively.

Finally, a systematic review and meta-analysis of two techniques of crosslinking (transepithelial versus epithelium-off) (37) reported a KMax variation of -0.06D at 12 months in the transepithelial cross linking group (440 eyes) compared to -0.54D in the epithelium-off group (486 eyes). Kmean progression was measured at -0.62D and -1.48D at 12 months and progression at 12 months was 7 and 2% in the trans-epithelial and epithelium-off groups, respectively. Significant complications such as corneal melt, persistent corneal ulcer, or visually significant stromal haze were seen in 2 and 4% of eyes in the trans-epithelial and epithelium-off groups, respectively.

Our patients showed a mean Kmax progression of -0.16D and +0.57D at 12 et 36 months, respectively, which is better than the natural progression reported by Ferdi et al. meta-analysis (36) and Wittig-Silva et al. control-group (20). We report a Kmean variation of -0.16D and +0.53D at 12 et 36 months, respectively, which

TABLE 7 Minimal pachymetry outcomes in keratoconus patients.

	Mean	SD	N	p [‡]
Baseline	0	0	153	
Δ M 6	-0.42	9.563	86	0.59
Δ M 12	-0.81	8.41	110	0.76
Δ M 24	-0.24	10.26	90	0.67
Δ M 36	-4.38	14.18	120	0.02*
Δ M 48	-3.25	15.52	84	0.59
$\Delta > M48$	-4.36	11.88	61	0.64

M, Months, SD, Standard Deviation. [‡]Unpaired Student's *t*-test comparing the statistically significant difference from the previous timepoint. *Indicates statistical significance ($p < 0.05$).

TABLE 8 Minimal pachymetry outcomes in keratoconus patients for each sub-group: no ARB nor RER, ARB only, RER only and both ARB and RER.

Δ PachyMin (μ m)	No ARB/RER	RER only	ARB only	ARB & RER	N	p-value
Baseline	0	0	0	0		
Δ M 6	1.51	-1.58	-4.41	7.50	86	0.07
Δ M 12	0.34	-2.64	-1.72	-2.00	110	0.32
Δ M 24	-0.34	-7.33*	2.27	5.38*	90	0.01
Δ M 36	0.03	-15.34*	-4.82	-4.38	119	0.03
Δ M 48	0.44	-22.46*	-2.23	6.20*	84	<0.01
$\Delta > M48$	-4.65	-0.25	0.67	-3.33	62	0.76

ARB, At-Risk Behavior, RER, Recurrent Eye-Rubbing, M, Months, [‡]Unpaired Student's *t*-test comparing the statistically significant difference from the previous timepoint, *Indicates statistical significance in this sub-group ($P < 0.05$).

outperforms Ferdi et al. meta-analysis (36) again. Regarding the pachymetry criteria, we demonstrate a loss of 0.42 μ m and 4.4 μ m at 12 and 36 months, respectively, which surpasses both Ferdi et al. (36) and Wittig-Silva et al. (20) groups.

Our cohort thus demonstrates fewer variation in all progression criteria compared to natural keratoconus progression as defined by Ferdi et al. large meta-analysis (36) and Wittig-Silva et al. control-group (20).

Regarding crosslinking data, both Wittig-Silva et al. (20) and Nath et al. (37) reported a significant Kmax flattening which seems to persist up to 36 months follow-up and outperforms our results. However, our keratoconus progression rate (1.96% in the absence of reported eye-rubbing or ARB at 53 months mean follow-up) equals if not supersedes Nath et al. (37) two cross-linking groups (2 and 7% at 12 months follow-up). One could discuss that cross-linked populations usually present more aggressive forms of keratoconus, resulting in a selection bias in those cohorts. But one should remember that our patients were all showing progression when referred to our department. On the other hand, one should also consider the significant complications rate observed by Nath et al. systematic review and meta-analysis (37), compared to their absence in our conservative approach.

In conclusion, our conservative treatment performs well with regards to keratoconus progression rate, in comparison to both its natural evolution and cross-linked populations. It can be described

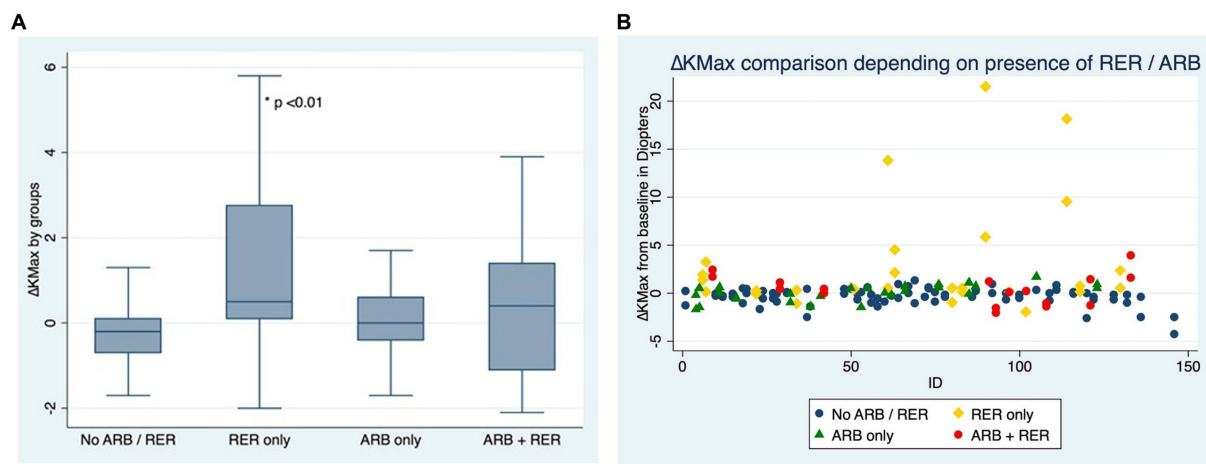


FIGURE 2

(A) Comparison of Kmax variation for each eye, depending on presence or absence of at-risk behaviors (ARB) and recurrent eye-rubbing (RER) - Box and whiskers for each sub-group. (B) Comparison of Kmax variation for each eye, depending on presence or absence of at-risk behaviors (ARB) and recurrent eye-rubbing (RER) - "Scattered-Dot" Plots Graph for each sub-group.

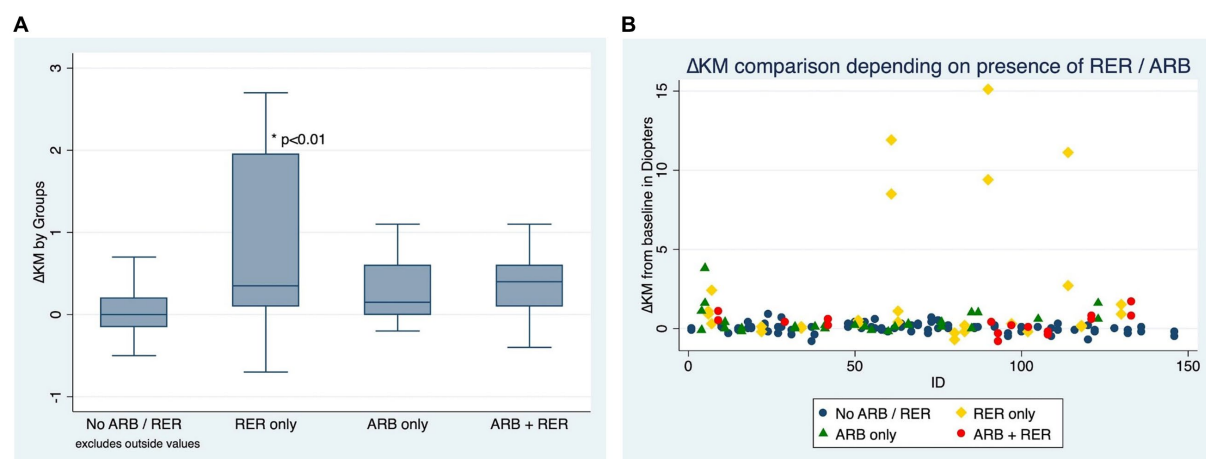


FIGURE 3

(A) Comparison of Kmean variation for each eye, depending on presence or absence of at-risk behaviors (ARB) and recurrent eye-rubbing (RER) - Box and whiskers for each sub-group. (B) Comparison of Kmean variation for each eye, depending on presence or absence of at-risk behaviors (ARB) and recurrent eye-rubbing (RER) - "Scattered-Dot" Plots Graph for each sub-group.

as a safe and efficient first-step treatment of keratoconus, which resolves most keratoconus progression cases. More invasive procedures, such as cross-linking can be indicated as second-step treatment if progression persists despite good compliance to recommendations.

When asked about performing anticipated cross-linking in pediatric patients, in absence of progression proof, we think that recent literature shows controversy in terms of cross-linking efficacy and safety, especially in pediatric populations. On one hand, Ferdi et al. (36) meta-analysis predicts an annual 1.5D Kmax progression in under 17 years old patients and McAnena et al. (38) meta-analysis and systematic review recommends cross-linking in pediatric keratoconus cases. On the other hand, Or et al. (39) five year follow-up suggests that there is no emergency to perform cross-linking in underaged

patients in absence of progression proof, and Achiron et al. (40) meta-analysis observes a rough 10% keratoconus progression risk after cross-linking in this same population. As therapists, we feel that performing a procedure carrying significant risks without proof of progression is aggressive.

Our approach would rather favor patient education to their chronic disease, removal of causative factors and close monitoring of high-risk populations such as the pediatric one. If progression is observed, further treatment such as cross-linking is more promptly and aggressively suggested, according to McAnena et al. (38) conclusions.

Regarding data, our cohort contains some young patients. Twenty-six patients were younger than 18 at diagnosis and were included in this study. When comparing progression criteria in this

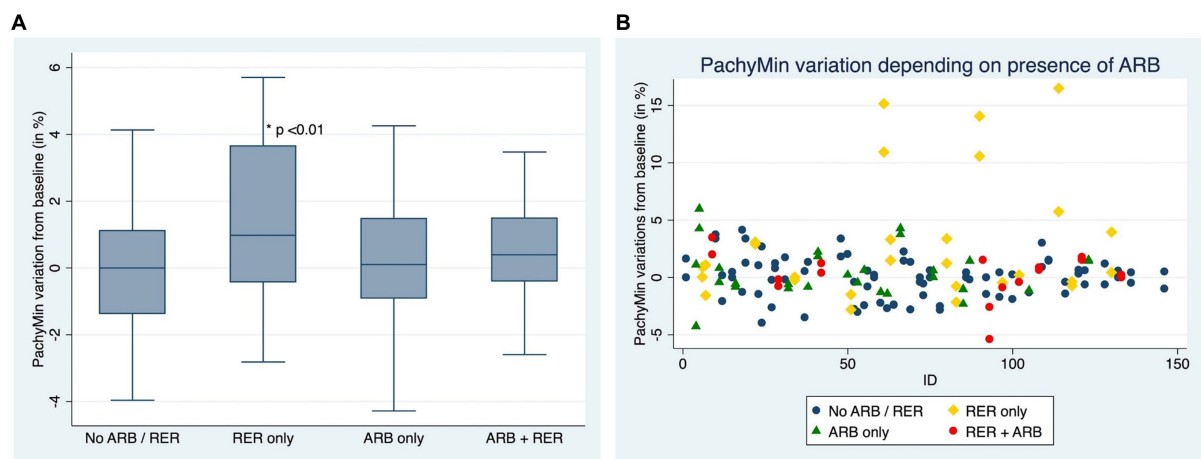


FIGURE 4

(A) Comparison of Pachymin variation for each eye, depending on presence or absence of at-risk behaviors (ARB) and recurrent eye-rubbing (RER) - Box and whiskers for each sub-group. (B) Comparison of Pachymin variation for each eye, depending on presence or absence of at-risk behaviors (ARB) and recurrent eye-rubbing (RER) - "Scattered-Dot" Plots Graph for each sub-group.

TABLE 9 Characteristics of patients with and without progression.

	General	Progressing	Non progressing	p-value
Total of patients	77			
Number of KC eyes	153	26 (16.99%)	127 (83.01%)	
Age (years)	26.4	24.83	26.70	0.24
Male (percentage of patients)	75.82%	69.23%	77.13%	0.39
Follow-up (months)	53.04	57.74	52.08	0.21
Kmax	51.6	53.47	51.16	0.08
Kmean	45.5	46.02	45.43	0.39
Pachymin (μm)	479.3	474.35	480.32	0.51

KC, Keratoconus; Kmax, Maximal keratometry reading; Kmean, Mean keratometry reading; PachyMin, Minimal corneal thickness measurement.

subgroup to the older patients, there was progression in 5/26 (19.23%) compared to 16/127 (12.60%) ($p=0.37$). Of the 5 young patients progressing, 4 admitted continuing daily eye rubbing despite the recommendations.

We hypothesize that young people are less compliant with the recommendations, probably because of poor understanding of the possible seriousness of their condition. We believe that if these patients developed keratoconus at an early age, it is because of more aggressive eye-rubbing habits, which are more difficult to give up.

Conversely, allergic conjunctivitis was more often reported in those patients' files than in older ones. Topical treatment was key to helping them eradicate their eye-rubbing habits, and thus keratoconus progression.

TABLE 10 Percentage of progression according to positive criteria in each sub-group.

Progression	KMAX (>1D)	KM (>1D)	PACHYMIN (>5%)
No ARB/RER	1/80 (1.25%)	0/80 (0%)	0/80 (0%)
RER only	11/28 (39.29%)	10/28 (35.71%)	6/28 (21.43%)
ARB only	2/28 (7.14%)	4/28 (14.29%)	1/28 (3.57%)
ARB & RER	7/17 (41.18%)	2/17 (11.76%)	0/17 (0%)

ARB, At-Risk Behavior; RER, Recurrent Eye-Rubbing; Kmax, Maximal keratometry reading; Kmean, Mean keratometry reading; PachyMin, Minimal corneal thickness measurement.

Finally, there is also known physiologic evidence that Maillard reaction enhances cornea rigidity in aging corneas (41). As younger patients do not benefit from this protective factor, we believe that shear-stress caused by eye-rubbing tends to be more impactful on their corneas, leading to more progress.

Mechanical models have shown that keratoconus progresses under environmental stresses, but only when there is an initial defect, especially a thinning defect such as that induced by continual eye rubbing (42). McMonnies (6) extensively reviewed the possible mechanisms for the association between chronic habitual eye rubbing and the development of keratoconus. He described several potential factors, including temperature increase from eye rubbing (2, 43–45), leading to increased activity of inflammatory mediators and enzymes; hydrostatic pressure increases combined with enzyme activation "tenderizing" the cornea; reduction of corneal shear strength; reduction of proteoglycan viscosity and displacement of proteoglycans from the corneal apex; and induction of keratocyte apoptosis from eye rubbing. It has been shown that healthy patients who rub their eyes mainly use the pulps of their fingers, producing a weak force equivalent to $0.45 \text{ cm kg}/2.54^2$, while keratoconus patients tend to use their knuckles, along with more

frequent and prolonged rubbing, producing a force greater than 4.5 cm kg/2.54² (46). Indeed there are many anecdotal reports in the literature which support a mechanical hypothesis, with reports of keratoconus associated with repeated and vigorous eye-rubbing alone in patients without a family history of KC (33, 47–50).

In addition, the mechanical hypothesis is consistent with the well-recognized association between allergy and keratoconus. In certain countries such as Israel (51), Lebanon (52), and Saudi Arabia (53), the association with allergy is even stronger. Patients with ocular allergy are more often subject to itch, therefore more likely to rub their eyes and induce further progression of keratoconus. Keratoconus has been shown to be more likely to progress in patients with ocular allergy (53, 54).

It is increasingly recognized that the development and progression of keratoconus is highly likely in the presence of external triggers, particularly repetitive vigorous corneal trauma such as eye-rubbing, compression of the globe during sleep (15), heat (43) and induced inflammation, atopy, and allergy, which may be or may not be associated with a coexisting genetic predisposition which renders the cornea more susceptible to trauma. This is then responsible for a cascade of biochemical events culminating in the development of keratoconus. Notably, only 6 patients in our study had a family history of keratoconus, while all patients admitted vigorous eye-rubbing, and indeed a specific genetic factor for keratoconus has proven difficult to identify. Although certain familial cases and genetic studies favor a genetic origin (55), no specific gene mutation has been clearly identified, and discordance for keratoconus in monozygotic twins have been reported (56).

One of the alarming issues with studies pertaining to keratoconus is the lack of consensus regarding the definition of disease progression, which often relies on the interpretation of multiple parameters such as subjective refraction, uncorrected and best-corrected visual acuity, and corneal topographies. Despite its important flaw of limiting the disease to just a focal corneal measurement, an increase in the maximum keratometry (≥ 1 D) remains the most frequently reported index of disease progression (18, 21, 22). However, a rising trend among corneal specialists suggests several criteria, especially non-focal ones, may prove more reliable (57).

We acknowledge that our study has limitations. Although patients are encouraged to maintain their follow-up, significant loss to follow-up occurred in the initial population. This is likely explained by the nature of the center, a specialized tertiary center in a capital city that receives many referrals from patients with long commutes who may prefer local care after the initial first specialized visits. This might explain the statistically significant difference in ΔK_{mean} and $\Delta PachyMin$ at one specific timepoint (year 3) with a loss of significance at later time points. The absence of further treatment escalation, such as an intervention date, in addition to the seemingly simplistic therapeutic approach proposed (in the eyes of the patients), may also have undermined the importance of regular follow-up in a population composed of young and active individuals with professional obligations. It has been observed that cross-linking studies are susceptible to loss of follow-up of between 6 and 15% depending on the duration of study (58). The loss of follow-up may have biased the results of this

study by excluding patients with relatively mild to moderate forms of stabilized keratoconus. In our experience, the present cohort illustrates a more pessimistic view of keratoconus progression than what one actually sees in daily practice.

The design of our study, which is based on retrospective self-reported behaviors, inevitably leads to recall bias. However, we did not find other better ways to assess and monitor patients' behavior. Progress in objective hand gesture detection and eye rubbing through monitoring devices such as smartwatches, as developed during the covid-pandemic to detect eye-or nose-touching (59), might be a solution in the future.

Meanwhile, eye-rubbing and its associated behaviors are, from our experience, often unconscious habits, and patients require time and awareness to detect and eradicate them. We take time with them during medical consultation, including listening to the testimonies of their relatives with them. We are aware of the risk that eye rubbing could represent for them, as well as being more careful not to perform this gesture. They are then often underestimated by the patient at their first appointment and later estimated more realistically either by the patient or their close ones. They often admit to having underestimated their unconscious habit at their second appointment.

The baseline was defined as the first consultation at the center, which ignores previous investigations and consultations in other centers and makes evaluating previous progression rates impossible. All patients were progressing at the time of referral to our tertiary center. Patients were referred either after initial diagnosis due to visual loss or because of progression observed by their referring ophthalmologist. We acknowledge that this fact, combined with the study's monocentric and retrospective nature, may lead to a partial selection bias which may hinder the generalization of our results to other populations.

However, the inclusion criteria and the outcome measures are comparable to non-pediatric studies evaluating long-term efficacy and tolerance after corneal cross-linking (CXL) (20, 57, 60).

The robust methods in our study and the use of objective judgment criteria and multimodal imaging with good repeatability also limit this potential bias. As the outcome measures were objective and quantitative, with measurements taken by independent operators, the influence on results is limited.

By further analyzing the patient's profile of progressing eyes, eye rubbing continuation despite recommendations predominated. However, careful follow-up must be maintained for all patients, and treatment escalation might be offered if progression is detected despite good compliance with recommendations.

Larger studies and longer follow-ups are needed to support our findings. While the relationship between mechanical trauma from eye rubbing and disease progression in keratoconus remains incompletely understood, based on these results, we believe that cessation of eye-rubbing is an important first step toward halting the progression of this condition in keratoconus patients. Our study demonstrates stable K_{max} , K_{mean} , and $Pachymin$ following cessation of eye-rubbing over a 3-year follow-up period. This highlights the importance of screening for eye-rubbing during patient evaluations, and our results suggest that definitive cessation of eye rubbing alone (albeit difficult) can be successful in limiting progression or achieving stabilization of keratoconus in the long-term in almost all eyes.

Data availability statement

The raw data supporting the conclusions of this article will be made available by the authors, without undue reservation.

Ethics statement

The studies involving human participants were reviewed and approved by Ethic committee of Fondation Ophtalmologique Adolphe de Rothschild, Paris, France. Written informed consent for participation was not required for this study in accordance with the national legislation and the institutional requirements.

Author contributions

AM wrote the core of this manuscript and initiated the database of the study. RF collected all the data and participated to the writing of the manuscript. SE did the statistical analysis of the data and participated to the writing of the manuscript. CP and RR reviewed

the manuscript and conducted data analysis. DG reviewed the manuscript and was the instigator of both the project and the hypothesis developed in this manuscript. All authors contributed to the article and approved the submitted version.

Conflict of interest

The authors declare that the research was conducted in the absence of any commercial or financial relationships that could be construed as a potential conflict of interest.

Publisher's note

All claims expressed in this article are solely those of the authors and do not necessarily represent those of their affiliated organizations, or those of the publisher, the editors and the reviewers. Any product that may be evaluated in this article, or claim that may be made by its manufacturer, is not guaranteed or endorsed by the publisher.

References

- Rabinowitz YS. Keratoconus. *Surv Ophthalmol.* (1998) 42:297–9. doi: 10.1016/S0039-6257(97)00119-7
- McMonnies CW. Eye rubbing type and prevalence including contact lens « removal-relief » rubbing. *Clin Exp Optom* juill. (2016) 99:366–2. doi: 10.1111/cxo.12343
- Moran S, Gomez L, Zuber K, Gatineau D. A case-control study of keratoconus risk factors. *Cornea. juil.* (2020) 39:697–1. doi: 10.1097/ICO.0000000000002283
- Sugar J, Macsai MS. What causes keratoconus? *Cornea. juil.* (2012) 31:716–9. doi: 10.1097/ICO.0b013e31823f8c72
- Norouzzpour A, Mehdizadeh A. A novel insight into keratoconus: mechanical fatigue of the cornea. *Med Hypothesis Discov Innov Ophthalmol J.* (2012) 1:14–7.
- McMonnies CW. Mechanisms of rubbing-related corneal trauma in keratoconus. *Cornea. juill.* (2009) 28:607–5. doi: 10.1097/ICO.0b013e318198384f
- McMonnies CW, Schief WK. Biomechanically coupled curvature transfer in normal and keratoconus corneal collagen. *Eye Contact Lens. janv.* (2006) 32:51–62. doi: 10.1097/01.icl.0000183177.22734.f3
- Gatineau D. Eye rubbing, a sine qua non for keratoconus? *Int J Keratoconus Ectatic Corneal Dis.* (2016) 5:6–12. doi: 10.5005/jp-journals-10025-1114
- Gatineau D. Challenging the “no rub, no cone” keratoconus conjecture. *Int J Keratoconus Ectatic Corneal Dis.* (2018) 7:66–81. doi: 10.5005/jp-journals-10025-1161
- McMonnies CW. Management of chronic habits of abnormal eye rubbing. *Contact Lens Anterior Eye J Br Contact Lens Assoc. avr.* (2008) 31:95–2. doi: 10.1016/j.clae.2007.07.008
- McMonnies CW. Behaviour modification in the management of chronic habits of abnormal eye rubbing. *Contact Lens Anterior Eye J Br Contact Lens Assoc. avr.* (2009) 32:55–63. doi: 10.1016/j.clae.2008.11.001
- de Azevedo MO, Gonçalves MC, Gatineau D. The role of environment in the pathogenesis of keratoconus. *Curr Opin Ophthalmol.* (2021) 32:379–4. doi: 10.1097/ICO.0000000000000764
- Gatineau D, Galvis V, Tello A, Niño CA, Rey JJ, Camacho PA, et al. Obstructive sleep Apnea-hypopnea syndrome and keratoconus: an epiphenomenon related to sleep position? *Cornea. avr.* (2020) 39:e11–2. doi: 10.1097/ICO.0000000000002219
- Tello A, Gatineau D, Galvis V, Prada AM, Duarte LM, Villamizar SJ, et al. Importance of the appropriate history-taking process in patients with keratoconus to reduce the risk of finding spurious associations. *Cornea.* (2023). doi: 10.1097/ICO.0000000000003244 [Epub ahead of print].
- Mazharian A, Panthier C, Courtin R, Jung C, Rampat R, Saad A, et al. Incorrect sleeping position and eye rubbing in patients with unilateral or highly asymmetric keratoconus: a case-control study. *Graefes Arch Clin Exp Ophthalmol Albrecht Von Graefes Arch Clin Exp Ophthalmol.* (2020) 258:2431–9. doi: 10.1007/s00417-020-04771-z
- Hashemi H, Heydarian S, Hooshmand E, Saatchi M, Yekta A, Aghamirsalim M, et al. The prevalence and risk factors for keratoconus: a systematic review and Meta-analysis. *Cornea. févr.* (2020) 39:263–0. doi: 10.1097/ICO.00000000000002150
- Guilbert E, Saad A, Elluard M, Grise-Dulac A, Rouger H, Gatineau D. Repeatability of keratometry measurements obtained with three topographers in Keratoconic and Normal corneas. *J Refract Surg Thorofare NJ* 1995. (2016) 32:187–2. doi: 10.3928/1081597X-20160113-01
- Gomes JAP, Tan D, Rapuano CJ, Belin MW, Ambrósio R, Guell JL, et al. Global consensus on keratoconus and ectatic diseases. *Cornea. avr.* (2015) 34:359–9. doi: 10.1097/ICO.0000000000000408
- Kandarakis A, Karampelas M, Soumplis V, Panos C, Makris N, Kandarakis S, et al. A case of bilateral self-induced keratoconus in a patient with tourette syndrome associated with compulsive eye rubbing: case report. *BMC Ophthalmol.* (2011) 11:28. doi: 10.1186/1471-2415-11-28
- Wittig-Silva C, Chan E, Islam FMA, Wu T, Whiting M, Snibson GR. A randomized, controlled trial of corneal collagen cross-linking in progressive keratoconus: three-year results. *Ophthalmology. avr.* (2014) 121:812–1. doi: 10.1016/j.ophtha.2013.10.028
- Schröder S, Langenbucher A, Schrecker J. Comparison of corneal elevation and pachymetry measurements made by two state of the art corneal tomographers with different measurement principles. *PLoS One.* (2019) 14:e0223770. doi: 10.1371/journal.pone.0223770
- McAlinden C, Schwiegerling J, Khadka J, Pesudovs K. Corneal aberrations measured with a high-resolution Scheimpflug tomographer: repeatability and reproducibility. *J Cataract Refract Surg. avr.* (2020) 46:581–0. doi: 10.1097/j.jcrs.0000000000000084
- Defeat Keratoconus (2023) The keratoconus diary [internet]. Defeat keratoconus. [cité 17 mars 2023]. Disponible sur Available at: <https://defeatkeratoconus.com/> (Accessed March 17, 2023).
- Gordon-Shaag A, Millodot M, Kaiserman I, Sela T, Barnett Itzhaki G, Zerbib Y, et al. Risk factors for keratoconus in Israel: a case-control study. *Ophthalmic Physiol Opt J Br Coll Ophthalmic Opt Optom.* (2015) 35:673–1. doi: 10.1111/opo.12237
- Naderan M, Shoor S, Rezagholizadeh F, Zolfaghari M, Naderan M. Characteristics and associations of keratoconus patients. *Contact Lens Anterior Eye J Br Contact Lens Assoc. juil.* (2015) 38:199–5. doi: 10.1016/j.clae.2015.01.008
- Salman A, Darwish T, Ghabra M, Kailani O, Haddeh Y, Askar M, et al. Prevalence of keratoconus in a population-based study in Syria. *J Ophthalmol.* (2022) 2022:1–9. doi: 10.1155/2022/6064533
- Santodomingo-Rubido J, Carracedo G, Suzuki A, Villa-Collar C, Vincent SJ, Wolffsohn JS. Keratoconus: an updated review. *Contact Lens Anterior Eye J Br Contact Lens Assoc. juil.* (2022) 45:101559. doi: 10.1016/j.clae.2021.101559
- Mou Y, Qin Q, Huang X, Jin X. Risk factors and severity of keratoconus on the East Coast of China. *Int Ophthalmol. juill.* (2022) 42:2133–40. doi: 10.1007/s10792-022-02212-w
- Song M, Fang QY, Seth I, Baird PN, Daniell MD, Sahebjada S. Non-genetic risk factors for keratoconus. *Clin Exp Optom.* (2022):1–11. doi: 10.1007/978-981-19-4262-4_2 [Epub ahead of print].
- Coyle JT. Keratoconus and eye rubbing. *Am J Ophthalmol. avr.* (1984) 97:527–8. doi: 10.1016/S0002-9394(14)76143-4
- Gunes A, Tok L, Tok Ö, Seyrek L. The youngest patient with bilateral keratoconus secondary to chronic persistent eye rubbing. *Semin Ophthalmol.* (2015) 30:454–6. doi: 10.1016/j.soph.2013.07.040

32. Fakhraie G, Vahedian Z. Post filtering surgery globe massage-induced keratoconus in an eye with iridocorneal endothelial syndrome: a case report and literature brief review. *J Ophthalmic Vis Res.* (2016) 11:319–2. doi: 10.4103/2008-322X.158896
33. Lindsay RG, Bruce AS, Gutteridge IF. Keratoconus associated with continual eye rubbing due to punctal agenesis. *Cornea. juill.* (2000) 19:567–9. doi: 10.1097/00003226-200007000-00034
34. Bawazeer AM, Hodge WG, Lorimer B. Atopy and keratoconus: a multivariate analysis. *Br J Ophthalmol août.* (2000) 84:834–6. doi: 10.1136/bjo.84.8.834
35. Rabinowitz YS, Galvis V, Tello A, Rueda D, García JD. Genetics vs chronic corneal mechanical trauma in the etiology of keratoconus. *Exp Eye Res janv.* (2021) 202:108328. doi: 10.1016/j.exer.2020.108328
36. Ferdi AC, Nguyen V, Gore DM, Allan BD, Rozema JJ, Watson SL. Keratoconus natural progression: a systematic review and Meta-analysis of 11 529 eyes. *Ophthalmology juill.* (2019) 126:935–5. doi: 10.1016/j.optha.2019.02.029
37. Nath S, Shen C, Koziarz A, Banfield L, Nowrouzi-Kia B, Fava MA, et al. Transepithelial versus epithelium-off corneal collagen cross-linking for corneal ectasia: a systematic review and Meta-analysis. *Ophthalmology août.* (2021) 128:1150–60. doi: 10.1016/j.optha.2020.12.023
38. McAnena L, Frank A, Michael O'Keefe A. Cross-linking in children with keratoconus: a systematic review and meta-analysis. *Acta Ophthalmol.* (2017) 95:229–39. doi: 10.1111/aos.13224
39. Or L, Rozenberg A, Abulafia A, Avni I, Zadok D. Corneal cross-linking in Pediatric patients: evaluating treated and untreated Eyes-5-year follow-up results. *Cornea août.* (2018) 37:1013–7. doi: 10.1097/ICO.0000000000001629
40. Achiron A, El-Hadad O, Leadbetter D, Hecht I, Hamiel U, Avadhanam V, et al. Progression of Pediatric keratoconus after corneal cross-linking: a systematic review and pooled analysis. *Cornea.* (2022) 41:874–8. doi: 10.1097/ICO.0000000000002808
41. Péterszegi G, Robert AM, Robert L, Renard G. The importance of the Maillard reaction in ophthalmology. *J Soc Biol.* (2007) 201:209–4. doi: 10.1051/jbio:2007026
42. Perone JM, Conart JB, Bertaux PJ, Sujet-Perone N, Ouamara N, Sot M, et al. Mechanical Modeling of a Keratoconic cornea. *Cornea.* (2017) 36:1263–6. doi: 10.1097/ICO.0000000000001293
43. McMonnies CW, Korb DR, Blackie CA. The role of heat in rubbing and massage-related corneal deformation. *Contact Lens Anterior Eye J Br Contact Lens Assoc août.* (2012) 35:148–4. doi: 10.1016/j.clae.2012.01.001
44. McMonnies CW. The possible significance of the baropathic nature of keratectasias. *Clin Exp Optom mars.* (2013) 96:197–0. doi: 10.1111/j.1444-0938.2012.00726.x
45. McMonnies CW, Boneham GC. Corneal responses to intraocular pressure elevations in keratoconus. *Cornea. juill.* (2010) 29:764–0. doi: 10.1097/ICO.0b013e3181ca2b75
46. Osuagwu UL, Alanazi SA. Eye rubbing-induced changes in intraocular pressure and corneal thickness measured at five locations, in subjects with ocular allergy. *Int J Ophthalmol.* (2015) 8:81–8. doi: 10.3980/j.issn.2222-3959.2015.01.15
47. McMonnies CW. The evidentiary significance of case reports: eye rubbing and keratoconus. *Optom Vis Sci Off Publ Am Acad Optom avr.* (2008) 85:262–9. doi: 10.1097/OPX.0b013e318169287a
48. Ioannidis AS, Speedwell L, Nischal KK. Unilateral keratoconus in a child with chronic and persistent eye rubbing. *Am J Ophthalmol févr.* (2005) 139:356–7. doi: 10.1016/j.ajo.2004.07.044
49. Bral N, Termote K. Unilateral keratoconus after chronic eye rubbing by the nondominant hand. *Case Rep Ophthalmol.* (2017) 8:558–1. doi: 10.1159/000484712
50. Saad A, Rizk M, Gatineau D. Fourteen years follow-up of a stable unilateral keratoconus: unique case report of clinical, tomographical and biomechanical stability. *BMC Ophthalmol.* (2022) 22:245. doi: 10.1186/s12886-022-02412-z
51. Millodot M, Shneor E, Albou S, Atlani E, Gordon-Shaag A. Prevalence and associated factors of keratoconus in Jerusalem: a cross-sectional study. *Ophthalmic Epidemiol avr.* (2011) 18:91–7. doi: 10.3109/09286586.2011.560747
52. Waked N, Fayad AM, Fadlallah A, El Rami H. Keratoconus screening in a Lebanese students' population. *J Fr Ophthalmol.* (2012) 35:23–9. doi: 10.1016/j.jfo.2011.03.016
53. Assiri AA, Yousuf BI, Quantock AJ, Murphy PJ. Incidence and severity of keratoconus in Asir province, Saudi Arabia. *Br J Ophthalmol.* (2005) 89:1403–6. doi: 10.1136/bjo.2005.074955
54. Mazzotta C, Traversi C, Mellace P, Bagaglia SA, Zuccarini S, Mencucci R, et al. Keratoconus progression in patients with allergy and elevated surface matrix metalloproteinase 9 point-of-care test. *Eye Contact Lens.* (2018) 44:S48–53. doi: 10.1097/ICL.0000000000000432
55. Edwards M, McGhee CN, Dean S. The genetics of keratoconus. *Clin Exp Ophthalmol.* (2001) 29:345–1. doi: 10.1046/j.1442-9071.2001.d01-16.x
56. McMahon TT, Shin JA, Newlin A, Edrington TB, Sugar J, Zadnik K. Discordance for keratoconus in two pairs of monozygotic twins. *Cornea. juill.* (1999) 18:444–1. doi: 10.1097/00003226-199907000-00010
57. Goldich Y, Marcovich AL, Barkana Y, Mandel Y, Hirsh A, Morad Y, et al. Clinical and corneal biomechanical changes after collagen cross-linking with riboflavin and UV irradiation in patients with progressive keratoconus: results after 2 years of follow-up. *Cornea. juin.* (2012) 31:609–4. doi: 10.1097/ICO.0b013e318226bf4a
58. Epstein RL, Chiu YL, Epstein GL. Pentacam HR criteria for curvature change in keratoconus and postoperative LASIK ectasia. *J Refract Surg Thorofare NJ.* (1995) 28:890–4.
59. Maeda A. Can not touching the nose or eyes help cold prevention? Possibility of application using a smartwatch and self-checking. *Annu Int Conf IEEE Eng Med Biol Soc IEEE Eng Med Biol Soc Annu Int Conf.* (2020) 2020:5722–8. doi: 10.1109/EMBC44109.2020.9176589
60. Vinciguerra P, Albé E, Frueh BE, Trazza S, Epstein D. Two-year corneal cross-linking results in patients younger than 18 years with documented progressive keratoconus. *Am J Ophthalmol sept.* (2012) 154:520–6. doi: 10.1016/j.ajo.2012.03.020



OPEN ACCESS

EDITED BY

Cristina Nicula,
University of Medicine and Pharmacy Iuliu
Hatieganu, Romania

REVIEWED BY

Mehran Zarei-Ghanavati,
Tehran University of Medical Sciences, Iran
Ahmed Abdelkareem Elmassry,
Alexandria University, Egypt

*CORRESPONDENCE

Qing-yan Zeng
✉ zengqingyan1972@163.com

RECEIVED 17 January 2023

ACCEPTED 16 June 2023

PUBLISHED 03 July 2023

CITATION

Liu Y, Shen D, Wang H-y, Qi M-y and Zeng Q-y
(2023) Development and validation to predict
visual acuity and keratometry two years after
corneal crosslinking with progressive
keratoconus by machine learning.
Front. Med. 10:1146529.
doi: 10.3389/fmed.2023.1146529

COPYRIGHT

© 2023 Liu, Shen, Wang, Qi and Zeng. This is
an open-access article distributed under the
terms of the [Creative Commons Attribution
License \(CC BY\)](#). The use, distribution or
reproduction in other forums is permitted,
provided the original author(s) and the
copyright owner(s) are credited and that the
original publication in this journal is cited, in
accordance with accepted academic practice.
No use, distribution or reproduction is
permitted which does not comply with these
terms.

Development and validation to predict visual acuity and keratometry two years after corneal crosslinking with progressive keratoconus by machine learning

Yu Liu^{1,2}, Dan Shen², Hao-yu Wang², Meng-ying Qi² and
Qing-yan Zeng^{1,2,3,4*}

¹Aier School of Ophthalmology, Central South University, Changsha, China, ²Aier Eye Hospital of Wuhan University, Wuhan, China, ³Aier Cornea Institute, Beijing, China, ⁴Aier School of Ophthalmology and Optometry, Hubei University of Science and Technology, Xianning, China

Purpose: To explore and validate the utility of machine learning (ML) methods using a limited sample size to predict changes in visual acuity and keratometry 2years following corneal crosslinking (CXL) for progressive keratoconus.

Methods: The study included all consecutive patients with progressive keratoconus who underwent CXL from July 2014 to December 2020, with a 2year follow-up period before July 2022 to develop the model. Variables collected included patient demographics, visual acuity, spherical equivalence, and Pentacam parameters. Available case data were divided into training and testing data sets. Three ML models were evaluated based on their performance in predicting case corrected distance visual acuity (CDVA) and maximum keratometry (K_{\max}) changes compared to actual values, as indicated by average root mean squared error (RMSE) and R-squared (R^2) values. Patients followed from July 2022 to December 2022 were included in the validation set.

Results: A total of 277 eyes from 195 patients were included in training and testing sets and 43 eyes from 35 patients were included in the validation set. The baseline CDVA (26.7%) and the ratio of steep keratometry to flat keratometry (K_2/K_1 ; 13.8%) were closely associated with case CDVA changes. The baseline ratio of K_{\max} to mean keratometry (K_{\max}/K_{mean} ; 20.9%) was closely associated with case K_{\max} changes. Using these metrics, the best-performing ML model was XGBoost, which produced predicted values closest to the actual values for both CDVA and K_{\max} changes in testing set ($R^2=0.9993$ and 0.9888) and validation set ($R^2=0.8956$ and 0.8382).

Conclusion: Application of a ML approach using XGBoost, and incorporation of identifiable parameters, considerably improved variation prediction accuracy of both CDVA and K_{\max} 2years after CXL for treatment of progressive keratoconus.

KEYWORDS

crosslinking (CXL) corneal collagen, machine learning, keratoconus, prediction model, XGBoost (extreme gradient boosting)

Introduction

Corneal collagen crosslinking (CXL) has been extensively used in clinical management of keratoconus since Wollensak et al. (1) originally demonstrated in 2003 that CXL enhances corneal stiffness. Although the effect of CXL in halting the progression of keratoconus has been widely recognized, long-term (≥ 2 years) randomized controlled (RCT) studies still indicated that its failure rate was highly variable (0–28%) (2–5) depending on CXL procedure type, age, race, disease severity, and other factors.

If CXL surgery fails, the progression of keratoconus continues, and CXL retreatment and/or keratoplasty are necessary. In China, there is a shortage of corneal donor tissue (6) which might induce patients to delay treatment. Meanwhile, this increases the financial and psychological burden on the patient. Therefore, accurate prediction of the postoperative outcome prior to CXL could help patients choose a newly alternative treatment options, such as intraocular lens or intrastromal implantation (7).

The most commonly used definition of keratoconus progression is maximum keratometry (K_{\max}) increase ≥ 1.0 D or corrected distance visual acuity (CDVA) decrease >2 lines (8). High preoperative K_{\max} , thin corneas thickness, and atopic diseases were widely recognized as the risk factors for progression of keratoconus after CXL (9–12). Female gender, young age, pronounced optical aberrations, and the cone location were also found as the risk factors of the progression in 2 years (10–12).

Several studies have utilized liner regression approaches to predict treatment outcomes including CDVA and K_{\max} , but these approaches failed to produce sufficiently reliable predictive power (13–17). An early study used a multivariate regression statistical model to predict CDVA and K_{\max} for pediatric keratoconus patients (1 year follow-up) (13), and obtained a low predictive value model with CDVA ($R^2 = 0.45$, $p < 0.01$) and K_{\max} ($R^2 = 0.15$, $p > 0.05$). A prior study (14) demonstrated that CDVA could potentially be predicted for 1 year postoperative following CXL, but did not evaluate the model's ability to predict K_{\max} . Similarly, other studies only provided the predictors such as baseline K_{\max} (15–17). However, the cornea biomechanics are not completely stable at 1 year following CXL.

Machine learning (ML) is a computer science discipline that utilizes algorithms and other approaches to automatically address complex problems that cannot easily be addressed by conventional data analysis means (18). Previous ML approaches have traditionally required very large datasets for training. With newly developed approaches, ML is now also suited for interrogation of small datasets with hundreds or dozens of variables using approaches such as few-shot learning (FSL) (19) and gradient boosting. The most widely used gradient boosting algorithms including categorical gradient boosting on decision trees (CatBoost), light gradient boosting machine (LightGBM), eXtreme gradient boosting (XGBoost), and Bayesian optimization (20).

Recently, ML has been used for keratoconus detection (21), classification (20), and candidacy for CXL treatment (23). However, no reports have used ML to predict the therapeutic outcome of CXL postoperatively. This study aimed to apply ML algorithms trained with a limited dataset to predict changes of visual acuity and keratometry 2 years following CXL for progressive keratoconus.

Materials and methods

Database

A retrospective medical chart review was conducted on all consecutive patients with progressive keratoconus who underwent CXL treatment between July 2014 and December 2020 at the Aier Eye Hospital of Wuhan University (Wuhan, Hubei province, China). Patients who returned for a follow-up visit at 2 years were included in the study. Data were collected using a convenient data management system supported by Empower Electronic Data Capture (EDC) system (<https://empoweredc.com>, Solution Inc., Shanghai, China).

An increase of at least 1 diopter (D) in maximum keratometry (K_{\max}) derived from computerized corneal topography during the preceding 12 months was required for inclusion. We enrolled keratoconus patients for all grades based on the Amsler-Krumeich keratoconus classification (24). Patients with previous refractive surgeries or corneal history of ocular surface or other eye disorders were excluded. In addition, patients whose data could not be reviewed for any reason were classified as being lost to follow-up and excluded from the study.

Surgical technique

Patients were included regardless of their treatment protocols, which were not included in the prediction model. Two different treatment combinations were included in the study. When the thinnest corneal thickness of the eye was ≥ 450 μm , patients were undergo the high-fluence accelerated CXL (HF A-CXL). When the thinnest corneal thickness of the eye was < 450 μm , they were undergo the accelerated transepithelial CXL (A-TE CXL).

- (1) **A-TE CXL:** In the first step, 0.25% riboflavin (Paracel Part I, Avedro Inc., USA) containing 0.02% benzalkonium chloride (BAC) and 0.85% hydroxypropyl methyl cellulose (HPMC) was applied onto the cornea every 90 s for 4 min. Thereafter, part I solution was rinsed with 0.22% riboflavin (Paracel Part II, Avedro), and part II solution was instilled every 90 s over the next 6 min. UV-A was applied using the Avedro KXL System (Avedro Inc., Waltham, USA) with 30 mW/cm² UV power for 8 min with a 1 s on/off cycle (7.2 J/cm²) (25).
- (2) **HF A-CXL:** The corneal epithelium was removed with a blunt knife in a 10 mm zone. CXL was then performed with 0.1% dextran-free riboflavin (VibeX Rapid, Avedro) instilled every 90 s for 10 min. Subsequently, it was placed under UA irradiation for 4 min at 30 mW/cm² (7.2 J/cm², Avedro) (26).

The operator verified irradiance prior to each treatment. The two CXL procedures are summarized in Table 1.

Pain medication and postoperative care

All patients received 0.5% levofloxacin drops four times daily for 3 days prior to surgery. Thirty minutes before surgery, patients received 2% pilocarpine (Sigma-Aldrich, St. Louis, MO, United States) and 0.4% oxybuprocaine hydrochloride (Bausch & Lomb Pty Ltd.,

TABLE 1 Crosslinking treatment procedures.

Parameter	A-TE CXL	HF A-CXL
Fluence (total) (J/cm ²)	7.2	7.2
Soak time and interval (minutes)	10 (1.5)	10 (1.5)
Intensity (mW/cm ²)	30	30
Treatment time (minutes)	8	4
Irradiation mode (interval)	Pulsed (1 s on/1 s off)	Continuous
Epithelium status	On	Off
Riboflavin	ParaCel	Vibex Rapid

CXL = corneal crosslinking; A-TE CXL = accelerated transepithelial corneal crosslinking; HF A-CXL = high fluence corneal crosslinking.

NSW, Australia) drops three times, with 5 min between each administration.

At the end of the surgery, the corneal surface was dressed with a therapeutic soft contact lens (Bausch & Lomb Pty Ltd.) for at least 24 h until the epithelium had completely healed.

Feature selection

Twenty-six preoperative variables were recorded in all patients: sex, age, uncorrected visual acuity (UCVA, logarithm of the minimum angle of resolution [LogMAR] units), CDVA (LogMAR units), spherical equivalence (SE), flat keratometry (K_1), steep keratometry (K_2), mean keratometry (K_{mean}), astigmatism (Astig), eccentricity (ecc), maximum keratometry (K_{max}), minimum corneal thickness (MCT), the most elevated points on the front corneal surfaces (F. Ele Th), the most elevated points on the back corneal surfaces (B. Ele Th), the index of surface variance (ISV), the index of vertical asymmetry (IVA), keratoconus index (KI), center keratoconus index (CKI), the index of height decentration (IHD), minimum radius of curvature (RMin), and Belin/Ambrósio final D value (BAD-D), which were measured by Pentacam (Oculus, Wetzlar, Germany). In addition, five incorporation parameters were also collected, including the ratio of K_2 to K_1 (K_2/K_1), the ratio of K_{max} to K_{mean} ($K_{\text{max}}/K_{\text{mean}}$), the ratio of K_{max} to K_1 (K_{max}/K_1), the ratio of K_{max} to K_2 (K_{max}/K_2), and the difference between K_{max} and K_{mean} ($K_{\text{max}} - K_{\text{mean}}$). All the exams were executed by the skilled examiners. The ‘quality specifications (QS)’ was used to evaluate the quality of Pentacam images. If the QS is not ‘OK’, the exams were executed more than two times. Finally, at least two experienced ophthalmologists validated the accuracy of the images and data.

Features that demonstrated the highest feature importance to the model on primary runs were included for further analysis. Histograms of each numerical attribute were generated to understand the distribution features across distinct values. Categorical features (sex) were encoded into a binary representation to enable machine learning (ML) readability of algorithms.

Model development

Patients who returned for a follow-up visit at 2 years before June 30, 2022 were included in the study to develop the model. Data processing and ML model development were performed in Python

3.9.7 using the *pandas* (version 1.3.4), *numpy* (version 1.20.3), and *scikit-learn* (version 1.0.2; [mode: *sklearn.model_selection* and *sklearn.metrics*]) packages. Three models were run by supervised ML methods, while examples of inputs (features chosen) and outputs (actual changes in CDVA and K_{max}) were provided to models as training inputs to build an algorithm for future predictions including, CatBoost, LightGBM, and XGBoost.

Model evaluation and statistical methods

The database was randomly split into two groups: 80% of data ($n=222$) was used for model training, while the remaining 20% of the dataset ($n=55$) was reserved to test the model's predicted case value for CDVA and K_{max} variation. The predicted values were compared to the actual case changes. Performance metrics included root mean squared error (RMSE) and R -squared (R^2). Models were compared using a Nadeau and Bengio's corrected resampled t-test (27, 28). Feature importance values were derived using prespecified methodology specific to the algorithms studied.

Model validation

To validate the accuracy of the prediction model, we established a free website and used data from patients followed from July 2022 to December 2022. We use the same RMSE and R^2 evaluations.

The workflow diagram detailing the data modeling process was showed in Figure 1. The website for validating the prediction model was showed in Figure 2.

Results

Patient characteristics

Data were recorded for 405 eyes from 289 patients who were diagnosed with progressive keratoconus and underwent CXL treatment. Thirty-nine patients (49 eyes) who were followed up at different clinics, and 30 patients (36 eyes) did not complete the 2 year follow-up, were excluded. Finally, the study included 277 eyes from 195 patients in training and testing sets and 43 eyes from 35 patients in the validation set. The demographic and baseline data of all patients are summarized in Table 2.

TABLE 2 Demographic and baseline data.

Parameter	Value in training and testing sets	Value in validation set
Patients	195 (151 males/44 females)	35 (28 males/7 females)
Eyes	277	43
Mean age (y, range)	20.09 (10 to 46)	20.31 (11 to 43)
UDVA (LogMAR)	0.71 ± 0.43	0.63 ± 0.44
CDVA (LogMAR)	0.27 ± 0.22	0.21 ± 0.19
SE (D)	−6.95 ± 0.22	−5.58 ± 3.04
K ₁ (D)	47.21 ± 4.59	45.17 ± 2.78
K ₂ (D)	51.12 ± 5.21	48.95 ± 3.96
K _{mean} (D)	49.05 ± 4.74	46.93 ± 3.11
Astig (D)	3.91 ± 2.36	3.78 ± 2.47
ecc	0.94 ± 0.27	0.83 ± 0.22
K _{max} (D, range)	58.13 ± 8.55 (44.1 to 83.4)	54.45 ± 5.82 (44.3 to 68.2)
MCT (μm)	454 ± 41	489 ± 29
F. Ele Th (μm)	23.77 ± 13.86	18.37 ± 9.73
B. Ele Th (μm)	52.71 ± 27.17	42.51 ± 20.41
BAD-D	9.62 ± 4.98	7.22 ± 3.1
ISV	88.64 ± 40.97	73.23 ± 31.54
IVA	0.83 ± 0.44	0.74 ± 0.42
KI	1.23 ± 0.14	1.18 ± 0.11
CKI	1.09 ± 0.08	1.06 ± 0.47
IHD	0.123 ± 0.075	0.098 ± 0.055
RMin	5.94 ± 0.82	6.27 ± 0.66
Follow-up (months, range)	24 (22 to 27)	24 (22 to 26)

UDVA = uncorrected distance visual acuity; CDVA = corrected distance visual acuity; LogMAR = logarithm of the minimum angle of resolution; SE = spherical equivalence; D = diopter; K₁ = flat keratometry, K₂ = steep keratometry, K_{mean} = mean keratometry; Astig = astigmatism; ecc = eccentricity; K_{max} = maximum keratometry; MCT = minimum corneal thickness; F. Ele Th = most elevated points on the front corneal surfaces; B. Ele Th = most elevated points on the back corneal surfaces; BAD-D = Belin/Ambrósio final D value; ISV = index of surface variance; IVA = index of vertical asymmetry; KI = keratoconus index; CKI = center keratoconus index; IHD = index of height decentration; RMin = minimum radius of curvature.

Data were presented as mean ± standard deviation or frequency.

Clinical outcomes

Both CDVA and K_{max} improved significantly over baseline at the 2 year follow-up. Average CDVA decreased by 0.08 from 0.27 to 0.19 LogMAR (range: −0.8 to 0.7 LogMAR; $p < 0.001$), and average K_{max} decreased by 1.06 D from 58.13 to 57.07 D (range: −14.6 to 5.8 D; $p < 0.001$) in training and testing sets.

Feature importance and model development

Feature importance was applied to select key features for improved performance. Baseline CDVA (26.7%), K₂/K₁ value (13.8%), and F. Ele Th (11.1%) were closely associated with case CDVA changes. The baseline K_{max}/K_{mean} (20.9%), UDVA (14%), and ecc (10%) were closely associated with case changes of K_{max}. The feature importance of each parameter is shown in Figure 3.

All baseline features were used as training features to construct a baseline regression model, to predict changes in CDVA and K_{max} 2 years after CXL while applying different algorithms. The XGBoost model demonstrated the best predictive ability in the training set (RMSE = 0.001 LogMAR and 0.013 D) compared to CatBoost and

LightGBM. Therefore, XGBoost was selected for model and website building. Finally, our predictive model performed robustly in the testing set ($R^2 = 0.9991$ and 0.9888). The performance of the three models in predicting changes of CDVA and K_{max} with the training and testing dataset were showed in Table 3.

Model validation

The CDVA also improved by 0.07 ± 0.21 LogMAR ($p = 0.029$) and K_{max} decreased by 1.16 ± 2.22 D ($p = 0.001$) in the validation set. The validation for the model achieved RMSE of 0.066 LogMAR and 0.907 D, and R^2 of 0.8956 and 0.8382, respectively. The scatterplot of the predicted values compared to actual value in validation set were showed in Figure 4 and the raw data was showed in Supplementary Table 1.

Adverse events

Opacity of the corneal stroma at the central and paracentral areas occurred in two eyes of one patients (10 years) during the follow-up in HF A-CXL treatment group. The minimum stromal thickness after epithelial removal were 411 and 429 μm. The patient had a history of

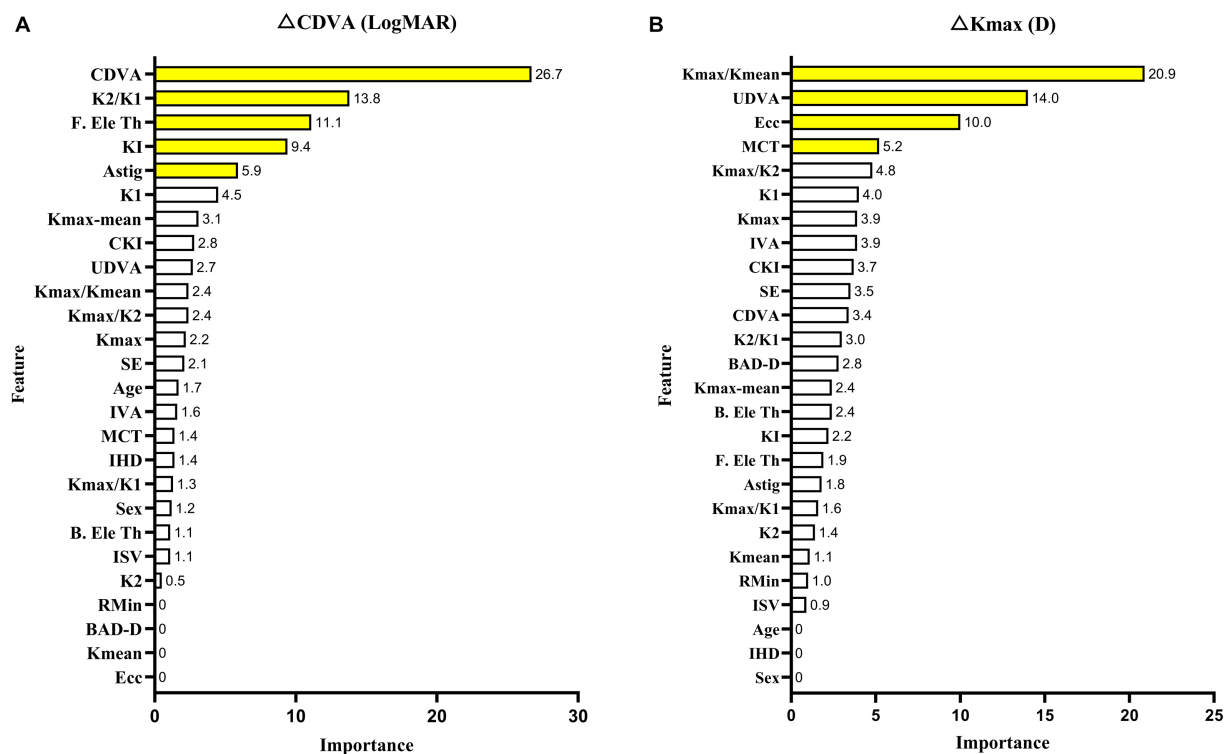


FIGURE 3 XGBoost model with the feature importance of each parameter in CDVA (A) and K_{\max} (B) changes with keratoconus 2years after crosslinking.

TABLE 3 Performance of three models with changes of CDVA and K_{\max} in training and testing data sets.

Dataset	Model	Δ CDVA (LogMAR)		Δ K_{\max} (D)	
		RMSE	R^2	RMSE	R^2
Training Set	CatBoost	0.040	0.9410	0.089	0.9724
	LightGBM	0.031	0.9639	0.095	0.9682
	XGBoost	0.001	0.9998	0.007	0.9991
Testing Set	CatBoost	0.098	0.8892	0.504	0.8785
	LightGBM	0.066	0.9144	0.541	0.8719
	XGBoost	0.001	0.9993	0.053	0.9888

CatBoost = categorical gradient boosting on decision trees, LightGBM = light gradient boosting machine, XGBoost = eXtreme gradient boosting, Δ = difference between 2-year post-CXL and pre-CXL; CDVA = corrected distance visual acuity; LogMAR = logarithm of the minimum angle of resolution; K_{\max} = maximum keratometry; D = diopter; RMSE = root mean squared error; R^2 = R square.

sunlight exposure early in the postoperative period. Thereafter, the corneal transparency was restored after treatment with 0.1% fluorometholone (Allergan, Irvine, CA) and corneal protection to avoid direct irritation from sunlight (Supplementary Figure 1). No infections or other adverse events were observed in slit-lamp examination.

Discussion

To our knowledge, this is the first study to use ML to predict the 2 year efficacy of CXL for keratoconus. Classical regression analysis

has used one regression equation (linear regression) or several equations (hierarchical regression) to explain outcomes. The algorithm we ultimately used was XGBoost, which is accomplished through a process known as boosting. Boosting is an iterative procedure that intelligently adds weak learners to the ensemble model. The new weak learners will focus on the unlearned and thus strengthen the ensemble (20). By increasing the iterative over time, XGBoost improves the accuracy of regression analysis. Further, the XGBoost model will overfit when the dataset is too large, even if lasso or ridge regression are used to filter variables. Therefore, XGBoost is commonly used for small datasets and is effective for this application (29–31). The present study tested a variety of machine learning algorithms to develop prediction models for changes in CDVA and K_{\max} 2 years following CXL for keratoconus, and XGBoost provided a superior models.

This research aimed to include five new incorporation variable indicators, including K_2/K_1 , K_{\max}/K_{mean} , K_{\max}/K_1 , K_{\max}/K_2 , and $K_{\max}\text{-mean}$. Further, some combinations of factors were relevant for improving model accuracy. Baseline CDVA was the most significant contributing feature in the CDVA change model, which is consistent with previous studies (13, 14, 32). The resultant feature importance could be simply defined as the extent to which the feature is incorporated into the model. In addition, we discovered that K_2/K_1 is another key feature in predicting CDVA changes. We hypothesized that K_2/K_1 was more important to CDVA changes than other indicators because CDVA monitors the overall visual function of the eye, which is directly connected to the shape of the cornea. Accordingly, the K_2/K_1 ratio is indicative of the general regularity of the front surface of the cornea. Some other combined parameters have been applied to develop a prediction model for keratoconus. A prior study indicated that the

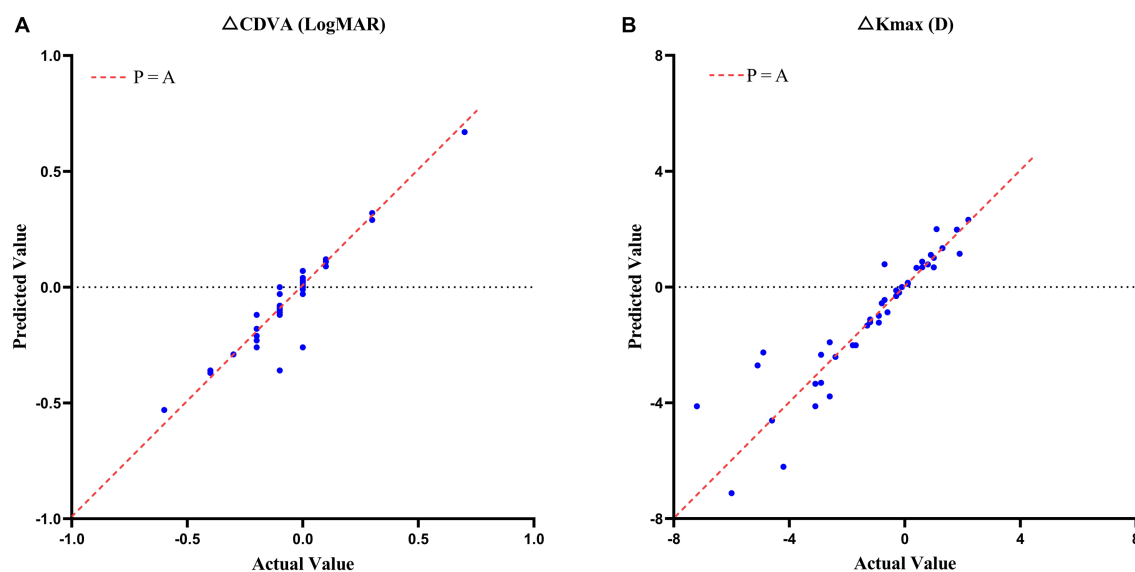


FIGURE 4
Scatterplots of the case predicted values compared to actual values in CDVA (A) and K_{max} (B) changes with keratoconus 2years after crosslinking in validation set.

ratio of anterior radius of curvature (ARC) to posterior radius of curvature (PRC) was linked to CDVA 1 year after CXL for keratoconus (11). The greatest obstacle to correcting ametropia for keratoconus is irregularity of the cornea. A new parameter developed by Pablo et al., the K-factor ($K_F = K_2 [K_2 - K_1]$) (33), was utilized to predict considerable improvement in CDVA after intracorneal ring segment implantation (ICRS). K_2/K_1 could determine the topographic form of the 3 mm of the central cornea, which contains the visual axis and is a crucial area for investigations focused on visual results. Similarity, KI and astigmatism (Astig) are two indicators of corneal regularity that can be used to evaluate corneal regularity, and account for 9.4 and 5.9%, respectively, of the feature importance outcomes in the CDVA change prediction model (Figure 3).

Concurrence of the highest elevated point on the front corneal surfaces (F. Ele Th) relative to the best fit sphere on the elevation maps was a novel important feature that could explain CDVA variations, consistent with a prior study (34). The study suggested that the difference in location between the most elevated areas on the corneal surfaces could be connected to biomechanical deterioration of the cornea. Corneal biomechanics could be connected to visual acuity, as the mechanical qualities of the cornea reflect its capacity to bear intraocular pressure. Furthermore, corneal curvature is intimately connected to visual acuity as described above.

According to prior studies, it is difficult to predict changes in K_{max} after CXL for keratoconus (13). This is most likely because K_{max} , as measured by Pentacam, simulates corneal morphology and calculates maximum curvature *via* three-dimensional reconstruction of the collected corneal Scheimpflug pictures, rather than using directly measured values (35). Hence, K_{max} is influenced by an excessive number of variables. In the present study, we used a novel incorporation parameter, the baseline K_{max}/K_{mean} ratio, to predict changes in K_{max} . This parameter was much more predictive of final K_{max} than was baseline K_{max} . This could be because baseline K_{max} is the

maximum curvature of the anterior corneal surface, which indicates the absolute preoperative convexity of a point. However, after the crosslinking reaction, corneal rigidity increases, changing the biomechanical characteristics of the integrated cornea, thus there are additional factors impacting postoperative K_{max} . Consistent with this notion, a recent study identified strong associations between corneal hysteresis (CH), corneal resistance factor (CRF), and K_{max} in keratoconic eyes, but not in crosslinked eyes (36). Variations in the biomechanics of the whole cornea result in more complex changes in K_{max} that are difficult to predict using preoperative data. Nevertheless, the K_{max}/K_{mean} ratio maybe normalized for some unclear confounding factor, which reflects the convexity of the cornea, can be used to measure the overall qualities of the cornea.

It is presently unclear why baseline UDVA is a secondary-importance feature in the K_{max} change prediction model. One possible explanation is that visual function and corneal structure are inextricably linked (37).

Eccentricity (ecc) was identified as another significant predictive factor for changes in K_{max} , consistent with prior findings (13, 15, 38). Additionally, central cones have a larger degree of postoperative corneal flattening than do peripheral cones (38). This conclusion could be explained by several factors. The efficacy of CXL is decreased in eccentric cones because UV devices cannot be applied uniformly across the treatment zone. UV rays could scatter in the perimeter, with a weaker and inconsistent beam in peripherally located cones. The second potential contributor is that even with homogenous light energy, the treatment power was relatively low in the peripheral cornea (39). Accordingly, cones in the periphery could be exposed to less crosslinking power, making ecc a significant predictor of K_{max} changes after CXL.

Minimum corneal thickness, the parameter of corneal thickness, was also of importance in predicting changes in K_{max} after CXL, which was consistent with an earlier study demonstrating a

link between MCT and K_{\max} variations (40). Corneal thinning in keratoconus results from defects in collagen lamellae caused by errors in the collagen lamellae manufacturing process (41). After stabilization with CXL, corneal collagen structural changes (42), primarily crimping (43), change corneal biomechanics. Therefore, using baseline data from MCT would enhance the prediction efficiency of K_{\max} .

Our pilot model still has several significant limitations that should be considered in its interpretation. First, even though XGBoost could effectively create a predictive model with a small dataset, our sample size was also limited, which could result in an unnecessarily complicated model. Second, parameters, such as atopic constitution, positive family history, and smoking, which did not have predictive potential in conventional linear regression analyses were excluded from the ML dataset (13, 16). However, XGBoost or other ML algorithms filter variables by lasso regression. The predictive potential of these parameters with ML approaches should be examined to determine their feature importance. Furthermore, a prior study found that keratoconus progression after CXL in one eye should be continuously monitored due to an increased chance of progression in the contralateral eye (44). This suggests that fellow eye data could also be incorporated into analysis.

Moreover, we found a pediatric patient who underwent HF A-CXL procedure has occurred the corneal opacity. Another study that used the same procedure to treat pediatric keratoconus patients did not report complications through 2 years postoperatively (45). Corneal haze following CXL has been reported in previous studies (46), but the reasons remain unclear at present. Potential reasons for this phenomenon are as follows: (1) more severe corneal ectasis caused by the fibroblast proliferation, which is more common in pediatric patients than in adults due to a more active proliferation response (47, 48); (2) the slow spontaneous crosslinking reactions triggered by residual riboflavin in the corneal stroma and UV-A rays in natural light (49); or (3) endothelial toxicity caused by reduced corneal thickness.

The study has several limitations that should be considered in its interpretation: the limited sample size, the multiplied CXL modalities, the various variable, the accuracy of pre-existing data, and the inherent biases introduced by retrospective analysis. Hence, these findings should be further confirmed by prospective trials with a longer follow-up period, larger sample size, and better variable selection.

Using an ML algorithm and incorporating identifiable parameters from historical case data improved prediction of case changes in CDVA and K_{\max} at 2 years after CXL for progressive keratoconus. These techniques could improve case accuracy and decrease patient treatment expenses. To improve the prediction model, more data sets and richer feature collections should be examined in further studies.

Data availability statement

The data analyzed in this study is subject to the following licenses/restrictions: The datasets used and analyzed during the current study are available from the corresponding author on reasonable request. Requests to access these datasets should be directed to Q-yZ, zengqingyan1972@163.com.

Ethics statement

The studies involving human participants were reviewed and approved by Ethics Committee of Aier Eye Hospital of Wuhan University. Written informed consent to participate in this study was provided by the participants' legal guardian/next of kin.

Author contributions

YL conceived the study and was the major contributor in design and coordination, in collecting data, in analyzing data, in the web designing, and in writing the manuscript. DS and H-yW helped to collect the data. M-yQ made the web design. Q-yZ participated in surgeries and contributed in its design and coordination, and made the analysis and interpretation of data. All authors have read and approved the final manuscript.

Funding

This study received support from the scientific research project of the Health Commission of Wuhan (Grant No. WX20Q19), and the Research Fund of the Clinical Research Institute of Aier Eye Hospital Group (No. AR2110D22).

Acknowledgments

The authors acknowledge Guang Zhao from the Department of Statistics of Tongji Medical College, Huazhong University of Science and Technology for his help in statistical analysis.

Conflict of interest

The authors declare that the research was conducted in the absence of any commercial or financial relationships that could be construed as a potential conflict of interest.

Publisher's note

All claims expressed in this article are solely those of the authors and do not necessarily represent those of their affiliated organizations, or those of the publisher, the editors and the reviewers. Any product that may be evaluated in this article, or claim that may be made by its manufacturer, is not guaranteed or endorsed by the publisher.

Supplementary material

The Supplementary material for this article can be found online at: <https://www.frontiersin.org/articles/10.3389/fmed.2023.1146529/full#supplementary-material>

References

- Wollensak G, Spoerl E, Seiler T. Riboflavin/ultraviolet-A-induced collagen crosslinking for the treatment of keratoconus. *Am J Ophthalmol.* (2003) 135:620–7. doi: 10.1016/S0002-9394(02)02220-1
- Wittig-Silva C, Chan E, Islam FM, et al. A randomized, controlled trial of corneal collagen cross-linking in progressive keratoconus: three-year results. *Ophthalmology.* (2014) 121:812–21. doi: 10.1016/j.ophtha.2013.10.028
- Iqbal M, Elmassry A, Saad H, Am Gad A, Ibrahim O, Hamed N, et al. Standard cross-linking protocol versus accelerated and transepithelial cross-linking protocols for treatment of paediatric keratoconus: a 2-year comparative study. *Acta Ophthalmol.* (2020) 98:e352–62. doi: 10.1111/aos.14275
- Lombardo M, Serrao S, Lombardo G, Schiano-Lomoriello D. Two-year outcomes of a randomized controlled trial of transepithelial corneal crosslinking with iontophoresis for keratoconus. *J Cataract Refract Surg.* (2019) 45:992–1000. doi: 10.1016/j.jcrs.2019.01.026
- Bikbova G, Bikbov M. Standard corneal collagen crosslinking versus transepithelial iontophoresis-assisted corneal crosslinking. 24 months follow-up: randomized control trial. *Acta Ophthalmol.* (2016) 94:e600–6. doi: 10.1111/aos.13032
- Zhong W, Montana M, Santosa SM, Isjwara ID, Huang YH, Han KY, et al. Angiogenesis and lymphangiogenesis in corneal transplantation—a review. *Surv Ophthalmol.* (2018) 63:453–79. doi: 10.1016/j.survophthal.2017.12.008
- Santodomingo-Rubido J, Carracedo G, Suzuki A, Villa-Collar C, Vincent SJ, Wolffsohn JS. Keratoconus: an updated review. *Cont Lens Anterior Eye.* (2022) 45:101559. doi: 10.1016/j.clae.2021.101559
- Raiskup-Wolf F, Hoyer A, Spoerl E, Pillunat LE. Collagen crosslinking with riboflavin and ultraviolet-A light in keratoconus: long-term results. *J Cataract Refract Surg.* (2008) 34:796–801. doi: 10.1016/j.jcrs.2007.12.039
- Lenk J, Herber R, Oswald C, Spoerl E, Pillunat LE, Raiskup F. Risk factors for progression of keratoconus and failure rate after corneal cross-linking. *J Refract Surg.* (2021) 37:816–23. doi: 10.3928/1081597X-20210830-01
- Sağlık A, Özcan G, Uçakhan Ö. Risk factors for progression following corneal collagen crosslinking in keratoconus. *Int Ophthalmol.* (2021) 41:3443–9. doi: 10.1007/s10792-021-01908-9
- Sot M, Gan G, François J, Chaussard D, Da Costa M, Luc MS, et al. Risk factors for keratoconus progression after treatment by accelerated cross-linking (A-CXL): a prospective 24-month study. *J Fr Ophtalmol.* (2021) 44:863–72. doi: 10.1016/j.jfo.2020.08.040
- Sarac O, Caglayan M, Cakmak HB, Cagil N. Factors influencing progression of keratoconus 2 years after corneal collagen cross-linking in pediatric patients. *Cornea.* (2016) 35:1503–7. doi: 10.1097/ICO.0000000000001051
- Wisse RP, Godefrooij DA, Soeters N, Imhof SM, Van der Lelij A. A multivariate analysis and statistical model for predicting visual acuity and keratometry one year after cross-linking for keratoconus. *Am J Ophthalmol.* (2014) 157:519–25.e1-2. doi: 10.1016/j.ajo.2013.11.001
- Gilevska F, Biscevic A, Popovic Suic S, Bohac M, Patel S. Are changes in visual acuity and astigmatism after corneal cross-linking (CXL) in keratoconus predictable? *Graefes Arch Clin Exp Ophthalmol.* (2021) 259:2259–68. doi: 10.1007/s00417-021-05173-5
- Tian M, Jian W, Zhang X, Sun L, Shen Y, Zhou X. Predictive factors of the accelerated transepithelial corneal cross-linking outcomes in keratoconus. *BMC Ophthalmol.* (2022) 22:7. doi: 10.1186/s12886-021-02235-4
- Godefrooij DA, Boom K, Soeters N, Imhof SM, Wisse RP. Predictors for treatment outcomes after corneal crosslinking for keratoconus: a validation study. *Int Ophthalmol.* (2017) 37:341–8. doi: 10.1007/s10792-016-0262-z
- Badawi AE, Abou Samra WA, El Ghafar AA. Predictive factors of the standard cross-linking outcomes in adult keratoconus: one-year follow-up. *J Ophthalmol.* (2017) 2017:4109208. doi: 10.1155/2017/4109208
- Rebala G, Ravi A, Churiwala S. Machine learning definition and basics In: . *An Introduction to Machine Learning*. Cham: Springer (2019) (pp. 1–17).
- Wang Y, Yao Q, Kwok JT, Ni LM. Generalizing from a few examples: A survey on few-shot learning[J]. *ACM Comput Surv.* (2020) 53:1–34. doi: 10.1145/3386252
- Korstanje J. Gradient boosting with XGBoost and LightGBM In: . *Advanced Forecasting With Python*. Berkeley, CA: Apress (2021)
- Maile H, Li JO, Gore D, Leucci M, Mulholland P, Hau S, et al. Machine learning algorithms to detect subclinical keratoconus: systematic review. *JMIR Med Inform.* (2021) 9:e27363. doi: 10.2196/27363
- Aatila M, Lachgar M, Hamid H, Kartit A. Keratoconus severity classification using features selection and machine learning algorithms. *Comput Math Methods Med.* (2021) 2021:9979560–26. doi: 10.1155/2021/9979560
- Kato N, Masumoto H, Tanabe M, Sakai C, Negishi K, Torii H, et al. Predicting keratoconus progression and need for corneal crosslinking using deep learning. *J Clin Med.* (2021) 10:844. doi: 10.3390/jcm10040844
- McMahon TT, Szczotka-Flynn L, Barr JT, Anderson RJ, Slaughter ME, Lass JH, et al. A new method for grading the severity of keratoconus: the keratoconus severity score (KSS). *Cornea.* (2006) 25:794–800. doi: 10.1097/01.icc.0000226359.26678.d1
- Cronin B, Ghosh A, Chang CY. Oxygen-supplemented transepithelial-accelerated corneal crosslinking with pulsed irradiation for progressive keratoconus: 1 year outcomes. *J Cataract Refract Surg.* (2022) 48:1175–82. doi: 10.1097/j.jcrs.0000000000000952
- Mazzotta C, Traversi C, Caragiuli S, Rechichi M. Pulsed vs continuous light accelerated corneal collagen crosslinking: in vivo qualitative investigation by confocal microscopy and corneal OCT. *Eye (Lond).* (2014) 28:1179–83. doi: 10.1038/eye.2014.163
- Nadeau C, Bengio Y. Inference for the generalization error. *Mach Learn.* (2003) 52:239–81. doi: 10.1023/A:1024068626366
- Bouckaert RR, Frank E. Evaluating the replicability of significance tests for comparing learning algorithms. *Lecture Notes Comput Sci.* (2004) 3056:3–12. doi: 10.1007/978-3-540-24775-3_3
- Kan J, Li A, Zou H, Chen L, Du J. A machine learning based dose prediction of lutein supplements for individuals with eye fatigue. *Front Nutr.* (2020) 7:577923. doi: 10.3389/fnut.2020.577923
- Zhao X, Wu S, Fang N, Sun X, Fan J. Evaluation of single-cell classifiers for single-cell RNA sequencing data sets. *Brief Bioinform.* (2020) 21:1581–95. doi: 10.1093/bib/bbz096
- Xia Y, Li X, Chen X, Lu C, Yu X. Inferring retinal degeneration-related genes based on Xgboost. *Front Mol Biosci.* (2022) 9:843150. doi: 10.3389/fmolb.2022.843150
- Tayfur M, Ocak SY, Elcioglu MN. Factors affecting visual gain after accelerated crosslinking in pediatric Keratoconic cases. *Beyoglu Eye J.* (2021) 6:267–71. doi: 10.14744/bej.2021.15046
- Peña-García P, Vega-Estrada A, Barraquer RI, Burguera-Giménez N, Alio JL. Intracorneal ring segment in keratoconus: a model to predict visual changes induced by the surgery. *Invest Ophthalmol Vis Sci.* (2012) 53:8447–57. doi: 10.1167/iov.12-10639
- Sedaghat MR, Momeni-Moghaddam H, Piñero DP, Akbarzadeh R, Moshirfar M, Bamdad S, et al. Predictors of successful outcome following intrastromal corneal ring segments implantation. *Curr Eye Res.* (2019) 44:707–15. doi: 10.1080/02713683.2019.1594945
- Motlagh MN, Moshirfar M, Murri MS, Skanchy DF, Momeni-Moghaddam H, Ronquillo YC, et al. Pentacam® corneal tomography for screening of refractive surgery candidates: A review of the literature, part I. *Med Hypothesis Discov Innov Ophthalmol.* (2019) 8:177–203.
- Viswanathan D, Kumar NL, Males JJ, Graham SL. Relationship of structural characteristics to biomechanical profile in Normal, Keratoconic, and crosslinked eyes. *Cornea.* (2015) 34:791–6. doi: 10.1097/ICO.0000000000000434
- Amanzadeh K, Elham R, Jafarzadehpour E. Effects of single-segment Intacs implantation on visual acuity and corneal topographic indices of keratoconus. *J Curr Ophthalmol.* (2017) 29:189–93. doi: 10.1016/j.joco.2016.10.004
- De Angelis F, Rateau J, Destrieux C, Patat F, Pisella PJ. Facteurs prédictifs de bonne réponse au crosslinking d'un kératocône évolutif: résultats réfractifs et topographiques à un an postopératoire [Predictive factors for visual outcome after corneal collagen crosslinking treatment in progressive keratoconus: One-year refractive and topographic results]. *J Fr Ophtalmol.* (2015) 38:595–606. doi: 10.1016/j.jfo.2014.11.017
- Greenstein SA, Fry KL, Hersh PS. Effect of topographic cone location on outcomes of corneal collagen cross-linking for keratoconus and corneal ectasia. *J Refract Surg.* (2012) 28:397–405. doi: 10.3928/1081597X-20120518-02
- Greenstein SA, Shah VP, Fry KL, Hersh PS. Corneal thickness changes after corneal collagen crosslinking for keratoconus and corneal ectasia: one-year results. *J Cataract Refract Surg.* (2011) 37:691–700. doi: 10.1016/j.jcrs.2010.10.052
- Takahashi A, Nakayasu K, Okisaka S, Kanai A. Quantitative analysis of collagen fiber in keratoconus. *Nippon Ganka Gakkai Zasshi.* (1990) 94:1068–73.
- Uçakhan OO, Kanpolat A, Yilmaz N, Ozkan M. In vivo confocal microscopy findings in keratoconus. *Eye Contact Lens.* (2006) 32:183–91. doi: 10.1097/01.icl.0000189038.74139.4a
- Bradford SM, Mikula ER, Juhasz T, Brown DJ, Jester JV. Collagen fiber crimping following in vivo UVA-induced corneal crosslinking. *Exp Eye Res.* (2018) 177:173–80. doi: 10.1016/j.exer.2018.08.009
- Mimouni M, Sorkin N, Hatch W, Slomovic ARKEI CXL Study Group, Singal N. Fellow eye as a predictor for keratoconus progression following accelerated corneal cross-linking. *J Refract Surg.* (2021) 37:186–91. doi: 10.3928/1081597X-20201229-02
- Ozgunhan EB, Kara N, Cankaya KI, Kurt T, Demirok A. Accelerated corneal cross-linking in pediatric patients with keratoconus: 24-month outcomes. *J Refract Surg.* (2014) 30:843–9. doi: 10.3928/1081597X-20141120-01
- Vinciguerra P, Albé E, Frueh BE, Trazza S, Epstein D. Two-year corneal cross-linking results in patients younger than 18 years with documented progressive keratoconus. *Am J Ophthalmol.* (2012) 154:520–6. doi: 10.1016/j.ajo.2012.03.020
- Olivo-Payne A, Abdala-Figuerola A, Hernandez-Bogantes E, Pedro-Aguilar L, Chan E, Godefrooij D. Optimal management of pediatric keratoconus: challenges and solutions. *Clin Ophthalmol.* (2019) 13:1183–91. doi: 10.2147/OPTH.S183347

48. Kotecha A, Elsheikh A, Roberts CR, Zhu H, Garway-Heath DF. Corneal thickness- and age-related biomechanical properties of the cornea measured with the ocular response analyzer. *Invest Ophthalmol Vis Sci.* (2006) 47:5337–47. doi: 10.1167/iops.06-0557

49. Jester JV, Huang J, Fisher S, Spiekerman J, Chang JH, Wright WE, et al. Myofibroblast differentiation of normal human keratocytes and hTERT, extended-life human corneal fibroblasts. *Invest Ophthalmol Vis Sci.* (2003) 44:1850–8. doi: 10.1167/iops.02-0973



OPEN ACCESS

EDITED BY

Cristina Nicula,
University of Medicine and Pharmacy Iuliu
Hatieganu, Romania

REVIEWED BY

Francesco Maria D'Alterio,
Imperial College Healthcare NHS Trust,
United Kingdom
Zhipeng Yan,
Third Hospital of Hebei Medical
University, China

*CORRESPONDENCE

Marco Ferrise
✉ ferrisemarco@gmail.com

RECEIVED 31 March 2023

ACCEPTED 01 August 2023

PUBLISHED 21 August 2023

CITATION

Mazzotta C, Pandolfi A and Ferrise M (2023)
Progressive high-fluence epithelium-on
accelerated corneal crosslinking: a novel
corneal photodynamic therapy for early
progressive keratoconus.
Front. Med. 10:1198246.
doi: 10.3389/fmed.2023.1198246

COPYRIGHT

© 2023 Mazzotta, Pandolfi and Ferrise. This is
an open-access article distributed under the
terms of the [Creative Commons Attribution
License \(CC BY\)](https://creativecommons.org/licenses/by/4.0/). The use, distribution or
reproduction in other forums is permitted,
provided the original author(s) and the
copyright owner(s) are credited and that the
original publication in this journal is cited, in
accordance with accepted academic practice.
No use, distribution or reproduction is
permitted which does not comply with these
terms.

Progressive high-fluence epithelium-on accelerated corneal crosslinking: a novel corneal photodynamic therapy for early progressive keratoconus

Cosimo Mazzotta^{1,2}, Anna Pandolfi³ and Marco Ferrise^{4*}

¹Departmental Ophthalmology Unit, USL Toscana Sudest, Postgraduate Ophthalmology School, Alta Val
d'Elsa Hospital, University of Siena, Siena, Italy, ²Siena Crosslinking Center, Siena, Italy, ³Civil and
Environmental Engineering Department, Politecnico di Milano, Milan, Italy, ⁴Studio Oculistico Ferrise,
Lamezia Terme, Italy

Purpose: To assess the preliminary clinical results of a new, progressively higher
fluence-pulsed light Epi-On accelerated crosslinking nomogram (PFPL M Epi-On
ACXL) in the treatment of progressive keratoconus (KC).

Setting: Siena Crosslinking Center, Siena, Italy.

Methods: A prospective pilot open, non-randomized interventional study,
including 32 eyes of 32 young-adult patients over 26 years old with Stages I-
III progressive KC undergoing PFPL M Epi-On ACXL, was conducted. Riboflavin
loading was performed by using Paracel I 0.25% for 4 min and Paracel II 0.22%
for 6 min. The Avedro KXL System (Glaukos-Avedro, Burlington, USA) was used
for pulsed-light accelerated crosslinking (ACXL) at air room 21% oxygenation and
13 min of UV-A irradiation. The treatment fluence was set at 7.2 J/cm², 8.6 J/cm²,
and 10.0 J/cm² in corneas with baseline pachymetry <420 μm (group 1: 8 eyes), ≥
420 μm < 460 μm (group 2, 11 eyes), and ≥ 460 μm (group 3, 13 eyes), respectively.
Uncorrected distance visual acuity (UDVA), best-spectacle corrected visual acuity
(BSCVA), Scheimpflug corneal tomography, and anterior segment OCT (AS-OCT)
data were collected at baseline and postoperatively at 1, 3, and 6 months.

Results: UDVA and BSCVA improved in all groups ($P \leq 0.05$). Maximum keratometry
values (K max) showed a significant decrease in the 10.0 J/cm² group ($\Delta -1.68$
D). The coma (HOAs) value improved significantly by the sixth month in all groups.
OCT average demarcation lines were $211 \pm 19 \mu\text{m}$ in group 1, $245 \pm 23 \mu\text{m}$ in
group 2, and $267 \pm 21 \mu\text{m}$ in group 3.

Conclusions: The preliminary results show that pachymetry-based PFPL M
Epi-On ACXL nomogram stabilizes ectasia progression. Higher fluence Epi-On
ACXL increases CXL penetration, with better functional outcomes in the absence
of complications.

KEYWORDS

keratoconus, corneal ectasia, corneal cross-linking, refractive surgery, Epi-On CXL

Introduction

To date, riboflavin–ultraviolet-A (UV-A) corneal collagen crosslinking (CXL) with epithelium removal (Epi-Off CXL) represents the gold standard of treatment for progressive keratoconus (KC) and other corneal ectasias (1). The main reason behind this is that the removal of the epithelial barrier allows for adequate diffusion of both riboflavin and oxygen into the corneal stroma, which is necessary to achieve an adequate photo-oxidative reaction and, consequent, the desired formation of collagen fibrils crosslinking with adjacent fibrils (1–3).

From a clinical and practical perspective, a safer and faster transepithelial crosslinking treatment with an efficacy profile comparable to Epi-Off CXL, with no adverse events and capable of quickly rehabilitating patients with progressive KC to resume their school or work activities, represents a great challenge and a highly interesting goal. In fact, there are several indisputable advantages to performing a corneal CXL whilst maintaining the epithelial layer. Some of the primary advantages are the elimination of the risk of infectious keratitis and persistent stromal haze, easier functional recovery for patients with minimal postoperative pain and discomfort, and the ability to avoid microstructural damage to the ocular surface so that patients may return to their normal activities the day after (4).

Another substantial advantage of Epi-On treatments is the possibility of performing the procedure fully in an outpatient modality, without the need for a sterile operating theater. This approach makes the clinical workflow more linear and is also cost-effective for the surgeon. In cases of bilateral progressive keratoconus (KC), a simultaneous bilateral treatment can also be performed, with a clear advantage for both the patient and the clinic in terms of organizational burden.

Unfortunately, many studies have shown that the initial adoption of the original 5.4 J/cm² Epi-On corneal crosslinking has been largely unsuccessful due to a lack of ectasia stabilization. In 2012, Koppen et al.'s cohort study evaluated the efficacy of CXL treatment without epithelial debridement. The standard CXL irradiation was preceded by the instillation of proparacaine drops 0.5% preserved with BAC 0.005% every 5 min for 30 min. The results showed significant continuous maximum K increasing and thinnest point decreasing (KC progression) throughout the study in 100% of eyes (5). Similarly, in 2013, Caporossi et al.'s study in a population of pediatric and young adult patients treated with transepithelial (Epi-On) CXL showed that, after relative improvement in the first 3 to 6 months, the UDVA and CDVA gradually returned to baseline preoperative values. After 12 months of stability, K max and pachymetry values worsened at 24 months. Functional results after transepithelial CXL showed keratoconus instability, particularly in pediatric patients 18 years old and younger. There was also functional regression in patients between 19 years and 26 years old after 24 months of follow-up. In fact, 50% of pediatric patients were retreated with Epi-Off CXL due to significant deterioration of all parameters after 1 year of follow-up (6).

In 2016, Gatziofias et al.'s prospective interventional multicentre study confirmed the clinical inefficacy of transepithelial CXL, documenting that after a 12-month follow-up, progression

(defined by an increase in K max >1.00 diopter) still occurred in 46% of eyes (7).

Fortunately, everything has changed, and everything is changing from the original Epi-On CXL protocol. In recent years, the failure of the outset of Epi-On CXL has prompted researchers to utilize all the gathered clinical experience and deepen their understanding of the physiochemical mechanisms underlying crosslinking kinetics through multiple pathways. It has driven them to implement every small detail to bring the efficacy of transepithelial techniques ever closer to Epi-Off CXL (8).

Many parameters have been adapted to optimize the effectiveness of Epi-On accelerated crosslinking. The most important was represented by the increased fluence that passed from the original 5.4 to 7 J/cm², which ensured greater penetration, visibility of deeper demarcation lines, and higher efficacy of the new Epi-On procedures without intraoperative supplemental oxygen (9).

The first international study on Epi-On customized crosslinking with intraoperative supplemental oxygen also demonstrated different depths of the demarcation line, according to a double fluence based on corneal curvature: 7.2 and 10 J/cm², respectively (10).

The fact that fluence was a major player in the crosslinking procedure was clinically proven only in 2016 by Seiler et al. and Mazzotta et al. The authors used topography-guided accelerated crosslinking protocols with 7.2, 10, and 15 J/cm² variable fluence in Epi-Off ACXL modality without adverse events for corneal stroma and endothelium (11, 12).

Another important parameter was the increased concentration of the chemically enhanced riboflavin solutions, now being used at 0.22 and 0.25% instead of 0.1%, which is significant considering that the penetration of riboflavin through the intact epithelium was more than halved compared with its passive diffusion after epithelium removal (13, 14).

An important method for improving riboflavin loading into the stroma through the epithelium *in situ* is the iontophoresis technique, which was recently renewed by Mazzotta et al. in the new iontophoresis protocol with enhanced fluence and pulsed light mode of UV-A irradiation (15, 16).

The use of pulsed UV-A light in a duty cycle of 1 s on 1 s off to partially enhance intraoperative oxygen diffusion and drive the aerobic photochemistry of the crosslinking reaction was based on lab demonstrations and on the literature showing a deeper stromal demarcation line when compared to the accelerated continuous light CXL protocol, with less microstructural damage and improved stromal oxygenation (17–20).

Recent laboratory studies have proven that higher fluences between 8 and 10 J/cm² increase the biomechanical impact of CXL (21). The progressively higher fluence protocols enhance Epi-Off and Epi-On efficacy, as demonstrated in past and recent literature (9–12, 15). The increased fluence variance may be the key to optimizing the photodynamic process of Epi-On crosslinking, paving the way to the final switch (9). We present the preliminary data of the new pachymetry-based progressively higher fluence Epi-On nomogram as a new paradigm of corneal photodynamic therapy for early progressive KC (22–24).

Materials and methods

A prospective pilot open, non-randomized interventional study, including 32 eyes of 32 young-adult patients over 26 years old with Stages I, II, and III progressive KC undergoing PFPL M Epi-On CXL, was conducted. The treatment protocol was approved by the Institutional Review Board of the Siena Crosslinking Center (Code: *PFPL.EPION 2.0*) under the tenets of the Helsinki Declaration, taking into account no expected risk of adverse events, as fluences between 5.4 and 15 J/cm² have already been safely used and published in the literature for both Epi-Off and Epi-On customized accelerated CXL treatments (10–12). Likewise, riboflavin solutions (Paracel parts 1 and 2 by Glaukos-Avedro, Burlington, USA) already approved in the market for ACXL therapy of progressive KC were adopted (10–12).

The progression of KC was defined as an increase in K max ≥ 1 diopter (D) using the Scheimpflug–Placido corneal tomography system Sirius, Costruzione Strumenti Oftalmici (C.S.O.), Florence, Italy. It was also defined by a minimum corneal thickness (MCT) reduction ≥ 10 μ m, worsening of uncorrected distance visual acuity (UDVA) and corrected distance visual acuity (CDVA) ≥ 0.1 decimal equivalent, or a change of ≥ 0.5 in the mean refractive spherical equivalent (MRSE) in the last 6 months of clinical and instrumental observation. MCT was required to be at least 400 μ m (including epithelium). Patients with clear corneas with no sub-apical opacities or scars, no history of previous herpes simplex virus infection and other infectious keratitis or autoimmune diseases, and no severe dry eye were included.

All patients signed a specific informed consent form.

The demographic data of the study are displayed in Table 1.

Measurements and devices

Ophthalmic evaluations were performed before CXL and at all follow-up visits (1, 3, and 6 months). The evaluation included UDVA, best-spectacle corrected distance visual acuity (BCDVA), biomicroscopic corneal examination, ocular surface disease index (OSDI) test, and non-invasive topographic break-up time test (NI-BUT) for excluding dry-eye disease. Scheimpflug-based corneal tomography (Sirius, CSO, Florence, Italy) was used to measure the maximum curvature simulated K reading (K max), high-order aberration (coma), and MCT. Anterior segment optical coherence tomography (AS-OCT) was performed using the I-Vue (Optovue, Fremont CA, USA) to assess the demarcation line depth on the first postoperative month.

Surgical procedure

The treatment parameters of PHFPL Epi-On ACXL are displayed in Table 2.

The surgical procedure was performed under topical anesthesia with 4% oxybuprocaine chlorhydrate 1.6 mg/0.4 ml drops, applied 5 min before the treatment (one drop per min). After applying a closed-valve eyelid speculum, it involved swiping the epithelial

TABLE 1 Demographic baseline data.

Patients	32 (28 male patients/4 female patients)
Group 1 (Fluence 7.2 J/cm ²)	8 (pachymetry < 420 μ m)
Group 2 (Fluence 8.6 J/cm ²)	11 (pachymetry ≥ 420 μ m < 460 μ m)
Group 3 (Fluence 10 J/cm ²)	13 (pachymetry ≥ 460 μ m)
Eyes total	32
Age	27.9 y (range 26–31 y).
M/F ratio	28/4 (87.5% male)
UDVA (uncorrected distance visual acuity, decimal equivalents)	Group 1: 0.32 \pm 0.07
	Group 2: 0.41 \pm 0.08
	Group 3: 0.44 \pm 0.11
BCDVA (best-corrected distance visual acuity, decimal equivalents)	Group 1: 0.63 \pm 0.15
	Group 2: 0.77 \pm 0.11
	Group 3: 0.75 \pm 0.12
K max (maximum curvature simulated K reading, dioptres)	Group 1: 48.76 \pm 0.9 D
	Group 2: 48.40 \pm 0.4 D
	Group 3: 48.33 \pm 0.6 D
COMA (high order aberration, μ m)	Group 1: 0.68 \pm 0.12
	Group 2: 0.69 \pm 0.07
	Group 3: 0.64 \pm 0.06
MCT (minimum corneal thickness, μ m)	Group 1: 401 \pm 11 μ m
	Group 2: 442 \pm 14 μ m
	Group 3: 481 \pm 15 μ m
Follow-up	6 months

surface with a sponge soaked in 0.25% Paracel 1 solution. This was followed by biphasic (4 min part one and 6 min part two) riboflavin soaking with Paracel 1 (Glaukos-Avedro, Burlington, USA) 0.25% riboflavin solution, dropped every min for 6 min, and Paracel 2 (Glaukos-Avedro, Burlington, USA) 0.22% riboflavin solution, dropped every 30 s for 4 min. Copious irrigation of the corneal surface was performed for 15–20 s with a balanced salt solution (BSS) before starting the UV-A irradiation with the New KXL I UV-A emitter (Glaukos-Avedro, Burlington, USA).

The new Epi-On protocol is a pachymetry-based variable fluence “corneal photodynamic therapy.” It consists of the application of a progressively higher fluence of 7.2 in corneas with baseline pachymetry <420 μ m (group 1: 8 eyes) using a UV-A power of 18 mW/cm², 8.6 J/cm² in corneas with baseline pachymetry ≥ 420 μ m < 460 μ m (group 2: 11 patients) using 22 mW/cm² UV-A power, and 10 J/cm² in patients with baseline pachymetry ≥ 460 μ m (group 3: 13 patients) using 26 mW/cm² UV-A power. Overall, an irradiation time of 13 min was maintained in all cases to achieve an overall treatment time of 23 min (10 min of riboflavin soaking plus 13 min of pulsed light 1 s on–1 s off UV-A irradiation), as shown in Table 2. At the end of the procedure,

TABLE 2 Progressive Fluence Pulsed Light Epi-On accelerated crosslinking M nomogram, developed by Mazzotta and Ferrise at the Siena crosslinking center, Italy.

Parameter	Variable	Variable	Variable
Treatment target	KC stabilization	KC stabilization	KC stabilization
Thinnest point	< 420 μ m	$\geq 420 \mu\text{m} < 460 \mu\text{m}$	$\geq 460 \mu\text{m}$
Fluence (total) (J/cm ²)	7.2 J/cm ²	8.6 J/cm ²	10 J/cm ²
Soak time and interval (min)	10 min (4 + 6)	10 min (4 + 6)	10 min (4 + 6)
Intensity (mW)	18 mW/cm ²	22 mW/cm ²	26 mW/cm ²
Irradiation time	13 min	13 min	13 min
Epithelium status	On	On	On
Chromophore	Riboflavin	Riboflavin	Riboflavin
Chromophore carrier and concentration. Paracel part 1 (0.25%)	BAK, EDTA, trometamol	BAK, EDTA, trometamol	BAK, EDTA, trometamol
	HPMC NaCl	HPMC NaCl	HPMC NaCl
	Phosphate buffered saline solution	Phosphate buffered saline solution	Phosphate buffered saline solution
Chromophore carrier and concentration. Paracel part 2 (0.22%)	NaCl Phosphate buffered saline solution	NaCl Phosphate buffered saline solution	NaCl Phosphate buffered saline solution
Chromophore osmolarity	Hypotonic	Hypotonic	Hypotonic
Chromophore concentration	0.22% (Paracel 1)	0.22% (Paracel 1)	0.22% (Paracel 1)
	0.25% (Paracel 2)	0.25% (Paracel 2)	0.25% (Paracel 2)
Epithelial rinsing	15 s with BSS	15 s with BSS	15 s with BSS
Light source	New KXL I (Glaukos-Avedro, USA)	New KXL I (Glaukos-Avedro, USA)	New KXL I (Glaukos-Avedro, USA)
Irradiation mode (interval)	Pulsed (1 s on–1 s off)	Pulsed (1 s on–1 s off)	Pulsed (1 s on–1 s off)
Protocol modifications	EFPL M ACXL	EFPL M ACXL	EFPL M ACXL
Protocol abbreviation	PFPL M ACXL	PFPL M ACXL	PFPL M ACXL

the cornea was medicated with preservative-free netilmicin plus dexamethasone, cyclopentolate, and Ketorolac eye drops plus Carbolol 974P 0.25 % gel. The eye was dressed with a therapeutic bandage soft contact lens, which was kept for 24 h. After therapeutic contact lens removal (the day after), fluorometholone 0.2% eye drops (tapered 4 times/day in the first week, 3 times/day in the second week, and 2 times/day in the third week) were administered in combination with sodium hyaluronate 0.2% lacrimal substitutes for 6 weeks. In case of pain, oral NSAID (10 mg Ketorolac) was prescribed in the first 24 h in combination with Ketorolac eye drops administered qid.

Statistical analysis

According to the study purpose, follow-up examinations were performed at 24 h, 1 month, 3 months, and 6 months. All patients completed the 6-month follow-up. A two-tailed paired samples *t*-test was performed to compare each baseline measurement with the respective follow-up measurements. Differences with $P < 0.05$ were considered statistically significant. Data were collected and analyzed with PRISM 6.0 GraphPad software (La Jolla, California, USA).

Results

Between the preoperative data and the 6-month postoperative control data, the UDVA did not show statistically significant changes in the 7.2 J/cm² (no detectable difference found) and 8.6 J/cm² ($\Delta +0.04$ decimal equivalents) groups, but it showed a statistically significant improvement in the 10.0 J/cm² group ($\Delta +0.15$ decimal equivalents) (Figure 1).

At 6 months postoperatively, the BCDVA did not show statistically significant changes in the 7.2 J/cm² ($\Delta +0.13$ decimal equivalents) and 8.6 J/cm² ($\Delta +0.04$ decimal equivalents) groups, but it showed a statistically significant improvement in the 10.0 J/cm² group ($\Delta +0.16$ decimal equivalents) (Figure 2).

K max reduced in all the groups at 6 months postoperatively. The difference between the 7.2 J/cm² and 8.6 J/cm² groups was not statistically significant, whilst the difference between the 10.0 J/cm² group and the other groups was statistically significant ($P < 0.05$) (Figure 3).

The coma (HOAs) value showed a statistically significant improvement in the 6th month in the 10.0 J/cm² group ($\Delta -0.26 \mu\text{m}$) (Figure 4).

The postoperative spectral-domain corneal OCT performed 1 month after the treatments revealed a clear demarcation line with a

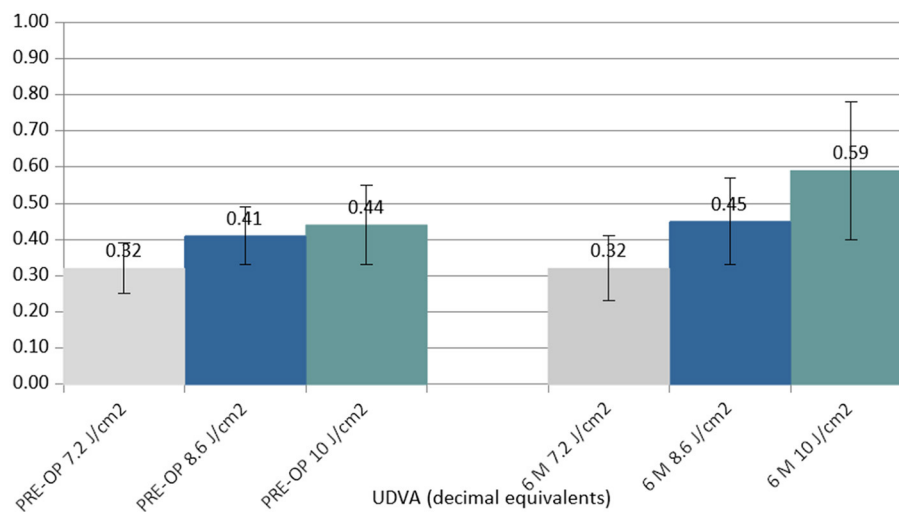


FIGURE 1

Column chart with preoperative (**Left** cluster) and 6-month postoperative (**Right** cluster) values of uncorrected distance visual acuity (UDVA) expressed in decimal equivalents. In each cluster, the first column (gray) corresponds to group 1 (7.2 J/cm², eight patients), the central column (blue) corresponds to group 2 (8.6 J/cm², 11 patients), and the right column (green) corresponds to group 3 (10.0 J/cm², 13 patients).

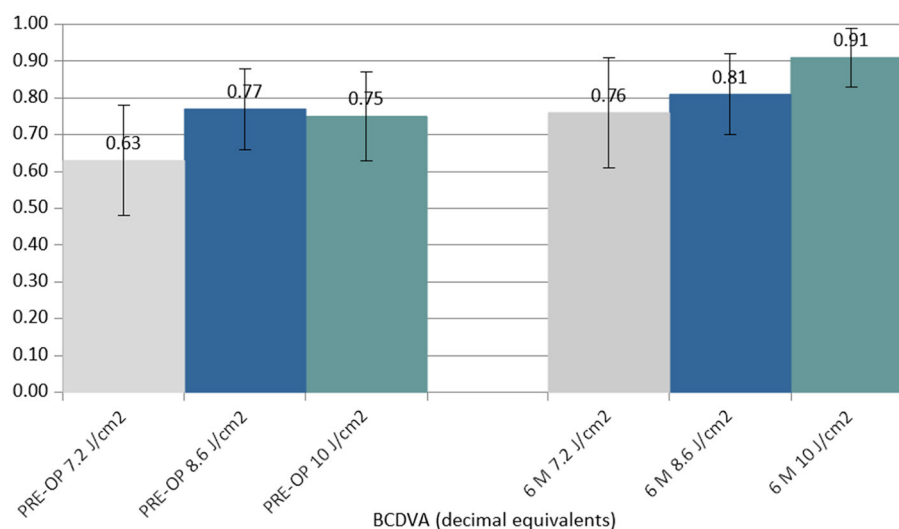


FIGURE 2

Column chart with preoperative (**Left** cluster) and 6-month postoperative (**Right** cluster) values of best-corrected distance visual acuity (BCDVA) expressed in decimal equivalents. In each cluster, the first column (gray) corresponds to group 1 (7.2 J/cm², eight patients), the central column (blue) corresponds to group 2 (8.6 J/cm², 11 patients), and the right column (green) corresponds to group 3 (10.0 J/cm², 13 patients).

mean depth of $211 \pm 19 \mu\text{m}$ in group 1, $245 \pm 23 \mu\text{m}$ in group 2, and $267 \pm 21 \mu\text{m}$ in group 3 (Figure 5).

No adverse events, such as haze or infections, were recorded during the follow-up. A punctate epitheliopathy was found in all cases after performing the fluorescein dye test, which resolved after 24–48 h when a soft contact lens bandage and lubricants were applied. According to the visual analog scale (VAS) pain scale, the average value as reported in our series was 2 ± 1 , from 0 (no pain) to mild annoying pain (2) in the first 2–4 postoperative hours. The postoperative endothelial count showed no significant variation in all three groups between preoperative and 6-month postoperative data.

Discussion

This pilot study demonstrated for the first time at the international level the efficacy and safety of a pachymetry-based progressively higher fluence Epi-On in halting KC progression in all treated patients. The treatment helped avoid pain, eliminated the risk of infectious keratitis, prevented persistent stromal haze, and resulted in faster functional recovery for the patients. This method is the ideal candidate as a possible future alternative to Epi-Off CXL in the management of progressive KC. What is even more relevant is the absence of risks and adverse events, which place this method amongst the prophylactic therapies of primary and

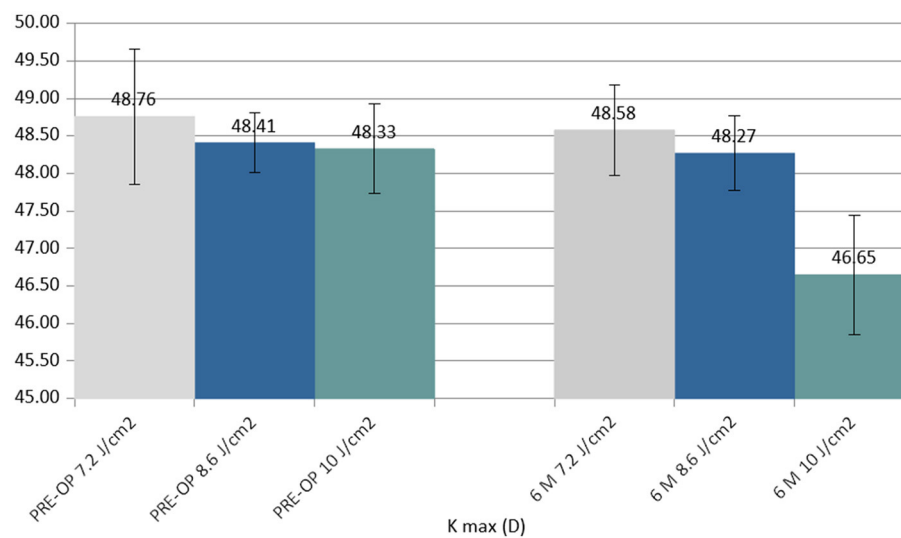


FIGURE 3

Column chart with preoperative (Left cluster) and 6-month postoperative (Right cluster) values of maximum curvature simulated K reading (K max), expressed in diopters (D). In each cluster, the first column (gray) corresponds to group 1 (7.2 J/cm², 8 patients), the central column (blue) corresponds to group 2 (8.6 J/cm², 11 patients), and the right column (green) corresponds to group 3 (10.0 J/cm², 13 patients).

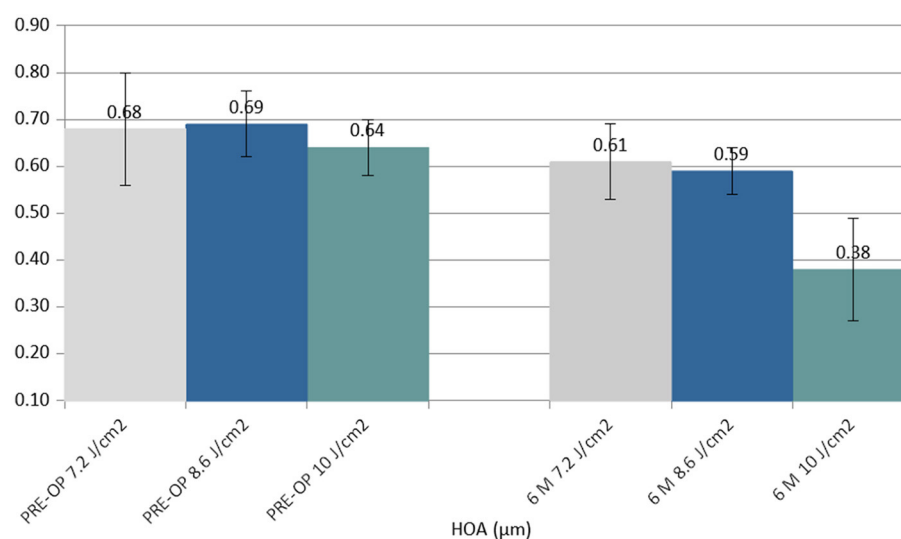


FIGURE 4

Column chart with preoperative (Left cluster) and 6-month postoperative (Right cluster) values of coma (high order aberration, HOA), expressed in micrometers (µm). In each cluster, the first column (gray) corresponds to group 1 (7.2 J/cm², eight patients), the central column (blue) corresponds to group 2 (8.6 J/cm², 11 patients), and the right column (green) corresponds to group 3 (10.0 J/cm², 13 patients).

iatrogenic corneal ectasia as it can be applied purely preventively, even in cases of ectasia that have not yet evolved, to safeguard patients' vision with excellent compliance. The approach also allows for the possibility of simultaneous outpatient interventions, causing minimal postoperative discomfort and avoiding microstructural damage to the ocular surface so that patients may return to their normal activities the day after (9). The high fluence era began in 2016, with studies on customized CXL by Seiler (the first study with 10 J/cm²) (11) and Mazzotta (the first study with PiXL at 10 and 15 J/cm²) (12). It is known that customized CXL with variable fluence shows multiple demarcation lines; this formed the

theoretical basis for the formulation of the "Epi-On M Nomogram" in this study. An increase in UV-A irradiation causes an increase in the density of cross-links in the corneal tissue, even in a low-oxygen environment. Thus, it is apparent that relatively higher fluences help improve stromal strength (9). Therefore, increasing the treatment fluence not only increases the demarcation line depth but also improves corneal resistance to progressive ectasia, which is crucial to Epi-On treatments (9). A higher fluence results in a deeper demarcation line, substantially increasing the treatment volume and the biomechanical power of crosslinking itself (11, 22–27). The clinical and experimental observations presented in the

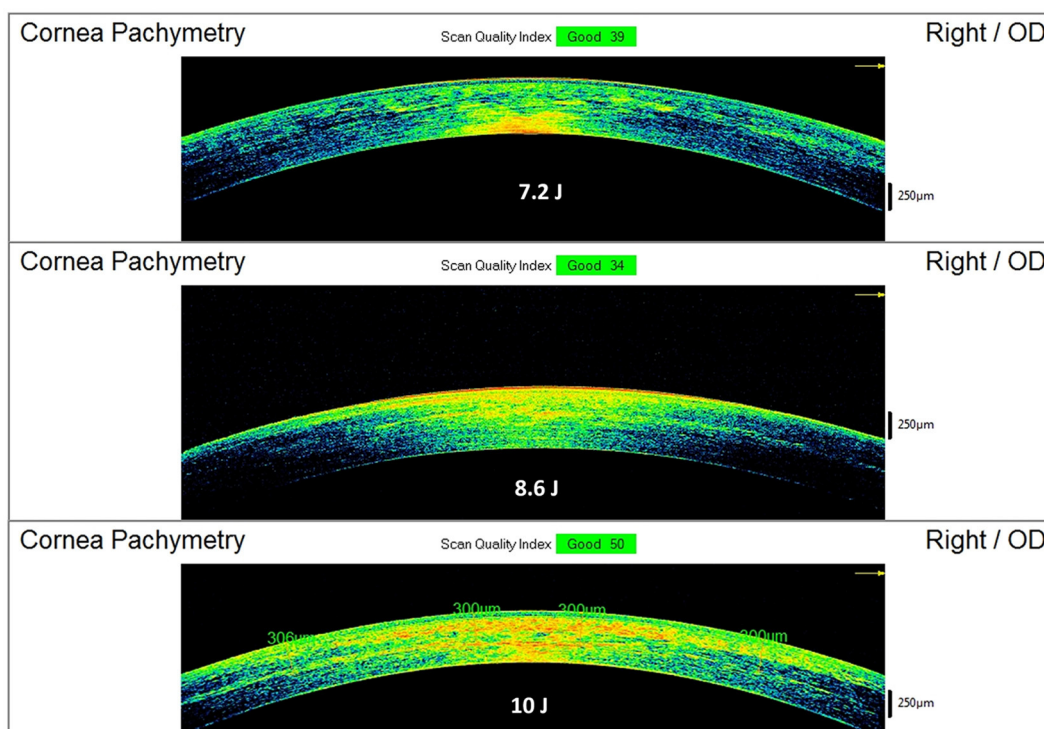


FIGURE 5

Spectral-domain corneal OCT scans performed 15 days after Progressive Fluence Pulsed Light Epi-On M nomogram (PFPL M Epi-On), showing the depth of the demarcation line and stromal reflectivity. The 7.2 J/cm² group (see example in the **Top** image) had an average demarcation line of $211 \pm 19 \mu\text{m}$; the 8.6 J/cm² group (see example in the **Middle** image) had an average demarcation line of $245 \pm 23 \mu\text{m}$; the 10 J/cm² group (see example in the **Bottom** image) had an average demarcation line of $267 \pm 21 \mu\text{m}$.

literature and in this paper suggest that, currently, the best practice of Epi-On CXL treatment could be setting a balance between the riboflavin concentration and a higher fluence between 7.2 and 10.0 J/cm² (22–24).

The morphological anterior segment OCT and tomographic observations of the demarcation line depth show evidence of fluence-dependent CXL penetration and biological impact (the higher the fluence, the deeper the demarcation line depth and the deeper the stromal density) (11, 12). This apparently demonstrates that we are moving in the right direction to permanently replace the Epi-Off CXL.

The preliminary results of this study demonstrate this protocol's ability to penetrate deeply into the stroma without the need to remove the corneal epithelium and to impart a reflectivity to cross-linked tissue, achieving significant corneal flattening that is comparable to that of the Epi-Off treatment, whilst avoiding its side effects, as shown in Figure 6. Moreover, this treatment allows for the possibility of carrying out the procedure in the outpatient mode with less invasiveness and no adjunctive costs (9). Experimental data have proven that higher fluences (irradiation doses) result in a larger increment of corneal stiffness (22–24).

It was previously known that the crosslinking density in the superficial layers ends after reaching saturation and cannot be increased indefinitely (28). Therefore, its overall efficiency attains a homogeneous distribution not only horizontally into the stroma but also in a “depth-dependent curve,” as recently reported in a

review study (25). Biochemical investigations have clearly proven that collagen molecules possess many amino acid reactive residues, such as lysine and proline, constituting over 80% of collagen amino acids that are recruited in the strong chemical (aldehydes-mediated) CXL. Contrarily, only a limited amount (<20%) of free reactive residues of aromatic amino acids, such as tyrosine and phenylalanine, are involved in the short-wave UV-mediated CXL (29).

The increase in the effectiveness of Epi-On protocols is due to the combination of several factors, such as high fluence, imbibition with a high concentration of riboflavin carried out by new chemical enhancers, and the use of pulsed UV light (18, 19). These combined factors enhance the anaerobic photodynamic pathways of CXL (8). This has been extensively demonstrated in both iontophoresis (15, 16) and non-iontophoresis (9) treatment protocols, using 7 J/cm² fluence, as well as in Epi-On customized ACXL protocols at variable higher fluences (between 7.2 and 10 J/cm²) with supplemental oxygen (10).

The fact that laboratory studies confirm that fluences between 8 and 10 J/cm² determine the best biomechanical result cuts the head off all low-fluence treatments especially if conveyed by transepithelial route (22–24).

In fact, it is known that the antioxidant systems of the corneal epithelium and Bowman's lamina absorb approximately 30% of the UV-A energy at a wavelength of 370 nm (30, 31). Corneal transepithelial photodynamic treatments with low

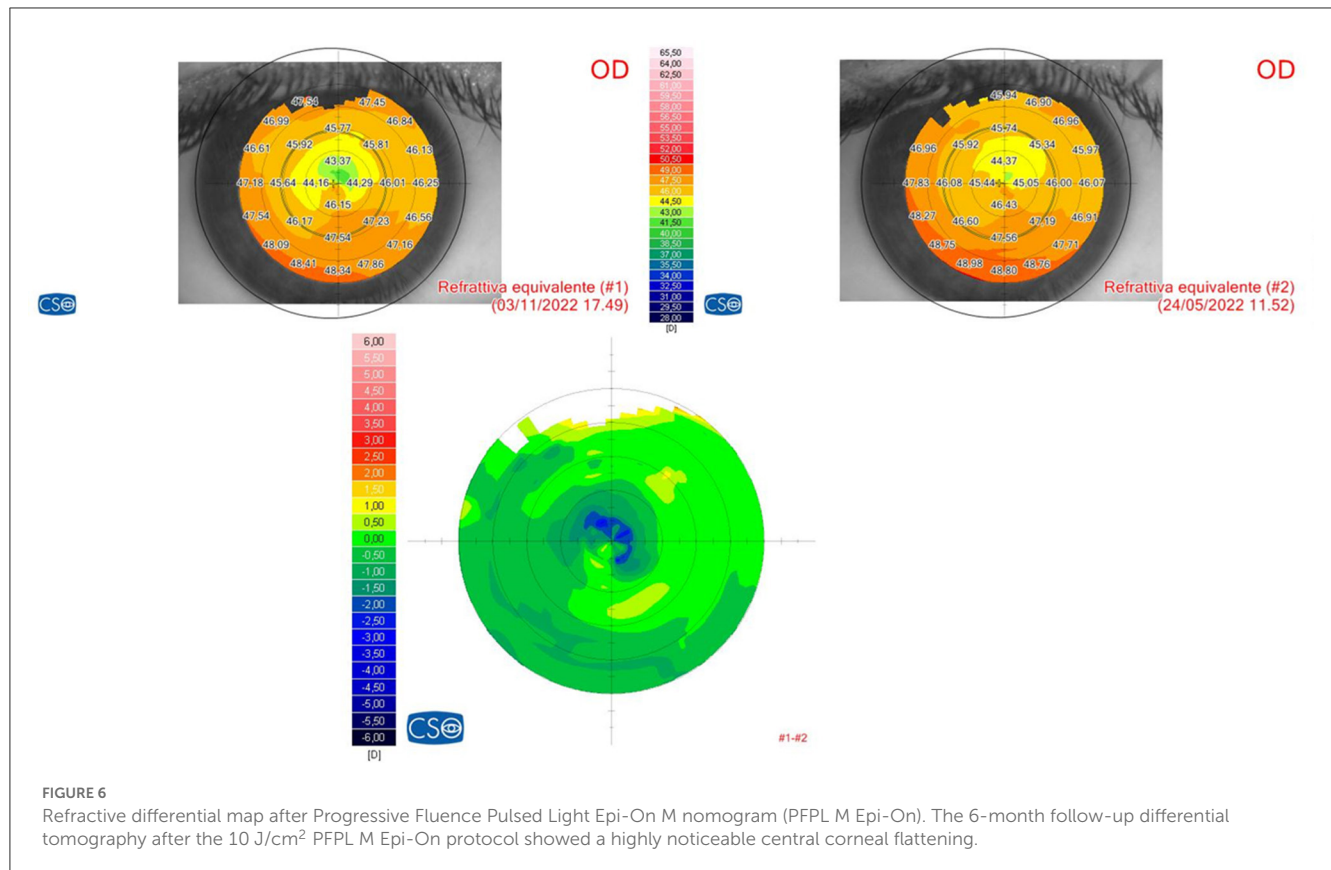


FIGURE 6

Refractive differential map after Progressive Fluence Pulsed Light Epi-On M nomogram (PFPL M Epi-On). The 6-month follow-up differential tomography after the 10 J/cm² PFPL M Epi-On protocol showed a highly noticeable central corneal flattening.

fluence between 2.7 and 3.6 J/cm² with pulsed light cannot prevent the long-term evolution of ectasia due to low CXL density. Additionally, they do not avoid the risk of developing ectasia in the presence of undiagnosed fruste keratoconus (FKFC) due to the obvious limitations outlined above (epithelium-Bowman's lamina complex antioxidants UV-energy absorption and low biomechanical efficacy) (30, 31) and due to high oxygen consumption provided by the epithelium *in situ*. This creates a further negative impact on oxygen kinetics and on the overall efficacy of the Epi-On treatment as a low-fluence corneal CXL photodynamic treatment (LF-CXL-PDT) (32, 33).

What we define as low-fluence crosslinking corneal photodynamic treatment (LF-CXL-PDT) may have a rationale for use in femto-LASIK (34) and corneal refractive lenticule extraction techniques (ReLEx) (35, 36) to prevent idiopathic iatrogenic ectasias. This approach helps avoid an aggressive impact that could negatively affect the corneal stroma, modifying the postoperative refraction stability due to uncontrolled apoptotic corneal flattening and stromal collagen fibril retraction. However, further studies are required to standardize the UV-A irradiation protocols and to evaluate the long-term safety, refractive predictability, and stability of these procedures.

The early evidence of our study will allow surgeons to extend the indications for the photodynamic variable fluence ACXL protocol to increasingly younger patients, potentially to treat developmental ectasias even in the pediatric age, before or after intrastromal refractive surgery procedures (LASIK and ReLEx). It may also allow them to perform bilateral treatments when needed,

with much-improved patient compliance and clinical workflow, including the possibility of outpatient treatments conducted on the same day to reduce the burden of time and organization for both the patient and the surgeon. Moreover, this treatment protocol can be repeated if the progression of ectasia restarts during the follow-up, and the advantages of Epi-On procedures can still be retained in terms of excellent compliance and the absence of infectious and uncontrolled corneal scarring (9).

In conclusion, the preliminary results of the study show that PFPL M Epi-On ACXL halted KC progression in young-adult patients and demonstrated increased efficacy closer to the standard Epi-Off CXL. The increase in efficacy was directly correlated with higher fluences, and significantly better results were obtained by adopting a fluence of 10 J/cm².

Further studies with longer follow-up time, larger patient cohorts, and with the implementation of additional parameters are necessary to improve the efficacy of epithelium-preserving CXL protocols and make them highly effective, more accessible, and feasible in outpatient modality.

Data availability statement

The raw data supporting the conclusions of this article will be made available by the authors, without undue reservation.

Ethics statement

The treatment protocol was approved by the Institutional Review Board of the Siena Crosslinking Center (Code: PFPL.EPION 2.0). The patients/participants provided their written informed consent to participate in this study.

Author contributions

Conceptualization, writing—original draft, writing—review and editing, methodology, and investigation: CM and MF. Supervision: AP. Data curation: CM and AP. All authors contributed to the article and approved the submitted version.

References

1. Raiskup F, Spoerl E. Corneal Crosslinking with Riboflavin and Ultraviolet A. *J Principles Ocul Surf.* (2013) 11:65–74. doi: 10.1016/j.jtos.2013.01.002
2. Kobashi H, Tsubota K. Accelerated vs. standard corneal cross-linking for progressive keratoconus: a meta-analysis of randomized controlled trials. *Cornea.* (2020) 39:2. doi: 10.1097/ICO.0000000000002092
3. Mazzotta C, Raiskup F, Hafezi F, Torres-Netto EA, Balamoun AA, Giannaccare G, et al. Long term results of accelerated 9 mW corneal crosslinking for early progressive keratoconus: the Siena Eye-Cross Study 2. *Eye Vis.* (2021) 8:16. doi: 10.1186/s40662-021-00240-8
4. Dhawan S, Rao K, Natrajan S. Complications of corneal collagen cross-linking. *J Ophthalmol.* (2011) 2011:869015. doi: 10.1155/2011/869015
5. Koppen C, Wouters K, Mathysen D, Rozema J, Tassignon MJ. Refractive and topographic results of benzalkonium chloride-assisted transepithelial crosslinking. *J Cataract Refract Surg.* (2012) 38:1000–5. doi: 10.1016/j.jcrs.2012.01.024
6. Caporossi A, Mazzotta C, Paradiso AL, Baiocchi S, Marigliani D, Caporossi T. Transepithelial corneal collagen crosslinking for progressive keratoconus: 24-month clinical results. *J Cataract Refract Surg.* (2013) 39:1157–63. doi: 10.1016/j.jcrs.2013.03.026
7. Gatziofufas Z, Raiskup F, O'Brart D, Spoerl E, Panos GD, Hafezi F. Transepithelial corneal crosslinking using an enhanced riboflavin solution. *J Refract Surg.* (2016) 32:372–7. doi: 10.3928/1081597X-20160428-02
8. Lin J-T. Critical Analysis of corneal cross-linking (part-II): resolving the controversial issues (theory vs. measurements). *Ophthalmol Res An Int J.* (2021). doi: 10.20944/preprints202108.0488.v1
9. Mazzotta C, Balamoun AA, Chabib A, Rechichi M, D'Oria F, Hafezi F, et al. Transepithelial enhanced fluence pulsed light m accelerated crosslinking for early progressive keratoconus with chemically enhanced riboflavin solutions and air room oxygen. *J Clin Med.* (2022) 11:5039. doi: 10.3390/jcm11175039
10. Mazzotta C, Sgheri A, Bagaglia SA, Rechichi M, Di Maggio A. Customized corneal crosslinking for treatment of progressive keratoconus: Clinical and OCT outcomes using a transepithelial approach with supplemental oxygen. *J Cataract Refract Surg.* (2020) 46:1582–7. doi: 10.1097/j.jcrs.0000000000000347
11. Seiler TG, Fischinger I, Koller T, Zapp D, Frueh BE, Seiler T. Customized corneal cross-linking: one-year results. *Am J Ophthalmol.* (2016) 166:14–21. doi: 10.1016/j.ajo.2016.02.029
12. Mazzotta C, Moramarco A, Traversi C, Baiocchi S, Iovieno A, Fontana L. Accelerated corneal collagen cross-linking using topography-guided UV-A energy emission: preliminary clinical and morphological outcomes. *J Ophthalmol.* (2016) 2016:2031031. doi: 10.1155/2016/2031031
13. Mastropasqua L, Nubile M, Calienno R, Mattei PA, Pedrotti E, Salgari N, et al. Corneal cross-linking: Intrastromal riboflavin concentration in iontophoresis-assisted imbibition vs. traditional and transepithelial techniques. *Am J Ophthalmol.* (2014) 157:3. doi: 10.1016/j.ajo.2013.11.018
14. Franch A, Birattari F, Mas GD, Lužnik Z, Parekh M, Ferrari S, et al. Evaluation of intrastromal riboflavin concentration in human corneas after three corneal cross-linking imbibition procedures: a pilot study. *J Ophthalmol.* (2015) 2015:794256. doi: 10.1155/2015/794256
15. Mazzotta C, Bagaglia SA, Vinciguerra R, Ferrise M, Vinciguerra P. Enhanced fluence pulsed-light iontophoresis corneal cross-linking: 1-year morphological and clinical results. *J Refract Surg.* (2018) 34:438–44. doi: 10.3928/1081597X-20180515-02
16. Mazzotta C, Bagaglia SA, Sgheri A, Di Maggio A, Fruschelli M, Romani A, Vinciguerra R, Vinciguerra P, Tosi GM. Iontophoresis corneal cross-linking with enhanced fluence and pulsed UV-A light: 3-year clinical results. *J Refract Surg.* (2020) 36:286–92. doi: 10.3928/1081597X-20200406-02
17. Kamaev P, Friedman MD, Sherr E, Muller D. Photochemical kinetics of corneal cross-linking with riboflavin. *Investig Ophthalmol Vis Sci.* (2012) 53:2360–7. doi: 10.1167/iovs.11-9385
18. Mazzotta C, Traversi C, Paradiso AL, Latronico ME, Rechichi M. Pulsed light accelerated crosslinking vs. continuous light accelerated crosslinking: one-year results. *J Ophthalmol.* (2014) 2014:604731. doi: 10.1155/2014/604731
19. Mazzotta C, Traversi C, Caragiuli S, Rechichi M. Pulsed vs continuous light accelerated corneal collagen crosslinking: *in vivo* qualitative investigation by confocal microscopy and corneal OCT. *Eye (Lond).* (2014) 28:1179–83. doi: 10.1038/eye.2014.163
20. Jiang LZ, Jiang W, Qiu SY. Conventional vs. pulsed-light accelerated corneal collagen cross-linking for the treatment of progressive keratoconus: 12-month results from a prospective study. *Exp Ther Med.* (2017) 14:4238–44. doi: 10.3892/etm.2017.5031
21. Fischinger I, Reifeltshammer SA, Seiler TG, Nambiar MH, Komninou MA, Büchler P, et al. Analysis of biomechanical response after corneal crosslinking with different fluence levels in porcine corneas. *Curr Eye Res.* (2023) 5:1–5. doi: 10.1080/02713683.2023.2205612
22. Cornaggia A, Boschetti F, Mazzotta C, Pandolfi A. Numerical investigation on epi-off crosslinking effects on porcine corneas. *Mech Soft Mat.* (2020) 2:15. doi: 10.1007/s42558-020-00030-7
23. Boschetti F, Conti D, Soriano EM, Mazzotta C, Pandolfi A. Experimental *in-vitro* investigation on epi-off-crosslinking on porcine corneas. *PLoS ONE.* (2021) 16:e0249949. doi: 10.1371/journal.pone.0249949
24. Xiao X, Xiao C, Yin Y. Effect of a gradient distribution of cross-links on the deformation behaviors of corneal stroma: theoretical model and finite element simulation. *Front Mater.* (2022) 9:870134. doi: 10.3389/fmats.2022.870134
25. Mazzotta C, Wollensak G, Raiskup F, Pandolfi AM, Spoerl E. The meaning of the demarcation line after riboflavin-UVAcornal collagen crosslinking. *Expert Rev Ophthalmol.* (2019) 14:115–31. doi: 10.1080/17469899.2019.1611425
26. Richoz O, Hammer A, Tabibian D, Gatziofufas Z, Hafezi F. The biomechanical effect of corneal collagen cross-linking (CXL) with riboflavin and UV-A is oxygen dependent. *Transl Vis Sci Technol.* (2013) 2:6. doi: 10.1167/tvst.2.7.6
27. Mazzotta C, Romani A, Burroni A. Pachymetry-based accelerated crosslinking: the “m nomogram” for standardized treatment of all-thickness progressive ectatic corneas. *Int J Kerat Ect Cor Dis.* (2018) 7:137–44. doi: 10.5005/jp-journals-10025-1171
28. Lanchares E, del Buey MA, Cristóbal JA, Lavilla L, Calvo B. Biomechanical property analysis after corneal collagen cross-linking in relation to ultraviolet A irradiation time. *Graefes Arch ClinExp Ophthalmol.* 249:1223–7. doi: 10.1007/s00417-011-1674-0

Conflict of interest

The authors declare that the research was conducted in the absence of any commercial or financial relationships that could be construed as a potential conflict of interest.

Publisher's note

All claims expressed in this article are solely those of the authors and do not necessarily represent those of their affiliated organizations, or those of the publisher, the editors and the reviewers. Any product that may be evaluated in this article, or claim that may be made by its manufacturer, is not guaranteed or endorsed by the publisher.

29. Weadock K, Olson RM, Silver FH. Evaluation of collagen crosslinking techniques. *Biomater Med Devices Artif Organs*. (1983–1984) 11:293–318. doi: 10.3109/10731198309118815
30. Podskochoy A. Protective role of corneal epithelium against ultraviolet radiation damage. *Acta Ophthalmol Scand*. (2004) 82:714–7. doi: 10.1111/j.1600-0420.2004.00369.x
31. Kolozsvári L, Nógrádi A, Hopp B, Bor Z. UV absorbance of the human cornea in the 240- to 400-nm range. *Invest Ophthalmol Vis Sci*. (2002) 43:2165–8.
32. Freeman RD. Oxygen consumption by the component layers of the cornea. *J Physiol*. (1972) 225:15–32. doi: 10.1113/jphysiol.1972.sp009927
33. Harvitt DM, Bonanno JA. Oxygen consumption of the rabbit cornea. *Invest Ophthalmol Vis Sci*. (1998) 39:444–8.
34. Mazzotta C, Balestrazzi A, Traversi C, Caragiuli S, Caporossi A. In vivo Confocal Microscopy Report after Lasik with Sequential Accelerated Corneal Collagen Cross-Linking Treatment. *Case Rep Ophthalmol*. (2014) 5:125–31. doi: 10.1159/000362327
35. Mo F, Di Y, Li Y. Changes in Corneal Morphology and Biomechanics in Cases of Small Incision Lenticule Extraction with Prophylactic Accelerated Collagen Cross-Linking. *J Ophthalmol*. (2022) 2022:1640249. doi: 10.1155/2022/1640249
36. Ganesh S, Brar S. Clinical outcomes of small incision lenticule extraction with accelerated cross-linking (ReLEx SMILE Xtra) in patients with thin corneas and borderline topography. *J Ophthalmol*. (2015) 2015:1–7. doi: 10.1155/2015/263412

Frontiers in Medicine

Translating medical research and innovation into
improved patient care

A multidisciplinary journal which advances our
medical knowledge. It supports the translation
of scientific advances into new therapies and
diagnostic tools that will improve patient care.

Discover the latest Research Topics

See more →

Frontiers

Avenue du Tribunal-Fédéral 34
1005 Lausanne, Switzerland
frontiersin.org

Contact us

+41 (0)21 510 17 00
frontiersin.org/about/contact



Frontiers in Medicine

